Interactions of Smc-ScpAB with the *Bacillus subtilis* chromosome

Dissertation

der Fakultät für Biologie

der Ludwig-Maximilians-Universität München

zur Erlangung des naturwissenschaftlichen Doktorgrades

Doctor rerum naturalium (Dr. rer. nat.)

vorgelegt von

Larissa Wilhelm

aus Wien (Österreich)

München, 22. August 2016

Die vom Autor beigesteuerten Experimente in den hier vorgestellten Publikationen wurden von März 2013 bis August 2016 in der Abteilung „Chromosomale Organisation und Dynamik“ (Dr. Stephan Gruber) am Max Planck Institut für Biochemie in Martinsried durchgeführt.

1. Gutachter: Prof. Dr. Marc Bramkamp
2. Gutachter: Prof. Dr. Heinrich Jung

Dissertation eingereicht: 22.08.2016
Tag der mündlichen Prüfung: 01.12.2016

Eidesstaatliche Erklärung

Ich, Larissa Wilhelm, versichere hiermit an Eides statt, dass die vorgelegte Dissertation von mir selbstständig und ohne unerlaubte Hilfe angefertigt ist. Keine als die angegebenen Quellen und Hilfsmittel wurden benutzt und alle Zitate wurden kenntlich gemacht.

………………………………… …………………………………

München, den Larissa Wilhelm

Erklärung

Hiermit erkläre ich, dass die Dissertation nicht ganz oder in wesentlichen Teilen einer anderen Prüfungskommission vorgelegt worden ist und, dass ich mich anderweitig einer Doktorprüfung ohne Erfolg nicht unterzogen habe.

………………………………… …………………………………

München, den Larissa Wilhelm

ABSTRACT

Every living organism relies on cell division for survival, which requires proper chromosomal organization and segregation. The SMC family of proteins is highly conserved in all branches of life and is known to play an important role in these processes. In *Bacillus subtilis* deletion of the Smc-ScpAB complex leads to severe defects in chromosome segregation. Presumably, Smc-ScpAB mediates the compaction and resolution of sister DNA molecules during cell division, however the molecular mechanism for this action is only poorly understood. A major aim of this work was to answer the question of how the ring-shaped Smc-ScpAB complex interacts with the chromosome.

I thus developed a novel biochemical assay and found that the *B. subtilis* Smc-ScpAB complex entraps chromosomal DNA inside its ring *in vivo*. I then aimed in establishing the requirements for chromosomal entrapment. In a second study I contributed to, the impact of the Smc-ScpAB ATPase activity on its chromosome-wide interaction was studied using ChIP combined with whole-genome sequencing. In combination both studies allowed us to gain a deeper mechanistic insight on the interactions of *B. subtilis* Smc-ScpAB with the chromosome.

ZUSAMMENFASSUNG

Die Vermehrung und das Überleben jeglichen zellulären Lebens hängt von der präzise koordinierten Zellteilung ab. Dafür müssen die Chromosomen in einer geordneten und kompakten Form vorliegen. Die Structural Maintenance of Chromosomes (SMC)-Komplexe sind eine hoch konservierte Protein-Familie, die für diese Prozesse eine fundamentale Rolle spielt. In *Bacillus subtilis* führt die Deletion von Smc-ScpAB zu schwerwiegenden Fehlern in der Chromosomen-Segregation. Vermutlich stellt Smc-ScpAB sicher, dass die Schwester-Chromosomen vor der Zellteilung voneinander getrennt vorliegen. Der molekulare Mechanismus dieses Vorgangs ist jedoch nur in geringen Teilen verstanden.

Ziel dieser Arbeit war es, die Interaktion von Smc-ScpAB mit dem *B. subtilis* Chromosom zu studieren. Der Komplex weist eine außergewöhnliche ringförmige Struktur auf. Ich entwickelte eine neue biochemische Methode, mit deren Hilfe ich zeigen konnte, dass Smc-ScpAB das Chromosom ringförmig umschließen kann. Dadurch konnte ich darlegen, dass diese Art der Interaktion evolutionär konserviert ist. Basierend auf diesem Resultat untersuchte ich die Voraussetzungen für das Umschließen chromosomaler DNA durch Smc-ScpAB. In einer zweiten Publikation an der ich mitwirkte, untersuchten wir die Chromosomen-weite Interaktion von Smc-ScpAB mit Hilfe von Chromatin Immunopräzipitation (ChIP) kombiniert mit Chromosomen-weiter Sequenzierung. Die Ergebnisse beider Publikationen ermöglichen uns nun detailliertere mechanistische Einblicke in die Interaktionen von *B. subtilis* Smc-ScpAB mit dem Chromosom.

PUBLICATIONS & CONTRIBUTION

Major parts of this thesis were published in:

Publication I

SMC condensin entraps chromosomal DNA by an ATP hydrolysis dependent loading mechanism in *Bacillus subtilis*

Larissa Wilhelm, Frank Bürmann, Anita Minnen, Ho-Chul Shin, Christopher P Toseland, Byung-Ha Oh, Stephan Gruber

eLIFE, 2015;4:e06659. DOI: 10.7554/eLife.06659

Author contribution

Larissa Wilhelm performed the majority of the experiments, prepared all figures and wrote the manuscript together with Stephan Gruber. The strains and experiments presented in Figure 5 and S5 were done by Frank Bürmann. The experiment in Figure S3 was performed by Anita Minnen. Ho-Chul Shin, Christopher P Toseland and Byung-Ha Oh contributed essential unpublished material to the manuscript.

Publication II

Control of Smc Coiled Coil Architecture by the ATPase Heads Facilitates Targeting to Chromosomal ParB/*parS* and Release onto Flanking DNA

Anita Minnen*, Frank Bürmann*, **Larissa Wilhelm**, Anna Anchimiuk, Marie-Laure Diebold-Durand, Stephan Gruber

Cell Reports; 14, 1-14, March 1, 2016. DOI: 10.1016/j.celrep.2016.01.066

*Co-First authors

Author contribution

Anita Minnen and Frank Bürmann performed the majority of the experiments of this publication. Larissa Wilhelm statistically analyzed all the data obtained from the microscopy experiments in the publication and did the ChIP-qPCR experiments in Figures S2 and S3. Anna Anchimiuk performed exploratory ChIP-qPCR experiments and Marie-Laure Diebold-Durand mapped the Smc coiled-coil register and did protein purifications. The manuscript was prepared by Anita Minnen, Frank Bürmann, Larissa Wilhelm and Stephan Gruber.

ABSTRACT I

ZUSAMMENFASSUNG III

PUBLICATIONS & CONTRIBUTION V

TABLE OF CONTENTS VI

ABBREVIATIONS VIII

1. INTRODUCTION - 1 -

1.1. Bacterial chromosome organization and dynamics - 1 -
  1.1.1. Historical view on chromosome organization - 1 -
  1.1.2. Spatial organization of bacterial chromosomes - 2 -
  1.1.3. Negative supercoiling and topological domains - 3 -
  1.1.4. Nucleoid-Associated Proteins (NAPs) - 4 -
  1.1.5. Macrodomains - 5 -

1.2. Bacterial cell division cycle - 6 -
  1.2.1. Chromosome replication - 6 -
  1.2.2. Chromosome segregation - 8 -

1.3. Eukaryotic cell division cycle - 11 -

1.4. SMC-kleisin complexes - 12 -
  1.4.1. Architecture and composition - 12 -
  1.4.2. Eukaryotic SMC-complexes - 15 -
  1.4.3. Prokaryotic SMC and SMC-like complexes - 19 -

1.5. The functions of the *Bacillus subtilis* Smc-ScpAB complex - 20 -
  1.5.1. Roles in chromosome organization and segregation - 20 -
  1.5.2. Interaction with DNA - 21 -
  1.5.3. Influence of the ParB protein on Smc-ScpAB - 23 -

2. AIM OF THE STUDIES - 24 -

3. RESULTS - 25 -

3.1. Publication I - 25 -

3.2. Publication II - 55 -

4. DISCUSSION - 91 -

4.1. Development of a chromosome-entrapment assay - 92 -
  4.1.1. Locking Smc-ScpAB rings *in vivo* - 92 -
  4.1.2. Efficiency of cross-linking - 93 -
  4.1.3. Degradation of chromosomal DNA - 95 -
  4.1.4. Quantification of entrapping proteins - 96 -
  4.1.5. A topological entrapment or a non-topological entrapment - 97 -

4.2. Functional implications of chromosomal entrapment by Smc-ScpAB - 101 -
  4.2.1. What is the mechanistic basis of chromosomal entrapment? - 101 -
  4.2.2. What is the role of chromosomal entrapment in *B. subtilis*? - 107 -

4.3. Conclusion - 113 -

5. REFERENCES - 115 -

6. CURRICULUM VITAE - 135 -

7. ACKNOWLEDGEMENTS - 137 -

ABBREVIATIONS

ABC transporter	ATP-binding cassette transporter
APC/C	Anaphase-promoting complex/cyclosome
BMOE	Bismaleimidoethane
bps	base pairs
CdLS	Cornelia de Lange Syndrome
CDK	Cyclin-dependent kinase
CID	Chromosome interacting domain
ChIP	Chromatin Immunoprecipitation
DCC	Dosage Compensation Complex
ds DNA	double stranded DNA
FISH	Fluorescence In Situ Hybridization
HR	Homologous Recombination
HTH motif	Helix-Turn-Helix motif
kDa	Kilo Dalton
Kite	Kleisin-interacting tandem winged-helix elements
MTOC	Microtubule-organizing centers
NAPs	Nucleoid Associating Proteins
NBD	Nucleotide Binding Domain
NO	Nucleoid Occlusion
PDB	Protein Data Bank
Rtp	Replication terminator protein
SCC	Sister Chromatid Cohesion
ss DNA	single stranded DNA
SMC	Structural Maintenance of Chromosomes
SUMO	Small ubiquitin-like modifier
TAD	Topological Associating Domain
WHD	Winged Helix Domain
3C	Chromosome Conformation Capture

1. INTRODUCTION

Every living organism relies on cell division for growth and survival. Precise replication and segregation of a genome depends on chromosomal organization in prokaryotes and eukaryotes. The structural maintenance of chromosome (SMC) complexes are highly conserved in all domains of life and play important roles in these processes. In eukaryotes, several kinds of SMC complexes are present within a cell, while prokaryotes usually encode only one of two types, Smc-ScpAB or MukBEF. The molecular mechanism of their action is only poorly understood. Here, members of the family of SMC proteins will be denoted as 'SMC', including both prokaryotic and eukaryotic origins. The bacterial complex will be referred to as 'Smc-ScpAB' and the prokaryotic SMC protein will be denoted as 'Smc'.

This doctoral thesis focuses on establishing a mechanistic basis of the interaction of the *Bacillus subtilis* Smc-ScpAB complex. The first part will provide a general introduction on bacterial chromosome organization, replication, segregation and cell division. Due to their high conservation, mechanistic insights on prokaryotic Smc-ScpAB might also provide a basis on our understanding of eukaryotic complexes. Therefore all known SMC-complexes will be shortly introduced thereafter. Finally the knowledge available on the *B. subtilis* Smc-ScpAB complex will be introduced in detail. Following the introduction two peer-reviewed publications by the author of this thesis are included as chapter 2 and 3. Finally, findings from those studies will be briefly summarized and thoroughly discussed in chapter 4.

1.1. BACTERIAL CHROMOSOME ORGANIZATION AND DYNAMICS

Most bacterial species contain a single circular chromosome between 2 and 8 mega-bps in size (Badrinarayanan et al., 2015). Extended chromosomal DNA of that size would measure approximately 1 to 4 mm in length. The rod-shaped *B. subtilis* cells are 2-5 µm long. Therefore mechanisms must exist to ensure at least 1000-fold compaction of its chromosome in order to fit DNA inside one cell (reviewed in Gruber, 2014). The nucleoid only occupies a fraction within the cell which further supports the existence of a compact and tight state (Dame, 2005). The circular genome is replicated bi-directionally by two forks established at one origin of replication ('*oriC*') with an average speed of 500-1000 bps per second (Chandler et al., 1975; reviewed in: Merrikh et al., 2012). Exponentially growing *B. subtilis* cells divide about every 20 minutes in nutrient-rich medium, hence chromosome replication takes longer than a cell division cycle. To do so, replication is reinitiated before the previous round is finished, resulting in several origins per chromosome (Cooper and Helmstetter, 1968; Niki and Hiraga, 1998).

1.1.1. HISTORICAL VIEW ON CHROMOSOME ORGANIZATION

Basic bacterial research not only promotes the identification of novel targets for antibiotics but is also of particular importance to identify processes that are evolutionary maintained in other domains of life.

Light microscopy approaches and highly specific DNA staining dyes such as the Feulgen staining procedure enabled visualization of nuclear material in bacteria in the mid 1920s (Feulgen and Rossenbeck, 1924). This led to first evidence that bacteria contain a compact chromosome (reviewed in: Robinow and Kellenberger, 1994). Especially, Piekarski (Piekarski, 1937) and Stille (Stille, 1937), consistently described the appearance of a regular number of stained bodies within bacterial cells, behaving in an ordered fashion. They were termed 'nucleoids' due to their cloud-like appearance in the cell. Microscopy studies showed that the nucleoid behaves highly dynamic in the cell, especially during fast growth conditions and undergoes several morphological changes (Mason and Powelson, 1956). The development and optimization of electron microscopy and of techniques for isolating whole bacterial chromosomes in the 1970s (Delius and Worcel, 1974; Kavenoff and Bowen, 1976; Pettijohn and Hecht, 1974) enabled detailed visualization of the chromosome. DNA spreads on EM grids do not reflect the *in vivo* situation, however at that time they provided for the first time an insight on the physical appearance of bacterial DNA. The isolated chromosomes mostly showed interwound DNA loops – called 'plectonemes'. Fluorescence microscopy and techniques for tagging proteins with GFP were another milestone (Chalfie et al., 1994; Shimomura et al., 1962). Advanced methods such as FISH or time-lapse microscopy allowed *in vivo* imaging of bacterial chromosomes, determination of the *oriC* position and co-labeling of DNA-interacting proteins in *E. coli* (Niki and Hiraga, 1998) and *B. subtilis* (Teleman et al., 1998; Webb et al., 1997). Methods such as Chromatin immunoprecipitation ('ChIP') combined with whole genome sequencing ('ChIP-seq') allowed chromosome-wide interaction studies (Solomon et al., 1988; reviewed in: Collas, 2010). The recent development of the Chromosome Conformation Capture ('3C') technologies (Dekker et al., 2002) led to a breakthrough in research on chromosomal organization. Hi-C is an extension of 3C that couples the technology to massive parallel sequencing. Hi-C already shed light into chromosomal organization of *C. crescentus* and *B. subtilis* (Dekker et al., 2002; Le et al., 2013; Lieberman-Aiden et al., 2009; Marbouty et al., 2015; Wang et al., 2015).

1.1.2. SPATIAL ORGANIZATION OF BACTERIAL CHROMOSOMES

The spatial localization of the nucleoid changes throughout the cell cycle (Adams et al., 2014; Wang and Rudner, 2014). In *B. subtilis oriC* is positioned close to mid-cell directly after cell division but is repositioned the cell poles upon replication initiation (Glaser et al., 1997; Lin et al., 1997; Webb et al., 1997). Consequently, replicating chromosomes adopt an 'ori-ter ter-ori' conformation in the cell (*see* **Figure 1.1**). Interestingly, in *E. coli* the chromosome adopts a 'left arm-ori-right arm' configuration throughout its whole cell cycle (Wang and Sherratt, 2010). And in contrast to both is the spatial organization of the *C. crescentus* chromosome. Each locus of the chromosome has a special subcellular localization (Viollier et al., 2004). Replication starts at the cell pole where *oriC* resides and Hi-C confirmed a longitudinal ori-ter ter-ori organization of *C. crescentus* (Le et al., 2013).

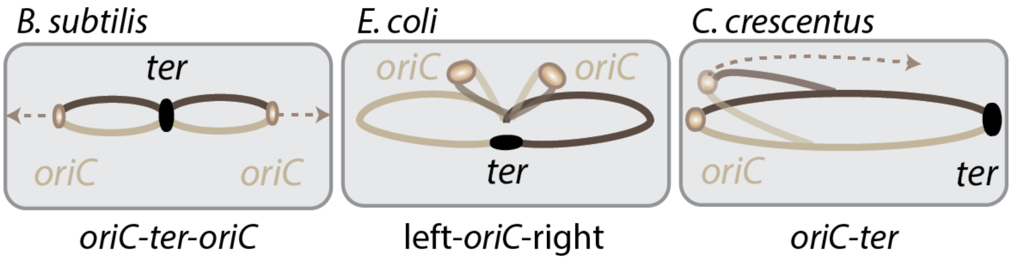

Figure 1.1: Spatial organization of bacterial chromosomes during replication. Three bacterial cells and their circular chromosomes are depicted. The left and right arms of the chromosome are colored in light (left arm) and dark brown (right arm), respectively. In *B. subtilis* the replicated *oriCs* (brown sphere) are repositioned to each cell pole. In *E. coli oriC* stays mid-cell. In *C. crescentus oriC* is positioned at one cell pole and its terminus *ter* (black sphere) at the opposite one, the replicated *oriC* is transferred to the opposite cell pole.

A longitudinal conformation means that the loci of each chromosomal arm are arranged linearly between the origin and the terminus. In *C. crescentus* the ParABS system (*see* **1.2.2.1**) is part of the machinery transferring the newly replicated *oriC* to the opposite cell pole (Ptacin et al., 2010). How *oriC* in the *B. subtilis* or *E. coli* chromosomes is segregated is unclear.

1.1.3. NEGATIVE SUPERCOILING AND TOPOLOGICAL DOMAINS

Organization of the bacterial chromosome can be subdivided into different hierarchical layers. The bottom layer is thought to be negative supercoiling (Badrinarayanan et al., 2015; Drlica, 1992). This describes 'underwinding' of the DNA double helix (*see* **Figure 1.2**), which is in bacteria mediated by the enzymes DNA gyrase, also called topoisomerase II, and RNA polymerase (Gellert et al., 1976; Liu and Wang, 1987). In contrast, topoisomerase I relaxes negative supercoils (Wang, 1971). Plectonemes are a result of negative supercoiling. The negatively supercoiled DNA is additionally twisted thereby forming intertwined loops (Vinograd and Lebowitz, 1966). Negative supercoiling with plectonemic loops is thought to generate separated topological domains on bacterial chromosomes (Postow et al., 2004). Hi-C studies in *C. crescentus* and *B. subtilis* have provided evidence for the existence of topological domains *in vivo* (Le et al., 2013; Marbouty et al., 2015; Wang et al., 2015). They were termed chromosome interacting domains ('CID's) and span on average between 60-340 kilo-bps. Interestingly, most CIDs are separated by 'plectoneme-free' regions that contain highly transcribed genes (Le et al., 2013; Wang et al., 2015). Indeed, supercoiling does not only play a role in chromosome organization but also in various other processes that include unwinding of DNA, such as transcription, replication or homologous recombination (reviewed in: Gilbert and Allan, 2014). It was hypothesized that unwinding of the DNA by the transcription machinery could generate the 'plectoneme-free' regions and thereby set the boundaries of the CIDs (Le et al., 2013). Moreover, single double strand breaks are unable to release negative supercoils suggesting that other proteins or DNA-bound molecules are barriers for DNA superhelicity (reviewed in: Gellert, 1981).

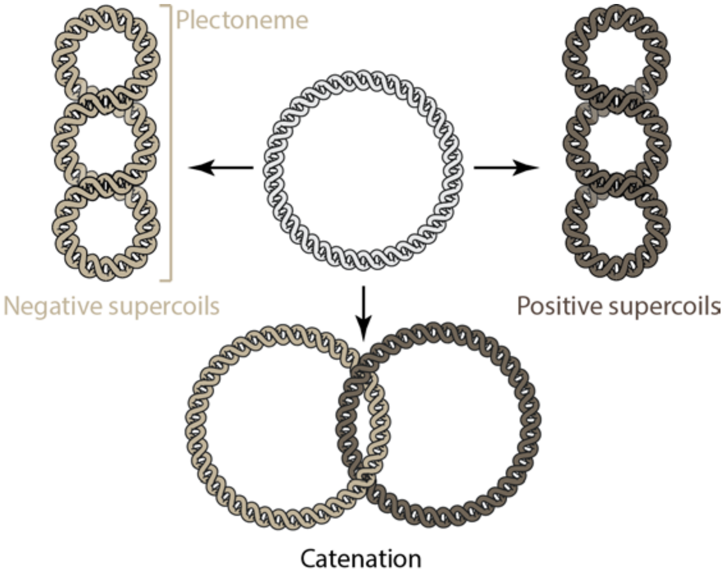

Figure 1.2: Topology of dsDNA. Right-handed underwinding of the circular dsDNA (middle) leads to negative supercoils (light brown, scheme on left side) and subsequently to plectoneme formation. Left-handed overwinding of circular dsDNA leads to positive supercoils (dark brown, scheme on right side). Catenation of two circular dsDNAs is depicted in the bottom scheme.

1.1.4. NUCLEOID-ASSOCIATED PROTEINS (NAPS)

Proteins that bind and also 'form' the bacterial chromosome have been identified and called Nucleoid-Associated Proteins ('NAP') (reviewed in: Dame, 2005). Many NAPs were identified by isolation of whole chromosomes and analysis of co-purified proteins (Paterczyk and Fornal, 1991; Varshavsky et al., 1977). In general NAPs are small proteins and highly abundant in number, they can sequence-specifically and non-specifically bind DNA and are often subdivided into two groups: The first group is called 'DNA bender' proteins. They are able to bend DNA such as the HU, IHF and Fis proteins, present in many bacterial species such as *E. coli*, *C. crescentus* and *B. subtilis* (reviewed in: Song and Loparo, 2015). The HU protein binds to the minor groove of a short stretch of DNA, intercalates and induces kinks in the DNA. A crystal structure of HU in complex with DNA revealed DNA-bends in angles ranging from 105° to 140° (Swinger et al., 2003). ChIP-seq experiments showed that HU has only little DNA specificity and is dispersed over the whole *E. coli* chromosome (Prieto et al., 2012). Quantification of NAPs in exponentially growing *E. coli* revealed on average 30.000-55.000 molecules of HU (Ali Azam et al., 1999). Deletion of HU in *C. crescentus* decreases short-range interactions along the chromosomal arms (Le et al., 2013). This finding supports the idea that the NAPs help to stabilize short (10 kilo-bps) topological domains, generated by negative supercoiling, or promote their formation (Le et al., 2013). The second group consists of proteins bridging DNA, thereby bringing far-distant loci on the chromosome into close proximity (reviewed in: Song and Loparo, 2015). One example is the *E. coli* H-NS protein that forms bridges between dsDNA in scanning force microscopy (Dame et al., 2000). ChIP-on-chip and ChIP-seq studies showed that H-NS binds several sites on the genome, preferentially AT-rich or curved DNA, and various of these sites are also bound by the RNA polymerase (Grainger et al., 2006;

Kahramanoglou et al., 2011), suggesting an influence of H-NS on regulation of gene expression (Navarre et al., 2006; Singh et al., 2014). H-NS proteins do not exist in all bacterial species, however, analogous proteins such as Rok in *B. subtilis* exist. Rok binds several regions of the chromosome non-specifically, with a preference for AT-rich DNA, but can specifically bind promotors e.g. of ComK (Albano et al., 2005; Hoa et al., 2002; Smits and Grossman, 2010).

1.1.5. MACRODOMAINS

First evidence for the existence of defined chromosomal domains was found in *E. coli* using FISH (Niki et al., 2000). Large chromosomal regions around *oriC* ('ori domain') and around the terminus ('ter domain') show different cellular localization patterns from other chromosomal regions and co-occupy the same cytoplasmatic space in *E. coli* (Niki et al., 2000). A further genetic study in *E. coli* describes the presence of four domains that were called 'macrodomains'. This study revealed a higher frequency of recombination events between chromosomal loci in the ori and ter domains as well as in two domains flanking the left and right side of the ter domain (Valens et al., 2004). Moreover, DNA movement within the macrodomains is more restricted than in unstructured chromosomal regions (Espeli et al., 2008).

In *B. subtilis* various studies support the existence of chromosomal domains that might be comparable to the macrodomains found in *E. coli*. In an early study different positions on the chromosome were visualized simultaneously using fluorescence microscopy. The origin region was usually arranged towards the cell poles whereas the terminus region was mid-cell, at the origin-opposing position (Lin et al., 1997; Teleman et al., 1998; Webb et al., 1997). More recently, Hi-C studies in *B. subtilis* and *C. crescentus* revealed the existence of CIDs (Le et al., 2013; Marbouty et al., 2015; Wang et al., 2015). A combination of super-resolution microscopy and Hi-C enabled the assembly of a 3D model of the chromosomal domain architecture in *B. subtilis*. In contrast to *C. crescentus*, a high number of the CID boundaries overlap with binding sites of the Rok protein (Marbouty et al., 2015; Smits and Grossman, 2010). The 3C technologies and super-resolution microscopy will allow detailed research on macrodomains of bacterial chromosomes.

1.2. BACTERIAL CELL DIVISION CYCLE

Bacterial chromosome replication, segregation and cell growth occur concomitantly in many bacteria (Adams et al., 2014). Replication always starts at *oriC* and continues bi-directionally along the two chromosomal arms. In parallel the cell grows and *oriC* is re-positioned. The cell division machinery is assembled, the sister chromosomes physically separate and the cell divides after which the cycle starts over again. *B. subtilis* can undergo one cell cycle in approximately 20 minutes at 37°C under nutrient-rich conditions (Hajduk et al., 2016). Moreover, *B. subtilis* is a spore-forming bacterium under conditions of environmental stress. The purpose of spore formation is to produce metabolically inactive offspring, able to survive long periods of harsh conditions such as lack of nutrients or high/low temperatures (Levin and Grossman, 1998). While during vegetative growth cell division is symmetric i.e. the cell divides exactly mid-cell, cells entering sporulation produce two different types of offspring – the mother cell and the forespore (Errington, 1996). Regulation and mechanistic details of sporulation are not only of interest from a developmental point of view, but also for mechanistic details of cell division (reviewed in: Errington, 2003). Although equally important, organization and segregation during sporulation will not be further introduced here, as for this thesis I have only focused on studying exponentially growing cells.

1.2.1. CHROMOSOME REPLICATION

Replication can be divided into three main stages: initiation, elongation and termination. Species such as *B. subtilis* reinitiate replication of replicating chromosomes during nutrient-rich conditions and consequently chromosomes will be segregated to the daughter cells with already re-replicated *oriC* regions (Cooper and Helmstetter, 1968; Nielsen et al., 2007; Niki and Hiraga, 1998).

Replication initiation and mechanics of the replisome have been extensively studied and established by Kornberg and colleagues in the 1980s for *E. coli*. Important insights on bacterial chromosome replication were obtained, however, not all keyplayers in that process are conserved among other bacterial species such as *B. subtilis* (Kornberg and Baker, 2005). In *B. subtilis oriC* harbours sequence repeats ('DnaA boxes') in between the DnaA encoding gene and the neighbouring DnaN gene (Moriya et al., 1992, 1994). The highly conserved DnaA protein, is an AAA+ ATPase and initiates the replication process by binding to the DnaA boxes followed by hydrolysis of ATP (Fukuoka et al., 1990; Sekimizu et al., 1987) and local unwinding of the dsDNA (Bramhill and Kornberg, 1988). Binding of DnaA sets the stage for the *B. subtilis* helicase DnaC to bind to the ssDNA (Sakamoto et al., 1995). *B. subtilis* requires at least three proteins to load the helicase onto the chromosome during replication start: DnaB, DnaD and DnaI (Bruand et al., 1995, 2001; Marsin et al., 2001; Velten et al., 2003). Next, DNA polymerases are recruited, bind to the chromosome and start replicating. In contrast to *E. coli*, *B. subtilis* requires two replicases called PolC and DnaE and there is evidence that DnaE is the lagging, and PolC the leading strand polymerase (Dervyn et al., 2001). *In vitro* reconstitution of *B. subtilis* replication revealed a complex of 13 proteins being essential to replication, including all proteins mentioned here (Sanders et al., 2010). Replication initiation must be tightly regulated to orchestrate chromosome segregation and cell division. In *B. subtilis* it is partially controlled by the chromosome partitioning proteins Soj and Spo0J (Murray and Errington, 2008). These proteins belong to the ParAB family and are also called 'ParA' (Soj) and 'ParB' (Spo0J).

Replication has to be frequently reinitiated as e.g. double strand breaks will inactivate the replication machinery (reviewed in: Cox et al., 2000). In conclusion, replication is initiated at *oriC* and the chromosome is replicated bi-directionally along both chromosomal arms (*see* **Figure 1.3**). This process stops at the terminus region, opposite of *oriC* where both replication forks eventually meet.

This region, also called '*terC*' in *B. subtilis* harbours at least nine inverted repeat sequences called TerI-TerIX (Duggin et al., 2008; Lewis et al., 1990; Mirkin and Mirkin, 2007). A protein called 'Rtp' ('Replication terminator protein'), was identified binding to them (Lewis et al., 1989) in a polar fashion (Smith and Wake, 1992; Smith et al., 1996). One hypothesis is that the replication forks are stopped by a 'replication fork trap'. As soon as one replication fork is blocked from progressing at a *ter* site, replication of the other fork will only continue to exactly this point, as the termination sites of the second are positioned ahead of the first.

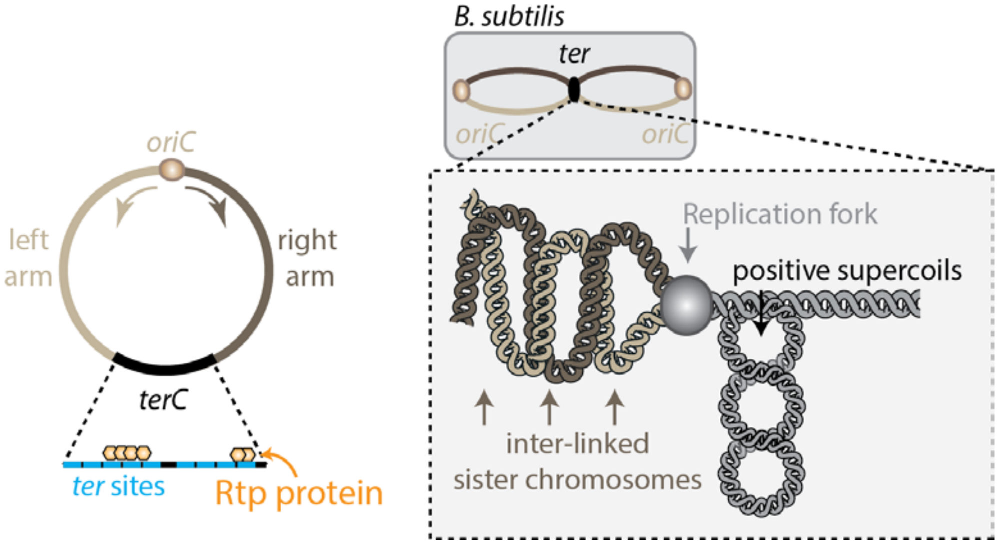

Figure 1.3: Bi-directional replication and topological problems at the replication fork. Replication forks eventually meet at a region called *terC*. It harbours at least nine *ter* sequences (blue) that will be bound by Rtp (yellow) to stop the replication forks. Right scheme: Replicated sister chromosomes behind the replication fork are colored in dark and light brown, respectively. They become inter-linked which causes the formation of pre-catenanes. In front of the replication fork positive supercoils are generated.

1.2.1.1. TOPOLOGICAL PROBLEMS DURING CHROMOSOME REPLICATION

After termination of replication the two sister chromosomes need to be separated from each other. The helical nature of dsDNA in combination with the nature of the circular chromosome causes various links between the sister DNA molecules during replication (reviewed in: Postow et al., 2001). During unwinding of the double helix, positive supercoils are generated in front of the elongating replication fork (*see* **Figure 1.3**; reviewed in: Jeppsson et al., 2014). Positive supercoils can be removed by DNA gyrase (Gellert et al., 1976) and by topoisomerase IV (Ullsperger and Cozzarelli, 1996). If not removed immediately, the positive supercoils can be propagated to the daughter strands behind the replication fork if the fork is able to rotate freely during replication which causes the formation of precatenanes (inter-linked sister DNA strands). These precatenanes must be removed by topoisomerase IV before chromosome segregation (Adams et al., 1992). A special situation occurs at the terminus as the positive superocils ahead of the replication fork presumably block replication of this small region, and topoisomerases cannot bind anymore. *In vitro* experiments on a circular virus DNA (SV40) suggested that the unreplicated structures are directly converted into catenanted sister chromosome dimers that have to be resolved by topoisomerase IV (Mirkin and Mirkin, 2007; Sundin and Varshavsky, 1980, 1981).

Positive supercoils and precatenanes are not the only topological problems during replication. Homologous recombination events happen frequently between sister DNA molecules at the replication forks, resulting in cross-over (Pérals et al., 2001; Steiner and Kuempel, 1998). Proper chromosome segregation will be impeded if the resultant chromosome dimers are not resolved into monomers. The XerCD system in *E. coli* is a major playor in resolving chromosome dimers after replication. *E. coli* harbours a site-specific recombinase consisting of XerC and XerD, acting near the replication terminus at *dif* sites (Blakely et al., 1993). Deletions of either *dif* or XerCD result in long filamentous cells, that fail in proper chromosome segregation (Kuempel et al., 1991). In *B. subtilis* the CodV and RipX proteins are homologues of XerCD (Sciochetti et al., 1999) and a *dif* site was found being located at a position of 166° on the chromosome (Sciochetti et al., 2001).

1.2.2. CHROMOSOME SEGREGATION

Several bacterial systems ensure that cell division occurs mid-cell in *B. subtilis* so that sister chromosomes are segregated equally. Chromosome segregation in *B. subtilis* follows a defined order and loci that are replicated first will also be segregated first (Teleman et al., 1998; Webb et al., 1997). Chromosome segregation is often described as a three-step process starting with segregation of *oriC*, followed by the bulk chromosome, and the terminus (Badrinarayanan et al., 2015; Bouet et al., 2014; Wang et al., 2013).

1.2.2.1. ORIGIN SEGREGATION AND THE PARABS SYSTEM

Soon after replication initiation, the duplicated origins move to opposite cell poles in *B. subtilis*. This is thought to be mediated by active partitioning systems such as the bacterial ParABS system (Glaser et al., 1997; Lee and Grossman, 2006; Lee et al., 2003; Lewis and Errington, 1997; Webb et al., 1997). ParABS systems are present in almost two thirds of all sequenced bacteria, including *B. subtilis*, and *C. crescentus* but not *E. coli* (Livny et al., 2007). It is a three-component system consisting of several centromeric DNA sequences called *parS*, the *parS*-binding protein ParB and a Walker-type ATPase ParA. The ParABS system is thought to play an important role in *oriC* segregation. In *B. subtilis* ten palindromic *parS* sites are distributed over the chromosome, eight of which are localized in 20% of the region around *oriC* (Breier and Grossman, 2007; Ebersbach and Gerdes, 2005). They are specifically bound by the Helix-Turn-Helix motif ('HTH') of a ParB dimer that thereby generates a nucleoprotein complex on the chromosome (Leonard et al., 2004; Sanchez et al., 2013). ParB was shown to spread unspecifically along several kilo-bps of neighboring DNA (Breier and Grossman, 2007; Lin and Grossman, 1998; Murray et al., 2006). In *C. crescentus* deletion of ParB is lethal. It was suggested that the ParABS system could be actively involved in chromosome segregation (reviewed in: Badrinarayanan et al., 2015). ParA binds non-specifically to DNA, when bound to ATP. One model is based on the ability of ParA to form dynamic filaments *in vitro* (Ptacin et al., 2010). It was suggested that the ParB-*parS* complex, itself bound to one of the newly replicated origins, binds to the edge of a ParA filament that is itself bound to the opposite cell pole. This would possibly induce ATP hydrolysis and dissociation of ParA from the filament. ParB would then follow the dissociating ParA filament (Ptacin et al., 2010; Shebelut et al., 2010; Toro et al., 2008). This 'pulling-force' model is based on the existence of a ParA filament, however *in vivo* evidence is missing. The model was challenged by *in vitro* experiments of Vecchiarelli et al. who proposed the 'Brownian ratchet' model (Vecchiarelli et al., 2010). In this model ParB binds to nucleoid-bound ParA-ATP which presumably induces hydrolysis and dissociation of ParA. It was proposed that ParB then moves to regions of more ParA based on Brownian dynamics (Vecchiarelli et al., 2010, 2013). A more recent study discovered elastic properties of the *C. crescentus* chromosome and proposed the 'DNA-relay' model, also based on the findings of Vecchiarelli et al. They propose that ParB-*parS* moves into the direction where most ParA molecules are bound, based on the elasticity of the chromosome rather than on a Brownian ratchet (Lim et al., 2014). Additionally, ParB-*parS* was found to be anchored to the cell pole through its interaction with an anchor protein termed PopZ which could possibly re-establish the ori-ter-ter-ori configuration of the replicated *C. crescentus* chromosome (Bowman et al., 2008; Ebersbach et al., 2008). In *B. subtilis* mutations in ParB only mildly affect chromosome segregation -as judged by the appearance of anucleate cells- but cause a severe sporulation defect (Autret et al., 2001; Ireton et al., 1994). In addition, mis-positioned *oriC*s were observed in its absence (Ireton et al., 1994; Lee and

Grossman, 2006). Possibly the system is catalyzing or improving the efficiency of origin segregation but does not serve as its basis. In *B. subtilis* the role of ParB in chromosome segregation is linked to the Smc-ScpAB complex. Recruitment and binding of Smc-ScpAB to the chromosome has been proposed to be largely dependent on the presence of ParB (Gruber and Errington, 2009; Sullivan et al., 2009). Available data on the role of Smc-ScpAB in chromosome segregation will be introduced later (*see* **chapter 1.5.1**).

1.2.2.2. BULK CHROMOSOME SEGREGATION

The main driving force of bulk chromosome segregation is thought to be chromosome organization itself. Hi-C studies revealed longitudinally organized bacterial chromosomes with juxtaposed chromosomal arms in *B. subtilis* and *C. crescentus* (Le et al., 2013; Wang et al., 2015). Loss of Smc-ScpAB or the ParB protein led to impairment of this organization and was also shown earlier to trigger bulk chromosome segregation defects (Britton et al., 1998; Jensen and Shapiro, 1999; Painbeni et al., 1997). Other models are based on computational modeling and propose that entropy could drive chromosome segregation as a physical force under the right conditions (Jun and Mulder, 2006; Jun and Wright, 2010).

1.2.2.3. TERMINUS SEGREGATION

Decatenation and dimer resolution are crucial for terminus segregation and are both largely dependent on a protein called FtsK in *E. coli* and SpoIIIE in *B. subtilis* (Bigot et al., 2005; Kaimer et al., 2009; Stouf et al., 2013). FtsK is a sequence-guided directional DNA pump that associates with the divisome and interacts with topoisomerase IV *in vitro* (Bigot et al., 2007; Espeli et al., 2003; Sherratt et al., 2010). It recognizes short motifs on the chromosome and can bring together *dif* sites of sister chromosomes before the XerCD recombinase is activated in *E. coli* to separate sister dimers (Bigot et al., 2005; Grainge et al., 2007; Löwe et al., 2008; Steiner et al., 1999). Terminus segregation can only occur when sister chromosomes are separated and segregated into opposite sides of the cell (Badrinarayanan et al., 2015). A major player in cytokinesis is the FtsZ protein. FtsZ assembles into a ring-scaffold, called Z-ring, positioned exactly mid-cell to mark the cell division site and to recruit other divisome proteins (reviewed in: Gamba et al., 2009; Oliferenko et al., 2009). Positioning the Z-ring is an essential step of faithful chromosome segregation, else 'guillotine-effects' can occur that separate the replicated chromosome into two asymmetrically units. Two systems are known to mediate the spatial regulation of cytokinesis: 1) The Min-system, preventing cell division at the cell poles and; 2) Nucleoid occlusion ('NO'), preventing cell division in regions occupied by the nucleoid (reviewed in: Bramkamp and van Baarle, 2009). The Min-system of *B. subtilis* consists of the membrane-associated ATPase MinD that localizes MinC to the plasma membrane and of DivIVA, spatially organizing MinCD. Deletion of any of the components leads to cell division close to the cell poles, generating anucleate mini-cells (Lutkenhaus, 2007). The effector protein of NO is Noc in *B. subtilis*. Noc localizes to specific binding sites on the chromosome lacking from the terminus region, where the FtsZ-ring will form (Wu and Errington, 2004). Although not experimentally proven, one current model is, that Noc recruits the bound DNA to the membrane periphery, inhibiting Z-ring formation in the regions along the chromosome and thereby only allowing its formation around the terminus region (Adams et al., 2015).

1.3. EUKARYOTIC CELL DIVISION CYCLE

The eukaryotic cell cycle is tightly controlled and separated into four major phases: 1) DNA-synthesis phase (S-Phase); 2) Gap 2 phase (G_2); 3) Mitosis (M-Phase); 4) Gap 1 phase (G_1) (reviewed in: Harashima et al., 2013). DNA is replicated only in S-Phase starting from several origins of replication and cells can only enter mitosis when they pass the G_2-checkpoint, making sure that the genome has been completely duplicated (reviewed in: Kelly and Brown, 2000). In general cell cycle progression and checkpoints are regulated by a system of Cyclin-dependent kinases ('CDK's) and cyclins (reviewed in: Morgan, 1997). Mitosis can be subdivided into four phases: 1) Prophase; 2) Metaphase; 3) Anaphase; and 4) Telophase. Entering mitosis, chromosomes have to be compacted in a process known as chromosome condensation, happening in mitotic prophase. This process depends on one side largely on histones, which have DNA wound around them and in mitosis fold into more compact chromatin fibers. An additional level of remodeling and condensation is added by topoisomerase II and condensin complexes, both associating with the chromosome (Coelho et al., 2003; Hirano and Mitchison, 1993, 1994; Maeshima and Laemmli, 2003; Shintomi et al., 2015). For faithful segregation, each sister chromatid has to be attached by the mitotic spindle from opposite directions in a process called bi-orientation (Sonoda et al., 2001; Tanaka et al., 2000). The basis of the mitotic spindle is the dynamic assembling of microtubules that nucleate from two microtubule-organizing centers ('MTOC's) or centrosomes, by polymerization and attach to the centromeres of sister chromatids through kinetochores (reviewed in: Duro and Marston, 2015). Sister chromatids are tightly hold together by the cohesin complexes in a process called sister chromatid cohesion ('SCC') (Michaelis et al., 1997; reviewed in: Peters and Nishiyama, 2012). SCC is established during S-phase and provides the opposing force to the mitotic spindle that applies pulling forces on the centromeres in direction towards the MTOCs (Goshima and Yanagida, 2000; He et al., 2000; Nasmyth and Haering, 2009; Tanaka et al., 2000; Uhlmann and Nasmyth, 1998).

The spindle checkpoint detects chromosomes that are wrongly attached to the mitotic spindle and will block the destruction of securin (and cyclin B) by inhibition of the APC/C complex (reviewed in: Peters, 2006). Securin binds and inhibits separase, and thereby blocks cleavage of the cohesin ring until all duplicated chromosomes are properly attached to the spindle (Uhlmann et al., 1999, 2000). Opening of cohesin at the metaphase-to-anaphase transition enables sister chromatid segregation. Subsequent cytokinesis marks the end of mitosis. The eukaryotic SMC-complexes cohesin, condensin and Smc5/6 play key roles throughout the eukaryotic cell cycle and will be introduced below (Duro and Marston, 2015; Nasmyth, 2002).

1.4. SMC-KLEISIN COMPLEXES

The structural maintenance of chromosome ('SMC')-complexes represent a highly conserved protein family conserved in all domains of life. The first SMC-like gene was isolated in *E. coli* and named 'MukB' after its anucleate phenotype upon deletion, originating from the Japanese word 'mukaku' (Hiraga et al., 1989). Subsequent biochemical analysis revealed that MukB is a 177 kDa protein with an extraordinary architecture and the ability to bind and hydrolyze ATP (Niki et al., 1991, 1992). Shortly after, a mutant of a protein sharing the same architecture combined with a defect in mini-chromosome segregation was identified in *Saccharomyces cerevisiae*. Its encoding gene was termed 'SMC1' (Strunnikov et al., 1993). Bioinformatics revealed that the Smc1 protein has highly conserved homologues in all domains of life and that MukB is a related SMC-like member of this family (Melby et al., 1998; Strunnikov et al., 1993). For their function the SMC-proteins assemble into a complex with accessory proteins that differ depending on the type of complex (Mascarenhas et al., 2002; Nasmyth and Haering, 2005; Soppa et al., 2002; Yamazoe et al., 1999).

1.4.1. ARCHITECTURE AND COMPOSITION

SMC-complexes comprise dimers of SMC-proteins, bridged by a protein from the 'kleisin' family that itself interacts with at least one accessory protein. The single bacterial Smc protein forms a homodimer. In contrast, eukaryotes encode for six different SMC-proteins that assemble into three specific SMC-complexes (Haering et al., 2002).

1.4.1.1. THE SMC PROTEIN

Most SMC proteins are molecules between 1000-1500 amino acids in length that fold back onto themselves almost in the middle of the protein. A folded SMC protein has a length of almost 50 nm and contains three distinct domains that are all functionally essential: 1) A globular 'head' domain formed by the N- and C-termini; 2) A globular dimerization domain called 'hinge', formed by back-folding in the middle of one Smc protein; 3) An intramolecular antiparallel coiled coil that separates the two globular domains (reviewed in: Nasmyth and Haering, 2005).

The 'head'-domain is a characteristic ATP-binding cassette ('ABC') ATPase domain, such as can be found in many membrane transporters (Davidson et al., 2008). ABC transporters usually have two nucleotide binding domains ('NBD') for binding and hydrolysis of ATP. In the SMC complexes one head-domain of SMC forms one NBD and both heads in a dimer are needed for ATP hydrolysis (Haering et al., 2004; Hopfner et al., 2000; Lammens et al., 2004; Löwe et al., 2001). All ABC ATPases harbor at least three distinct motifs: The Walker A motif, the Walker B motif and the signature motif or C-loop (Davidson et al., 2008; Lammens et al., 2004; Walker et al., 1982). In SMC the Walker A motif resides in the N-terminus whereas the Walker B and signature motif are present in the C-terminal part.

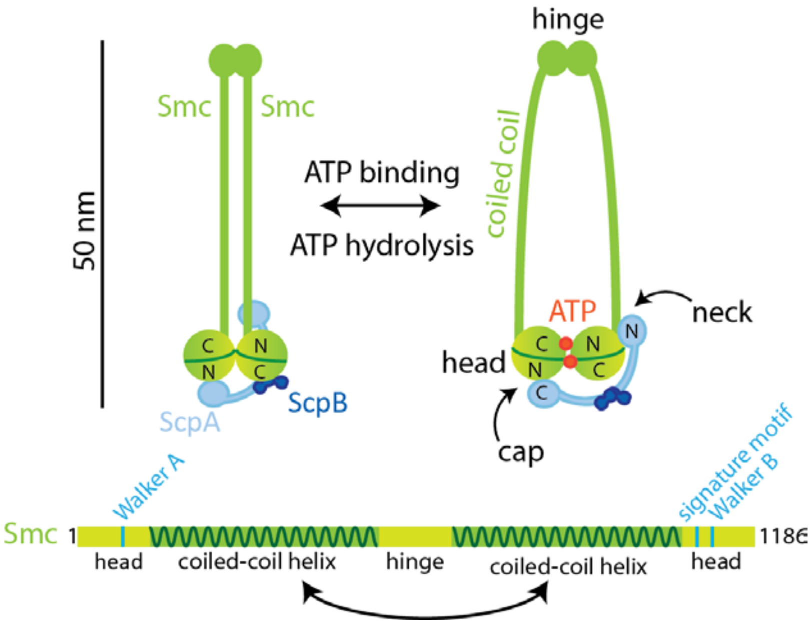

Figure 1.4: Architecture of the *B. subtilis* Smc-ScpAB complex. The complex has a length of approximately 50 nm and consists of a dimer of two Smc proteins (green) that is bound to one molecule of ScpA (light blue) at the cap (Nt-Smc) and neck (Ct-Smc) interface. There is evidence that Smc-ScpAB undergoes a conformational change upon binding of ATP (red sphere) that could lead to opening of its coiled coils. At the bottom a scheme of the Smc protein is depicted. The protein folds at its hinge domain and N- and C-termini bind to each other. This image is modified from: (Wilhelm and Gruber, 2016).

The SMC heads dimerize upon binding of two molecules of ATP, which are sandwiched between the Walker A motif of one SMC head and the signature motif of the second SMC head (Haering et al., 2004; Hopfner et al., 2000; Lammens et al., 2004; Löwe et al., 2001). The Walker B motif coordinates a magnesium ion needed for the ATP hydrolysis reaction (Davidson et al., 2008; Hopfner et al., 2000; Walker et al., 1982). In summary, ATP binds to a pocket formed by N- and C-termini of one SMC-protein, harboring Walker A/B and the signature motif. In the SMC-homodimer this induces ATP-dependent dimerization of two SMC-heads, stabilized by the signature motif (Ames and Lecar, 1992) and subsequent ATP hydrolysis. ATP binding, head engagement and ATP hydrolysis are needed for the function of SMC complexes and their interaction with DNA, described later in detail (Hirano and Hirano, 2006; Minnen et al., 2016; Wilhelm et al., 2015).

The second globular domain of a SMC-protein is separated from the head by a long intramolecular antiparallel coiled coil of more than 300 amino acids in length. The coiled-coil sequence contains a very distinctive heptad repeat pattern and can therefore be predicted very well from the primary sequence (Lupas and Gruber, 2005). To date the least structural information is available on the SMC coiled-coil domain, mostly because high-resolution crystal structures of coiled coils are hard to obtain, possibly because of too much intrinsic flexibility (Waldman et al., 2015). A recent study in *B. subtilis* used site-specific cross-linking to analyze the Smc coiled-coil register. Accordingly, it forms a pretty continuous structure with only two major coiled-coil interruptions on the C-terminal strand. While one interruption seems to be only three amino acids in length and is located more hinge-proximal, the second was proposed to be considerably longer (≈24 AA) and close to the C-terminal head domain (Waldman et al., 2015). These results are in accordance with bioinformatics predictions of the structure of the SMC-protein (prediction tool: Gruber et al., 2006a). Seemingly, the C-terminal half of the SMC-protein is minimally longer compared to the N-terminal half.

The hinge domain of a SMC-protein builds the basis of its homo- or heterodimerization. Structural analysis revealed its ring or doughnut-like structure that is very similar in prokaryotes and eukaryotes (Griese and Hopfner, 2011; Haering et al., 2002; Ku et al., 2010; Soh et al., 2015). Studies of Hirano and colleagues have identified four glycine residues in the *B. subtilis* hinge domain (G657, G658, G662, G663) that when mutated to alanines result in the formation of single-armed monomeric Smc proteins in solution. Almost all of these residues are conserved between prokaryotes and eukaryotes (Hirano, 2001; Hirano and Hirano, 2002). This and other sequence motifs in the hinge have been of particular interest for studying the interaction of the SMC-complex with DNA and will be introduced later (*see* **chapter 1.5.2**).

The coiled-coil region is associated with the hinge domain in different conformations amongst different SMC-complexes based on electron microscopy images. For example the coiled coil emerging from the eukaryotic cohesin hinge displays are more open conformation in comparison to the one from eukaryotic condensin (Anderson et al., 2002; Soh et al., 2015). Also in prokaryotes different conformations of the coiled-coil region below the hinge domain have been described (Anderson et al., 2002; Soh et al., 2015). The potential functional relevance of these different conformational arrangements still needs to be determined and will be addressed in the discussion of this thesis.

1.4.1.2. KLEISIN

SMC proteins interact with additional essential non-SMC components. In cohesin, the kleisin protein Scc1 binds to the Smc1/3 heterodimer, thereby generating a tripartite protein ring (Gruber et al., 2003). In *B. subtilis* the ScpA protein binds a homodimer of Smc (Bürmann et al., 2013). Both, Scc1 and ScpA belong to the same family of proteins called ‘kleisin’, from the Greek word ‘kleisimo’ for ‘closure’, as this protein unit closes the SMC-dimer into a ring-like complex (Schleiffer et al., 2003). The kleisin-family shares most sequence homology between their N- and C-termini. The region in between can be of variable length and is in general less conserved (Schleiffer et al., 2003). Four major classes of eukaryotic kleisins can be separated based on sequence analysis: Kleisin-α/β/γ/δ whereas the ScpA protein represents the class of prokaryotic kleisins (Schleiffer et al., 2003). Kleisins contain a winged-helix domain (‘WHD’) at their C-terminus that interacts in case of eukaryotic cohesin with the bottom of the NBD of Smc1 called ‘cap’ (Haering et al., 2004; Weitzer et al., 2003). Crystal structures of SMC in *B. subtilis* and

S. cerevisiae shed light into the binding of the kleisin N-terminus to SMC and revealed a region above the head in the coiled coil, which was called 'neck' (Bürmann et al., 2013; Gligoris et al., 2014). The *B. subtilis* Smc-ScpAB thereby forms an asymmetric Smc-kleisin complex, as it is also the case for its eukaryotic counterparts where asymmetry is also introduced by the formation of the SMC-heterodimer (Bürmann et al., 2013). It is still unclear, what origin the asymmetric binding of *B. subtilis* ScpA to the Smc-homodimer has.

1.4.1.3. ACCESSORY PROTEINS

All known SMC-complexes contain at least one accessory protein, also essential for their function. These proteins are very divergent but most of them bind to the kleisin subunit of the complex (reviewed in: Nasmyth and Haering, 2005; Nolivos and Sherratt, 2013; Palecek and Gruber, 2015). Also their role within the SMC-complex is not well understood for both prokaryotes and eukaryotes. Crystal structures of the accessory proteins revealed that most of the prokaryotic complexes such as *B. subtilis* Smc-ScpAB and the SMC-like MukBEF can be structurally aligned very well (Bürmann et al., 2013; Gloyd et al., 2011; Kamada et al., 2013; Woo et al., 2009). Moreover structural homology was also found between the Nse1/3 proteins that are part of the accessory proteins in the eukaryotic Smc5/6 complex and the bacterial proteins (Palecek and Gruber, 2015). Interestingly the eukaryotic cohesin and condensin complexes do not display high structural homology with the prokaryotic accessory proteins. It was speculated that this could mean that the Smc5/6 complex is functionally more related to prokaryotic Smc-ScpAB than cohesin and condensin (Palecek and Gruber, 2015).

1.4.2. EUKARYOTIC SMC-COMPLEXES

1.4.2.1. COHESIN

Cohesin forms a Smc1/Smc3 heterodimer which interacts with Scc1, in an asymmetric manner (Michaelis et al., 1997; Strunnikov et al., 1993). Additionally, Scc1 is bound by Scc3 and Pds5, characterized by HEAT sequence repeats (Neuwald and Hirano, 2000; Panizza et al., 2000). To date cohesin is the best studied SMC-complex and a lot of its understanding has been established in the buddying yeast *S. cerevisiae* (reviewed in: Nasmyth and Haering, 2005). Cohesin is essential for holding sister chromatids together during mitosis, a process called sister chromatid cohesion (Michaelis et al., 1997). Cohesin's presence on the chromosome during the eukaryotic cell cycle differs among eukaryotic species, however a fraction always seems to be present from S-phase to mitosis (Uhlmann and Nasmyth, 1998). In yeast, cohesin is loaded onto the chromosome in late G_1-phase, before S-phase, mediated by ATP-hydrolysis and by the loader complex Scc2/4 (Arumugam et al., 2003; Ciosk et al., 2000). Entering S-phase, a fraction of cohesin becomes more stably attached to the chromosome. This is needed because the Wpl1/Rad61 protein that forms a complex with the Pds5 subunit of cohesin displaces cohesin from chromosomes in prophase (Gandhi et al., 2006; Kueng et al., 2006). Unloading by Wpl1/Rad61 can be prevented by acetylation of the Smc3 subunit by the acetyltransferase Eco1 in yeast, and homologous proteins in higher eukaryotes such as ESCO1/ESCO2 in human cells (Ben-Shahar et al., 2008; Gerlich et al., 2006a; Sutani et al., 2009; Unal et al., 2007; Zhang et al., 2008). In metazoans, inhibition of WAPL (Wpl1) and stabilization of cohesin also requires binding of the sororin protein before entry into mitosis (Lafont et al., 2010; Nishiyama et al., 2010; Rankin et al., 2005). In mitosis, cohesin bound along the chromosomal arms is phosphorylated by several kinases (Aurora B, Cdk1, Polo-like kinase 1) which enables their Wpl1-induced release from the chromosome (Hegemann et al., 2011; Losada et al., 2002; Sumara et al., 2002). Importantly, complexes at the centromeres are specifically dephosphorylated by Shugoshin-PP2A complexes to hinder their release (Kitajima et al., 2006; Waizenegger et al., 2000). SCC is resolved in anaphase by proteolytic cleavage of the cohesin ring at the Scc1-kleisin subunit, mediated by the enzyme separase (Uhlmann et al., 1999).

Cohesin does not exclusively function in SCC and was also shown to participate in DNA damage pathways, chromosome condensation and regulation of gene expression (Kagey et al., 2010; Lopez-Serra et al., 2014; Nativio et al., 2009; Strom et al., 2007; Tedeschi et al., 2013; Unal et al., 2007). Mutations in human cohesin cause severe developmental disorders such as the Cornelia de Lange syndrome (‘CdLS’) (Deardorff et al., 1993; Krantz et al., 2004).

In mammals, many cohesin enrichment sites on the chromosome are bound by the CCCTC-binding factor (‘CTCF’) (Parelho et al., 2008; Rubio et al., 2008; Stedman et al., 2008; Wendt et al., 2008), a DNA binding protein involved in transcriptional regulation and chromatin architecture (Phillips and Corces, 2009). Interestingly, depletion of CTCF does not affect SCC although cohesin does not localize to the CTCF binding sites anymore (Parelho et al., 2008; Wendt et al., 2008). In contrast, cohesin depletion reduces the amount of CTCF on the chromosome and disables its function as transcriptional insulator (Wendt et al., 2008). Although it is still unclear how cohesin affects eukaryotic transcription, its interplay with CTCF could provide one possible answer. In yeast, cohesin localizes to intergenic regions between convergently transcribed genes (Lengronne et al., 2004; Schmidt et al., 2009; Tanaka et al., 1999). In contrast, the cohesin loader Scc2/4 is enriched at centromeres and there is evidence that the chromatin structure remodeling complex (RSC) recruits Scc4 to nucleosome-free regions (Hu et al., 2011; Lopez-Serra et al., 2014). Although Scc2/4 is needed for loading of cohesin their localization on the chromosome seems to be different. This suggests that cohesin relocates from its initial Scc2/4 loading sites. Moreover this activity seems to be dependent on ATP hydrolysis (Hu et al., 2011). The relocation was also suggested to be mediated by the active transcription which could explain the high localization of cohesin at convergent transcription sites (Hu et al., 2011).

1.4.2.2. DNA ENTRAPMENT AND THE 'RING'-MODEL

Based on the finding that SMC-complexes form tripartite rings *in vivo* it was proposed that the ring-form mediates 'entrapment' of chromosomes by encircling one or more DNA fibers (Gruber et al., 2003; Haering et al., 2002). There are two ways of how proteins can interact with DNA: 1) physical protein-DNA interactions and; 2) a topological association of the protein ring with DNA. Physical and topological interactions are mostly lost upon denaturation conditions. Only the interaction between a covalently linked protein ring that topologically associates with DNA is resistant to denaturation.

A topological interaction in case of SMC-complexes displays embracement of DNA within the ring that is generated by the interaction of two Smc proteins with a kleisin subunit. A discrimination can be made between: 1) Non-topological entrapment of DNA loops; and 2) A topological entrapment that requires transient opening of the ring, such as a clothespin would be clamped onto a rope.

Cleavage of the *S. cerevisiae* Scc1-kleisin subunit by separase at the onset of anaphase triggers dissociation of cohesin from chromosomes (Hauf et al., 2001; Uhlmann and Nasmyth, 1998; Uhlmann et al., 1999). This was first evidence supporting the 'ring' model that proposes a topological association of cohesin with chromosomal DNA. Moreover, cleavage of the Smc3 coiled coil is sufficient to release cohesin from chromosomes and abolishes SCC, also being consistent with the ring model (Gruber et al., 2003). One way of testing the interaction of SMC-complexes with DNA directly was the establishment of mini-chromosome assays for yeast cohesin and condensin (Cuylen et al., 2011; Farcas et al., 2011; Haering et al., 2008; Ivanov and Nasmyth, 2005). The mini-chromosomes are stably maintained in yeast and specifically isolated from cells from different cell cycle phases, where cohesin is known to bind to the chromosome. In theory, a topological entrapment is lost upon cleavage of either the SMC ring or by linearization of the mini-chromosome, both was observed in the assays. Thereby it was shown that *S. cerevisiae* cohesin topologically entraps DNA inside its ring (*see* Discussion, **chapter 4.1.5**). Basis of the establishment of a topological entrapment, however, is opening of one SMC-complex ring interface upon loading and unloading from the chromosome. In *S. cerevisiae* there is evidence that the hinge interface is involved in loading onto chromosomes (Gruber et al. 2006). A fusion of the Smc3/Scc1 interface reduces the turnover of cohesin on the chromosome once it has loaded on chromatin suggesting that this interface could be the exit gate (Chan et al., 2012). The mechanistic details of establishing topological entrapment are still to a large extend unclear and will be discussed extensively in my discussion (*see* **chapter 4.2.1.3**).

1.4.2.3. CONDENSIN

At least three condensin complexes have been identified in eukaryotes to date. Condensin I was identified originally in *Xenopus laevis* egg extracts as an essential chromosomal component. It is essential for proper segregation and condensation of chromosomes *in vivo* and the complex is ubiquitously present in eukaryotes (Hirano and Mitchison, 1994; Hirano et al., 1997; Houlard et al., 2015; Ono et al., 2003; Sutani et al., 1999). A variant of condensin I in *Caenorhabditis elegans* is part of the dosage-compensation complex ('DCC') that controls expression levels of the X-chromosome in XX-animals (Chuang et al., 1994; Lieb et al., 1998; Meyer, 2010). Many but not all eukaryotes have a second condensin complex, condensin II, that was first identified in vertebrates (Ono et al., 2003; Yeong et al., 2003). The core component of condensin I and II is a heterodimer formed by the Smc2 and Smc4 proteins. The heterodimer associates with the γ-kleisin Brn1 in condensin I of budding yeast and CAP-H in higher eukaryotes such as *D. melanogaster* or humans. Condensin II associates with a β-kleisin named CAP-H2. Each complex has a unique set of non-SMC subunits. Budding yeast condensin I associates with the HEAT-repeat proteins Ycs4 and Ycg1, whereas in higher eukaryotes condensin I and II subunits are termed CAP-D2/D3 and CAP-G/G2 (Haering and Gruber, 2016; Hirano, 2012).

Condensin was suggested to facilitate compaction and disentanglement of sister chromatids, crucial for their separation at anaphase (Kimura and Hirano, 1997; Kimura et al., 1999; Losada and Hirano, 2001; Strick et al., 2004). Several lines of evidence suggest that it promotes the function of the type II topoisomerase ('Top2') that is involved in disentanglement of sister chromatids. Depletion of either Top2 or condensin in yeast leads to similar chromosome mis-segregation phenotypes (Bhalla, 2002; Bhat et al., 1996; Coelho et al., 2003).

There is evidence that condensin complexes entrap DNA inside their tripartite ring, as described for cohesin. It was suggested that entrapment of chromosomal loops could serve as basis for chromosomal compaction (Cuylen et al., 2011). Indeed, depletion of condensin II in *Xenopus* egg cell-free extracts suggests that it contributes to axial shortening of chromatids while condensin I supports the lateral compaction (Shintomi and Hirano, 2011). While condensin II is present in the eukaryotic nucleus throughout the cell cycle, condensin I does not access the chromosome until the nuclear envelope dismantles during mitosis. Both localize differently on the chromosome, however, their localization seems to be somewhat interdependent (Hirota et al., 2004; Ono et al., 2003, 2004). Moreover, condensin I was suggested to interact in a more dynamic way with mitotic chromosomes than condensin II (Gerlich et al., 2006b; Oliveira et al., 2007). Finally, there is evidence that condensins are also needed for transcriptional control, DNA damage response, repair and recombination (Hirano, 2012). An example for transcriptional control in budding yeast is the association of condensin I with the RNA polymerase II transcription factor TFIIIC (D'Ambrosio et al., 2008).

1.4.2.4. SMC5/6

Smc5/6 was first identified as part of the DNA repair proteins during homologous recombination in fission yeast *Schizisaccharomyces pombe* (Fousteri and Lehmann, 2000; Lehmann et al., 1995). In most species the complex consists of a Smc5/6 heterodimer, a kleisin called Nse4, two tandem-WHD proteins

Nse3 and the Nse1 ubiquitin ligase, both associating with the kleisin subunit, and a SUMO ligase called Nse2 in most species (Haering and Gruber, 2016; Jeppsson et al., 2014). A striking structural similarity between the prokaryotic complexes Smc-ScpAB and MukBEF and eukaryotic Smc5/6 has been described recently (Palecek and Gruber, 2015). A class of proteins, containing tandem WHD-elements interacting with the central part of kleisin proteins, was identified and termed kleisin-interacting tandem winged-helix elements ('kite'-proteins). Kite proteins were not identified for cohesin or condensin (Palecek and Gruber, 2015).

The protein complex is most known for its involvement in double-strand break repair (Jeppsson et al., 2014). Fission yeast Smc6 was shown to be needed for DNA repair after UV- or γ-ray irradiation (Lehmann et al., 1995). In *S. cerevisiae*, all components of the Smc5/6 complex are essential (Pebernard et al., 2006). Several studies reported a delay of chromosome segregation upon Smc5/6 depletion and also revealed an accumulation of unusual recombination intermediate structures between replicated sister chromatids, which possibly hinder their efficient separation (Betts Lindroos et al., 2006; Torres-Rosell et al., 2005). Interestingly, Smc5/6 and cohesin are both recruited to double-strand breaks on the replicated genome and 60% of Smc6 binding sites overlap with the cohesin subunit Scc1 (Betts Lindroos et al., 2006; De Piccoli et al., 2006; Potts et al., 2006). Based on this finding a role in resolution of sister chromatid intertwinings was suggested (Betts Lindroos et al., 2006).

Inhibition of Smc5 or Smc6 has been linked with SCC defects in yeast, chicken and humans, such as observed upon cohesin-depletion (Almedawar et al., 2012; Gallego-Paez et al., 2014; Stephan et al., 2011). Its exact role in SCC is unknown, however, one hint could be the Nse2 (Mms21) SUMO-ligase subunit of Smc5/6, that sumoylates several substrates including cohesin (Almedawar et al., 2012; McAleenan et al., 2012; Zhao and Blobel, 2005). However, there is also evidence that chromosomal localization of Smc5/6 requires itself SCC (Jeppsson et al., 2014).

1.4.3. PROKARYOTIC SMC AND SMC-LIKE COMPLEXES

Identification of the MukB protein, member of the SMC family marked the beginning of research on SMC-kleisin complexes in the 1990's. Prokaryotic SMC-complexes are present in a wide range of bacteria and archaea. Smc-like MukB protein, however, was only found in a limited branch of γ-proteobacteria (reviewed in: Gruber, 2011). MukB shares structural features with canonical SMC proteins, such as the ATP binding domain at its N- and C-termini, a long coiled coil and a hinge domain for dimerization of two MukB proteins (Niki et al., 1991, 1992). MukB is encoded in an operon with its associating proteins MukE and MukF, which together form the MukBEF complex (Yamanaka et al., 1996). With its N-termini two MukF proteins dimerize and each C-terminus binds one MukB head thereby possibly forming a tetrapartite ring (reviewed in: Nolivos and Sherratt, 2013). ATP binding to the

MukB dimer leads to disruption of one MukF binding site, a finding that has not been seen for any other SMC-complex so far (Upton and Sherratt, 2013; Woo et al., 2009).

A *mukBEF* deletion causes accumulation of anucleate cells and temperature sensitive growth (Niki et al., 1991). On the other hand, overexpression generates more condensed chromosomes, suggesting a role in chromosome organization (Wang et al., 2011). Fluorescence microscopy studies indicate that MukBEF co-localizes with *oriC* such as Smc-ScpAB in *B. subtilis* (Badrinarayanan et al., 2012; Danilova et al., 2007). A physical interaction of the MukBEF hinge with topoisomerase IV was observed and several lines of evidence support a model in which their interaction facilitates chromosome segregation (Hayama and Marians, 2010; Li et al., 2010; Nicolas et al., 2014; Vos et al., 2013).

There is no answer to the question why only some bacteria have MukBEF instead of Smc-ScpAB. Only recently a third prokaryotic SMC-like complex has been identified in *Pseudomonas aeruginosa* as a distant relative of MukBEF (Petrushenko et al., 2011; reviewed in: Gruber, 2011). The complex is not conserved at sequence level with MukBEF, but equally genetically organized. Moreover their predicted secondary structures are very similar. Based on these similarities the complex was termed MksBEF for 'Muk-like SMC'. Surprisingly, MksBEF was then found in many more bacterial species often in combination with Smc-ScpAB (Petrushenko et al., 2011). Mutations in MksBEF cause anucleate cells in *P. aeruginosa*. Where both, MksBEF and Smc-ScpAB are present, overexpression of MksBEF can rescue the *smc* deletion phenotype, suggesting that both complexes share functions (Gruber, 2011; Petrushenko et al., 2011).

1.5. THE FUNCTIONS OF THE *BACILLUS SUBTILIS* SMC-SCPAB COMPLEX

1.5.1. ROLES IN CHROMOSOME ORGANIZATION AND SEGREGATION

B. subtilis harbors prokaryotic Smc-ScpAB (Britton et al., 1998; Melby et al., 1998). Our understanding of prokaryotic SMC complexes is largely based on work in *B. subtilis*. Due to the high conservation of its structure and the ATPase domain our knowledge from prokaryotes might contribute considerably to our general and mechanistic understanding of all SMC-kleisin complexes.

Prokaryotic Smc-ScpAB is often termed 'prokaryotic condensin', due to perceived functional similarities with the eukaryotic condensin complex (reviewed in: Hirano, 2016; Palecek and Gruber, 2015). In early studies a condensation phenotype of a *smc* deletion has been described that has encouraged the idea that the prokaryotic complex could function similar to eukaryotic condensin (Britton et al., 1998). However this phenotype might be caused indirectly by defective chromosome segregation. Only recently Hi-C has brought evidence, that Smc contributes to chromosome organization in *B. subtilis*, its mechanistic action, however, still remains unknown (Marbouty et al., 2015; Wang et al., 2015). Null mutations of either Smc, ScpA or ScpB are lethal in *B. subtilis* in nutrient-rich growth conditions (Britton et al., 1998; Gruber et al., 2014; Wang et al., 2014). The cells are able to grow under slow growth conditions such as in minimal growth medium where an accumulation of anucleate cells is observed (Britton et al., 1998; Moriya et al., 1998; Niki et al., 1991). Moreover, decreasing levels of negative supercoiling by DNA gyrase inhibitors even further enhance these phenotypes. Contrarily, increasing negative supercoiling by depletion of topoisomerase I can suppress to some extend the chromosome partitioning defect of *smc* null mutants (Lindow et al., 2002). On the basis of its sequence *B. subtilis* Smc shares most sequence homology with eukaryotic Smc1/3 and Smc2/4, however, in general the sequences are poorly comparable (Palecek and Gruber, 2015). Moreover, structural similarities between eukaryotic Smc5/6 and prokaryotic Smc-ScpAB were identified ('kite' proteins) and it therefore remains to be determined, if the term 'prokaryotic condensin' is justified for Smc-ScpAB (Palecek and Gruber, 2015).

Deletion of eukaryotic cohesin leads to premature sister chromosome separation, in contrast to a deletion of Smc-ScpAB in *B. subtilis*, where interlinked sister chromosomes arise due to a partitioning defect of *oriC* (Gruber et al., 2014; Wang et al., 2014). During normal growth, the replication forks of *B. subtilis* proceed with an approximate speed of 1000 bps per second (Merrikh et al., 2012). Surprisingly, a reduction of this speed can suppress the growth defect of the *smc* deletion in rich medium, suggesting that Smc-ScpAB is needed primarily upon fast replicating conditions (Gruber et al., 2014).

Different experimental approaches revealed that Smc-ScpAB localizes onto the bacterial chromosome *in vivo*. ChIP experiments showed that Smc binds along the whole chromosome, but is enriched at *oriC* and its vicinity (Gruber and Errington, 2009; Sullivan et al., 2009). Eight of total ten ParB-bound *parS* sites in *B. subtilis* are in the vicinity of *oriC* (*see* **chapter 1.2.2.1**). Strikingly, the localization of Smc to origin-proximal DNA is largely abolished upon *parB* deletion. This was also shown by a second independent approach using fluorescence microscopy (Gruber and Errington, 2009; Sullivan et al., 2009). The Hi-C studies that observed a longitudinal folding of the *B. subtilis* chromosome, provided evidence that this organization is dependent on the presence of ParB, Smc-ScpAB and at least one *parS* site (Marbouty et al., 2015; Wang et al., 2015). Moreover, one single *parS* site can define the apex from which adjacent loci become juxtaposed along the entire length of the chromosome. These data suggest that Smc-ScpAB binds to ParB-bound *parS* sites near *oriC* and then promotes juxtaposition of DNA flanking the *parS* sites. Thereby replicated sister-origins could be separated from each other, which would explain the origin segregation effect in absence of Smc-ScpAB (Marbouty et al., 2015; Wang et al., 2015). These data will be discussed thoroughly in the light of our results in **chapter 4.2.2.2**.

1.5.2. INTERACTION WITH DNA

SMC-complexes are ABC-like ATPases containing a Walker A, Walker B and a signature motif in their Smc-head domains (Ames and Lecar, 1992; Walker et al., 1982). Binding of Smc-ScpAB to DNA *in vitro* has been extensively studied by Hirano and colleagues (Hirano, 2005, 2016).

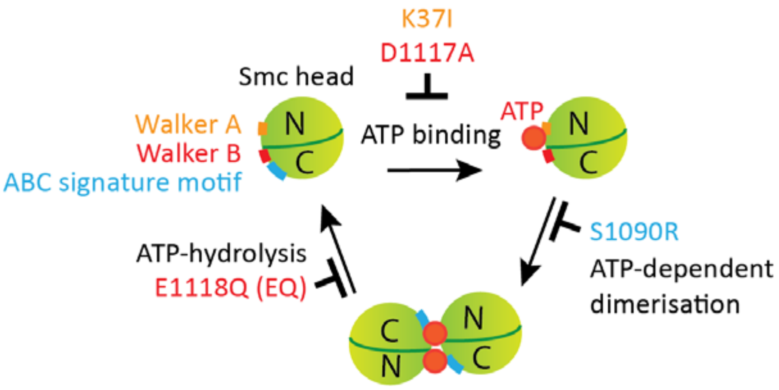

Figure 1.5: **ATP hydrolysis cycle of Smc-ScpAB**. The N-terminus of the Smc-head ('N' on green sphere) harbors the Walker A motif (yellow). The Walker B (red) and C-motif (blue) are present at the C-terminus ('C'). ATP binding is inhibited by the Smc K37I and D1117A mutations whereas dimerization of two NBDs is inhibited the Smc S1090R mutation. The E1118Q mutation close to the Walker B motif almost completely abolishes ATP hydrolysis. Image modified from: (Minnen et al., 2016)

These studies have been performed *in vitro* with tagged proteins and artificial DNA substrates. Nevertheless, basic mechanistic features of the *B. subtilis* Smc-ScpAB complex were successfully established thereby. Smc-ScpAB binds to ds and ssDNA and both DNA substrates stimulate the ATPase activity of the complex (Hirano and Hirano, 1998). Mutants specifically blocked in certain steps of the ATP hydrolysis cycle were constructed in *B. subtilis* and are still of outstanding importance for studying the function and mechanism of Smc-ScpAB (*see* **Figure 1.5**; Hirano and Anderson, 2001; Hirano and Hirano, 2004; Hopfner et al., 2000). The Walker A motif mutant K37I and the Walker B motif mutant D1117A abolish binding of ATP to Smc. Mutation in the C motif S1090R abolishes ATP dependent dimerization of two Smc heads. All three mutants do not show any ATP hydrolysis activity nor do they normally bind to DNA (Hirano, 2001; Hirano and Hirano, 2004). The E1118Q mutation in the Walker B motif ('EQ-mutant') almost completely abolishes ATP hydrolysis and Smc-ScpAB complex is left in a head-engaged state. Strikingly, this mutant has strongly enhanced DNA binding activity *in vitro* compared to wild-type Smc (Hirano and Hirano, 2004; Kamada et al., 2013).

Head and hinge interfaces are separated by the coiled-coil domain, with a length of almost 50 nm (Melby et al., 1998). It was suggested, that the coiled coil could serve as communication device between head and hinge, propagating the energy from ATP hydrolysis resulting in a conformational change of the complex (Thadani et al., 2012). Hirano et al. identified residues in the hinge dimerization interface of *B. subtilis* that monomerize the complex, when mutated to alanine (Hirano and Hirano, 2002). The Smc monomer still binds to DNA *in vitro* and hydrolyzes ATP, however, at very low levels. Interestingly, a basic patch at the inner surface of the hinge that consists of three consecutive lysine residues (K666, K667, K668) was identified, being exposed in the monomeric hinge. It was suggested that this patch could be necessary for stable interaction with DNA upon hinge opening (Hirano and Hirano, 2006). And there is evidence for eukaryotic cohesin that opening of the hinge domain is needed for loading of DNA into the cohesin ring (Gruber et al., 2006b). Electron microscopy and atomic force microscopy of SMC-complexes showed that they adopt different configurations, from O-shapes, V-shapes to more I-shapes (Anderson et al., 2002; Fuentes-Perez et al., 2012; Haering et al., 2002; Melby et al., 1998). Apart from ChIP data only few data is available on the interaction of the *B. subtilis* Smc-ScpAB complex with DNA *in vivo*. It was shown that the formation of a tripartite ring is conserved in *B. subtilis* (Bürmann et al., 2013). Therefore the hypothesis arose that Smc-ScpAB could interact with DNA similar as the eukaryotic complexes through DNA entrapment (Bürmann et al., 2013). This was a central question of this thesis.

1.5.3. INFLUENCE OF THE PARB PROTEIN ON SMC-SCPAB

ParABS is of particular interest for studying the *B. subtilis* Smc-ScpAB complex. It is needed for specific chromosomal recruitment of the complex as shown by ChIP experiments and fluorescence microscopy (Gruber and Errington, 2009; Sullivan et al., 2009). Deletion of *parB* is not lethal for *B. subtilis* but shows an increase in the number of anucleate cells (Autret et al., 2001; Ebersbach and Gerdes, 2005; Ireton et al., 1994; Lee et al., 2003). ParB has at least two independent functions, one in regulation of DNA replication where its interaction with ParA is needed, and a second in the recruitment of Smc-ScpAB to the chromosome and therefore presumably in chromosome segregation (Gruber and Errington, 2009).

As introduced, ParB binds specifically to *parS* sites on the *B. subtilis* chromosome (Livny et al., 2007). Moreover, it associates unspecifically with DNA adjacent to the *parS* sites, a phenomenon termed ‘spreading’ (Lin and Grossman, 1998; Rodionov et al., 1999). The unspecifically bound regions span 10-20 kilo-bps, however the mechanism of how spreading is established still remains somewhat unclear (Breier and Grossman, 2007; Graham et al., 2014; Murray et al., 2006; Sanchez et al., 2015). One suggestion was that ParB forms long filaments by polymerization, emerging from *parS* sites (Murray et al., 2006; Rodionov et al., 1999). Only very recently a study using quantitative immunoblotting revealed that ParB is a very low abundant protein in the cell with approximately 20 dimers in *B. subtilis.* This challenges the ParB-filament model (Graham et al., 2014). ParB-dimers can interact with neighboring ParB complexes, an interaction called ‘nearest-neighbor interaction’ (Broedersz et al., 2014). Furthermore, an additional form of ParB binding was identified called ‘DNA bridging’, which is the ability of ParB-nucleoprotein complexes to interact with others located at different positions on the chromosome and thereby bridging distant chromosomal segments (Graham et al., 2014). Moreover, a DNA condensation effect and the formation of large ParB nucleoprotein complexes was observed *in vitro* (Taylor et al., 2015). Until now a direct interaction between Smc and ParB was never observed. However, the described activities of ParB were proposed to mediate organization of *oriC* and could thereby facilitate the interaction of Smc-ScpAB with the chromosome. Lastly the Hi-C studies on the *B. subtilis* chromosome showed that the observed longitudinal organization is dependent on Smc-ScpAB, ParB and the presence of *parS* indicating an interplay of the two proteins (Marbouty et al., 2015; Wang et al., 2015).

2. AIM OF THE STUDIES

The SMC-complexes are structurally highly conserved from prokaryotes to eukaryotes and almost ubiquitously present in all domains of life. Most of the current knowledge on bacterial Smc-ScpAB has been established in the model organism *Bacillus subtilis*. Deletion of *B. subtilis* Smc-ScpAB is lethal and both, chromosome segregation and organization are severely impaired. However, the functional role of Smc-ScpAB in these processes is still largely unknown. On the basis of this question it is essential to study how Smc-ScpAB interacts with the chromosome *in vivo*.

To start answering this question the major goal of this thesis was to study the nature of interaction of Smc-ScpAB with the *B. subtilis* chromosome and to establish its requirements. So far, only i*n vitro* studies have brought evidence that Smc-ScpAB binds both ssDNA and dsDNA and that its ATPase activity plays a major role in this process. Therefore I developed a novel biochemical assay in *B. subtilis* that allowed us to specifically isolate proteins entrapping whole chromosomes *in vivo*. The 'entrapment assay' isolates proteins or complexes that capture at least one DNA strand inside its ring structure and eliminates proteins that are only physically interacting with the chromosome. After establishing the entrapment assay my aim was to establish the requirements of chromosomal entrapment by Smc-ScpAB. It was therefore a major experiment to assess the dependence of entrapment on the ATP hydrolysis activity of Smc-ScpAB. In a second publication to which I contributed to, ChIP experiments and whole-genome sequencing experiments were performed to obtain a broader perspective on the chromosomal localization of Smc-ScpAB. A central aim was also here to study the impact of the ATP hydrolysis cycle on the interaction of the complex. Together the studies present a fruitful approach for elucidating the interaction of Smc-ScpAB with the *B. subtilis* chromosome.

3. RESULTS

3.1. PUBLICATION I

SMC condensin entraps chromosomal DNA by an ATP hydrolysis dependent loading mechanism in *Bacillus subtilis*

Wilhelm, L., Bürmann, F., Minnen, A., Shin, H.-C., Toseland, C.P., Oh, B.-H., and Gruber, S. 2015. *Elife* **4**:1–18. doi:10.7554/eLife.06659.

Abstract:

Smc–ScpAB forms elongated, annular structures that promote chromosome segregation, presumably by compacting and resolving sister DNA molecules. The mechanistic basis for its action, however, is only poorly understood. Here, we have established a physical assay to determine whether the binding of condensin to native chromosomes in *Bacillus subtilis* involves entrapment of DNA by the Smc–ScpAB ring. To do so, we have chemically cross-linked the three ring interfaces in Smc–ScpAB and thereafter isolated intact chromosomes under protein denaturing conditions. Exclusively species of Smc–ScpA, which were previously cross-linked into covalent rings, remained associated with chromosomal DNA. DNA entrapment is abolished by mutations that interfere with the Smc ATPase cycle and strongly reduced when the recruitment factor ParB is deleted, implying that most Smc–ScpAB is loaded onto the chromosome at *parS* sites near the replication origin. We furthermore report a physical interaction between native Smc–ScpAB and chromosomal DNA fragments.

On the following pages the original publication is attached as published online on May 26, 2015 without any modifications. http://dx.doi.org/10.7554/eLife.06659

This article is distributed under the terms of the **Creative Commons Attribution License**, which permits unrestricted use and redistribution provided that the original author, the source of the publication and the license are credited. https://creativecommons.org/licenses/by/4.0/

eLIFE
elifesciences.org

RESEARCH ARTICLE

SMC condensin entraps chromosomal DNA by an ATP hydrolysis dependent loading mechanism in *Bacillus subtilis*

Larissa Wilhelm[1], Frank Bürmann[1], Anita Minnen[1], Ho-Chul Shin[2†], Christopher P Toseland[1], Byung-Ha Oh[2], Stephan Gruber[1]*

[1]Chromosome Organization and Dynamics, Max Planck Institute of Biochemistry, Martinsried, Germany; [2]Department of Biological Sciences, KAIST Institute for the Biocentury, Cancer Metastasis Control Center, Korea Advanced Institute of Science and Technology, Daejeon, Republic of Korea

Abstract Smc–ScpAB forms elongated, annular structures that promote chromosome segregation, presumably by compacting and resolving sister DNA molecules. The mechanistic basis for its action, however, is only poorly understood. Here, we have established a physical assay to determine whether the binding of condensin to native chromosomes in *Bacillus subtilis* involves entrapment of DNA by the Smc–ScpAB ring. To do so, we have chemically cross-linked the three ring interfaces in Smc–ScpAB and thereafter isolated intact chromosomes under protein denaturing conditions. Exclusively species of Smc–ScpA, which were previously cross-linked into covalent rings, remained associated with chromosomal DNA. DNA entrapment is abolished by mutations that interfere with the Smc ATPase cycle and strongly reduced when the recruitment factor ParB is deleted, implying that most Smc–ScpAB is loaded onto the chromosome at *parS* sites near the replication origin. We furthermore report a physical interaction between native Smc–ScpAB and chromosomal DNA fragments.

DOI: 10.7554/eLife.06659.001

Introduction

Compaction and individualization of sister DNA molecules is a prerequisite for efficient segregation of the genetic material to daughter cells during cell division. Multi-subunit Structural Maintenance of Chromosomes (SMC) protein complexes—such as cohesin and condensin—are major determinants of chromosome structure and dynamics during the cell cycle in eukaryotes as well as in prokaryotes (***Hirano, 2006***; ***Thadani et al., 2012***; ***Gruber, 2014***). Condensin subunits were initially identified as abundant, non-histone components of mitotic chromosomes in metazoans (***Hirano and Mitchison, 1994***). In mitosis, condensin localizes together with topoisomerase II in punctate structures to the longitudinal core of chromatids, called the chromosome axis (***Coelho et al., 2003***; ***Maeshima and Laemmli, 2003***; ***Ono et al., 2004***). Inactivation of condensin subunits by mutation or depletion results in severe morphological aberrations and mechanical sensitivity of metaphase chromosomes, and subsequently to defects in their segregation during anaphase (***Hirano and Mitchison, 1994***; ***Ono et al., 2003***; ***Gerlich et al., 2006***). In bacteria, Smc–ScpAB is the prevalent version of SMC protein complexes. Its distant relatives MksBEF and MukBEF can be found scarcely scattered over most of the bacterial phylogenetic tree and in isolated branches of proteobacteria, respectively (***Gruber, 2011***). In *Bacillus subtilis* and *Streptococcus pneumoniae*, Smc–ScpAB is recruited to a region around the replication origin by ParB/Spo0J protein bound to *parS* sites, thereby forming a discrete focus—also called condensation center—on each nascent copy of the chromosome (***Gruber and Errington, 2009***; ***Sullivan et al., 2009***; ***Minnen et al., 2011***). Inactivation of Smc–ScpAB in *B. subtilis* under nutrient rich

***For correspondence:** sgruber@biochem.mpg.de

Present address: †Functional Genomics Research Center, Korea Research Institute of Bioscience and Biotechnology, Daejeon, Republic of Korea

Competing interests: The authors declare that no competing interests exist.

Funding: See page 16

Received: 25 January 2015
Accepted: 06 May 2015
Published: 07 May 2015

Reviewing editor: Bernard de Massy, Institute of Human Genetics, CNRS UPR 1142, France

Copyright Wilhelm et al. This article is distributed under the terms of the Creative Commons Attribution License, which permits unrestricted use and redistribution provided that the original author and source are credited.

eLife digest The genome of any living organism holds all the genetic information that the organism needs to live and grow. This information is written in the sequence of the organism's DNA, and is often divided into sub-structures called chromosomes. Different species have different sized genomes, but even bacteria with some of the smallest genomes still contain DNA molecules that are thousand times longer than the length of their cells. DNA molecules must thus be highly compacted in order to fit inside the cells. DNA compaction is particularly important during cell division, when the DNA is being equally distributed to the newly formed cells.

In plants, animals and all other eukaryotes, large protein complexes known as condensin and cohesin play a major role in compacting, and then separating, the cell's chromosomes. Many bacteria also have condensin-like complexes. At the core of all these complexes are pairs of so-called SMC proteins. However, it is not clear how these SMC proteins direct chromosomes to become highly compacted when cells are dividing.

Wilhelm et al. have now developed two new approaches to investigate how SMC proteins associate with bacterial DNA. These approaches were then used to study how SMC proteins coordinate the compaction of chromosomes in a bacterium called *Bacillus subtilis*. The experiments revealed that SMC proteins are in direct physical contact with the bacterial chromosome, and that bacterial DNA fibers are physically captured within a ring structure formed by the SMC proteins.

Wilhelm et al. suggest that these new findings, and recent technological advances, have now set the stage for future studies to gain mechanistic insight into these protein complexes that organize and segregate chromosomes.

DOI: 10.7554/eLife.06659.002

growth conditions blocks separation of sister replication origins and consequentially leads to lethal defects in chromosome partitioning (**Gruber et al., 2014**; **Wang et al., 2014**). Smc–ScpAB thus promotes the initial stages of chromosome segregation in *B. subtilis*, likely by condensing and individualizing the emerging copies of the chromosome in preparation for their segregation to opposite halves of the cell.

The canonical SMC complex in bacteria comprises five subunits: (1) two Smc proteins, which each form a 45 nm long antiparallel coiled coil that connects an ABC-type ATPase 'head' domain at one end of the coiled coil with a 'hinge' homodimerization domain at the other end (**Hirano et al., 2001**), (2) a single ScpA subunit, which belongs to the kleisin family of proteins and associates via its C-terminal winged-helix domain (WHD) with the bottom 'cap' surface of one Smc head and via its N-terminal helical domain with the 'neck' coiled coil region of the other Smc protein (**Bürmann et al., 2013**), and (3) a dimer of ScpB protein, which binds to the central region of ScpA (**Bürmann et al., 2013**; **Kamada et al., 2013**). Overall, the pentameric Smc–ScpAB complex displays a highly extended conformation harboring a central channel, which is surrounded by a closed tripartite ring formed by the Smc dimer and the ScpAB$_2$ sub-complex. The *B. subtilis* Smc coiled coils associate with one another to form rod-shaped Smc dimers (**Soh et al., 2015**). Furthermore, the Smc head domains can interact directly with one another—via a composite interface that includes two molecules of ATP. Binding to ATP, head engagement and ATP hydrolysis likely control and drive the biochemical action of Smc–ScpAB.

Models for SMC condensation activity have been proposed based on observations made with isolated SMC dimers, SMC fragments or holo-complexes. Such protein preparations support the bridging of given DNA molecules in vitro as indicated by the re-annealing of single stranded DNA, intermolecular DNA ligation, DNA catenation and the co-purification of labeled and unlabeled DNA molecules (**Sutani and Yanagida, 1997**; **Losada and Hirano, 2001**; **Cui et al., 2008**). Many SMC complexes bound to different segments of DNA might thus come together and anchor DNA in condensation centers or at the chromosome axis. Oligomeric assemblies of bacterial Smc proteins have indeed been observed by Atomic Force Microscopy and Electron Microscopy (**Mascarenhas et al., 2005**; **Fuentes-Perez et al., 2012**). This model provides a straightforward explanation for the compaction activity of SMC. However, it is unclear how such apparently indiscriminate DNA aggregation would promote rather than block the individualization of sister chromosomes (**Gruber, 2014**). Local wrapping of DNA around the SMC complex could result in well-defined lengthwise condensation of DNA. However, too little SMC protein appears to be present in chromosomes to yield decent levels of compaction by simple wrapping. A different hypothesis is based on the finding that the structurally related cohesin complex holds sister chromatids in eukaryotes together by entrapping sister DNA fibers within its ring (***Gruber et al., 2003***; ***Gligoris et al., 2014***). Accordingly, individual SMC complexes might entrap and expand loops of DNA, thereby driving lengthwise condensation of chromosomes with little limitations in the attainable levels of compaction (***Nasmyth, 2001***; ***Alipour and Marko, 2012***).

Here, we investigate how the prokaryotic SMC–kleisin complex binds to chromosomes in vivo using a novel whole-chromosome assay.

Results

A chromosome entrapment assay

We initially attempted to detect topological interactions between *B. subtilis* Smc–ScpAB and plasmid DNA using pull-down assays as previously described (***Ivanov and Nasmyth, 2005***; ***Ghosh et al., 2009***; ***Cuylen et al., 2011***). However, several attempts failed to provide clear evidence for entrapment of small circular DNA by prokaryotic condensin. Conceivably, Smc–ScpAB does not interact with these artificial substrates in a physiological manner. To circumvent this possibility, we established an inverse assay by immobilizing whole chromosomes of *B. subtilis* in agarose plugs and monitoring their association with covalently closed rings of Smc–ScpA under harsh protein denaturing conditions (***Figure 1A***). To develop the chromosome entrapment assay we first performed experiments with the replicative sliding clamp, DnaN, in *B. subtilis*, which is known to entrap DNA in a topological manner. Furthermore, most of cellular DnaN protein is maintained in the vicinity of active replication forks in *B. subtilis*, presumably by its topological association with leading and lagging strand DNA (***Su'etsugu and Errington, 2011***).

Based on the crystal structure of *S. pneumoniae* DnaN we engineered a pair of cysteine residues (N114C, V313C) into the *B. subtilis* protein so that DnaN can be cross-linked into covalent rings in the presence of a cysteine-specific cross-linker such as BMOE (***Figure 1B***). For detection a cys-less variant of the HaloTag ('HT') was fused to the C-terminus of DnaN (***Figure 1—figure supplement 1B***) and the construct was integrated into the genome of *B. subtilis* via allelic replacement at the endogenous locus. The *dnaN-ht* genes with and without cysteine mutations supported normal growth of *B. subtilis*, implying that they encoded functional DnaN proteins (data not shown). In vivo cross-linking of DnaN-HT resulted in two additional, slow migrating bands in SDS-PAGE gels (***Figure 1C***), corresponding to single and double cross-linked species of DnaN dimers, designated as X-DnaN-HT and XX-DnaN-HT, respectively (***Figure 1—figure supplement 1A***). We next embedded cells in agarose plugs and disrupted their cell walls by lysozyme digestion. Agarose plugs were then subjected to an electric field in the presence of SDS to denature and remove any unattached proteins from chromosomes. Plugs were finally treated with benzonase to digest genomic DNA and to release any stably entrapped protein. DnaN-HT protein was then analysed by in-gel fluorescence. Non-crosslinkable DnaN-HT was efficiently depleted from agarose plugs during the entrapment assay (***Figure 1C***). In contrast, the double cross-linked, circular form of DnaN(N114C, V313C)-HT (XX-DnaN-HT) was retained in the agarose plug during electrophoresis with high efficiency (~50% of input). A minor fraction of single cross-linked DnaN dimer (X-DnaN-HT) was also observed. This is likely generated from XX-DnaN-HT by spontaneous hydrolysis of thiol-malemide adducts during protein isolation (***Kalia and Raines, 2007***; ***Baldwin and Kiick, 2013***). Importantly, the presence of benzonase during cell lysis eliminated all DnaN from the plug, indicating that circular DnaN is retained in plugs via its interaction with cellular DNA. Furthermore, in the absence of the cross-linker BMOE, no DnaN-HT was detected in the eluate fraction (***Figure 1—figure supplement 1C***). The chromosome entrapment assay thus specifically detects a topological association of intact chromosomes with DNA sliding clamps and confirms that a major fraction (at least 50%) of DnaN is loaded onto DNA in rapidly growing cells.

Prokaryotic condensin entraps chromosomal DNA

Next, we used the newly developed chromosome entrapment assay to test for an association between native chromosomes and Smc–ScpAB complexes. Cysteine pairs were introduced at the Smc–Smc and at both Smc–ScpA interfaces and a HT was fused at the C-terminus of Smc to allow in-gel fluorescence detection (***Figure 2A***) (***Bürmann et al., 2013***). Strains bearing the cysteine mutations and the

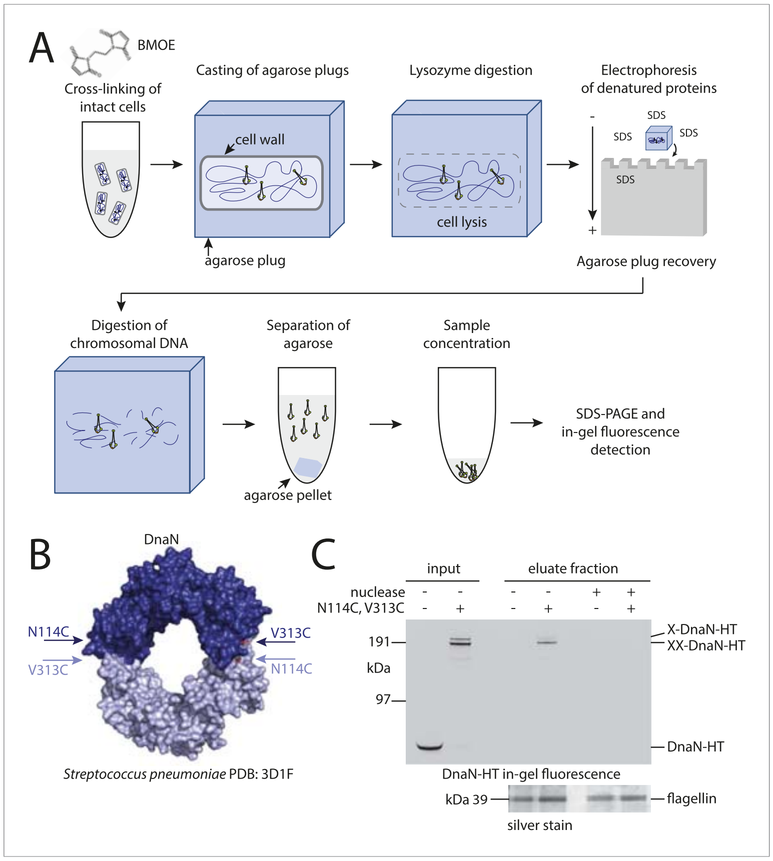
A
BMOE
Cross-linking of intact cells
Casting of agarose plugs
cell wall
agarose plug
Lysozyme digestion
cell lysis
Electrophoresis of denatured proteins
-
SDS
SDS
SDS
SDS
+
Agarose plug recovery
Digestion of chromosomal DNA
Separation of agarose
agarose pellet
Sample concentration
SDS-PAGE and in-gel fluorescence detection
B
DnaN
N114C
V313C
V313C
N114C
Streptococcus pneumoniae PDB: 3D1F
C
input
eluate fraction
nuclease - - - - + +
N114C, V313C - + - + - +
191
kDa
97
X-DnaN-HT
XX-DnaN-HT
DnaN-HT
DnaN-HT in-gel fluorescence
kDa 39
flagellin
silver stain

Figure 1. Development of the chromosome entrapment assay using DnaN. (**A**) Scheme for the chromosome entrapment assay. Cells are incubated with the cysteine cross-linker BMOE, lysed in agarose plugs and subjected to an electric field in the presence of SDS buffer. Proteins stably bound to chromosomal DNA are re-isolated from nuclease treated agarose plugs, concentrated and analyzed by SDS-PAGE. (**B**) Crystal structure of *S. pneumoniae* DnaN (PDB: 3D1F) in surface representation. The monomers of DnaN are shown in dark and light blue colours, respectively. The positions of an engineered pair of cysteine residues (N114C and V313C) at the monomer–monomer interface of *B. subtilis* DnaN are indicated by arrows. (**C**) Chromosome entrapment by DnaN. Cells of strains BSG1449 (*dnaN-HT*) and BSG1459 (*dnaN(N114C, V313C)-HT*) were cross-linked with BMOE and subjected to the chromosome entrapment assay. Input and eluate fractions were analysed by in-gel detection of fluorescently labeled HT fused to DnaN (top panel). Eluate fractions of samples treated with or without nuclease during cell lysis are indicated as nuclease '+' or '–', respectively. Eluate fractions were further analyzed by silver staining revealing that another protein was consistently co-isolated during the chromosome entrapment assay (bottom panel). This protein—identified as flagellin by mass spectrometry—was retained independently of the integrity of the chromosome. The following figure supplement is available: ***Figure 1—figure supplement 1***: DNA entrapment by DnaN.

DOI: 10.7554/eLife.06659.003

The following figure supplement is available for figure 1:

Figure supplement 1. DNA entrapment by DnaN.

DOI: 10.7554/eLife.06659.004

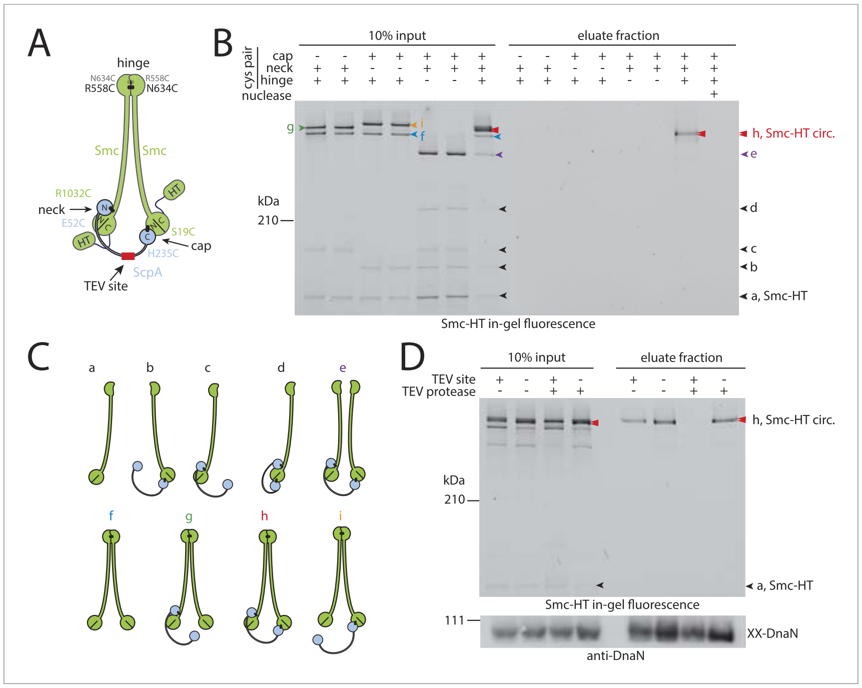

Figure 2. Prokaryotic condensin entraps the chromosome. (**A**) Scheme for the cross-linking of Smc-HaloTag ('HT') and ScpA into a covalent Smc–ScpA–Smc ring. (**B**) Chromosome entrapment of covalent Smc$_2$–ScpA rings. Cells of strains BSG1782, BSG1809-1813 and BSG1831 were cross-linked and subjected to the chromosome entrapment assay. Cross-linked Smc-HT species were visualized by in-gel fluorescence detection. The presence or absence of cysteine pairs at each of the three ring interfaces are indicated by '+' and '–', respectively. An aliquot of cells of strains BSG1782 was incubated with benzonase during cell lysis (nuclease '+'). The positions of uncross-linked Smc-HT and fully cross-linked, circular Smc–ScpA–Smc species are indicated by 'Smc-HT' and 'Smc-HT circ.'; all species are labelled by colour-coded arrowheads (see panel **C** for legend). Circular species ('h') are labeled by a double pointed arrowhead. (**C**) Schematic depiction of the structure of cross-linked Smc–ScpA species ('a'–'i'). (**D**) TEV cleavage of ScpA prevents entrapment of Smc–ScpAB in agarose plugs. In-gel fluorescence detection of Smc-HT derived from strains BSG1807 and BSG1832. The presence or absence of TEV sites in ScpA and of TEV protease during cell lysis is indicated by '+' and '–', respectively. Cleavage of ScpA(TEVs) by TEV protease creates new species of cross-linked Smc-HT (see 'input' samples) and prevents entrapment of Smc-HT in agarose plugs (see 'eluate fraction') (top panel). 'XX-DnaN' serves as internal assay control visualized by immunoblotting of cross-linked species of DnaN protein (bottom panel). The following figure supplement is available: ***Figure 2—figure supplement 1***: DNA entrapment by wild-type Smc–ScpAB (I) and ***Figure 2—figure supplement 2***: DNA entrapment by wild-type Smc–ScpAB (II).

DOI: 10.7554/eLife.06659.005

The following figure supplements are available for figure 2:

Figure supplement 1. DNA entrapment by wild-type Smc–ScpAB (I).

DOI: 10.7554/eLife.06659.006

Figure supplement 2. DNA entrapment by wild-type Smc–ScpAB (II).

DOI: 10.7554/eLife.06659.007

Smc-HaloTag fusion supported normal growth on nutrient rich medium demonstrating the functionality of the modified Smc complex (***Figure 2—figure supplement 1A***). Cells were treated with BMOE and extracts were analysed by SDS-PAGE. As internal control for the chromosome entrapment assay we employed the DnaN(N114C, V313C) protein, whose double cross-linked form was detected in input and eluate samples by immunoblotting (***Figure 2—figure supplement 1B***). Various species of Smc–ScpAB were identified in extracts of BMOE cross-linked cells by in-gel fluorescence. These correspond to fully cross-linked Smc–ScpA–Smc rings and several intermediate cross-linking species as reported previously (**Figure 2B,C**) (**Bürmann et al., 2013**). To reveal the identity of all species, strains lacking one of six engineered cysteines were used as controls that collectively form several intermediate cross-linked species but no fully cross-linked rings of Smc–ScpAB (**Figure 2—figure supplement 1C**). In these control samples little or no Smc-HT protein was retained in agarose plugs under denaturing conditions as expected for any non-circular protein (**Figure 2B**). In the presence of all pairs of cysteine, however, a set of two closely migrating species was consistently detected at significant levels after the chromosome entrapment assay (~10–20% of input material) (**Figure 2B**). We argued that the two closely migrating species might correspond to Smc–ScpAB with a single or a double cross-link at the Smc hinge. Consistent with this notion we find that only a single species of Smc_2–ScpA accumulated during the chromosome entrapment assay when a single cysteine residue (R643C) was used to cross-link the Smc hinge domains (**Figure 2—figure supplement 2A**). These findings strongly suggest that Smc–ScpAB is bound to chromosomes via entrapment of chromosomal DNA. If this were indeed the case, then its retention in agarose plugs should depend on the integrity of Smc–ScpAB rings and of chromosomal DNA. Incubation of agarose plugs with the nuclease benzonase during cell lysis eliminated the Smc-HT and DnaN signal in the sample (**Figure 2B**, **Figure 2—figure supplement 1B**). To disrupt covalent Smc–ScpAB rings, we inserted cleavage sites for TEV protease into the linker region preceding the C-terminal WHD of ScpA and incubated cells during lysozyme treatment with recombinant TEV protease to open any circular Smc_2–ScpA species. As expected, little or no Smc-HT signal was detected in agarose plugs after TEV cleavage of ScpA (**Figure 2D**). To exclude any artefacts due to the presence of the HT on Smc we have repeated the chromosome entrapment assay with an untagged allele of Smc using immunoblotting with anti-Smc antibodies for the detection of cross-linked species, which yielded very similar results (**Figure 2—figure supplement 2C**). Furthermore, we found that Smc_2-ScpA rings are stably trapped in agarose plugs over extended periods of time in constant or alternating electric fields (data not shown). Thus, our chromosome entrapment assay specifically detects the association between intact chromosomal DNA and rings of Smc–ScpAB in *B. subtilis*, demonstrating that DNA fibers pass through the Smc ring.

A full Smc ATPase cycle is required for loading of condensin onto chromosomes

Next, we established the requirements for the formation of interconnections between Smc–ScpAB rings and chromosomes. The intrinsic ATPase activity of cohesin has previously been implicated in stable association with chromosomes (**Arumugam et al., 2003**; **Weitzer et al., 2003**). More specifically, ATP hydrolysis has been hypothesized to transiently open an entry gate for DNA in the cohesin ring during its loading onto chromosomes (**Gruber et al., 2006**; **Hu et al., 2011**). To test what steps of the ATP hydrolysis cycle in Smc–ScpAB are involved in the entrapment of chromosomal DNA, we made use of *smc* alleles harboring mutations that specifically prevent ATP binding (K37I), engagement of Smc head domains (S1090R) or ATP hydrolysis (E1118Q) (**Figure 3A**) (**Hirano and Hirano, 2004**). The three mutant proteins are expressed at normal levels in *B. subtilis* being indicative of proper protein folding (**Figure 3—figure supplement 1A**). However, they do not support growth on nutrient rich medium similar to *smc* null mutants, implying that all steps of the ATPase cycle are essential for Smc functionality (**Figure 3—figure supplement 1B**) (**Gruber et al., 2014**). For the chromosome entrapment assay, these Smc ATPase mutations were combined with cysteine mutations for BMOE cross-linking. To support their viability, the resulting strains as well as the wild-type controls were grown in minimal medium. The three mutant Smc proteins assembled into normal Smc–ScpAB complexes as judged by Smc–ScpA cross-linking, albeit there is a slight decrease in the fraction of ScpA proteins bridging Smc dimers and a concomitant minor increase in ScpA subunits bound to single Smc proteins (**Figure 3—figure supplement 1C**, species 'e' and 'd', respectively) (**Bürmann et al., 2013**). Intriguingly, the ATP binding and engagement mutants abolished the fraction of covalent ring species retained in the agarose plug during the chromosome entrapment assay (**Figure 3B**). In case of the ATP hydrolysis mutant Smc(E1118Q) only minute amounts of cross-linked rings were recovered from SDS treated plugs. This small fraction of stably bound condensin conceivably arises as a consequence of residual levels of ATP hydrolysis activity in Smc(E1118Q) (**Hirano and Hirano, 2004**). Thus, ATP binding and ATP dependent Smc head engagement—and most probably also ATP hydrolysis—are essential for entrapment of chromosomal DNA by condensin

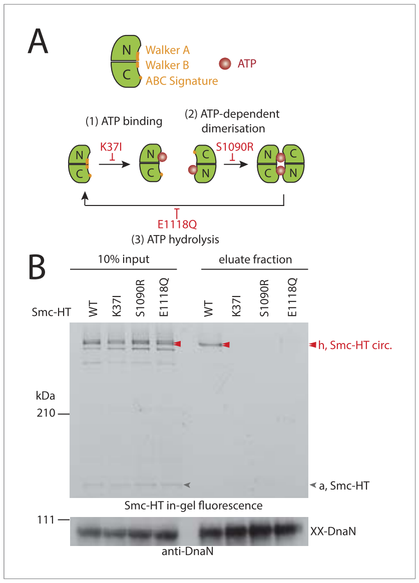

Figure 3. The Smc ATPase is required for loading of DNA into Smc–ScpAB. (**A**) A scheme for the ATP hydrolysis cycle of Smc. Schematic positions for Walker A, Walker B and ABC-signature motifs on the Smc head domain are shown (top row). ATP binding to the Walker A domain is blocked in Smc(K37I) '(1)'. ATP-dependent engagement of two Smc heads is abolished in the Smc (S1090R) mutant '(2)'. The E1118Q mutation strongly reduces ATP hydrolysis '(3)'. (**B**) Smc ATPase mutations abolish chromosomal loading of Smc–ScpAB. In-gel fluorescence detection of Smc-HT of input and eluate fractions from a representative chromosome entrapment assay performed with strains BSG1782 and BSG1784-6. Protein extracts (10% of input) were loaded next to samples subjected to the entrapment assay. Selected cross-linked species of Smc-HT are labeled (top panel). Detection of cross-linked species of DnaN by immunoblotting was used as internal assay control (bottom panel). The following figure supplement is available: ***Figure 3—figure supplement 1***: ATPase mutants of Smc–ScpAB.

DOI: 10.7554/eLife.06659.008

The following figure supplement is available for figure 3:

Figure supplement 1. ATPase mutants of Smc-ScpAB.

DOI: 10.7554/eLife.06659.009

in bacteria, as has been supposed for cohesin in yeast. Furthermore, the strict requirement of several steps of the ATPase cycle strongly suggests that entrapment of DNA corresponds to the physiological form of association with the bacterial chromosome.

ScpB and ParB proteins are essential for normal loading of condensin onto chromosomes

What other factors might be required for the loading of condensin onto DNA? The ScpB subunit forms homodimers that bind in an asymmetric manner to the central region of a single ScpA monomer. It thus is in close proximity of the Smc ATPase domains. Together with ScpA it putatively plays a role in the regulation of the Smc ATPase activity (***Kamada et al., 2013***). Its precise molecular function, however, is not clear yet. To test whether ScpB is involved in the association of Smc–ScpA rings with chromosomes we combined the cysteine mutations in Smc and ScpA with an *scpB* in-frame deletion (***Figure 4—figure supplement 1***). Ring formation was only mildly affected by the absence of ScpB as judged by BMOE cross-linking and in-gel fluorescence detection (***Figure 4A***) (***Bürmann et al., 2013***). However, Smc complexes lacking ScpB subunits failed to entrap chromosomes altogether demonstrating that ScpB is absolutely required for loading of prokaryotic condensin onto chromosomal DNA.

ParB proteins—bound to *parS* sites—are crucial for efficient targeting of Smc–ScpAB to a large region of the chromosome near the replication origin (***Gruber and Errington, 2009***; ***Sullivan et al., 2009***; ***Minnen et al., 2011***). ParB might act by simply increasing the local concentration of Smc–ScpAB around *oriC* either before or after its loading onto the chromosome. Alternatively, ParB bound to *parS* sites might be more directly involved in the loading reaction itself, for example, as catalytic factor, and its absence might thus affect levels of chromosomal condensin. To test this, we performed the chromosome entrapment assay with cells lacking the *parB* gene. Intriguingly, the levels of Smc–ScpAB entrapping chromosomal DNA were strongly reduced in the *parB* null mutant as judged by the limited retention of Smc–ScpA species in agarose plugs (***Figure 4B***). Thus, ParB protein likely promotes the entrapment of chromosomal DNA by Smc–ScpAB. This strongly suggests that most condensin is loaded onto the chromosome at *parS* sites, where ParB protein is bound. In all other parts of the chromosome entrapment of DNA fibers by Smc–ScpAB might be very inefficient. The cysteine bearing *smc* allele causes growth defects when combined with *ΔparB* (***Figure 4—figure supplement 1***). Therefore, we cannot formally exclude the possibility that the decreased loading of Smc observed in *ΔparB* are due to the cysteine

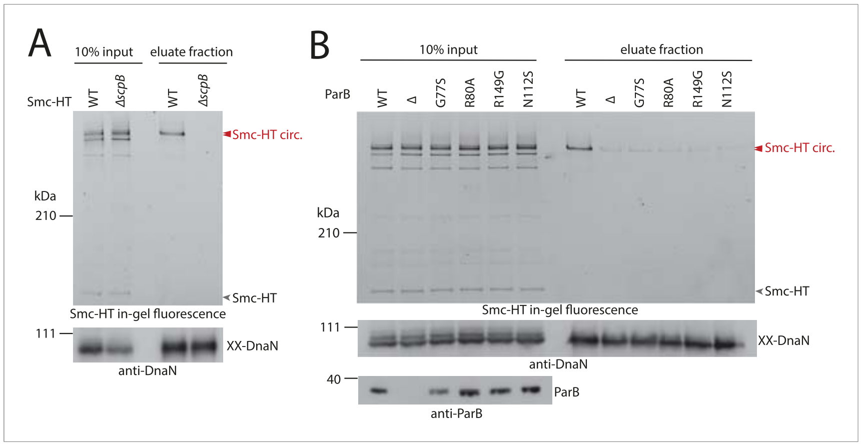

Figure 4. ScpB and ParB are essential for efficient DNA entrapment by Smc complexes. (**A**) Deletion of *scpB* eliminates loading of chromosomal DNA into Smc complexes. In-gel fluorescence detection of Smc-HT in input and eluate fractions is shown from chromosome entrapment assays performed with strains BSG1782 ('WT') and BSG1850 ('Δ*scpB*') (top panel). DnaN was used as internal control (bottom panel). (**B**) Several *parB* mutations interfere with efficient chromosomal loading of Smc–ScpAB. Input and eluate fractions from chromosome entrapment assays with strains BSG1782, BSG1783 and BSG1960-3 were analysed by in-gel fluorescence detection of Smc-HT (top panel). DnaN was used as internal control (middle panel). Immunoblotting using polyclonal rabbit anti-ParB antiserum confirms near-normal expression of mutant ParB proteins (bottom panel). The following figure supplement is available: ***Figure 4—figure supplement 1***: Growth of *smc*, *parB* double mutants.

DOI: 10.7554/eLife.06659.010

The following figure supplement is available for figure 4:

Figure supplement 1. Growth of *smc(Cys)* mutants.

DOI: 10.7554/eLife.06659.011

modifications in Smc and that chromosomal loading of wild-type Smc is not or much less affected by *parB* deletion.

Previously, two *parB* point mutations (N112S and R149G), which prevent the formation of Smc-GFP foci, have been isolated in *B. subtilis* (***Gruber and Errington, 2009***). We found that these mutations strongly impair loading of Smc onto the chromosome in the entrapment assay similar to Δ*parB* (***Figure 4B***). The R149G mutation is positioned on the helix-turn-helix motif of ParB and might thus directly affect binding to *parS* sites (***Leonard et al., 2004***). The N112S mutation, however, is located in another highly conserved region, which has been implicated in the 'spreading' of ParB protein from *parS* sequences into adjacent DNA (***Leonard et al., 2004***; ***Graham et al., 2014***). The spreading of ParB along several kb of DNA is a feature conserved in plasmid and chromosome derived ParB proteins, however, the underlying mechanism is only poorly understood (***Rodionov et al., 1999***). It might possibly involve the formation of a large nucleoprotein complex (***Broedersz et al., 2014***). Several other mutants of ParB (including *B. subtilis* ParB G77S and R80A) have been reported to be defective in spreading from *parS* sites (***Breier and Grossman, 2007***; ***Graham et al., 2014***). Intriguingly, also these mutations resulted in largely reduced levels of Smc on the chromosome in our entrapment assay, being comparable to the levels found in a *parB* deletion mutant (***Figure 4B***). This implies that ParB spreading from *parS* sites or formation of large nucleoprotein complexes might be essential for loading of DNA into the Smc ring by ParB. These findings are consistent with the observation that formation of Smc-GFP foci near the origin of replication are affected by the G77S mutation (***Sullivan et al., 2009***). In summary, these results demonstrate that several factors—including ScpB protein, a ParB/*parS* nucleoprotein complex and the Smc ATPase cycle—are required to promote efficient loading of condensin rings onto the chromosome.

Smc–ScpAB rings physically associate with chromosomal DNA fragments

Smc proteins and fragments thereof exhibit affinity for single- and double-stranded DNA in vitro (***Chiu et al., 2004***; ***Hirano and Hirano, 2006***; ***Soh et al., 2015***). The physical contacts with DNA might occur once condensin has been successfully loaded onto chromosomes and thus be a permanent feature of chromosomal Smc–ScpAB. Alternatively, the direct association with DNA might be restricted to certain intermediates in the chromosomal loading reaction. To test for interactions between Smc–ScpAB and specific chromosomal DNA fragments, we have affinity-purified endogenous Smc–ScpAB from *B. subtilis* cell lysates using a short Avitag peptide fused to the C-terminus of the Smc protein, which gets biotinylated when the biotin ligase gene *birA* is co-expressed ('Smc-Avitag'). We then examined fractions for the co-purification of fragments of chromosomal DNA—generated by restriction digest with XbaI—using quantitative PCR with primer pairs specific for different parts of the chromosome. Since we worried that Smc–ScpAB might not be sufficiently stable in diluted cell extracts, we cross-linked the three ring interfaces in Smc–ScpAB using BMOE cross-linking of engineered pairs of cysteines. A small fraction of chromosomal DNA was reproducibly co-purified with wild-type Smc-Avitag, whereas the yield of co-purified DNA was significantly improved by the presence of cross-linkable cysteine residues in Smc–ScpAB (***Figure 5***). In both cases origin-proximal regions (*yyaD*, *parS-359*, *dnaA* and *dnaN*) of the chromosome were more efficiently enriched than distal regions (*amyE*, *trnS* and *ter*) by the co-purification with Smc implying that the observed Smc-DNA contacts are dependent on chromosomal loading of Smc–ScpAB by ParB protein at *parS* sites and are thus physiologically relevant (***Figure 5***, ***Figure 5—figure supplement 1***) (***Gruber and Errington, 2009***). The association of DNA with wild-type and BMOE cross-linked Smc–ScpAB was highly sensitive to washes with a salt solution (2M NaCl), suggesting that it was dependent on electrostatic contacts between DNA and protein. These DNA contacts are presumably formed by the Smc–ScpAB complex itself. Alternatively, albeit less likely, other chromosomal proteins physically bound to DNA could prevent the release of condensin from DNA by blocking its sliding towards DNA ends.

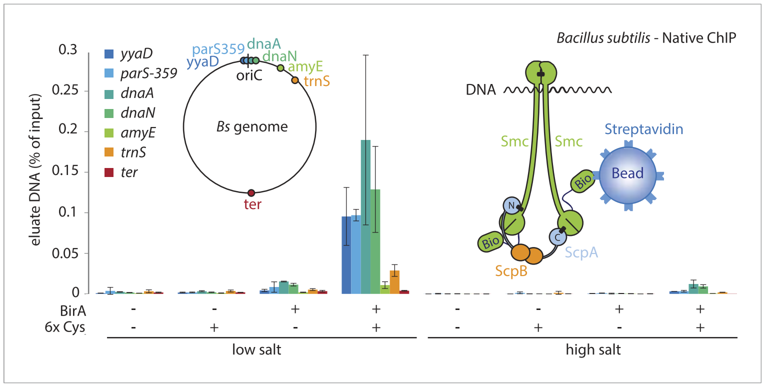

Figure 5. A physical interaction of Smc–ScpAB rings and chromosomal DNA. Co-purification of chromosomal DNA fragments with native Smc–ScpAB. Cells of strains BSG1104-5 and BSG1107-8 were treated with the cross-linker BMOE prior to cell lysis. Strains carrying ('+') or lacking ('−') cysteine mutations ('6xCys') in the Smc-AviTag construct were expressed in presence ('+') or absence ('−') of the biotin ligase ('BirA'). Beads were washed in the presence of either a 150 mM ammonium acetate buffer ('low salt') or a 2 M sodium chloride buffer ('high salt'). The co-purification of DNA fragments with Smc-biotin on streptavidin beads was measured by quantitative PCR using primer pairs specific for genomic positions indicated on a representation of the circular *B. subtilis* genome. Mean values and standard deviations were calculated from two independent biological replicates. The following figure supplement is available: ***Figure 5—figure supplement 1***: Chromatin immuno-precipitation of Smc.

DOI: 10.7554/eLife.06659.012

The following figure supplement is available for figure 5:

Figure supplement 1. Chromatin immuno-precipitation of Smc.

DOI: 10.7554/eLife.06659.013

Discussion

The agarose entrapment assay

In many cases, it is challenging to measure the activity and outcome of biochemical processes in the living cell. Here, we report the establishment of a straight-forward method to determine the physical association of ring-shaped protein complexes with whole bacterial chromosomes. Two examples, the SMC condensin complex and the sliding clamp DnaN, document the significant potential of our simple entrapment approach. In principle, similar assays should also be possible with eukaryotic cells and for many other chromosomal proteins such as for example hexameric helicases and certain transcription factors. Furthermore, analogous procedures might be useful to address biological questions related to other denaturation-resistant cellular structures such as cell wall polymers (e.g., made up of peptidoglycan, chitin or cellulose).

DNA entrapment by an ancestral SMC–kleisin complex

SMC–kleisin complexes are major governors of chromosome superstructure in most branches of the phylogenetic tree. The eukaryotic variants cohesin and condensin have been suggested to work as concatenases, which hold selected stretches of DNA together by simple embracement in their ring (***Haering et al., 2008***; ***Cuylen et al., 2011***). Whether DNA entrapment is an ancestral and thus fundamentally conserved function of SMC–kleisin complexes, however, remained elusive so far. Furthermore, interaction studies developed for cohesin and condensin are based on small, artificial DNA substrates and might thus not necessarily reflect the mode of binding to native chromosomes. These assays also fall short of providing an estimate for the fraction of SMC complexes involved in interlocked associations with DNA and thus leave open the possibility that DNA entrapment might be an insignificant side reaction. Finally, it has not been tested under physiological conditions, whether the ATPase cycle is required for proper loading of DNA into any SMC–kleisin complex. To provide answers to these questions, we have established the chromosome entrapment assay to determine the association of prokaryotic condensin with native chromosomes. Our results clearly demonstrate that chromosomal DNA is loaded into condensin complexes in *B. subtilis*—in a manner that depends on the non-SMC subunit ScpB and at least one full cycle of Smc ATPase activity. The chromosome entrapment assay recovers about 10–20% of the fully cross-linked input material. This number probably understates the real proportion of chromosomally entrapped Smc complexes due to the loss of material during protein re-isolation from agarose plugs, due to possible adverse effects of cysteine mutations on Smc–ScpAB loading and because cysteine-maleimide linkages are vulnerable to hydrolytic reversal during and after the entrapment assay (***Kalia and Raines, 2007***; ***Baldwin and Kiick, 2013***). Interestingly, a recent single-molecule tracking study in *B. subtilis* revealed two major populations of Smc: 80% of Smc-YFP proteins are displaying highly dynamic behavior on the nucleoid, whereas the other 20% (and most ScpA-YFP protein) are immobile and constrained within a small volume of the cell (***Kleine Borgmann et al., 2013***). This immobile fraction possibly represents Smc–ScpAB complexes embracing origin proximal DNA after loading at *parS* sites as observed in the entrapment assay.

Our results show that embracement of chromosomal DNA is a predominant feature of Smc–ScpAB, which has been evolutionarily retained in cohesin and likely all other SMC–kleisin complexes as well. Since the chromosome entrapment assay is based on the immobilization of intact replicating chromosomes, which possibly represent internally knotted and branched DNA structures, it is conceivable that Smc–ScpAB rings are linked to chromosomal DNA by non-topological capture of DNA loops, which themselves might be interlinked (i.e., knotted) with other parts of the chromosome. Therefore, it remains to be determined whether DNA entrapment by Smc–ScpAB is of topological (***Figure 6A***) and/or non-topological (***Figure 6B***) nature.

How might entrapment of DNA at ParB/*parS* nucleoprotein complexes promote sister DNA segregation?

Smc–ScpAB plays a crucial role in the segregation of replication origins in *B. subtilis* cells (***Gruber, 2014***; ***Wang et al., 2014***), presumably by organizing nascent sister chromosomes so that their spatial overlap and entanglement is minimized. It is tempting to speculate that ParB/*parS* not only enriches Smc in the vicinity of the replication origin but also sets up lengthwise compaction of chromosomes by

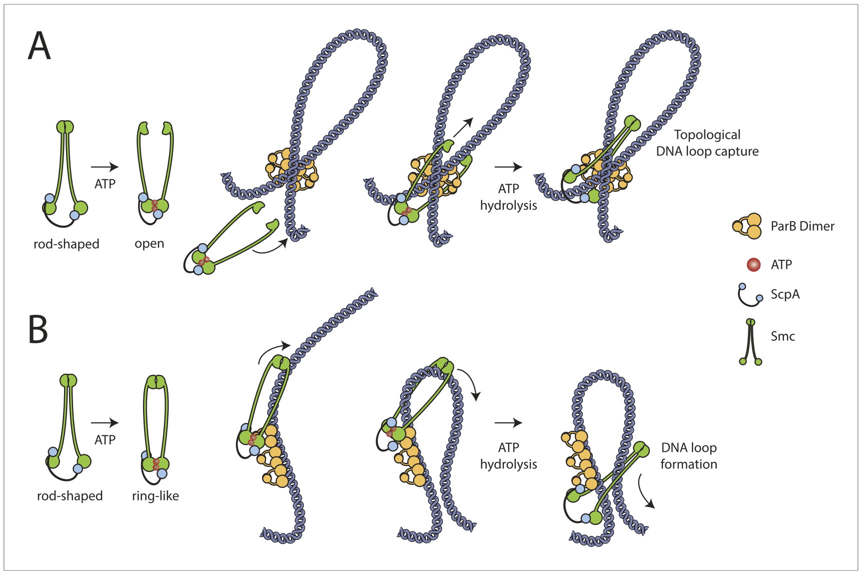

Figure 6. Models for entrapment of chromosomal DNA by Smc–ScpAB. (**A**) Loop capture model. DNA loops might be pre-formed within ParB/*parS* nucleoprotein assemblies. Driven by ATP dependent engagement of Smc head domains Smc–ScpAB adopts a ring-like configuration. Occasional opening of the Smc hinge then allows capture of ParB-DNA loops within Smc–ScpAB. Subsequent ATP hydrolysis by Smc locks the hinge in a closed state and stabilizes the structure. (**B**) Loop formation model. ParB/*parS* might serve as a landing platform for Smc–ScpAB allowing Smc–ScpAB in its ring-like conformation to guide DNA into its central cavity. Continuous extrusion of DNA through Smc–ScpAB then drives lengthwise condensation of chromosomes. Ring opening is not required in this model and DNA entrapment by Smc–ScpAB is thus strictly non-topological here. The following figure supplement is available: ***Figure 6—figure supplement 1***: Quantitative Blotting of Smc protein and *parB* DNA.

DOI: 10.7554/eLife.06659.014

The following figure supplement is available for figure 6:

Figure supplement 1. Quantitative Blotting of Smc protein and *parB* DNA.

DOI: 10.7554/eLife.06659.015

presenting DNA of a certain topology to the Smc–ScpAB complex. Consistent with this notion, we found that several *parB* mutants, which are defective in the ability to form large nucleoprotein complexes and to spread from *parS* sites, fail to promote loading of Smc–ScpAB onto the chromosome. Thus, Smc–ScpAB might capture, stabilize and expand structures–such as DNA loops or coils–that are pre-formed within larger ParB/*parS* nucleoprotein assemblies (***Figure 6A***). Alternatively, ParB/*parS* might serve as an elaborate landing platform on the chromosome, where Smc–ScpAB initiates with the help of ParB the lengthwise compaction of chromosomes by forming and extruding loops of DNA (***Figure 6B***). Extrusion of DNA might involve the translocation of Smc–ScpAB along DNA fibers made up of naked or ParB coated DNA. These models are not mutually exclusive. A reasonable first step towards understanding the architecture of Smc/ParB/*parS* assemblies might be the investigation of physical interactions between ParB/*parS* and Smc–ScpAB and their functional interconnection with the Smc ATPase cycle. In the future, Smc/ParB/*parS* structures could serve as a relatively simple paradigm for chromosome organization by the more intricately regulated cohesin and condensin complexes in eukaryotes.

The role of ScpB and ATP hydrolysis in Smc–ScpAB loading

ParB serves a supplemental—albeit important—role in the Smc loading process. In contrast, Smc functionality and its loading onto DNA in vivo is critically dependent on the ScpB subunit and the

ATPase cycle. It remains unclear though what the exact role of ScpB and ATP hydrolysis in the entrapment of DNA might be. If loading indeed depends on transient opening of a DNA entry gate, the open state would likely represent an energetically unfavorable reaction intermediate (**Figure 6A**). Timely opening would require energy input as well as tight regulation. We have recently demonstrated that the ATP dependent engagement of Smc head domains—together with DNA binding to the Smc hinge domain—can transform the configuration of the Smc coiled coil from a rod to a more open ring-like conformation (***Soh et al., 2015***). Hydrolysis of ATP and/or ScpB binding could drive a subsequent conformational change that might open the SMC–kleisin ring (**Figure 6A**). Alternatively, ScpB and/or ATP hydrolysis might stabilize Smc–ScpAB once loaded onto DNA or promote Smc's sliding along DNA to allow efficient extrusion of DNA loops by the Smc–ScpAB ring (**Figure 6B**).

How do so few Smcs organize so much DNA?

Deletion or mutation of the *parB* gene results in a clear drop in the levels of chromosomally bound condensin (~5–10 fold less) in our chromosome entrapment assay (**Figure 4B**, ***Figure 2—figure supplement 2C***). In addition to this loading defect, also the specific recruitment of Smc–ScpAB towards the replication origin is lost in the absence of ParB (***Gruber and Errington, 2009***; ***Sullivan et al., 2009***). Thus, in *parB* mutants only a very small proportion of cellular Smc–ScpAB is bound to chromosomes within the replication origin region, where it presumably performs its essential function by promoting the separation of nascent sister chromosomes (***Gruber et al., 2014***; ***Wang et al., 2014***). Nevertheless, defects in chromosome segregation are rather mild in *parB* mutants when compared to mutants of *smc*. Using quantitative blotting of Smc protein and replication origin DNA from cell extracts, we have estimated the average number of Smc protein to be around 30 dimers per replication origin in a fast growing population of cells (***Figure 6—figure supplement 1***). Assuming that all Smc complexes entrap chromosomal DNA in wild-type cells, only three to six Smc dimers (10–20% of total) are loaded onto the chromosome in *parB* mutants according to our measurements. Thus, a handful of Smc–ScpAB complexes, which are presumably randomly distributed over the chromosome, appears to be capable of supporting near-normal chromosome segregation under these conditions—when chromosome segregation is already compromised by the loss of the *parABS* system. Few Smc–ScpAB therefore seem to be able to provide enough organization to the replication origin region and the remainder of the chromosome to prevent lethal accumulation of inter-linked sister chromosomes. It is conceivable that individual Smc–ScpAB complexes are able to organize large chunks of a bacterial chromosome, possible by forming giant loops of DNA. Alternatively, Smc activity might be needed only at a limited number of defined locations on the *B. subtilis* chromosome and/or for very short periods of time. However, when levels of functional Smc dimers are in addition reduced for example by hypomorphic mutations in the *smc* gene itself, the loss of ParB protein becomes lethal (***Gruber and Errington, 2009***).

This work reveals the mode of association of Smc–ScpAB with bacterial chromosomes, highlights its striking evolutionary conservation and demonstrates the involvement of the SMC ATPase cycle in chromosomal loading. Future work must address the underlying biochemical mechanisms to get basic insight into the architectural role of SMC in chromosome biology.

Materials and methods

B. subtilis strains and media

Genetic modifications at *smc*, *scpAB*, *parB* and *dnaN* loci were generated via double cross-over recombination in strains derived from *B. subtilis* 1A700 or *B. subtilis* 168ED. Genotypes of strains used in this study are listed in ***Supplementary file 1***. Cells were transformed with plasmids or *B. subtilis* genomic DNA using a 2-step starvation protocol as previously described (***Hamoen et al., 2002***; ***Bürmann et al., 2013***). Transformants were selected by growth on nutrient agar (NA) plates (Oxoid, UK) supplemented with antibiotics as required: 5 μg ml^{-1} kanamycin, 80 μg ml^{-1} spectinomycin, 10 μg ml^{-1} tetracycline, 5 μg ml^{-1} chloramphenicol, 1 μg ml^{-1} erythromycin and 25 μg ml^{-1} lincomycin. Strains displaying a condensin null phenotype were selected on SMG medium instead: SMM salt solution (2 g l^{-1} ammonium sulphate, 14 g l^{-1} dipotassium hydrogen phosphate, 6 g l^{-1} potassium dihydrogen phosphate, 1 g l^{-1} trisodium citrate, 0.2 g l^{-1} magnesium sulphate, 6 g l^{-1} potassium hydrogen phosphate) supplemented with 5 g l^{-1} glucose, 20 mg l^{-1} tryptophan and 1 g l^{-1} glutamate with the respective antibiotics. Strains were single-colony purified and grown in the absence of antibiotics for experiments.

Colony formation assay

Cells were pre-grown in a 96-well plate in SMG medium for 24 hr at 37˚C. Overnight cultures were diluted 9^2-fold (high density spots) or 9^5-fold (low density spots) and spotted onto NA or SMG agar plates. Plates were incubated at 37˚C for 12 hr on NA or 24 hr on SMG agar.

Growth conditions and in vivo cysteine cross-linking

Cells were grown in either LB Miller medium (10 g l^{-1} tryptone, 5 g l^{-1} yeast extract, 10 g l^{-1} sodium chloride) or SMG medium to mid-exponential phase at 37˚C (in LB Miller medium, OD_{600} of 0.4; in SMG medium, OD_{600} of 0.03). Cells were harvested by centrifugation or vacuum filtration and washed in ice-cold PBS supplemented with 0.1% glycerol ('PBSG'). Cell aliquots (corresponding to 1 ml at an OD_{600} of 1.25) were re-suspended in PBSG and incubated with the cross-linker BMOE (bis-maleimidoethane, Applichem, Germany) at a concentration of 1 mM (diluted from a 20 mM stock solution in DMSO). After a 10 min incubation on ice the reaction was quenched by addition of 2-mercaptoethanol ('2-ME') to a final concentration of 28 mM.

For the preparation of protein extracts ('input') a mixture of following components was added to an aliquot of cells: 400 units ready-lyse lysozyme (Epicentre, Madison, WI), 12.5 units benzonase (Sigma-Aldrich, St. Louis, MO) and a protease-inhibitor cocktail (Sigma). In addition, 1 μM HT Oregon Green substrate (Promega, Madison, WI) was added to cell suspensions with HaloTag bearing alleles. Samples were then incubated for 20 min at 37˚C protected from light. Finally, the samples were heated to 70˚C for 5 min in LDS Sample Buffer (NuPage, Thermo Scientific, Waltham, MA) containing 200 mM DTT and loaded onto a SDS-PAGE gel (see below). Gels with Oregon Green labeled samples were scanned on a Typhoon scanner (GE Healthcare, UK) with Cy3-DIGE filter setup.

Chromosome entrapment assay

Cells were grown, cross-linked and quenched as described above. Lysozyme stock solution, protease inhibitor and HT substrate were added to an aliquot of cells at concentrations given above. The cell suspension was mixed immediately in a 1:1 ratio with a 2% solution of Megabase agarose (BioRad, Hercules, CA) or low-melt agarose (BioRad) and casted into 100 μl agarose plugs using plug molds (BioRad). Agarose plugs were incubated for 20 min at 37˚C, protected from light, and then loaded into the wells of a 6% SDS-PAGE Tris-glycine gel. The polyacrylamide mini-gel was run for 60 min at 25 mA protected from light. Agarose plugs were then re-extracted from the gel and transferred into 1.5 ml Eppendorf tubes. 1 ml of Wash Buffer ('WB': 0.01 mM EDTA, 0.5 mM Tris, 0.5 mM $MgCl_2$, 0.01% SDS) was added per agarose plug. Plugs were incubated for 10 min with gentle agitation protected from light. This step was repeated once. Wash buffer was then discarded and replaced by 100 μl fresh WB supplemented with 50 units of benzonase (Sigma). Plugs were incubated at 37˚C for 30 min. Plugs were melted at 85˚C for 2 min under vigorous agitation. The samples were frozen at −80˚C and stored overnight. Samples were then thawed, centrifuged for 10 min at 4˚C and 14,000×*g* and transferred to a 0.45 μm Cellulose acetate spin column (Costar, Tewksbury, MA) and spun for 1 min at 10,000×*g*. The flow-through was concentrated in a Speed Vac (Thermo Scientific, no heating, 2.5 hr running time). The concentrated sample was resuspended in LDS Sample Buffer (NuPage) containing 200 mM DTT and heated for 3 min at 70˚C. Samples were loaded onto Tris-acetate gels (3–8% Novex, Thermo Scientific) and run for 2.5 hr at 35 mA per gel at 4˚C. For DnaN detection Bis-Tris gels (8–12% Novex) were run for 1 hr at 200 V at room temperature. Gels were either scanned on a Typhoon scanner (FLA 9000, GE Healthcare) with Cy3-DIGE filter setup or immuno-blotted using antibodies against DnaN or Smc (see below). For cleavage of ScpA(TEVs) or degradation of chromosomal DNA 15 units of His-TEV protease or 12.5 units of benzonase, respectively, was added before casting agarose plugs.

Co-purification of chromosomal DNA fragments with Smc-AviTag protein

B. subtilis strains containing *smc-tev-avitag* alleles were grown to OD_{600} of 0.4 in 100 ml LB Miller at 37˚C. Part of the culture was fixed with formaldehyde and subjected to chromatin immunoprecipitation (ChIP) as described by (***Gruber and Errington, 2009***) using a rabbit anti-Smc antiserum. In parallel, 10 ml of the culture were mixed with ice, harvested by centrifugation and washed in cold

PBSG. Cells were resuspended in 200 µl PBSG and treated with 0.5 mM BMOE for 10 min on ice. The reaction was quenched with 14 mM 2-ME and cells were washed once in CutSmart buffer (New England Biolabs, Ipswich, MA). Cells were resuspended in 200 µl CutSmart containing 10 kU Ready-Lyse lysozyme (Epicentre), 40 U XbaI (New England Biolabs) and a protease inhibitor cocktail (Sigma). The suspension was incubated for 15 min at 37˚C before addition of 1800 µl buffer LS (10 mM Tris/HCl, 150 mM NH_4OAc, 1 mM EDTA, 6 mM 2-ME, 0.05% Tween-20, 0.01% NaN_3, final pH 7.9 at 23˚C). Lysates were centrifuged for 5 min at 20,000×*g*. Subsequently, 1400 µl of the extract were incubated with 100 µl Dynabeads Streptavidin C1 for 30 min at room temperature. Beads were washed once in buffer LS, then split, resuspended either in buffer LS or in buffer HS (10 mM Tris/HCl, 2 M NaCl, 1 mM EDTA, 6 mM 2-ME, 0.05% Tween-20, 0.01% NaN_3, final pH 7.9 at 23˚C) and incubated for 15 min at room temperature. Beads were washed twice with buffer LS, and protein/DNA complexes were eluted for 1 hr at 22˚C by incubation with 350 µl LS containing TEV protease and 1 mM DTT. DNA from input and eluate fractions was purified by treatment with 0.5 mg/ml Proteinase K for 1 hr at 55˚C followed by phenol/chloroform extraction. Samples were analysed by quantitative PCR using the second derivative maximum of a four parameter logistic model similar to the method described by (**Zhao and Fernald, 2005**).

Immunoblotting and antibodies

After gels were scanned for in-gel fluorescence detection, they were immediately transferred onto a PVDF membrane (Immobilon-P, Merck Millipore, Germany) using semi-dry transfer. Membranes were blocked with 3.5% (wt/vol) milk powder in PBS with 0.1% Tween 20. Rabbit polyclonal sera against *B. subtilis* DnaN (**Lenhart et al., 2013**), *B. subtilis* Smc (this paper) and *B. subtilis* ParB (this paper) were used as primary antibodies for immunoblotting at dilutions of 1:5000 each. The membrane was developed with HRP-coupled secondary antibodies and chemiluminescence (Super-Signal West Femto, Thermo Scientific) and visualized on a LAS-3000 scanner (FujiFilm, Germany).

DnaN cross-linking time-course

To estimate DnaN cross-linking kinetics (**Figure 1—figure supplement 1A**) samples were grown as described above. An aliquot of cells was incubated with the cross-linker BMOE (1 mM) for the indicated length of time before the reaction was quenched with 2-ME (28 mM).

Estimation of cellular Smc Protein and *parS-359* DNA

Protein purification and quantification

The expression plasmid for unmodified wild-type Smc was a gift from Mark Dillingham (Uni. of Bristol, UK). Wild-type Smc protein was expressed and purified as described in (**Fuentes-Perez et al., 2012**) with an additional Superose 6 10/300 GL (GE Healthcare) gel filtration added as a final step in the purification. Gel filtration was performed in storage buffer 50 mM Tris–HCl at pH 7.5, 150 mM NaCl, and 1 mM DTT. The concentration of purified untagged Smc protein was determined by measuring the absorption of the protein at 280 nm in 6 M guanidine chloride (**Grimsley and Pace, 2004**). An extinction coefficient (51,230 M^{-1} cm^{-1} at 280 nm) for the *B. subtilis* Smc protein was obtained using the ProtParam tool at www.expasy.org.

Spike-in PCR product and Southern probe

The spike-in DNA was generated by PCR using wild-type genomic DNA preparation as template DNA and forward ('STG246': cttgcgatttttgcttctcc; complementary to the *yyaD* locus) and reverse primers ('STH602': ttatcgtgcgaaagcagttg; complementary to the *gidA* locus) producing a DNA fragment of 7238 bp in size covering the *parS-359* site within the *parB* gene. The PCR product was purified using a PCR-purification kit (QIAquick PCR purification kit, Qiagen, Germany) and its concentration was measured by absorption at 260 nm on a Nanodrop 2000c (Thermo Scientific) photometer. The molecular weight was calculated based on the base composition of the DNA. For generation of the *parS-359*-specific Southern probe a PCR with primers annealing within and downstream of the *parB* locus ('STG301': acatgagaattcgtttttcatttatgattctcgttcagacaaaagctc and 'STK534': gcaatctgcagcatggcattcttcag) was performed on a wild-type genomic DNA preparation generating a 714 bp long PCR product. This PCR DNA was used as a template for a second PCR for random incorporation of digoxigenin ('DIG') labelled nucleotides following the 'random PCR DIG labelling protocol' (Roche, Germany).

Cell culture and harvesting

Wild-type *B. subtilis* strain BSG1001 and the doubly modified strain BSG2058 were grown in LB Miller medium (10 g l^{-1} tryptone, 5 g l^{-1} yeast extract, 10 g l^{-1} sodium chloride) to mid exponential phase at 37˚C (OD_{600} of 0.3). Cells were harvested by centrifugation and washed in ice-cold PBS supplemented with 0.1% glycerol ('PBSG').

Protein extracts for quantitative Western blotting

Protein extracts were prepared from 1 ml of a cell suspension at OD_{600} of 2. Cells of BSG1001 and BSG2058 were pelleted and resuspended in 50 µl PBSG and mixed in the appropriate ratios. Cells were lysed by addition of a mix of following enzymes: 400 units ready-lyse lysozyme (Epicentre), 12.5 units benzonase (Sigma) and a protease-inhibitor cocktail (Sigma) in a total volume of 5 µl. After 30 min incubation at 37˚C the purified Smc protein was spiked into the whole cell lysates in a total volume of 10 µl as given in ***Figure 6—figure supplement 1B***. Finally, the samples were heated to 70˚C for 5 min in LDS Sample Buffer (NuPage) containing 100 mM DTT. 1/20 of the final protein extracts were loaded onto a SDS-PAGE gel. For immunoblotting and antibodies see 'Materials and methods'.

Genomic DNA preparation for quantitative Southern blotting

Bacterial cell cultures were identical to the ones used for Quantitative Western blotting. Aliquots of BSG1001 and BSG2058 were taken (equivalent to 1 ml of culture at OD_{600} of 4) and resuspended in 95 µl 50 mM EDTA pH 8.0. 5 µl lysozyme was added to a final concentration of 0.5 mg/ml and samples were incubated for 30 min at 37˚C. 500 µl of a commercially available Lysis Buffer ('Nuclei Lysis Solution', Wizard Genomic DNA Purification Kit, Promega) was added, followed by 5 min incubation at 80˚C. Samples were incubated with a final concentration of 0.05 mg/ml RNAse A for 10 min at 37˚C. Then each sample was sonicated very gently (4× 0.1 s pulses at lowest power setting, Bandelin 'Sonoplus', Germany) to solubilize chromosome fragments. Cell lysates of BSG1001 and BSG2058 were mixed and purified PCR product was spiked in as given in the figure. 200 µl of 'Protein Precipitation Solution' (Wizard Genomic DNA Purification Kit, Promega) was added to each sample followed by a 10 s vortexing step and 5 min incubation on ice. Samples were spun 3 min at 13,000×*g* and supernatant was transferred into a fresh 1.5 ml tube containing 600 µl 100% isopropanol. The tubes were inverted 20 s until the DNA precipitated and DNA was pelleted by centrifugation for 2 min at 13,000×*g*. Pellets were washed with 70% ethanol and finally resuspended in 41 µl 10 mM Tris-Cl pH 8.5. Restriction digest was performed using 80 units PstI enzyme (NEB) per reaction for 1 hr at 37˚C and the enzyme was inactivated for 20 min at 80˚C. 1/3 of each preparation (equivalent to 1 ml OD_{600} of 1.3) was loaded onto a 0.6% Megabase agarose (BioRad) gel containing 1 µg/ml Ethidiumbromide (Sigma) in 44.5 mM Tris, 44.5 mM Boric acid, 1 mM EDTA ('0.5× TBE Buffer'). Gel was run 16 hr at 1V/cm. Transfer for Southern Blotting was performed using an alkaline buffer (1.5 M NaCl, 0.4 N NaOH) for 24 hr onto a nylon membrane ('Hybond-N', GE Healthcare Life Sciences). Hybridisation was done using the digoxigenin-labelled Southern probe (see above) specific to the *parS359* locus in a commercial hydridisation buffer ('DIG Easy Hyb Granules', Roche) for 4 hr at 42˚C. Stringency washes, blocking and detection was performed following the 'CDP-Star' Manual (Roche, Cat.No. 12 041 677 001).

Data quantification and calculation

The intensity of the individual wt Smc and wt *parS-359* bands from the Western and Southern blots, respectively, were quantified using ImageJ 1.48v software and values were plotted against the calculated concentrations of Smc protein and *parS-359* PCR DNA in each sample. The concentration of Smc protein and *parS-359* DNA in wild-type extracts was determined from the intensity of the Smc/*parS-359* band using a linear fit of the standard curve.

Acknowledgements

We are very grateful to Lyle Simmons for providing *B. subtilis dnaN-gfp* strains and α-DnaN antiserum and to Mark Dillingham for sharing expression plasmids and purification protocols for untagged Smc protein. We thank Boris Pfander and Stefan Jentsch for sharing resources, Anna Reisenbichler for technical help and all members of the Gruber laboratory for stimulating discussions and helpful comments on the manuscript. This work was supported by an ERC Starting Grant (DiseNtAngle, #260853) to SG and by the Max Planck Society and by the National Research Foundation of Korea (NRF) grant funded by the Korea government (#2014-022694) to B-HO.

Additional information

Funding

Funder	Grant reference	Author
European Research Council (ERC)	ERC StG 260853	Stephan Gruber, Larissa Wilhelm, Frank Bürmann, Anita Minnen, Christopher P Toseland
Max-Planck-Gesellschaft		Stephan Gruber
National Research Foundation of Korea	2013-034955	Ho-Chul Shin, Byung-Ha Oh

The funders had no role in study design, data collection and interpretation, or the decision to submit the work for publication.

Author contributions

LW, FB, Conception and design, Acquisition of data, Analysis and interpretation of data, Drafting or revising the article; AM, Acquisition of data, Drafting or revising the article; H-CS, CPT, B-HO, Drafting or revising the article, Contributed unpublished essential data or reagents; SG, Conception and design, Analysis and interpretation of data, Drafting or revising the article

Additional files

Supplementary file

- Supplementary file 1. Genotypes of *Bacillus subtilis* strains. All strains are derivatives of either *Bacillus subtilis* 1A700 (Bacillus Genetic Stock Centre) or *Bacillus subtilis* 168 ED.

DOI: 10.7554/eLife.06659.016

References

Alipour E, Marko JF. 2012. Self-organization of domain structures by DNA-loop-extruding enzymes. *Nucleic Acids Research* **40**:11202–11212. doi: 10.1093/nar/gks925.

Arumugam P, Gruber S, Tanaka K, Haering CH, Mechtler K, Nasmyth K. 2003. ATP hydrolysis is required for cohesin's association with chromosomes. *Current Biology* **13**:1941–1953. doi: 10.1016/j.cub.2003.10.036.

Baldwin AD, Kiick KL. 2013. Reversible maleimide-thiol adducts yield glutathione-sensitive poly(ethylene glycol)-heparin hydrogels. *Polymer Chemistry* **4**:133–143. doi: 10.1039/C2PY20576A.

Breier AM, Grossman AD. 2007. Whole-genome analysis of the chromosome partitioning and sporulation protein Spo0J (ParB) reveals spreading and origin-distal sites on the *Bacillus subtilis* chromosome. *Molecular Microbiology* **64**:703–718. doi: 10.1111/j.1365-2958.2007.05690.x.

Broedersz CP, Wang X, Meir Y, Loparo JJ, Rudner DZ, Wingreen NS. 2014. Condensation and localization of the partitioning protein ParB on the bacterial chromosome. *Proceedings of the National Academy of Sciences of USA* **111**:8809–8814. doi: 10.1073/pnas.1402529111.

Bürmann F, Shin H-C, Basquin J, Soh Y-M, Giménez-Oya V, Kim Y-G, Oh B-H, Gruber S. 2013. An asymmetric SMC-kleisin bridge in prokaryotic condensin. *Nature Structural & Molecular Biology* **20**:371–379. doi: 10.1038/nsmb.2488.

Chiu A, Revenkova E, Jessberger R. 2004. DNA interaction and dimerization of eukaryotic SMC hinge domains. *The Journal of Biological Chemistry* **279**:26233–26242. doi: 10.1074/jbc.M402439200.

Coelho PA, Queiroz-Machado J, Sunkel CE. 2003. Condensin-dependent localisation of topoisomerase II to an axial chromosomal structure is required for sister chromatid resolution during mitosis. *Journal of Cell Science* **116**:4763–4776. doi: 10.1242/jcs.00799.

Cui Y, Petrushenko ZM, Rybenkov VV. 2008. MukB acts as a macromolecular clamp in DNA condensation. *Nature Structural & Molecular Biology* **15**:411–418. doi: 10.1038/nsmb.1410.

Cuylen S, Metz J, Haering CH. 2011. Condensin structures chromosomal DNA through topological links. *Nature Structural & Molecular Biology* **18**:894–901. doi: 10.1038/nsmb.2087.

Fuentes-Perez ME, Gwynn EJ, Dillingham MS, Moreno-Herrero F. 2012. Using DNA as a fiducial marker to study SMC complex interactions with the atomic force microscope. *Biophysical Journal* **102**:839–848. doi: 10.1016/j.bpj.2012.01.022.

Gerlich D, Hirota T, Koch B, Peters J-M, Ellenberg J. 2006. Condensin I stabilizes chromosomes mechanically through a dynamic interaction in live cells. *Current Biology* **16**:333–344. doi: 10.1016/j.cub.2005.12.040.

Grimsley GR, Pace CN. 2004. Spectrophotometric determination of protein concentration. *Current Protocols in Protein Science. Chapter 3:Unit 3.1.* *doi: 10.1002/0471140864.ps0301s33.*

Ghosh SK, Huang CC, Hajra S, Jayaram M. 2009. Yeast cohesin complex embraces 2 micron plasmid sisters in a tri-linked catenane complex. *Nucleic Acids Research* **38**:570–584. doi: 10.1093/nar/gkp993.

Gligoris TG, Scheinost JC, Bürmann F, Petela N, Chan K, Uluocak P, Beckouët F, Gruber S, Nasmyth K, Löwe J. 2014. Closing the cohesin ring: structure and function of its Smc3-kleisin interface. *Science* **346**:963–967. doi: 10.1126/science.1256917.

Graham TGW, Wang X, Song D, Etson CM, van Oijen AM, Rudner DZ, Loparo JJ. 2014. ParB spreading requires DNA bridging. *Genes & Development* **28**:1228–1238. doi: 10.1101/gad.242206.114.

Gruber S. 2011. MukBEF on the march: taking over chromosome organization in bacteria? *Molecular Microbiology* **81**:855–859. doi: 10.1111/j.1365-2958.2011.07764.x.

Gruber S. 2014. Multilayer chromosome organization through DNA bending, bridging and extrusion. *Current Opinion in Microbiology* **22**:102–110. doi: 10.1016/j.mib.2014.09.018.

Gruber S, Errington J. 2009. Recruitment of condensin to replication origin regions by ParB/SpoOJ promotes chromosome segregation in *B. subtilis*. *Cell* **137**:685–696. doi: 10.1016/j.cell.2009.02.035.

Gruber S, Haering CH, Nasmyth K. 2003. Chromosomal cohesin forms a ring. *Cell* **112**:765–777. doi: 10.1016/S0092-8674(03)00162-4.

Gruber S, Arumugam P, Katou Y, Kuglitsch D, Helmhart W, Shirahige K, Nasmyth K. 2006. Evidence that loading of cohesin onto chromosomes involves opening of its SMC hinge. *Cell* **127**:523–537. doi: 10.1016/j.cell.2006.08.048.

Gruber S, Veening J-W, Bach J, Blettinger M, Bramkamp M, Errington J. 2014. Interlinked sister chromosomes arise in the absence of condensin during fast replication in *B. subtilis*. *Current Biology* **24**:293–298. doi: 10.1016/j.cub.2013.12.049.

Haering CH, Farcas A-M, Arumugam P, Metson J, Nasmyth K. 2008. The cohesin ring concatenates sister DNA molecules. *Nature* **454**:297–301. doi: 10.1038/nature07098.

Hamoen LW, Smits WK, de Jong A, Holsappel S, Kuipers OP. 2002. Improving the predictive value of the competence transcription factor (ComK) binding site in *Bacillus subtilis* using a genomic approach. *Nucleic Acids Research* **30**:5517–5528. doi: 10.1093/nar/gkf698.

Hirano T. 2006. At the heart of the chromosome: SMC proteins in action. *Nature Reviews. Molecular Cell Biology* **7**:311–322. doi: 10.1038/nrm1909.

Hirano M, Anderson DE, Erickson HP, Hirano T. 2001. Bimodal Activation of SMC ATPase by intra- and inter-molecular interactions. *The EMBO Journal* **20**:3238–3250. doi: 10.1093/emboj/20.12.3238.

Hirano M, Hirano T. 2004. Positive and negative regulation of SMC-DNA interactions by ATP and accessory proteins. *The EMBO Journal* **23**:2664–2673. doi: 10.1038/sj.emboj.7600264.

Hirano M, Hirano T. 2006. Opening closed arms: long-distance activation of SMC ATPase by hinge-DNA interactions. *Molecular Cell* **21**:175–186. doi: 10.1016/j.molcel.2005.11.026.

Hirano T, Mitchison TJ. 1994. A heterodimeric coiled-coil protein required for mitotic chromosome condensation in vitro. *Cell* **79**:449–458. doi: 10.1016/0092-8674(94)90254-2.

Hu B, Itoh T, Mishra A, Katoh Y, Chan K-L, Upcher W, Godlee C, Roig MB, Shirahige K, Nasmyth K. 2011. ATP hydrolysis is required for relocating cohesin from sites occupied by its Scc2/4 loading complex. *Current Biology* **21**:12–24. doi: 10.1016/j.cub.2010.12.004.

Ivanov D, Nasmyth K. 2005. A topological interaction between cohesin rings and a circular minichromosome. *Cell* **122**:849–860. doi: 10.1016/j.cell.2005.07.018.

Kalia J, Raines RT. 2007. Catalysis of imido group hydrolysis in a maleimide conjugate. *Bioorganic & Medicinal Chemistry Letters* **17**:6286–6289. doi: 10.1016/j.bmcl.2007.09.002.

Kamada K, Miyata M, Hirano T. 2013. Molecular basis of SMC ATPase activation: role of internal structural changes of the regulatory subcomplex ScpAB. *Structure* **21**:581–594. doi: 10.1016/j.str.2013.02.016.

Kleine Borgmann LA, Ries J, Ewers H, Ulbrich MH, Graumann PL. 2013. The bacterial SMC complex displays two distinct modes of interaction with the chromosome. *Cell Reports* **3**:1483–1492. doi: 10.1016/j.celrep.2013.04.005.

Lenhart JS, Sharma A, Hingorani MM, Simmons LA. 2013. DnaN clamp zones provide a platform for spatiotemporal coupling of mismatch detection to DNA replication. *Molecular Microbiology* **87**:553–568. doi: 10.1111/mmi.12115.

Leonard TA, Butler PJ, Löwe J. 2004. Structural analysis of the chromosome segregation protein Spo0J from *Thermus thermophilus*. *Molecular Microbiology* **53**:419–432. doi: 10.1111/j.1365-2958.2004.04133.x.

Losada A, Hirano T. 2001. Intermolecular DNA interactions stimulated by the cohesin complex in vitro: implications for sister chromatid cohesion. *Current Biology* **11**:268–272. doi: 10.1016/S0960-9822(01)00066-5.

Maeshima K, Laemmli UK. 2003. A two-step scaffolding model for mitotic chromosome assembly. *Developmental Cell* **4**:467–480. doi: 10.1016/S1534-5807(03)00092-3.

Mascarenhas J, Volkov AV, Rinn C, Schiener J, Guckenberger R, Graumann PL. 2005. Dynamic assembly, localization and proteolysis of the *Bacillus subtilis* SMC complex. *BMC Cell Biology* **6**:28. doi: 10.1186/1471-2121-6-28.

Minnen A, Attaiech L, Thon M, Gruber S, Veening JW. 2011. SMC is recruited to oriC by ParB and promotes chromosome segregation in *Streptococcus pneumoniae*. *Molecular Microbiology* **81**:676–688. doi: 10.1111/j.1365-2958.2011.07722.x.

Nasmyth K. 2001. Disseminating the genome: joining, resolving, and separating sister chromatids during mitosis and meiosis. *Annual Review of Genetics* **35**:673–745. doi: 10.1146/annurev.genet.35.102401.091334.

Ono T, Losada A, Hirano M, Myers MP, Neuwald AF, Hirano T. 2003. Differential contributions of condensin I and condensin II to mitotic chromosome architecture in vertebrate cells. *Cell* **115**:109–121. doi: 10.1016/S0092-8674(03)00724-4.

Ono T, Fang Y, Spector DL, Hirano T. 2004. Spatial and temporal regulation of Condensins I and II in mitotic chromosome assembly in human cells. *Molecular Biology of the Cell* **15**:3296–3308. doi: 10.1091/mbc.E04-03-0242.

Rodionov O, Lobocka M, Yarmolinsky M. 1999. Silencing of genes flanking the P1 plasmid centromere. *Science* **283**:546–549. doi: 10.1126/science.283.5401.546.

Soh Y, Bürmann F, Shin H, Oda T, Jin KS, Toseland CP, Kim C, Lee H, Kim SJ, Kong M, Durand-Diebold M-L, Kim Y-G, Kim HM, Lee NK, Sato M, Oh B, Gruber S. 2015. Molecular basis for smc rod formation and its Dissolution upon DNA binding. *Molecular Cell* **57**:1–14. doi: 10.1016/j.molcel.2014.11.023.

Su'etsugu M, Errington J. 2011. The replicase sliding clamp dynamically accumulates behind progressing replication forks in *Bacillus subtilis* cells. *Molecular Cell* **41**:720–732. doi: 10.1016/j.molcel.2011.02.024.

Sullivan NL, Marquis KA, Rudner DZ. 2009. Recruitment of SMC by ParB-parS organizes the origin region and promotes efficient chromosome segregation. *Cell* **137**:697–707. doi: 10.1016/j.cell.2009.04.044.

Sutani T, Yanagida M. 1997. DNA renaturation activity of the SMC complex implicated in chromosome condensation. *Nature* **388**:798–801. doi: 10.1038/42062.

Thadani R, Uhlmann F, Heeger S. 2012. Condensin, chromatin crossbarring and chromosome condensation. *Current Biology* **22**:R1012–R1021. doi: 10.1016/j.cub.2012.10.023.

Wang X, Tang OW, Riley EP, Rudner DZ. 2014. The SMC condensin complex is required for origin segregation in *Bacillus subtilis*. *Current Biology* **24**:287–292. doi: 10.1016/j.cub.2013.11.050.

Weitzer S, Lehane C, Uhlmann F. 2003. A model for ATP hydrolysis-dependent binding of cohesin to DNA. *Current Biology* **13**:1930–1940. doi: 10.1016/j.cub.2003.10.030.

Zhao S, Fernald RD. 2005. Comprehensive algorithm for quantitative real-time polymerase chain reaction. *Journal of Computational Biology* **12**:1047–1064. doi: 10.1089/cmb.2005.12.1047.

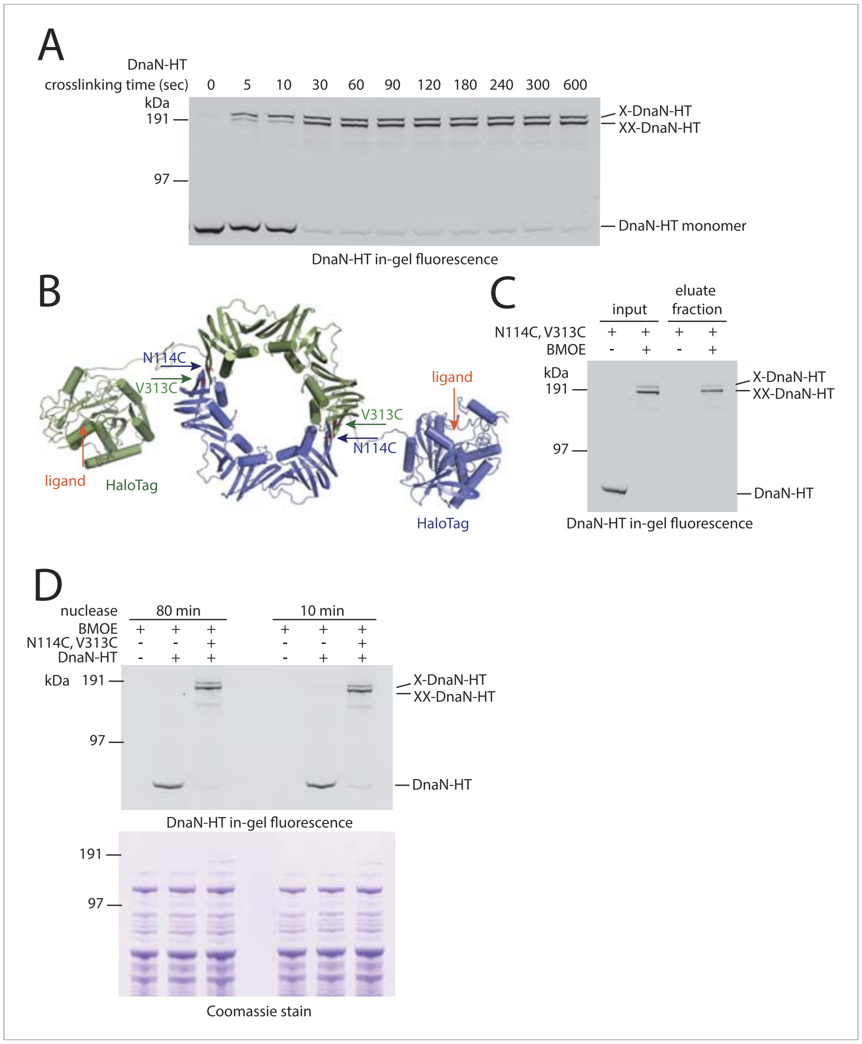

Figure 1—figure supplement 1. DNA entrapment by DnaN. (**A**) Cross-linking time course of DnaN-HT. Cells of strain BSG1459 were incubated with the cross-linker BMOE and quenched at the indicated times. Extracts were analysed by in-gel fluorescence detection of DnaN-HT. At later time points the double cross-linked DnaN species ('XX-DnaN-HT') is enriched over non-cross-linked and single cross-linked DnaN-HT. (**B**) Cartoon represenation of the DnaN-HT construct based on the crystal structure of *S. pneumoniae* DnaN (PDB: 3D1F) and *Rhodococcus* Haloalkane dehalogenase (PDB: 1BN6). The structure of the DnaN dimer (monomers in green and blue colours, respectively) was juxtaposed to the structure of the Haloalkane dehalogenase linked by a flexible peptide. The binding pockets for HT ligand binding are indicated by orange arrows. The positions of the engineered pair of cysteine residues (N114C and V313C) at the DnaN–DnaN interface are indicated by blue and green arrows. (**C**) Chromosome entrapment assay of strain BSG1459 (*dnaN(N114C, V313C)-HT*) in presence or absence of the cross-linker BMOE. (**D**) Effect of benzonase ('nuclease') on protein extracts of strains BSG1001, BSG1449 and BSG1459. Cell extracts were analysed by in-gel fluorescence detection (upper panel) of DnaN-HT after long-time ('80 min') or short-time ('10 min') incubation with benzonase. Lower panel shows Coomassie staining of the same SDS-PAGE gel to control for equal protein extraction efficiency.

DOI: 10.7554/eLife.06659.004

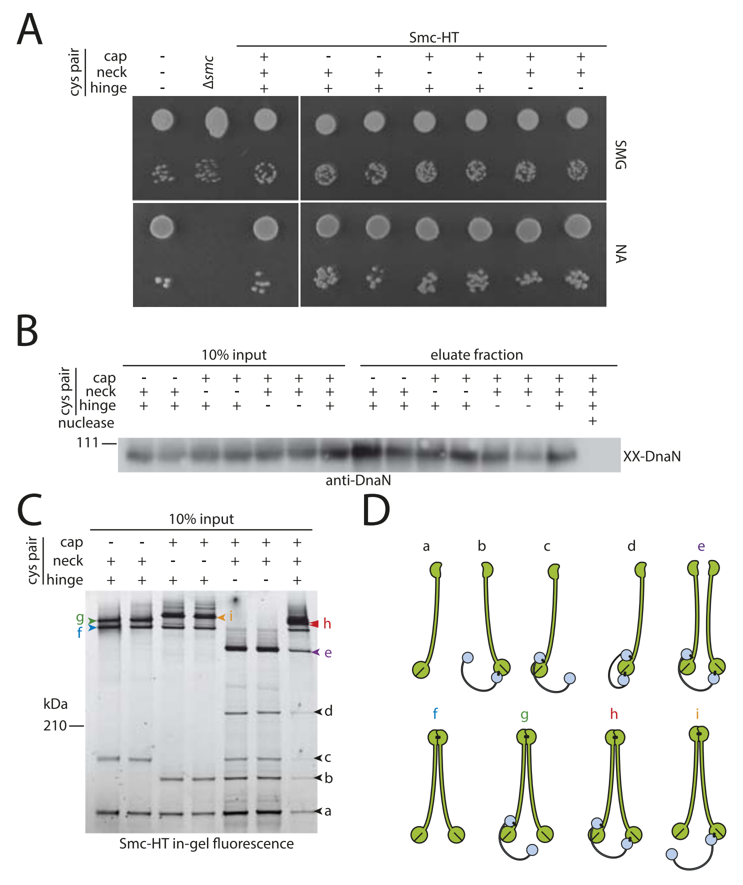

Figure 2—figure supplement 1. DNA entrapment by wild-type Smc–ScpAB (I). (**A**) Colony formation assays of strains BSG1002, BSG1007, BSG1782, 1809–1813 and BSG1831 were performed on minimal medium agar (SMG) or nutrient agar (NA). Cultures were diluted 9^2-fold (top row) and 9^5-fold (bottom row) and grown at 37˚C for 24 hr (SMG) and 14 hr (NA), respectively. The presence and absence of cysteine pairs for cross-linking of the hinge, cap and neck interface are indicated by '+' and '–', respectively. (**B**) Immunoblot of SDS-PAGE gels shown in ***Figure 2B*** using anti-DnaN antibody. All strains carry cysteine mutations for DnaN cross-linking. Doubly cross-linked DnaN ('XX-DnaN') serves as internal assay control as visualized by immunoblotting. (**C**) Identification of cross-linked species of Smc-HT and ScpA. The gel image is identical to ***Figure 2A*** with higher contrast settings to visualize low-intensity species. All cross-linked species are labelled (with a colour-coded letter) ('a'–'i'). Circular species ('h') are labeled by a double pointed arrowhead. (**D**) Same as ***Figure 2***, panel **C**. Schematic depiction of the structure of cross-linked Smc–ScpA species ('a'–'i').

DOI: 10.7554/eLife.06659.006

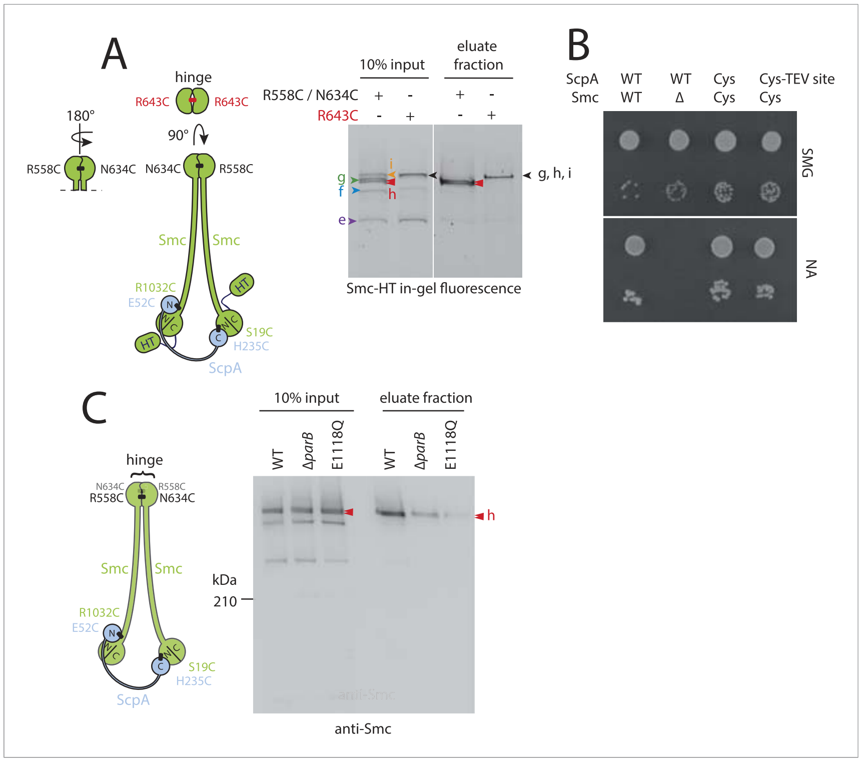

Figure 2—figure supplement 2. DNA entrapment by wild-type Smc–ScpAB (II). (**A**) Cross-linking of the Smc hinge interface with different cysteine residues. Cross-linking of the Smc hinge using cysteine residue ('R643C') instead of the 'R558C' and 'N643C' cysteine pair results in different migration pattern of cross-linked Smc-ScpA species (see input fractions). In this case species 'g' and 'i' have the same migration behavior as the circular form 'h'. Only a single species of Smc-ScpA is retained in the agarose plug after the entrapment assay (see eluate fractions). (**B**) Colony formation assay of strains BSG1002, BSG1007, BSG1807 and BSG1832 were performed as described before. The *smc* and *scpA* loci lacking mutations ('WT'), harbouring cysteine mutations for cross-linking alone ('Cys') or in combination with a TEV cleavage site ('Cys-TEV site') are denoted. (**C**) Chromosome entrapment of Smc–ScpAB lacking fusion tags (see scheme on the left). The right panel shows immunoblotting of input and eluate fractions using an anti-Smc antibody. All strains harbour cysteine residues for crosslinking of Smc-ScpA in an otherwise wild-type background ('WT') in BSG680, combined with a deletion of the *parB* gene ('Δ*parB*') in BSG1991 or with the E1118Q mutation at the *smc* locus in BSG1995. The position of fully cross-linked, circular Smc_2-ScpA species is indicated by double pointed arrowhead labelled 'h' (see ***Figure 2—figure supplement 1C***), respectively.

DOI: 10.7554/eLife.06659.007

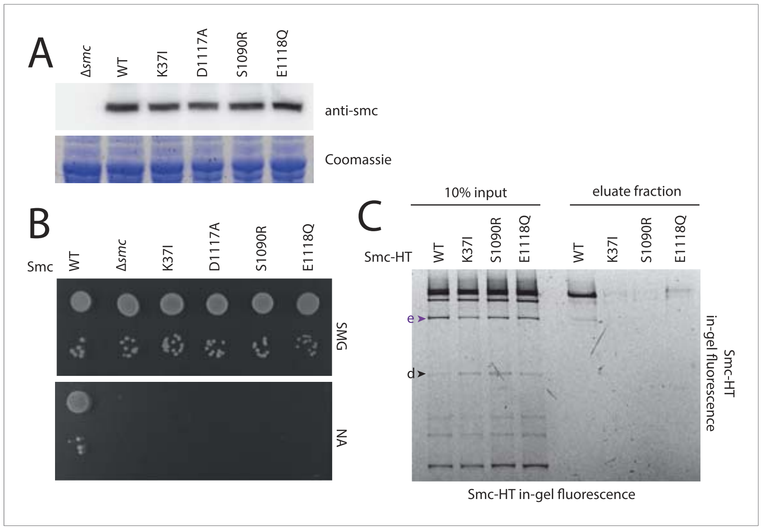
A
Δsmc
WT
K37I
D1117A
S1090R
E1118Q
anti-smc
Coomassie
B
Smc
WT
Δsmc
K37I
D1117A
S1090R
E1118Q
SMG
NA
C
10% input
eluate fraction
Smc-HT
WT
K37I
S1090R
E1118Q
WT
K37I
S1090R
E1118Q
e
d
Smc-HT in-gel fluorescence
Smc-HT in-gel fluorescence

Figure 3—figure supplement 1. ATPase mutants of Smc-ScpAB. (**A**) Upper panel shows Smc expression levels of strains with mutant *smc* alleles (BSG1002, 1007, 1008, 1045, 1046, 1047 and 1074) determined by immunoblotting using anti-Smc antibodies. Lower panel shows Coomassie staining of a SDS-PAGE gel loaded with the same whole cell extract samples to control for equal protein extraction efficiency. (**B**) Overnight cultures of strains (BSG1002, 1007, 1008, 1045, 1046, 1047) were spotted on SMG and NA as described before (see ***Figure 2—figure supplement 1***). Smc locus was without mutation ('WT'), a smc deletion ('Δ*smc*') or mutations in the Smc ATPase domain. (**C**) Smc ATPase mutations show slightly decreased levels of cross-linking species 'e' and increased levels of 'd'. Image is identical to ***Figure 3B***, with higher contrast.

DOI: 10.7554/eLife.06659.009

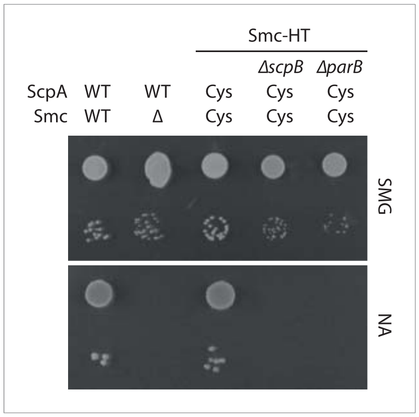
Smc-HT
ΔscpB
ΔparB
ScpA WT WT Cys Cys Cys
Smc WT Δ Cys Cys Cys
SMG
NA

Figure 4—figure supplement 1. Growth of *smc(Cys)* mutants. Overnight cultures of strains (BSG1002, BSG1007, BSG1782, BSG1850 and BSG1783) were serially diluted and spotted as described before (***Figure 2—figure supplement 1***). Strains were wild-type ('WT'), harboured the smc deletion ('Δ') or cysteine mutations for cross-linking the Smc-ScpA ring ('Cys'). In addition, scpB ('Δ*scpB*') or parB ('Δ*parB*') were deleted where indicated.

DOI: 10.7554/eLife.06659.011

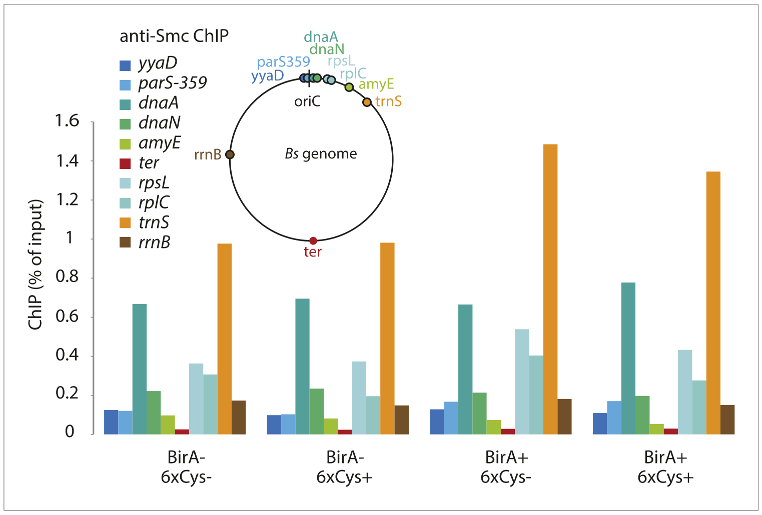

Figure 5—figure supplement 1. Chromatin immuno-precipitation of Smc. All Smc variants used in ***Figure 5*** behave similarly in standard ChIP experiments using anti-Smc antibodies. Cells of strains BSG1104-5 and 1107-8 were grown to mid-exponential phase and subjected to chromatin immunoprecipitation (ChIP) using polyclonal rabbit anti-Smc serum. Input and eluate DNA samples were analysed by quantitative PCR using specific primer pairs for the genomic positions indicated on a circular representation of the *B. subtilis* genome. Pull-down efficiency (ChIP-DNA/input-DNA *100%) was plotted for each primer pair. The lack and presence of the BirA biotin ligase or cysteines for cross-linking of Smc and ScpA proteins are denoted as 'BirA−' and 'BirA+' or '6xCys−' and '6xCys+', respectively. It is noted that the highly transcribed tRNA locus, *trnS*, is highly enriched by Smc-Avitag using standard ChIP (but not native ChIP, see ***Figure 5***), being consistent with the notion that enrichment of highly transcribed genes by ChIP is prone to artefacts due to non-uniform formaldehyde cross-linking.

DOI: 10.7554/eLife.06659.013

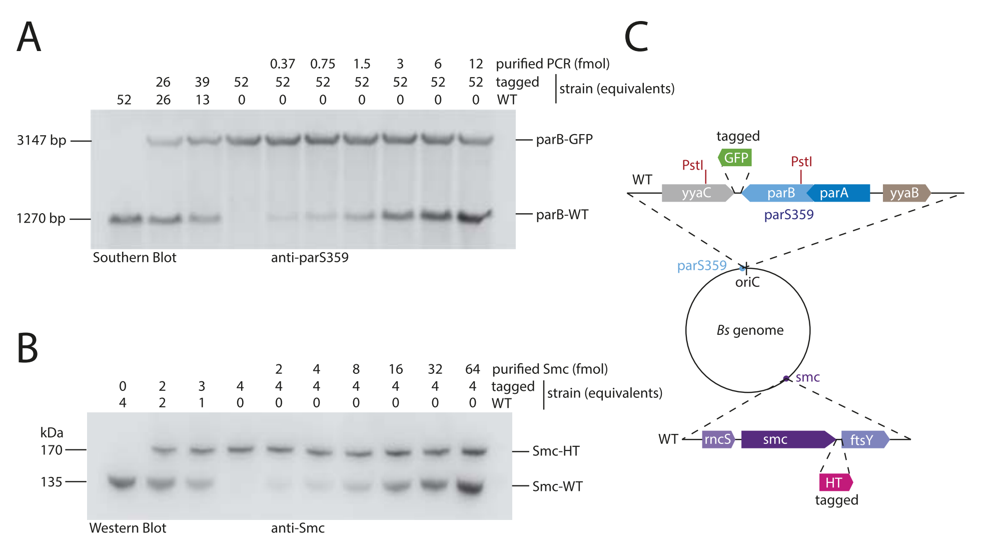

Figure 6—figure supplement 1. Quantitative Blotting of Smc protein and *parB* DNA. To estimate Smc protein and *parS-359* DNA abundance in *B. subtilis* cells, levels of Smc and *parS-359* in extracts of wild-type cells were compared to defined amounts of purified Smc protein and *parS-359* DNA spiked into equivalent extracts from cell harboring a tagged version of Smc and a modified *parS-359* locus (see panel **C**). The ratio of Smc protein (see panel **B**) to *parS-359* DNA (see panel **A**) was calculated as average from three independent experiments (biological replicates) to be 61 (±12 SEM, standard error of mean) Smc monomers per *parS-359* DNA. Due to potential loss of chromosomal DNA during genomic DNA preparation this might be a slight over-estimation of the real number. (**A**) Quantitative Southern blotting to estimate the number of molecules (in fmol) of the *parS359* locus in a given number of cells. Genomic DNA from 52× cell culture equivalents (1 equivalent equals 0.025 ml*OD_{600}) of wild type ('WT', BSG1001) has been digested with the PstI restriction enzyme (see panel **C**) and loaded into the left lane. DNA loaded into the second and third lane is derived from mixtures of wild-type and tagged ('parB-GFP', BSG2058) cells. Defined amounts of a purified PCR product covering the wild-type *parS-359* locus have been spiked into cell extracts of the tagged strain. Digested DNA was detected using a Southern probe specific for the *parS-359* locus. (**B**) Quantitative Western blot to estimate the number of molecules of the Smc protein (in fmol) in a given number of cells. Cultures were identical to the ones used in (**A**). Whole cell protein extract corresponding to 4 culture equivalents of wild-type cells ('WT', BSG1001) was loaded into the left lane. Other lanes were loaded with samples derived from wild-type and tagged cells or mixtures thereof with or without spiked-in purified Smc protein as indicated in the figure panel. Smc protein was detected by immunoblotting using a polyclonal rabbit anti-Smc antibody. (**C**) Protein and DNA spike-in was performed in extracts derived from cells (BSG2058) with modifications at the *parS-359* locus (blue filled circle) and the *smc* gene (purple filled circle). PstI restriction sites (in red) in the *parB* gene (light blue box) and the neighbouring *yyaC* gene (grey box) generate a fragment of 1270 bp in size in case of the wild-type locus. From *parB-gfp* cells (BSG2058), however, a bigger DNA fragment of 3147 bp in size is generated. Strain BSG2058 also harboured a modified *smc* gene, which is fused to a *halotag* cassette (pink box).

DOI: 10.7554/eLife.06659.015

Supplementary File 1: Genotypes of *Bacillus subtilis* strains. All strains are derived from *Bacillus subtilis* 1A700 (Bacillus Genetic Stock Centre) or from *Bacillus subtilis* 168 ED (Domínguez-Cuevas et al., 2012).

Name	Genotype
BSG1001	*1A700, trpC2*
BSG1002	*1A700, smc ftsY::ermB, trpC2*
BSG1007	*1A700, Δsmc ftsY::ermB, trpC2*
BSG1008	*1A700, smc(E1118Q) ftsY::ermB, trpC2*
BSG1045	*1A700, smc(K37I) ftsY::ermB, trpC2*
BSG1046	*1A700, smc(S1090R) ftsY::ermB, trpC2*
BSG1047	*1A700, smc(D1117A) ftsY::ermB, trpC2*
BSG1104	*1A700, smc-TEV-AviTag ftsY::(ermB birA), cat::scpA scpB, trpC2*
BSG1105	*1A700, smc(S19C, R558C, N634C, R1032C)-TEV-AviTag ftsY::(ermB, birA), cat::scpA(E52C, H235C), trpC2*
BSG1107	*1A700, smc-TEV-AviTag ftsY::tetL, cat::scpA scpB, trpC2*
BSG1108	*1A700, smc(S19C, R558C, N634C, R1032C)-TEV-AviTag ftsY::tetL, cat::scpA(E52C, H235C), trpC2*
BSG1449	*1A700, dnaN-HISx12-HaloTag::specR, trpC2*
BSG1459	*1A700, dnaN(N114C, V313C)-HISx12-HaloTag::specR, trpC*
BSG1494	*1A700, smc(S19C, R558C, N634C, R1032C)-TEV-HaloTag ftsY::ermB, cat::scpA(E52C, H235C), trpC2*
BSG1743	*1A700, smc(S19C, R643C, R1032C)-TEV-HaloTag ftsY::ermB, cat::scpA(E52C, H235C), trpC2*
BSG1782	*1A700, smc(S19C, R558C, N634C, R1032C)-TEV-HaloTag ftsY::ermB, cat::scpA(E52C, H235C), dnaN(N114C, V313C)::specR, trpC2*
BSG1783	*1A700, smc(S19C, R558C, N634C, R1032C)-TEV-HaloTag ftsY::ermB, cat::scpA(E52C, H235C), ΔparB::kanR, dnaN(N114C, V313C)::specR, trpC2*
BSG1784	*1A700, smc(S19C, K37I, R558C, N634C, R1032C)-TEV-HaloTag ftsY::ermB, cat::scpA(E52C, H235C), dnaN(N114C, V313C)::specR, trpC2*
BSG1785	*1A700, smc(S19C, R558C, N634C, S1090R, R1032C)-TEV-HaloTag ftsY::ermB, cat::scpA(E52C, H235C), dnaN(N114C, V313C)::specR, trpC2*
BSG1786	*1A700, smc(S19C, R558C, N634C, R1032C, E1118Q)-TEV-HaloTag ftsY::ermB, cat::scpA(E52C, H235C), dnaN(N114C, V313C)::specR, trpC2*
BSG1807	*1A700, smc(S19C, R558C, N634C, R1032C)-TEV-HaloTag ftsY::ermB, cat::scpA(E52C, H235C), dnaN(N114C, V313C)::specR, trpC2*
BSG1809	*1A700, smc(S19C, R558C, N634C)-TEV-HaloTag ftsY::ermB, cat::scpA(E52C, H235C), dnaN(N114C, V313C)::specR, trpC2*
BSG1810	*1A700, smc(S19C, N634C, R1032C)-TEV-HaloTag ftsY::ermB, cat::scpA(E52C, H235C), dnaN(N114C, V313C)::specR, trpC2*
BSG1811	*1A700, smc(S19C, R558C, N634C, R1032C)-TEV-HaloTag ftsY::ermB, cat::scpA(E52C), dnaN(N114C, V313C)::specR, trpC2*
BSG1812	*1A700, smc(S19C, R558C, R1032C)-TEV-HaloTag ftsY::ermB, cat::scpA(E52C, H235C),dnaN(N114C, V313C)::specR, trpC2*
BSG1813	*1A700, smc(S19C, R558C, N634C, R1032C)-TEV-HaloTag ftsY::ermB, cat::scpA(H235C), dnaN(N114C, V313C)::specR, trpC2*
BSG1831	*1A700, smc(R558C, N634C, R1032C)-TEV-HaloTag-ftsY::ermB; camR::scpA(E52C, H235C), dnaN(N114C, V313C)::specR, trpC2*

BSG1832	*1A700, smc(S19C, R558C, N634C, R1032C)-HaloTag ftsY::ermB, camR::scpA(E52C, TEV, H235C), dnaN(N114C, V313C)::specR, trpC2*
BSG1850	*1A700, smc(S19C, R558C, N634C, R1032C)-TEV-HaloTag ftsY::ermB, camR::scpA(E52C, H235C) ΔscpB, dnaN(N114C, V313C)::specR, trpC2*
BSG1960	*1A700, smc(S19C, R558C, N634C, R1032C)-TEV-HaloTag ftsY::ermB, cat::scpA(E52C, H235C), dnaN(N114C, V313C)::specR, parB(G77S)::kanR, trpC2*
BSG1961	*1A700, smc(S19C, R558C, N634C, R1032C)-TEV-HaloTag ftsY::ermB, cat::scpA(E52C, H235C), dnaN(N114C, V313C)::specR, parB(R80A)::kanR, trpC2*
BSG1962	*1A700, smc(S19C, R558C, N634C, R1032C)-TEV-HaloTag ftsY::ermB, cat::scpA(E52C, H235C), dnaN(N114C, V313C)::specR, parB(R149G)::kanR, trpC2*
BSG1963	*1A700, smc(S19C, R558C, N634C, R1032C)-TEV-HaloTag ftsY::ermB, cat::scpA(E52C, H235C), dnaN(N114C, V313C)::specR, parB(N112S)::kanR, trpC2*
BSG2058	*1A700, smc-TEV-HaloTag ftsY::tetL, parB-mGFPmut1::ermB, fabG::specR::tos-rtp, trpC2*
BSG680	*168 ED, CAT::scpA(E52C, H235C), smc(S19C, R558C, N634C, R1032C) ftsY::ermB, trpC2*
BSG1991	*168 ED, CAT::scpA(E52C, H235C), smc(S19C, R558C, N634C, R1032C) ftsY:ermB, ΔparB::kanR, trpC2*
BSG1995	*168 ED, CAT::scpA(E52C, H235C), smc(S19C, R558C, N634C, R1032C, E1118Q) ftsY::ermB, trpC2*

Domínguez-Cuevas, P., Mercier, R., Leaver, M., Kawai, Y., and Errington, J. 2012. The rod to L-form transition of Bacillus subtilis is limited by a requirement for the protoplast to escape from the cell wall sacculus. *Mol. Microbiol.* **83**:52–66. doi:10.1111/j.1365-2958.2011.07920.x.

3.2. PUBLICATION II

Control of Smc Coiled Coil Architecture by the ATPase Heads Facilitates Targeting to Chromosomal ParB/*parS* and Release onto Flanking DNA

Minnen, A., Bürmann, F., **Wilhelm, L.**, Anchimiuk, A., Diebold-Durand, M.-L., and Gruber, S. 2016. *Cell Rep.* **14**:2003–2016. doi:10.1016/j.celrep.2016.01.066.

Abstract:

Smc/ScpAB promotes chromosome segregation in prokaryotes, presumably by compacting and resolving nascent sister chromosomes. The underlying mechanisms, however, are poorly understood. Here, we investigate the role of the Smc ATPase activity in the recruitment of Smc/ScpAB to the *Bacillus subtilis* chromosome. We demonstrate that targeting of Smc/ScpAB to ParB/*parS* loading sites is strictly dependent on engagement of Smc head domains and relies on an open organization of the Smc coiled coils. We find that dimerization of the Smc hinge domain stabilizes closed Smc rods and hinders head engagement as well as chromosomal targeting. Conversely, the ScpAB sub-complex promotes head engagement and Smc rod opening and thereby facilitates recruitment of Smc to *parS* sites. Upon ATP hydrolysis, Smc/ScpAB is released from loading sites and relocates within the chromosome—presumably through translocation along DNA double helices. Our findings define an intermediate state in the process of chromosome organization by Smc.

On the following pages the original publication is attached as published on March 1, 2016 without any modifications. http://dx.doi.org/10.1016/j.celrep.2016.01.066

This article is distributed under the terms of the **Creative Commons Attribution License**, which permits redistribution provided that the original author, the source of the publication and the license are credited. https://creativecommons.org/licenses/by-nc-nd/4.0/

Cell Reports

Article

Control of Smc Coiled Coil Architecture by the ATPase Heads Facilitates Targeting to Chromosomal ParB/*parS* and Release onto Flanking DNA

Graphical Abstract

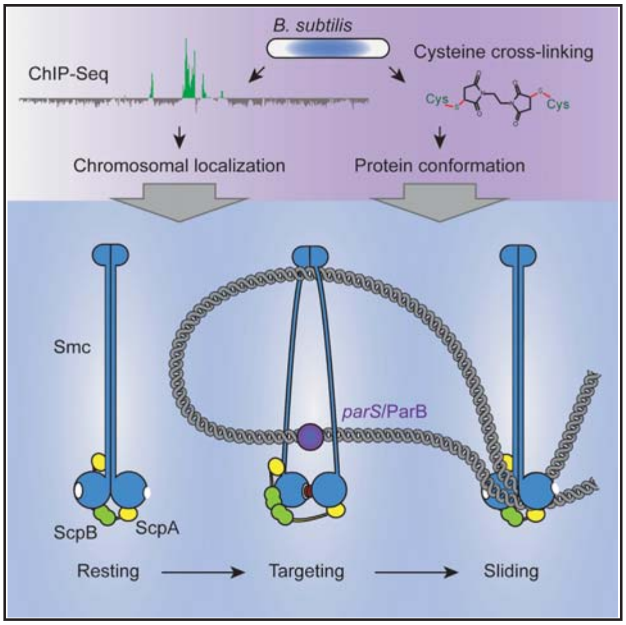
B. subtilis
ChIP-Seq
Cysteine cross-linking
Cys
Cys
Chromosomal localization
Protein conformation
Smc
parS/ParB
ScpB
ScpA
Resting
Targeting
Sliding

Authors

Anita Minnen, Frank Bürmann,
Larissa Wilhelm, Anna Anchimiuk,
Marie-Laure Diebold-Durand,
Stephan Gruber

Correspondence

sgruber@biochem.mpg.de

In Brief

Smc/ScpAB is an important chromosome-organizing machine in bacteria. Minnen et al. show that targeting of Smc/ScpAB to chromosomal *parS*/ParB sites requires ATP-dependent engagement of Smc heads, which promotes disengagement of the Smc coiled coils and drives the complex into a targeting-competent open conformation.

Highlights

- ATP-dependent head engagement is required for chromosomal targeting of Smc/ScpAB
- ATP-dependent head engagement drives coiled-coil opening of Smc in vivo
- Targeting of Smc/ScpAB to *parS*/ParB requires the head-proximal coiled coil of Smc
- Hinge dimerization antagonizes head engagement, coiled-coil opening, and targeting

Accession Numbers

GSE76949

Minnen et al., 2016, Cell Reports *14*, 1–14
March 1, 2016 ©2016 The Authors
http://dx.doi.org/10.1016/j.celrep.2016.01.066

Please cite this article in press as: Minnen et al., Control of Smc Coiled Coil Architecture by the ATPase Heads Facilitates Targeting to Chromosomal ParB/*parS* and Release onto Flanking DNA, Cell Reports (2016), http://dx.doi.org/10.1016/j.celrep.2016.01.066

Cell Reports
Article

OPEN ACCESS
CellPress

Control of Smc Coiled Coil Architecture by the ATPase Heads Facilitates Targeting to Chromosomal ParB/*parS* and Release onto Flanking DNA

Anita Minnen,[1,2] Frank Bürmann,[1,2] Larissa Wilhelm,[1] Anna Anchimiuk,[1] Marie-Laure Diebold-Durand,[1] and Stephan Gruber[1,*]
[1]Research Group 'Chromosome Organization and Dynamics', Max Planck Institute of Biochemistry, Am Klopferspitz 18, 82152 Martinsried, Germany
[2]Co-first author
*Correspondence: sgruber@biochem.mpg.de
http://dx.doi.org/10.1016/j.celrep.2016.01.066
This is an open access article under the CC BY-NC-ND license (http://creativecommons.org/licenses/by-nc-nd/4.0/).

SUMMARY

Smc/ScpAB promotes chromosome segregation in prokaryotes, presumably by compacting and resolving nascent sister chromosomes. The underlying mechanisms, however, are poorly understood. Here, we investigate the role of the Smc ATPase activity in the recruitment of Smc/ScpAB to the *Bacillus subtilis* chromosome. We demonstrate that targeting of Smc/ScpAB to ParB/*parS* loading sites is strictly dependent on engagement of Smc head domains and relies on an open organization of the Smc coiled coils. We find that dimerization of the Smc hinge domain stabilizes closed Smc rods and hinders head engagement as well as chromosomal targeting. Conversely, the ScpAB sub-complex promotes head engagement and Smc rod opening and thereby facilitates recruitment of Smc to *parS* sites. Upon ATP hydrolysis, Smc/ScpAB is released from loading sites and relocates within the chromosome—presumably through translocation along DNA double helices. Our findings define an intermediate state in the process of chromosome organization by Smc.

INTRODUCTION

Proper segregation of the genetic material during cell division relies on the organization of replicated DNA molecules into compact and individualized sister chromosomes. In eukaryotes, condensation and resolution of chromatin into morphologically distinct chromatids occurs early in mitosis and depends on the interplay of nucleosomes, DNA topoisomerase II and structural maintenance of chromosomes (SMC) protein complexes such as condensin and cohesin (Houlard et al., 2015; Shintomi et al., 2015). In bacteria, segments of the circular chromosome are sequentially partitioned to opposite halves of the cell in line with their duplication by the two replication forks. Resolution of bacterial chromosomes is thus an ordered process, which initiates near the replication origin and concludes with the separation of the replication terminus region. Prokaryotic SMC complexes, called Smc/ScpAB and MukBEF, are enriched in the vicinity of the replication origin on the bacterial chromosome (Badrinarayanan et al., 2012; Danilova et al., 2007; Gruber and Errington, 2009; Minnen et al., 2011; Sullivan et al., 2009; Wilhelm et al., 2015). In rapidly growing cells of *Bacillus subtilis*, inactivation of Smc/ScpAB is lethal due to a severe block in replication origin separation and nucleoid partitioning (Britton et al., 1998; Gruber et al., 2014; Mascarenhas et al., 2002; Moriya et al., 1998; Soppa et al., 2002; Wang et al., 2014). How Smc/ScpAB enables timely resolution of sister replication origins is largely unclear.

A 50-nm long intramolecular coiled-coil constitutes the central part of SMC proteins, which connects a "hinge" domain with an ATPase "head" domain (Haering et al., 2002; Hirano and Hirano, 2002; Melby et al., 1998). In bacteria, homotypic interaction of two Smc proteins at their hinge supports the alignment of the two Smc coiled coils to produce a highly elongated rod-shaped Smc dimer (Soh et al., 2015). At the hinge-distal end of the Smc rod a single subunit of the kleisin family of proteins (named ScpA in bacteria) binds to the Smc dimer via two separate interfaces (Bürmann et al., 2013; Gruber et al., 2003; Haering et al., 2002; Schleiffer et al., 2003). A helical bundle is formed by ScpA's N-terminal domain and the "neck" coiled coil of one Smc subunit (Bürmann et al., 2013; Gligoris et al., 2014). ScpA's C-terminal winged-helix domain attaches to the "cap" of the head in the other Smc subunit (Bürmann et al., 2013; Haering et al., 2004). Asymmetric tripartite rings made up of one ScpA and two Smc proteins are thus formed. Like its eukaryotic descendants, Smc/ScpAB entraps chromosomal DNA molecules within the confines of its SMC/kleisin ring (Cuylen et al., 2011; Gligoris et al., 2014; Wilhelm et al., 2015). DNA entrapment depends on the ScpB subunit, which forms dimers and associates with a central segment of ScpA, as well as on ATP hydrolysis by the Smc complex (Bürmann et al., 2013; Kamada et al., 2013; Wilhelm et al., 2015).

Smc/ScpAB localizes in foci within the bacterial cell. These Smc protein clusters are generally positioned in the vicinity of a copy of the replication origin in *B. subtilis* and *Streptococcus pneumoniae* (Graumann et al., 1998; Gruber and Errington, 2009; Kleine Borgmann et al., 2013; Minnen et al., 2011; Sullivan

Please cite this article in press as: Minnen et al., Control of Smc Coiled Coil Architecture by the ATPase Heads Facilitates Targeting to Chromosomal ParB/*parS* and Release onto Flanking DNA, Cell Reports (2016), http://dx.doi.org/10.1016/j.celrep.2016.01.066

et al., 2009). Targeting of Smc/ScpAB to the replication origin region and formation of Smc foci relies on ParB protein and *parS* sites. ParB binds to short palindromic *parS* sequences, the six most prominent of which are scattered within a 350 kb region (<10% of the genome) surrounding the replication origin in *B. subtilis*. In several bacteria, the replicating chromosome displays a distinctive ''longitudinal'' organization within the cell (Le et al., 2013; Marbouty et al., 2014, 2015; Umbarger et al., 2011; Vallet-Gely and Boccard, 2013; Wang et al., 2015): The newly replicated origins are generally found at the outer edges of the elongating chromosome, while other loci on the nascent chromosome are linearly arranged between the replication origin and the more centrally located terminus. Corresponding positions on opposite arms of the chromosome are frequently juxtaposed. The Smc/ScpAB complex as well as ParB protein and *parS* sites are essential for establishing this longitudinal organization of bacterial chromosomes (Le et al., 2013; Marbouty et al., 2015; Umbarger et al., 2011; Wang et al., 2015). How the loading of Smc/ScpAB by ParB/*parS* at few genomic positions governs global chromosome organization, however, is unclear (Bürmann and Gruber, 2015).

The SMC head domains share a common fold with nucleotide binding domains (NBD) found in ABC transporters. These domains undergo cycles of engagement and disengagement driven by ATP binding and ATP hydrolysis. In Smc/ScpAB, the Smc ATPase controls DNA binding to the distant hinge domain (Hirano and Hirano, 2006; Soh et al., 2015). Head engagement appears to promote the dissolution of the Smc coiled coil rod and thereby exposes an otherwise occluded binding site for DNA at the Smc hinge (Soh et al., 2015). If, and how, such a potential ATP-driven conformational transition might be relevant for the ParB-dependent recruitment of Smc/ScpAB toward the replication origin region of the bacterial chromosome is unclear. In yeast, ATP hydrolysis by cohesin has been implicated in its chromosomal relocation from sites occupied by the loading complex. However, the underlying molecular mechanisms remain elusive (Hu et al., 2011).

Here, we show that the Smc ATPase cycle controls the dynamic association of Smc/ScpAB with the bacterial chromosome. It determines the initial targeting of Smc/ScpAB to its chromosomal loading sites and subsequent re-distribution into flanking DNA. Smc head engagement is crucial for the recognition of the ParB/*parS* loading platform. We find that Smc head engagement is remarkably inefficient in Smc/ScpAB, due to the inhibitory action of Smc hinge and Smc rod, which is partially relieved by ScpAB. A head-proximal region of the Smc coiled coil is critical for targeting to ParB/*parS*. An Smc mutant defective in ATP hydrolysis is highly enriched at *parS* sites but fails to localize to other parts of the chromosome, including the neighboring replication origin and distant chromosomal arm loci. Smc appears to be released from loading sites to relocate along DNA to other parts of the chromosome in a manner that requires at least one round of ATP hydrolysis. Overall, our results demonstrate that engagement and disengagement of Smc heads define two distinct modes of chromosome association by Smc/ScpAB. Furthermore, they support the intriguing notion that movement of Smc/ScpAB along chromosome DNA is a critical aspect of its activity, which might be related to DNA loop extrusion by Smc.

RESULTS

Smc ATPase Activity Controls the Dynamic Distribution of Smc/ScpAB over the Bacterial Chromosome

To investigate a potential role of the Smc ATP hydrolysis cycle in the localization of Smc/ScpAB complexes within the bacterial cell and on the bacterial chromosome, we made use of well-characterized, single amino-acid substitutions in the Smc head domain, which specifically block ATP binding (K37I or D1117A) or ATP-dependent head engagement (S1090R), alleviate a proposed stimulatory effect of DNA on ATP hydrolysis (R57A), or strongly reduce Smc ATP hydrolysis (E1118Q; or EQ for short) (Figure 1A) (Hirano et al., 2001; Hirano and Hirano, 2004, 2006; Lammens et al., 2004; Schwartz and Shapiro, 2011). These mutant proteins, with the exception of Smc(R57A), fail to support growth of *B. subtilis* on rich medium indicating that the mutations render the Smc protein non-functional (Figure S1A) (Gruber et al., 2014). All non-functional Smc proteins, however, are expressed to normal levels as judged by immunoblotting using an α-Smc antiserum (Figure 1B) and efficiently bind to the kleisin subunit ScpA (Bürmann et al., 2013; Wilhelm et al., 2015). The *smc* alleles were then tagged at their C terminus with a monomeric version of *gfp* and integrated into the endogenous locus by allelic replacement. Cells were analyzed by fluorescence imaging on minimal medium, which supports near normal growth of *smc* mutant strains. Wild-type Smc-GFP protein formed approximately one GFP focus per μm cell length (Figures 1C and S1H) (Graumann et al., 1998; Gruber and Errington, 2009; Sullivan et al., 2009). The cellular localization of the R57A mutant protein was indistinguishable from wild-type Smc. In contrast, K37I, D1117A, and S1090R mutant proteins failed to form any discernible structures in fluorescence images being indicative of a dispersed cellular localization (Mascarenhas et al., 2005). Crucially, the Smc(EQ) protein produced bright GFP foci, which on average occurred slightly less frequently than in wild-type cells (Figures 1C and S1H). These observations demonstrate the involvement of the Smc ATPase activity in the sub-cellular organization of Smc complexes and indicate that Smc is able to localize within the cell when its ATP hydrolysis activity is reduced but not when ATP binding or Smc head engagement is blocked.

Next, we used untagged alleles of all ATPase mutants to examine their chromosomal distribution in *B. subtilis* by chromatin immunoprecipitation (ChIP) with an antiserum raised against the Smc protein. qPCR with primer pairs specific for selected regions of the chromosome was performed to measure the co-purification of chromosomal DNA with Smc. As predicted from their inability to form GFP foci in the cell, ATP binding and head engagement mutants resulted in little DNA co-purification similar to the Δ*smc* control—being consistent with the notion that ATP binding and engagement mutants fail to localize to the chromosome (Figure 1D). Wild-type Smc produced highly significant ChIP enrichment of origin proximal DNA (*parS-356*, *parS-359*, and *dnaA*) as observed before with tagged alleles of *smc* (Gruber and Errington, 2009). Intriguingly, the Smc(EQ) protein showed on the one hand markedly stronger localization to *parS* DNA than wild-type Smc and on the other hand quite low enrichment at the juxtaposed *dnaA* locus. Clearly, Smc(EQ) protein is able to efficiently target specific regions of the

Please cite this article in press as: Minnen et al., Control of Smc Coiled Coil Architecture by the ATPase Heads Facilitates Targeting to Chromosomal ParB/*parS* and Release onto Flanking DNA, Cell Reports (2016), http://dx.doi.org/10.1016/j.celrep.2016.01.066

OPEN ACCESS
CellPress

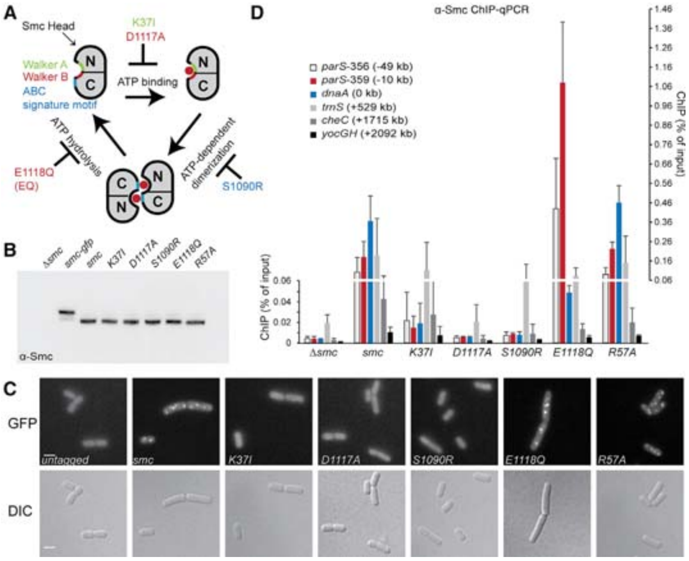

Figure 1. Smc ATPase Activity Determines the Chromosomal Distribution of Smc/ScpAB

(A) Schematic representation of the Smc ATPase cycle.

(B) Immunoblotting of ATPase mutant Smc proteins with α-Smc antiserum. Whole-cell extracts from strains BSG1002, BSG1007–BSG1008, BSG1067, BSG1045–BSG1047, and BSG1083. See also Figure S1B.

(C) Fluorescence images of cells harboring mGFP-tagged Smc alleles: BSG1002, BSG1067–BSG1068, BSG1855–BSG1857, and BSG1881. Scale bar, 2 μm. Differential interference contrast (DIC) (bottom) and GFP fluorescence images (top) are shown. Quantification of foci number per cell is given in Figure S1H.

(D) ChIP-qPCR analysis of cells from strains BSG1002, BSG1007–BSG1008, BSG1045–BSG1047, and BSG1083 using α-Smc antiserum. Error bars were calculated from two independent experiments as SD. Please note that values of ChIP enrichment below and above 0.06% are displayed on different scales given on the left and right side of the graph, respectively. The analysis of chromosomal loci harboring highly transcribed genes (such as the tRNA cluster *trnS*) generally produce ambiguous results with relatively high levels of ChIP signal in control samples (Δ*smc*). This seems to be a widely observed phenomenon in ChIP and it remains unclear whether the enrichment is physiologically relevant.

See also Figure S1.

chromosome. However, wild-type distribution of Smc on the bacterial chromosome—including its prominent localization to the replication origin—requires hydrolysis of ATP by Smc. Smc(R57A) showed a ChIP-qPCR pattern indistinguishable from wild-type Smc indicating that cellular ATP hydrolysis might be (if at all) only mildly affected by this amino-acid substitution in *B. subtilis*.

Smc/ScpAB Specifically Recognizes ParB/*parS* Nucleoprotein Complexes in Its Pre-hydrolysis State

To get a global view of the chromosomal distribution of Smc and Smc(EQ) proteins, we then analyzed ChIP input and eluate fractions by next-generation sequencing. Individual sequence reads were mapped to 1 kb sliding windows spaced at 100-bp intervals (Figure 2A) or to 5 kb bins (Figure 2C). In order to normalize for the copy number differences between origin-proximal and -distal loci caused by ongoing DNA replication, the ratio of the normalized number of reads in input and eluate fractions was calculated for each window. The resulting ChIP sequencing (ChIP-seq) profile for the Smc(EQ) sample showed striking peaks that are overlapping with several *parS* sites on the chromosome (Figure 2A). The profile of the wild-type sample is markedly different from the Smc(EQ) profile (Figure 2A) (Gruber and Errington, 2009). Its peaks at *parS* sites are less pronounced. Instead, other more prominent peaks are present at and near the replication origin (*oriC*) and generally more signal was detected all along the chromosome arms. Largely similar ChIP-seq results were obtained with an antiserum raised against the ScpB subunit (Figures S2 and 7A; discussed below), indicating that the observed enrichments are not caused by antibody artifacts and suggesting that substantial fractions of Smc and ScpB co-localize on the chromosome, presumably by forming Smc/ScpAB holo-complexes (Kleine Borgmann et al., 2013). ChIP-qPCR experiments using several primer pairs for chromosomal arm sites (Figure S2D) confirmed that Smc (but not Smc(EQ)) was significantly enriched at several positions on the two chromosome arms with levels of enrichment inversely correlating with distance from the replication origin. Together, these results confirm the specific localization of the Smc(EQ) protein to *parS* sites and strongly suggest that Smc head engagement is essential for Smc/ScpAB recruitment to the chromosome. However, a full cycle of ATP hydrolysis appears to be involved in the localization of Smc/ScpAB to other chromosomal sites—such as the replication origin and the chromosome arms (Figure 2A).

Furthermore, we found that the high levels of enrichment of Smc and Smc(EQ) at *parS-359* are fully dependent on the presence of ParB protein (Figure 3A). To compare the distribution of Smc and ParB proteins near *parS* sites, we next performed ChIP-seq analysis using an antiserum against the ParB protein. ChIP-seq peaks of ParB and Smc(EQ) (but not Smc) proteins at *parS* sites are very similar in terms of positioning and shape, strongly indicating that the two proteins are closely co-localized on chromosomal DNA (Figures 2A–2C and 2E).

In the absence of ScpA or ScpB, the Smc protein is non-functional and Smc-GFP fails to form foci in vivo (Lindow et al., 2002; Mascarenhas et al., 2002). We observed that the chromosomal

Please cite this article in press as: Minnen et al., Control of Smc Coiled Coil Architecture by the ATPase Heads Facilitates Targeting to Chromosomal ParB/*parS* and Release onto Flanking DNA, Cell Reports (2016), http://dx.doi.org/10.1016/j.celrep.2016.01.066

OPEN ACCESS
CellPress

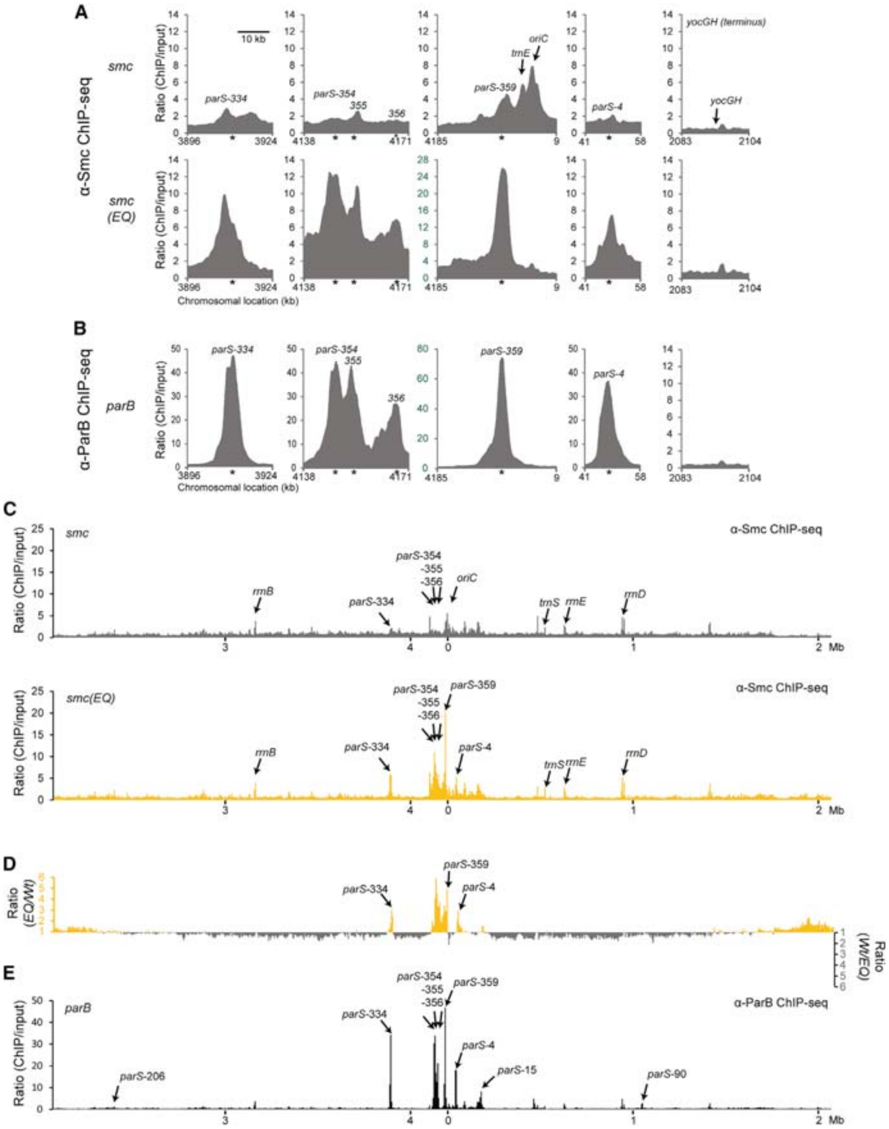

Figure 2. Hydrolysis Mutant but Not Wild-Type Smc Co-localizes with ParB/*parS*

(A) Close-up view of ChIP-seq profiles for wild-type Smc (BSG1002) (top panel) and Smc(EQ) (BSG1008) (bottom panel) generated using antiserum raised against the *Bs* Smc protein. Sequence reads were mapped to 1 kb windows spaced at 100-bp intervals and normalized for input DNA as follows. The number of reads for the ChIP sample in a given window was divided by the number of reads in the input sample for the same window (after normalizing the total number of reads). Raw input and ChIP data are shown in Figure S2. Axes labeled in green color highlights different scaling. Asterisks indicate the positions of *parS* sites.

(B) Close-up view of the ChIP-seq profile of ParB protein (from BSG1470 cells) generated using antiserum raised against purified *Bs*ParB-His6 protein. Data analysis and presentation as in (A).

(C) Whole-genome views of data presented in (A). Sequence reads were mapped to 5-kb windows spaced at 5-kb intervals across the genome and normalized for input DNA.

(legend continued on next page)

Please cite this article in press as: Minnen et al., Control of Smc Coiled Coil Architecture by the ATPase Heads Facilitates Targeting to Chromosomal ParB/*parS* and Release onto Flanking DNA, Cell Reports (2016), http://dx.doi.org/10.1016/j.celrep.2016.01.066

localization of wild-type Smc measured by ChIP-qPCR is strongly reduced when *scpA* or *scpB* is deleted (Figure 3B). Poor localization was also observed in Smc(EQ) cells in the absence of ScpA or ScpB. We thus conclude that ATP-dependent engagement of Smc heads as well as ScpA and ScpB proteins are crucial for efficient localization of Smc to ParB/*parS* on the chromosome. Apparently, a particular conformation of Smc/ScpAB recognizes ParB/*parS* nucleoprotein structures.

Dimerization at the Smc Hinge Controls Chromosomal Association of Smc/ScpAB

Next, we investigated the role of the Smc hinge domain in the localization of Smc/ScpAB to the bacterial chromosome. We made use of a previously characterized mutation of four highly conserved glycine residues to alanine at the *Bs* Smc hinge-hinge interface (designated as ''mH'' for mutant hinge) to block formation of stable dimers at the Smc hinge domain (Hirano and Hirano, 2002) (Figures S3C and S3D). The ChIP-qPCR enrichment of Smc(mH) was clearly reduced at *parS-359* as well as *dnaA* (Figure 3C). Dimerization of Smc at the hinge thus seems to be important for localization of wild-type Smc/ScpAB to the chromosome. This is consistent with the notion that Smc/ScpAB associates with the chromosome by entrapping the chromosomal DNA double helix within its SMC/kleisin ring (Wilhelm et al., 2015). In stark contrast, however, the enrichment of Smc(mH-EQ) protein at *parS-359* (but not at *dnaA*) was strongly enhanced (~4-fold) compared to Smc(EQ) (Figure 3C). Thus, hinge dimerization has strikingly antagonistic effects on the association of Smc and Smc(EQ) with the chromosome. Remarkably, ScpA and ScpB are dispensable for targeting of Smc(mH-EQ) to the chromosome (Figures 3C and S3H), while they are essential for wild-type Smc and Smc(EQ) to localize to the chromosome (Figure 3B). A plausible explanation for these striking observations is that the ScpAB sub-complex counteracts an inhibitory function of hinge dimerization on chromosomal targeting of Smc.

To ensure that these surprising findings are not caused by artifacts in the chromatin immunoprecipitation procedure, we have analyzed a set of Smc mutants by live-cell imaging of fluorescently labeled Smc proteins (Figure 3D). As predicted from the ChIP experiments, Smc(EQ)-GFP failed to form chromosomal foci when *scpA* is deleted, while Smc(mH-EQ)-GFP produced bright foci irrespective of the presence and absence of *scpA*. Together, these findings corroborate the view that Smc complexes associate with the bacterial chromosome in two fundamentally distinct manners, which are defined by the state of the Smc ATPase.

Smc Hinge Dimerization Inhibits Smc Head Engagement

How might the ScpAB sub-complex and dimerization at the Smc hinge control targeting of Smc to chromosomal *parS* sites in antagonistic ways? Conceivably, ScpAB and the Smc hinge might positively and negatively influence the engagement of Smc head domains, respectively, and thereby regulate the recruitment of Smc/ScpAB to *parS*. If so, then the levels of head engagement should correlate with the efficiency of chromosomal targeting. To address this, we made use of the efficient chemical cross-linking of closely juxtaposed pairs of cysteines by a thiol-specific bis-maleimide compound (BMOE) in *B. subtilis* (Bürmann et al., 2013; Soh et al., 2015). Based on the crystal structure of the *Pyrococcus furiosus* Smc(EQ) head dimer in the presence of ATP (Lammens et al., 2004), we engineered a cysteine residue into the bottom surface of the *Bs* Smc head (K1151C), so that it is located in close proximity to its pair mate at the 2-fold symmetry axis of the dimer (Figure 4A). In order to be able to precisely quantitate the levels of cross-linking, we fused the cysteine bearing *smc* gene at its C terminus with a HaloTag thus allowing in-gel fluorescence detection of Smc. In addition, the four endogenous cysteines in Smc were replaced by serine residues to reduce the propensity for any off-target cross-linking (Hirano and Hirano, 2006). The corresponding *smc* allele supports growth on nutrient rich medium, implying that it is functional (Figure S4A). Cross-linking of K1151C in otherwise wild-type Smc was barely detectable (<4%), while the ATP hydrolysis mutant Smc produced a low but substantial fraction (~14%) of cross-linked Smc dimers (Figure 4B). Intriguingly, K1151C cross-linking was undetectable in Smc(mH) but very pronounced in Smc(mH-EQ). The latter is cross-linked with an efficiency comparable to those previously observed for other Smc-Smc, Smc-ScpA, and DnaN-DnaN interfaces, which strongly suggests that the K1151C residue is a good reporter for head-head association (Bürmann et al., 2013; Soh et al., 2015; Wilhelm et al., 2015). The low levels of cross-linking observed with wild-type Smc and Smc(EQ) are therefore in most likelihood due to poor efficiency of head engagement. Deletion of *scpA* or *scpB* decreased the cross-linking of K1151C in Smc and Smc(EQ) protein even further (Figures 4B and S4B) being consistent with the notion that ScpAB might stimulate the targeting of Smc(EQ) to the chromosome (Figures 3B and S3H)—at least partly—by promoting head engagement (Bürmann et al., 2013; Kamada et al., 2013).

Smc head engagement must be a transient or rare phenomenon since it is barely detectable by cross-linking in wild-type Smc/ScpAB (Figure 4B). The maintenance of its association with the chromosome is thus very likely independent from continuous engagement of head domains. Smc head engagement, however, must be crucial during the establishment of chromosome association, because mutants defective in head engagement are unable to bind to the chromosome altogether. A stable association with the chromosome is likely created via the entrapment of chromosomal DNA within the Smc/ScpAB ring, a process that we have recently shown to be dependent on ATP hydrolysis (Wilhelm et al., 2015). We thus propose that Smc/ScpAB displays two distinct modes of binding to the

---

(D) To highlight differences between the distribution of wild-type Smc and Smc(EQ) the normalized ratios for Smc(EQ) in a given window was divided by the equivalent ratio for Smc(wt). Numbers above one are shown in yellow colors (axis on the left side). For numbers below one, the inverse ratio was calculated and displayed in gray colors (axis on the right side).
(E) Whole-genome view of the ParB ChIP-seq data presented in (B). Data analysis as in (C).
See also Figure S2.

Please cite this article in press as: Minnen et al., Control of Smc Coiled Coil Architecture by the ATPase Heads Facilitates Targeting to Chromosomal ParB/*parS* and Release onto Flanking DNA, Cell Reports (2016), http://dx.doi.org/10.1016/j.celrep.2016.01.066

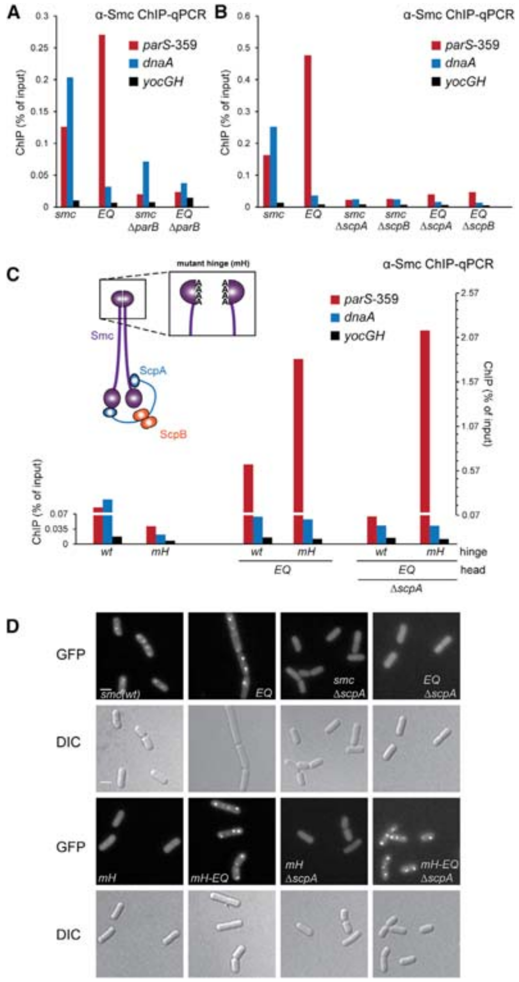

Figure 3. Dimerization at the Smc Hinge Hinders Chromosomal Association of Smc/ScpAB

(A) ChIP-qPCR was performed on exponentially growing cells of strains BSG1051–BSG1052, BSG1406, and BSG1387 using α-Smc antiserum. Quantification of input and eluate material was done by qPCR using primer pairs specific for the indicated loci.

(B) As in (A) using strains BSG1889–BSG1894.

(C) The scheme indicates the disruptive effect of mutations in the Smc hinge domain on dimerization. ChIP-qPCR was performed with α-Smc antiserum on strains BSG1620–BSG1621, BSG1624, BSG1890, and BSG1892–BSG1893.

(D) Fluorescence imaging of Smc-mGFP fusion proteins in cells of strains BSG1067–BSG1068, BSG1378, BSG1413, BSG1662, BSG1677, and BSG1798–BSG1799. Scale bar, 2 μm. Quantification of foci number per cell is given in Figure S4C. Same experiments as in Figure 1C.

See also Figure S3.

chromosome. The first one, designated as pre-hydrolysis mode, occurring mostly or exclusively at *parS* sites presumably via a physical interaction with the chromosome, has a strict requirement for Smc head engagement. The second one, generated by transient head engagement and subsequent ATP hydrolysis, designated as post-hydrolysis mode, features a much more dispersed distribution on the bacterial chromosome and likely involves the entrapment of one or more DNA double helices within the Smc/ScpAB ring.

Rod-Shaped Smc Dimers Poorly Target ParB/*parS*

The levels of head engagement in Smc, Smc(EQ), and Smc(mH-EQ) correlate well with their efficiency of targeting to *parS* on the chromosome (Figures 3C and 4B). However, when *scpA* is deleted, both Smc(EQ) and Smc(mH-EQ) display similarly low levels of head cross-linking, whereas Smc(mH-EQ) but not Smc(EQ) exhibits strong enrichment at *parS* on the chromosome (Figures 3C and 4B). We conclude that hinge dimerization must have additional effects on Smc(EQ), through which it restricts chromosomal targeting, and Smc head engagement—albeit being essential—is not sufficient for targeting of Smc/ScpAB to *parS* sites.

Smc dimers form straight rods via the close juxtapositioning of the Smc coiled coils (Soh et al., 2015). Upon Smc head engagement and DNA binding, however, they have been proposed to undergo an extensive conformational change to a more open, possibly ring-like configuration in vitro (Soh et al., 2015). Conceivably, this structural transition might also regulate the binding of Smc/ScpAB to ParB/*parS*. If this were the case, then any Smc mutant that efficiently targets to *parS* might harbor unstable Smc rods. To investigate this, we employed in vivo cross-linking of a cysteine residue (A715C) located at the hinge-proximal interface between the two Smc coiled coils as an indicator for the formation of Smc rods (Figure 4C) (Soh et al., 2015). As reported previously, ∼35% of wild-type Smc(A715C) proteins were cross-linked into covalent dimers by BMOE (Figure 4C). The mutant hinge strongly decreased the fraction of Smc dimers displaying coiled coil rods, irrespective of the presence or absence of ScpA protein (Figure 4C). Similarly, the E1118Q mutation lead to a significant reduction in the fraction of Smc dimers with rod-shaped coiled coils providing direct evidence that the ATPase cycle affects the architecture of the Smc coiled coils near the Smc hinge in vivo. Crucially, the partial dissolution of Smc(EQ) rods was lost when the *scpA* gene was deleted, whereas the more pronounced opening of the coiled coils in Smc(mH, EQ) was unaffected by *ΔscpA*. The ScpA subunit thus facilitates the opening of the Smc rod (Figures 4B and 4C). Altogether, these data strongly support the notion that dimerization at the Smc hinge promotes Smc rod formation, which in turn opposes head engagement. ScpA is required to antagonize rod-stabilization exerted by the Smc hinge and consistent with this notion it becomes dispensable for rod opening (and chromosomal targeting) in the absence of a functional hinge. Hence, a combination of two interrelated structural features seems to be responsible for the targeting of Smc/ScpAB to *parS* sites on the chromosome: (1) engagement of Smc head domains, and (2) dissolution of the Smc rod. Both features appear to be rare

Please cite this article in press as: Minnen et al., Control of Smc Coiled Coil Architecture by the ATPase Heads Facilitates Targeting to Chromosomal ParB/*parS* and Release onto Flanking DNA, Cell Reports (2016), http://dx.doi.org/10.1016/j.celrep.2016.01.066

OPEN ACCESS
CellPress

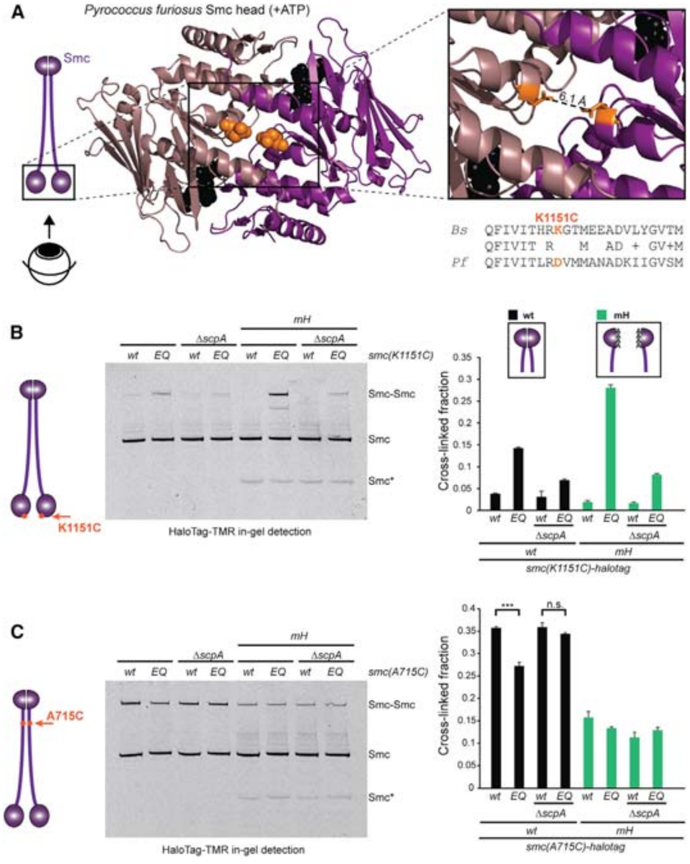

Figure 4. Hinge Dimerization and Head Engagement Control the Conformation of Smc/ScpAB

(A) Structure of ATP engaged *Pf* Smc head domains (PDB: 1XEX) in brown and pink colors, respectively, (bottom view). Residue D1131 is indicated in ball representation in orange colors (middle panel). The distance between the carboxyl carbon atom in the side chains of the D1131 symmetry mates is estimated to be ~6 Å (right panel). A sequence alignment between *Pf*Smc and *Bs*Smc shows that K1151 in *Bs*Smc corresponds to D1131 in *Pf*Smc.

(B) In vivo BMOE crosslinking of Smc(K1151C)-HaloTag in cells of strains BSG1488, BSG1509, BSG1512, BSG1547, BSG1597–BSG1598, BSG1791, and BSG1800. Four endogenous cysteine residues were replaced by serines. Cross-linked Smc-Halotag species were detected by in-gel fluorescence of the HaloTag-TMR substrate (left panel). Smc* indicates a degradation product of Smc(mH). The graph (right panel) shows mean values and SDs from three replicates.

(C) Same as in (B) using A715C as sensor cysteine for formation of Smc rods by the hinge proximal Smc coiled coil. In vivo crosslinking of Smc (A715C) with bismaleimidoethane (BMOE) in strains BSG1921–BSG1924, BSG1949–BSG1951, and BSG2036. T test statistics: ***p ≤ 0.001; not significant (n.s.), p > 0.05.

See also Figure S4.

or short-lived in wild-type Smc/ScpAB, presumably due to the inhibition by the hinge and the destabilizing action of the Smc ATPase. Nevertheless, a large fraction of cellular Smc/ScpAB must at least transiently adopt this conformation in order to localize to the replication origin region and to be able to form Smc-GFP foci in vivo (Figure 1) (Gruber and Errington, 2009; Sullivan et al., 2009).

Concomitantly, our A715C cross-linking experiments indicate that Smc coiled coils can be juxtaposed in a sizeable fraction of proteins even when dimerization at the Smc hinge is impaired, the ScpA bridge absent and Smc heads almost completely disengaged (Figure 4B). Thus, the association between Smc coiled coils contributes considerably to Smc dimerization.

The Smc Hinge Domain Is Dispensable for Targeting to *parS* DNA

A DNA binding site has previously been mapped to the bottom surface of the *Bs* Smc hinge dimer (Hirano and Hirano, 2006; Soh et al., 2015). DNA binding at the coils/hinge junction appears to be sterically blocked by the juxtapositioning of the Smc coiled coils and promoted by ATP-dependent dissolution of the Smc rod (Soh et al., 2015). The same mechanism could be responsible for the targeting of Smc/ScpAB to *parS* sites on the chromosome. If ParB/*parS*—like naked DNA—were to bind to the bottom of the Smc hinge dimer, then the presence of the hinge domain would be crucial for localization of Smc(EQ) to the chromosome. To test this, we constructed an Smc fragment lacking the entire hinge domain ("ΔH" for hinge deletion) by connecting the end of Smc's N-terminal coiled coil helix (amino acids 1–499) to the start of the C-terminal coiled coil helix (aa 674–1186) using a flexible linker peptide (-GGGSGGGSGGG-). The Smc(ΔH) construct was fused to a TAP tag at its C terminus and integrated at the endogenous *smc* locus. Smc(ΔH) was expressed at normal levels in *B. subtilis* but failed to localize to the chromosome as judged by α-TAP ChIP (Figures 5A and S5A). However, a Smc(ΔH) variant harboring the E1118Q mutation displayed robust localization to *parS*-359 in the presence and absence of the ScpA subunit (Figure 5A). Overall, strains harboring either a mutant Smc hinge domain or a complete deletion of the Smc hinge produced very similar results, clearly demonstrating that the Smc hinge is dispensable for the targeting of Smc(EQ) to *parS* (Figure 5A) and confirming that the hinge domain regulates chromosomal targeting indirectly—likely by affecting other parts of the Smc/ScpAB complex.

OPEN
ACCESS
CellPress

Please cite this article in press as: Minnen et al., Control of Smc Coiled Coil Architecture by the ATPase Heads Facilitates Targeting to Chromosomal ParB/*parS* and Release onto Flanking DNA, Cell Reports (2016), http://dx.doi.org/10.1016/j.celrep.2016.01.066

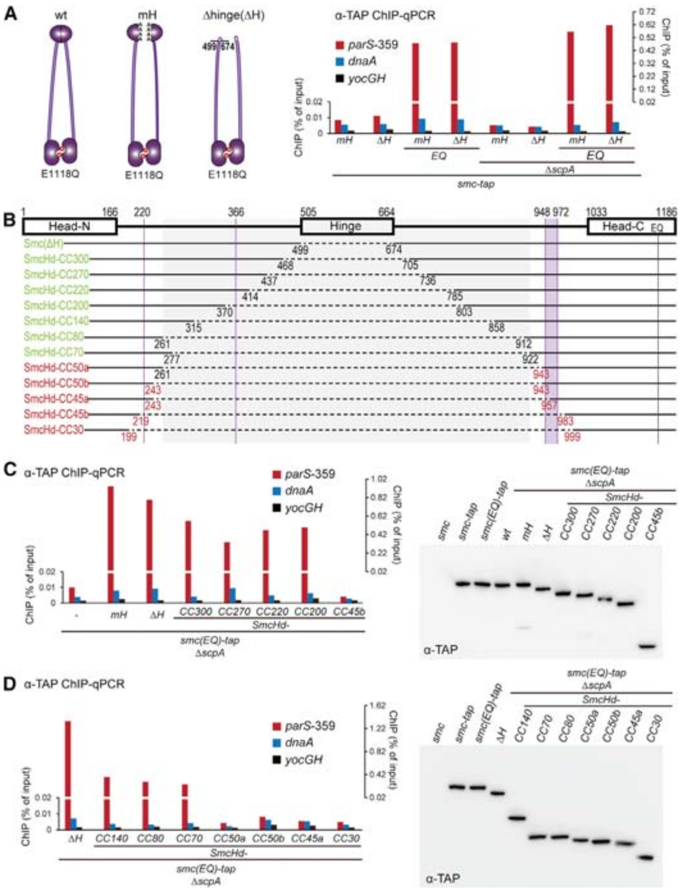

Figure 5. A Large Central Part of Smc Is Dispensable for Targeting to *parS*

(A) ChIP-qPCR was performed with TAP-tagged alleles of Smc using IgG-coupled magnetic beads for immunoprecipitation. Strains: BSG1671–BSG1672, BSG1689, BSG1691, BSG1779–BSG1780, and BSG1895–BSG1896. The schemes on top represent modifications to the Smc hinge in Smc(mH) (left) and Smc(ΔH) (right).

(B) Schematic overview of the series of internal Smc truncation constructs. Solid and dashed horizontal lines denote the presence and absence of Smc sequences in a given truncation construct. A gray box demarcates the central portion of the Smc protein, which is dispensable for targeting to *parS-359*. N-terminal and C-terminal Smc sequences are fused via a short peptide linker (-GGGSGGGSGGG-). The name of a given truncation construct indicates the predicted length of its Smc coiled coil. Labels in green and red colors indicate efficient and inefficient targeting to *parS*. All proteins are tagged with a TAP tag at their C terminus. Purple vertical lines and boxes indicate disruptions in the Smc coiled coil (Waldman et al., 2015).

(C) ChIP-qPCR against the TAP tag of strains BSG1520, BSG1689, BSG1779, BSG1825, BSG1871–BSG1872, and BSG1874–BSG1875 (left panel). Immunoblot against the TAP tag with strains BSG1002, BSG1016, BSG1475, BSG1520, BSG1689, BSG1779, BSG1825, BSG1871–BSG1872, and BSG1874–BSG1875 (right panel).

(D) Same as in (C) with another set of Smc truncation constructs. ChIP-qPCR with strains BSG1779, BSG1824, BSG1826–BSG1830 and BSG1873 (left panel). Anti-TAP immunoblot with strains BSG1002, BSG1016, BSG1475, BSG1779, BSG1824, BSG1826–BSG1830, and BSG1873 (right panel).

See also Figure S5.

A Mini-Smc Localizes to *parS* Sites on the Chromosome

The above results demonstrate that neither the Smc hinge nor the ScpA and ScpB subunits are strictly required for the localization of Smc(EQ) to *parS* sites. In order to fine map potential binding sites for ParB/*parS* on the Smc(EQ) protein, we removed increasingly larger segments of the central part of a Smc(EQ)-TAP allele by fusing selected N- and C-terminal Smc sequences using a short linker peptide (Figure 5B). Twelve such Smc fragments (designated as SmcHd-CC330 to SmcHd-CC30) were integrated into the endogenous *smc* locus by allelic replacement in a Δ*scpA* strain. All these truncated Smc(EQ) proteins were expressed at normal levels in *B. subtilis* as judged by immunoblotting against the TAP tag (Figures 5C and 5D). Intriguingly, the seven larger fragments (SmcHd-CC330–SmcHd-CC70) yielded strong and specific enrichment at the *parS-359* locus similar to the Smc(mH-EQ) and Smc(ΔH-EQ) proteins. In contrast, the five shorter constructs (SmcHd-CC50a– SmcHd-CC30) lacked any specificity for *parS-359* and instead displayed background levels of enrichment at all tested loci (Figures 5C and 5D). These results demonstrate that a large, central portion of Smc—comprising its hinge domain and approximately two-thirds of the hinge proximal coiled coil—is dispensable for the specific recognition of ParB/*parS*. A region located within the head proximal part of the Smc coiled coil, however, appears to be critical for *parS* targeting because even small truncations in this region totally abolish localization to *parS*. An Smc moiety critical for localization to *parS* thus appears to be located around hundred amino acid residues away from the Smc head domain on the Smc coiled coil. Mapping of the coiled coil register demonstrates that this head-proximal third of the Smc coiled coil includes a region in which the heptate register is interrupted in the N-terminal coiled coil helix and a 24 amino acid long peptide is inserted into the C-terminal α-helix (Figure S5D), (Waldman et al., 2015). Possibly, these extra sequences protrude from the Smc coiled coil and might be involved in the interaction with ParB protein and/or *parS* DNA. In the rod configuration, however, the protrusions might be sterically obstructed or otherwise masked.

Please cite this article in press as: Minnen et al., Control of Smc Coiled Coil Architecture by the ATPase Heads Facilitates Targeting to Chromosomal ParB/*parS* and Release onto Flanking DNA, Cell Reports (2016), http://dx.doi.org/10.1016/j.celrep.2016.01.066

Smc/ScpAB Relocates from *parS* Loading Sites to Distant Parts of the Chromosome in an ATP Hydrolysis-Dependent Manner

Smc/ScpAB exhibits very high specificity for *parS* sites on the bacterial chromosome when it is locked in its pre-hydrolysis conformation (Figures 1D and 2D). Nonetheless, only a small proportion of wild-type Smc/ScpAB actually localizes to *parS* sites in *B. subtilis* as judged from anti-ScpB and anti-Smc ChIP-seq profiles (Figures 2A and 6A). In fact, Smc/ScpAB rather displays a very broad distribution over the bacterial chromosome with a moderate peak at the replication origin and shallow gradients toward the replication terminus along both arms of the chromosome (Figures 6A and S2C) (Gruber and Errington, 2009). Formation of this long range gradient is completely abolished in the absence of ParB protein (Figure 6A). This raises the intriguing question of how a highly-localized pool of ParB protein might establish a very wide gradient of Smc/ScpAB on the chromosome. Conceivably, Smc/ScpAB might first load onto the chromosome at a *parS* site and then redistribute into neighboring and more distant regions of the chromosome. To test this, we modified the pattern of chromosomal recruitment of Smc/ScpAB by inserting a single additional *parS* site into the *B. subtilis* chromosome and observed changes in the chromosomal distribution of wild-type Smc/ScpAB. We inserted a 75-bp fragment of the *parB* gene including the *parS*-359 site or its non-functional variant, *mparS*, into the non-essential *amyE* gene located ~330 kb away from the replication origin on the right arm of the chromosome. The presence of the ectopic *parS* site at *amyE*, designated as *parS-amyE*, had no discernible effects on the growth of *B. subtilis*. We then tested whether the artificial *parS-amyE* locus serves as chromosomal landing site for Smc/ScpAB using ScpB ChIP-seq experiments in strains harboring the *smc(EQ)* gene (Figure S6). Efficient targeting of Smc(EQ) to *parS-amyE* suggests that also a significant fraction of wild-type Smc/ScpAB is loaded onto the chromosome at the synthetic *parS-amyE* locus (Figure S6). The pattern of wild-type Smc/ScpAB localization measured by ScpB ChIP-seq was superficially similar in cells harboring the ectoptic *parS* or *mparS* site (Figure 6B). However, the levels of ScpB enrichment were moderately—but consistently—higher for example in a region between the replication origin and the *amyE* locus when the additional *parS* site was present. In order to get a global and more quantitative picture of the differences between the two ChIP samples, we calculated enrichment ratios for each window along the chromosome (Figure 6B). Strikingly, the differences between the two samples followed a clear pattern with opposite trends on the two arms of the chromosome. Almost all loci on the right arm of the chromosome, which includes the ectopic *parS* site, were more highly enriched (on average by ~20%) in the *parS-amyE* sample, whereas DNA from the left arm of the chromosome was generally more enriched (~20%) in the *mparS* sample. Clearly, the addition of a single *parS* site at a defined position on the chromosome affects Smc distribution in a chromosome arm-specific manner. What might be the underlying molecular mechanism? Smc/ScpAB could relocate from *parS* by three-dimensional (3D) diffusion within a chromosomal domain or by one-dimensional (1D) translocation along the DNA backbone. 3D diffusion seems a highly unlikely explanation for intra-arm-specific relocation because loci on opposite chromosome arms are thought to be in close proximity in *B. subtilis* (Le et al., 2013; Marbouty et al., 2014, 2015; Umbarger et al., 2011; Wang et al., 2015). Our data is much more consistent with 1D translocation of Smc/ScpAB along a DNA double helix within a chromosome arm. According to this hypothesis, loading of Smc/ScpAB at the ectopic *parS* site might titrate condensin away from endogenous *parS* sites and thereby reduce loading on one arm of the chromosome, while increasing the fraction loaded onto the other. Curiously, the re-distribution of Smc complexes loaded onto the chromosome at the ectopic *parS* site appears to occur differently toward the replication origin and the terminus. In *B. subtilis*, most genes are co-oriented with respect to DNA replication. Thus, the apparent difference in relocation toward and away from the replication origin might be due to head-on encounters with transcription or replication complexes (Wang et al., 2015). Overall, these experiments provide evidence that Smc/ScpAB is able to translocate along a DNA double helix over large distances on the bacterial chromosome after its release from *parS* sites.

DISCUSSION

The mechanistic bases for SMC's dynamic association with chromosomes are in many ways mysterious. Here, we reveal that the Smc ATPase cycle defines two different configurations of Smc/ScpAB, which distinctly interact with the bacterial chromosome. The pre-ATP hydrolysis state displays high specificity for *parS* proximal DNA, whereas the specificity for *parS* is lost upon ATP hydrolysis leading to the redistribution of Smc/ScpAB within the chromosome.

Pre-ATP Hydrolysis Smc/ScpAB: A Tightly Regulated Configuration for ParB/*parS* Targeting

Our findings define the ATP engaged form of SmcHd(EQ)-CC80 as minimal structure for the specific recognition of Smc/ScpAB's chromosomal target (Figure 5). They highlight the importance of a head proximal segment of the Smc coiled coil in *parS*-DNA targeting and raise intriguing questions. How is binding of Smc/ScpAB to ParB/*parS*-DNA enabled by Smc head engagement? And conversely, how is physical association with the chromosome blocked when Smc heads are disengaged? Based on the strict dependence of *parS* targeting on Smc head engagement and its inverse correlation with Smc rod formation, we propose that a putative interface for ParB/*parS* on the head-proximal Smc coiled coil is concealed or distorted within the Smc rod. Smc head engagement might simply trigger the opening of the Smc rod and thereby unmask an interfaces for binding to ParB/*parS*. However, dimerization defective Smc proteins only very poorly localize to *parS* sites, despite featuring mostly "disengaged" Smc coiled coils (Figures 4 and 5). Conceivably, the interaction via a single interface on monomeric Smc is too transient for significant levels of targeting to *parS*. If so, then Smc head engagement might arrange the two interfaces on a given Smc dimer in a way that allows them to co-operatively and thus more stably bind a ParB protein/*parS* DNA complex. In this regard, it is tempting to speculate that DNA passes between the Smc coiled coils, because in this instance the 2-fold

Please cite this article in press as: Minnen et al., Control of Smc Coiled Coil Architecture by the ATPase Heads Facilitates Targeting to Chromosomal ParB/*parS* and Release onto Flanking DNA, Cell Reports (2016), http://dx.doi.org/10.1016/j.celrep.2016.01.066

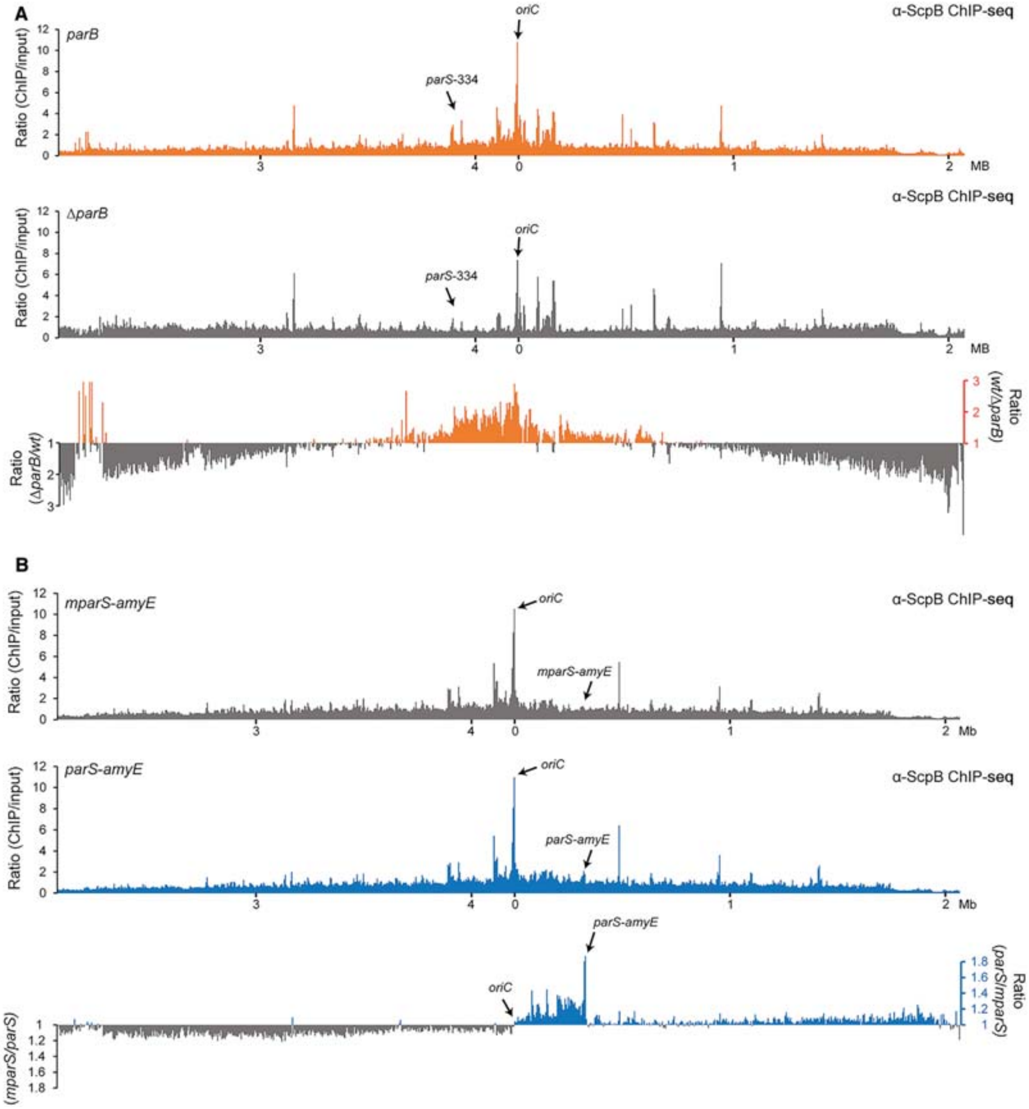

Figure 6. Smc/ScpAB Relocates from *parS* Loading Sites to Distant Parts of the Chromosome upon ATP Hydrolysis

(A) ChIP-seq using α-ScpB antiserum on strains BSG1002 (*parB*) (top panel) and BSG1052 (Δ*parB*) (middle panel). Reads were mapped to 5-kb bins. Signals for IP samples were divided by the signals of the normalized input. Ratios were calculated by dividing the values obtained for the wild-type strain by the numbers of the Δ*parB* strain (bottom panel). All values above one are shown in orange colors. For all other windows the inverse ratio was calculated and displayed in gray colors.

(B) ChIP-seq using α-ScpB antiserum on strains BSG1470 (*mparS-amyE*) (top panel) and BSG1469 (*parS-amyE*) (middle panel). Reads were mapped to 5-kb bins. Signals for IP samples were divided by the signals of the normalized input. Ratios were calculated by dividing the values of the *parS-amyE* strain by the *mparS-amyE* strain (bottom panel). A number above one indicates more reads in the *parS-amyE* sample (shown in the blue colors), for all other windows, the inverse ratios were calculated and displayed in gray colors.

See also Figure S6.

Please cite this article in press as: Minnen et al., Control of Smc Coiled Coil Architecture by the ATPase Heads Facilitates Targeting to Chromosomal ParB/*parS* and Release onto Flanking DNA, Cell Reports (2016), http://dx.doi.org/10.1016/j.celrep.2016.01.066

OPEN ACCESS
CellPress

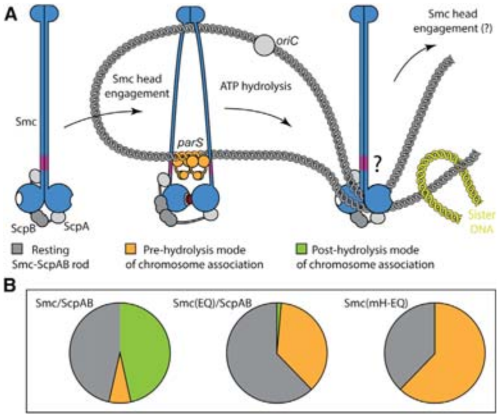

Figure 7. Model for the Recruitment of Smc/ScpAB to and Release from *parS* Sites

(A) Model for the targeting to and release from ParB/*parS* by holo-Smc/ScpAB. Most Smc/ScpAB exists as a rod-shaped structure, which is unable to bind to DNA via its hinge or to ParB/*parS* via the coiled coils. Dissolution of the Smc rod and engagement of Smc head domains are prerequisites for the targeting of Smc/ScpAB to *parS*. Upon ATP hydrolysis, the ring-like structure might revert to the rod conformation and is released from *parS* DNA. Sister DNA segments (in green colors) might be excluded from the Smc rod due to steric restrictions. Repetitive rod-ring-rod transitions might drive DNA loop extrusion.

(B) Pie charts displaying rough estimates for the relative occupancy of the different states illustrated in (A) based on Smc head cross-linking efficiency (Figure 4B). Please note that the fraction of wild-type Smc complexes on and off the chromosome (depicted as green and gray pies in the left chart) is unknown. A tiny fraction of chromosomally loaded Smc(EQ)/ScpAB has been detected (Wilhelm et al., 2015).

symmetry axis in the Smc dimer is matched to the one in ParB dimers. Binding of Smc to ParB/*parS*-DNA would therefore be restricted to the rare occasions when Smc head domains engage with one another to dissolve the Smc rod.

Although we have not been able to directly detect the recruitment of wild-type Smc to *parS* sites, at least three observations strongly suggest that wild-type Smc (like Smc(EQ)) is targeted to *parS* on the chromosome. First of all, the formation of chromosomal foci by wild-type Smc/ScpAB as well as its localization to the replication origin depend on ParB protein and *parS* sites (Gruber and Errington, 2009; Sullivan et al., 2009). Second, the efficiency of DNA entrapment by Smc/ScpAB is strongly decreased by the absence of ParB, indicating that most Smc/ScpAB is loaded onto the chromosome at *parS* sites (Wilhelm et al., 2015). Third, the chromosomal distribution of Smc is changed by an additional *parS* site. We propose that transient head engagement in Smc/ScpAB governs its brief encounters with chromosomal *parS* sites. It is important to note that the Smc(EQ) protein might display residual levels of ATP hydrolysis activity (Hirano and Hirano, 2004). It is thus conceivable that some observations made with Smc(EQ) such as its dependence on ScpAB during head engagement and *parS* localization and the inhibition by hinge dimerization might be specific to this partially defective ATP hydrolysis mutant. Furthermore, it is possible that the association of Smc(mH-EQ) (and Smc(EQ)/ScpAB) with ParB/parS might be structurally somewhat different from wild-type Smc/ScpAB.

Smc/ScpAB Relocation on the Bacterial Chromosome

The chromosomal distribution of Smc/ScpAB displays a single, broad peak centered on the replication origin and extending all the way to the replication terminus region (Figure 6A). Formation of such molecular gradients can be explained by a localized source of molecules and their random/diffusional or directed motion away from the source. Loading at *parS* establishes a tightly localized source of chromosomal Smc/ScpAB. Here, we present evidence for the subsequent relocation of Smc/ScpAB from its loading sites into flanking DNA. Our findings are consistent with the idea that Smc/ScpAB is able to translocate on the bacterial chromosome over hundreds of kilobases. Interestingly, cohesin has also been suggested to move away from its loading sites upon ATP hydrolysis possibly over several tens of kilobases (Hinshaw et al., 2015; Hu et al., 2011). What might be the purpose of such a striking and apparently conserved propensity for chromosomal relocation and what could be the molecular driving force?

The association of SMC complexes with chromosomes by DNA entrapment provides an obvious basis for a DNA sliding mechanism. Sliding of Smc/ScpAB rings along a single DNA molecule could help to identify and eliminate tangles within chromosomal DNA or between sister DNA molecules and thus promote chromosome segregation. However, this simple mechanism by itself fails to explain how Smc/ScpAB could organize the chromosome. Conceivably, Smc/ScpAB (like cohesin in eukaryotes) acts as a DNA clamp by capturing two or more DNA double helices within a single Smc/ScpAB ring or through the association of two or more Smc/ScpAB rings each entrapping a single DNA double helix. Taking into account the proposed DNA relocation activity, DNA loops could be formed by Smc/ScpAB and continuously expanded by the translocation of DNA through Smc/ScpAB rings. Extrusion of DNA loops—created at a *parS* site—explains how the left arm of the chromosome might be brought together with its right counterpart to establish the longitudinal organization of the chromosome observed in *Caulobacter crescentus* and *B. subtilis* (Le et al., 2013; Marbouty et al., 2014, 2015; Umbarger et al., 2011; Wang et al., 2015). Loop extrusion by SMC complexes also provides a simple solution for the formation of linearly condensed rod-shaped chromosomes during mitosis (Alipour and Marko, 2012; Bürmann and Gruber, 2015; Nasmyth, 2001). However, the driving force for any proposed relocation and loop extrusion mechanisms remains enigmatic. Smc/ScpAB appears to be able to translocate on the bacterial chromosome against the flow of replication forks and active transcription units, making a role of RNA polymerase and replication fork proteins in translocation unlikely (Figure 6) (Wang et al., 2015). Smc itself is an enzyme that could harbor energy from the hydrolysis of ATP to perform work. In principle, it could act as a motor protein for example by using its head engagement/disengagement cycle to progressively move DNA through its ring in a directional manner (Figure 7). For example, repetitive transitions between Smc rod

Please cite this article in press as: Minnen et al., Control of Smc Coiled Coil Architecture by the ATPase Heads Facilitates Targeting to Chromosomal ParB/*parS* and Release onto Flanking DNA, Cell Reports (2016), http://dx.doi.org/10.1016/j.celrep.2016.01.066

and Smc ring states might allow continuous expansion of loops of chromosomal DNA formed at *parS* (Figure 7) (Alipour and Marko, 2012; Nasmyth, 2001). Our data indeed suggest that ATP hydrolysis by Smc/ScpAB is involved in its chromosomal redistribution after loading. However, it remains to be determined whether continuous ATP hydrolysis by Smc is needed for relocation to distant positions on the chromosome or whether a single round of ATP hydrolysis is sufficient to trigger the relocation process.

The Mechanics of Smc Rod Making and Rod Breaking

We discovered an unexpected antagonistic functional relationship between the two globular domains located at distal ends of the long Smc coiled coil: dimerization at the Smc hinge has a clear inhibitory activity on the engagement of Smc head domains. Conversely, head engagement reduces the level of Smc coiled coil alignment. How might this long-distance communication happen mechanistically? We propose that the Smc coiled coil acts as rather stiff rod, which positions the Smc head in a way that is incompatible with ATP-dependent head engagement when the two Smc coiled coils are being aligned side-by-side. Dimerization of Smc hinge domains (“rod maker”) promotes Smc rod formation presumably by simply bringing the ends of two Smc coiled coils in close proximity in a way that allows them to zip up. Head engagement with the help of ScpAB (“rod breakers”), however, positions the two other ends of the Smc coiled coils at a distance to each other, thus favoring the unzipping of the Smc rod. In analogy, to the role of NBDs in ABC transporters, engagement and disengagement of Smc head domains might transform the Smc coiled coil between a rod-like state and a more open ring-like state. Only the open state appears to be able to contact DNA and the ParB/*parS* substrates via two separate interfaces located at the Smc hinge and within the head proximal coiled coil, respectively. Substrate binding is then likely triggering ATP hydrolysis, thereby driven head disengagement and rod re-formation, which in turn releases DNA and ParB/*parS* from its binding sites (Figure 7). We propose that transitions between open and closed states are central aspects of SMC biochemistry – conceivably regulating substrate binding to many or all SMC/kleisin complexes.

EXPERIMENTAL PROCEDURES

Strain Construction

Genetic modifications were introduced via double cross-over recombination into the genome of *B. subtilis 1A700*. Cells were made competent and grown on SMG or NA medium supplied with antibiotics as previously described (Bürmann et al., 2013). Relevant genotypes are given in Table S1.

ChIP-qPCR

ChIP-qPCR experiments were essentially performed as previously described (Gruber and Errington, 2009). Detailed information is available in the Supplemental Information.

ChIP-Seq

ChIP samples were prepared as described above with the exception that several immunoprecipitate (IP) samples were loaded onto the same PCR purification column to obtain sufficient DNA material. DNA (1–5 ng) was analyzed by Illumina sequencing at the Max Planck Genome Centre in Cologne. Briefly, DNA was fragmented by sonication (Covaris S2) to fragment sizes ranging from 220–280 bp with a main peak of ~250 bp. DNA libraries were prepared using the Ovation Ultralow Library System (NuGEN) kit (version V1) including 15 cycles of PCR amplification. Five to ten million sequence reads were obtained on a HiSeq2500 (Illumina) with 100-bp read length. The obtained reads were mapped to the genome with Bowtie (http://GalaxyProject.org) using default settings and randomly assigning sequencing reads from repetitive DNA elements to a single location. Subsequent data analysis was performed using Seqmonk (http://www.bioinformatics.babraham.ac.uk/projects/seqmonk/) and Microsoft Excel.

BMOE Cross-Linking

In vivo cross-linking of cysteine-modified Smc protein was performed as described previously (Soh et al., 2015).

Microscopy

Overnight cultures in SMG medium were diluted to an OD_{600} of 0.005 and grown to OD_{600} 0.02–0.03 in SMG medium. Cells were mounted on agarose pads and visualized on an Applied Precision DeltaVision RT system equipped with an Olympus IX-71 inverted base microscope, an Olympus UPlanApo 100 ×/NA1.35 oil immersion objective and a Photometrics CoolSNAP HQ 12 bit monochrome camera at the Imaging Facility of the Max Planck Institute of Biochemistry, Martinsried.

ACCESSION NUMBERS

The accession number for ChIP-seq data reported in this paper is GEO: GSE76949.

SUPPLEMENTAL INFORMATION

Supplemental Information includes Supplemental Experimental Procedures, six figures, and one table and can be found with this article online at http://dx.doi.org/10.1016/j.celrep.2016.01.066.

AUTHOR CONTRIBUTIONS

Strain Construction, A.M., L.W., and F.B.; Live-Cell Imaging, A.M. and L.W.; ChIP-qPCR, A.M. and L.W.; ChIP-Seq Experiments, A.M.; Cys Cross-Linking Experiments, F.B.; Exploratory ChIP-qPCR Experiments, A.A.; Mapping of the Smc Coiled Coil Register and Protein Purification, M.-L.D.-D; Conception and Interpretation of Experiments, A.M., F.B., and S.G.; Manuscript Preparation, A.M., F.B., L.W., and S.G.

ACKNOWLEDGMENTS

Next-generation sequencing (NGS) library preparation and sequencing was performed at the Max Planck-Genome-Centre Cologne. We thank Thomas Gerland and Verena Kuttenberger for strain construction and exploratory experiments. We are grateful to Stefan Jentsch for sharing equipment and the Max Planck Institute of Biochemistry core facility for SEC-MALS analysis. This work was supported by a European Research Council Starting Grant to S.G. (DiseNtAngle 260853) and the Max Planck Society. M.-L.D.-D. is supported by an EMBO long-term fellowship.

Received: September 23, 2015
Revised: December 22, 2015
Accepted: January 21, 2016
Published: February 18, 2016

REFERENCES

Alipour, E., and Marko, J.F. (2012). Self-organization of domain structures by DNA-loop-extruding enzymes. Nucleic Acids Res. *40*, 11202–11212.

Badrinarayanan, A., Reyes-Lamothe, R., Uphoff, S., Leake, M.C., and Sherratt, D.J. (2012). In vivo architecture and action of bacterial structural maintenance of chromosome proteins. Science *338*, 528–531.

Please cite this article in press as: Minnen et al., Control of Smc Coiled Coil Architecture by the ATPase Heads Facilitates Targeting to Chromosomal ParB/*parS* and Release onto Flanking DNA, Cell Reports (2016), http://dx.doi.org/10.1016/j.celrep.2016.01.066

OPEN ACCESS
CellPress

Britton, R.A., Lin, D.C., and Grossman, A.D. (1998). Characterization of a prokaryotic SMC protein involved in chromosome partitioning. Genes Dev. *12*, 1254–1259.

Bürmann, F., and Gruber, S. (2015). SMC condensin: promoting cohesion of replicon arms. Nat. Struct. Mol. Biol. *22*, 653–655.

Bürmann, F., Shin, H.C., Basquin, J., Soh, Y.M., Giménez-Oya, V., Kim, Y.G., Oh, B.H., and Gruber, S. (2013). An asymmetric SMC-kleisin bridge in prokaryotic condensin. Nat. Struct. Mol. Biol. *20*, 371–379.

Cuylen, S., Metz, J., and Haering, C.H. (2011). Condensin structures chromosomal DNA through topological links. Nat. Struct. Mol. Biol. *18*, 894–901.

Danilova, O., Reyes-Lamothe, R., Pinskaya, M., Sherratt, D., and Possoz, C. (2007). MukB colocalizes with the oriC region and is required for organization of the two Escherichia coli chromosome arms into separate cell halves. Mol. Microbiol. *65*, 1485–1492.

Gligoris, T.G., Scheinost, J.C., Bürmann, F., Petela, N., Chan, K.L., Uluocak, P., Beckouët, F., Gruber, S., Nasmyth, K., and Löwe, J. (2014). Closing the cohesin ring: structure and function of its Smc3-kleisin interface. Science *346*, 963–967.

Graumann, P.L., Losick, R., and Strunnikov, A.V. (1998). Subcellular localization of Bacillus subtilis SMC, a protein involved in chromosome condensation and segregation. J. Bacteriol. *180*, 5749–5755.

Gruber, S., and Errington, J. (2009). Recruitment of condensin to replication origin regions by ParB/SpoOJ promotes chromosome segregation in B. subtilis. Cell *137*, 685–696.

Gruber, S., Haering, C.H., and Nasmyth, K. (2003). Chromosomal cohesin forms a ring. Cell *112*, 765–777.

Gruber, S., Veening, J.W., Bach, J., Blettinger, M., Bramkamp, M., and Errington, J. (2014). Interlinked sister chromosomes arise in the absence of condensin during fast replication in B. subtilis. Curr. Biol. *24*, 293–298.

Haering, C.H., Löwe, J., Hochwagen, A., and Nasmyth, K. (2002). Molecular architecture of SMC proteins and the yeast cohesin complex. Mol. Cell *9*, 773–788.

Haering, C.H., Schoffnegger, D., Nishino, T., Helmhart, W., Nasmyth, K., and Löwe, J. (2004). Structure and stability of cohesin's Smc1-kleisin interaction. Mol. Cell *15*, 951–964.

Hinshaw, S.M., Makrantoni, V., Kerr, A., Marston, A.L., and Harrison, S.C. (2015). Structural evidence for Scc4-dependent localization of cohesin loading. eLife *4*, e06057.

Hirano, M., and Hirano, T. (2002). Hinge-mediated dimerization of SMC protein is essential for its dynamic interaction with DNA. EMBO J. *21*, 5733–5744.

Hirano, M., and Hirano, T. (2004). Positive and negative regulation of SMC-DNA interactions by ATP and accessory proteins. EMBO J. *23*, 2664–2673.

Hirano, M., and Hirano, T. (2006). Opening closed arms: long-distance activation of SMC ATPase by hinge-DNA interactions. Mol. Cell *21*, 175–186.

Hirano, M., Anderson, D.E., Erickson, H.P., and Hirano, T. (2001). Bimodal activation of SMC ATPase by intra- and inter-molecular interactions. EMBO J. *20*, 3238–3250.

Houlard, M., Godwin, J., Metson, J., Lee, J., Hirano, T., and Nasmyth, K. (2015). Condensin confers the longitudinal rigidity of chromosomes. Nat. Cell Biol. *17*, 771–781.

Hu, B., Itoh, T., Mishra, A., Katoh, Y., Chan, K.L., Upcher, W., Godlee, C., Roig, M.B., Shirahige, K., and Nasmyth, K. (2011). ATP hydrolysis is required for relocating cohesin from sites occupied by its Scc2/4 loading complex. Curr. Biol. *21*, 12–24.

Kamada, K., Miyata, M., and Hirano, T. (2013). Molecular basis of SMC ATPase activation: role of internal structural changes of the regulatory subcomplex ScpAB. Structure *21*, 581–594.

Kleine Borgmann, L.A., Ries, J., Ewers, H., Ulbrich, M.H., and Graumann, P.L. (2013). The bacterial SMC complex displays two distinct modes of interaction with the chromosome. Cell Rep. *3*, 1483–1492.

Lammens, A., Schele, A., and Hopfner, K.P. (2004). Structural biochemistry of ATP-driven dimerization and DNA-stimulated activation of SMC ATPases. Curr. Biol. *14*, 1778–1782.

Le, T.B., Imakaev, M.V., Mirny, L.A., and Laub, M.T. (2013). High-resolution mapping of the spatial organization of a bacterial chromosome. Science *342*, 731–734.

Lindow, J.C., Kuwano, M., Moriya, S., and Grossman, A.D. (2002). Subcellular localization of the Bacillus subtilis structural maintenance of chromosomes (SMC) protein. Mol. Microbiol. *46*, 997–1009.

Marbouty, M., Cournac, A., Flot, J.F., Marie-Nelly, H., Mozziconacci, J., and Koszul, R. (2014). Metagenomic chromosome conformation capture (meta3C) unveils the diversity of chromosome organization in microorganisms. eLife *3*, e03318.

Marbouty, M., Le Gall, A., Cattoni, D.I., Cournac, A., Koh, A., Fiche, J.B., Mozziconacci, J., Murray, H., Koszul, R., and Nollmann, M. (2015). Condensin- and replication-mediated bacterial chromosome folding and origin condensation revealed by Hi-C and super-resolution imaging. Mol. Cell *59*, 588–602.

Mascarenhas, J., Soppa, J., Strunnikov, A.V., and Graumann, P.L. (2002). Cell cycle-dependent localization of two novel prokaryotic chromosome segregation and condensation proteins in Bacillus subtilis that interact with SMC protein. EMBO J. *21*, 3108–3118.

Mascarenhas, J., Volkov, A.V., Rinn, C., Schiener, J., Guckenberger, R., and Graumann, P.L. (2005). Dynamic assembly, localization and proteolysis of the Bacillus subtilis SMC complex. BMC Cell Biol. *6*, 28.

Melby, T.E., Ciampaglio, C.N., Briscoe, G., and Erickson, H.P. (1998). The symmetrical structure of structural maintenance of chromosomes (SMC) and MukB proteins: long, antiparallel coiled coils, folded at a flexible hinge. J. Cell Biol. *142*, 1595–1604.

Minnen, A., Attaiech, L., Thon, M., Gruber, S., and Veening, J.W. (2011). SMC is recruited to oriC by ParB and promotes chromosome segregation in Streptococcus pneumoniae. Mol. Microbiol. *81*, 676–688.

Moriya, S., Tsujikawa, E., Hassan, A.K., Asai, K., Kodama, T., and Ogasawara, N. (1998). A Bacillus subtilis gene-encoding protein homologous to eukaryotic SMC motor protein is necessary for chromosome partition. Mol. Microbiol. *29*, 179–187.

Nasmyth, K. (2001). Disseminating the genome: joining, resolving, and separating sister chromatids during mitosis and meiosis. Annu. Rev. Genet. *35*, 673–745.

Schleiffer, A., Kaitna, S., Maurer-Stroh, S., Glotzer, M., Nasmyth, K., and Eisenhaber, F. (2003). Kleisins: a superfamily of bacterial and eukaryotic SMC protein partners. Mol. Cell *11*, 571–575.

Schwartz, M.A., and Shapiro, L. (2011). An SMC ATPase mutant disrupts chromosome segregation in Caulobacter. Mol. Microbiol. *82*, 1359–1374.

Shintomi, K., Takahashi, T.S., and Hirano, T. (2015). Reconstitution of mitotic chromatids with a minimum set of purified factors. Nat. Cell Biol. *17*, 1014–1023.

Soh, Y.M., Bürmann, F., Shin, H.C., Oda, T., Jin, K.S., Toseland, C.P., Kim, C., Lee, H., Kim, S.J., Kong, M.S., et al. (2015). Molecular basis for SMC rod formation and its dissolution upon DNA binding. Mol. Cell *57*, 290–303.

Soppa, J., Kobayashi, K., Noirot-Gros, M.F., Oesterhelt, D., Ehrlich, S.D., Dervyn, E., Ogasawara, N., and Moriya, S. (2002). Discovery of two novel families of proteins that are proposed to interact with prokaryotic SMC proteins, and characterization of the Bacillus subtilis family members ScpA and ScpB. Mol. Microbiol. *45*, 59–71.

Sullivan, N.L., Marquis, K.A., and Rudner, D.Z. (2009). Recruitment of SMC by ParB-parS organizes the origin region and promotes efficient chromosome segregation. Cell *137*, 697–707.

Umbarger, M.A., Toro, E., Wright, M.A., Porreca, G.J., Baù, D., Hong, S.H., Fero, M.J., Zhu, L.J., Marti-Renom, M.A., McAdams, H.H., et al. (2011). The three-dimensional architecture of a bacterial genome and its alteration by genetic perturbation. Mol. Cell *44*, 252–264.

Vallet-Gely, I., and Boccard, F. (2013). Chromosomal organization and segregation in Pseudomonas aeruginosa. PLoS Genet. *9*, e1003492.

Please cite this article in press as: Minnen et al., Control of Smc Coiled Coil Architecture by the ATPase Heads Facilitates Targeting to Chromosomal ParB/*parS* and Release onto Flanking DNA, Cell Reports (2016), http://dx.doi.org/10.1016/j.celrep.2016.01.066

Waldman, V.M., Stanage, T.H., Mims, A., Norden, I.S., and Oakley, M.G. (2015). Structural mapping of the coiled-coil domain of a bacterial condensin and comparative analyses across all domains of life suggest conserved features of SMC proteins. Proteins *83*, 1027–1045.

Wang, X., Tang, O.W., Riley, E.P., and Rudner, D.Z. (2014). The SMC condensin complex is required for origin segregation in Bacillus subtilis. Curr. Biol. *24*, 287–292.

Wang, X., Le, T.B., Lajoie, B.R., Dekker, J., Laub, M.T., and Rudner, D.Z. (2015). Condensin promotes the juxtaposition of DNA flanking its loading site in Bacillus subtilis. Genes Dev. *29*, 1661–1675.

Wilhelm, L., Bürmann, F., Minnen, A., Shin, H.C., Toseland, C.P., Oh, B.H., and Gruber, S. (2015). SMC condensin entraps chromosomal DNA by an ATP hydrolysis dependent loading mechanism in Bacillus subtilis. eLife *4*, 4.

Cell Reports, Volume *14*

Supplemental Information

Control of Smc Coiled Coil Architecture by the ATPase Heads Facilitates Targeting to Chromosomal ParB/*parS* and Release onto Flanking DNA

Anita Minnen, Frank Bürmann, Larissa Wilhelm, Anna Anchimiuk, Marie-Laure Diebold-Durand, and Stephan Gruber

I.) Supplemental Data

Figure S1 Expression, functionality and localization of ATPase mutant Smc proteins. Related to Figure 1.
(A) Colony formation assay using strains BSG1002, 1007, 1045, 1047, 1046, 1008 and 1083. Notably, Smc(EQ) mutant cells form colonies on minimal medium slightly more slowly than wild type or *smc* deletion mutants, suggesting that the mutant protein is mildly toxic when normal Smc function is lacking (Figure S1C, D) (Schwartz and Shapiro, 2011). The slow growth is likely due to a defect in replication origin segregation (Gruber et al., 2014; Schwartz and Shapiro, 2011; Wang et al., 2014), which provides a plausible explanation for the lower number of (replication origin-proximal) Smc foci in Smc(EQ) cells (see Figure S1H). (B) Protein extracts stained by Commassie Brilliant Blue. Immunoblotting of identical protein samples is shown in Figure 1B. (C) Same as in (A) with strains BSG1002, 1007, 1008, 1067, 1068 and 1855. (D) Immunoblotting of extracts from strains BSG1002, 1067, 1855, 1857, 1856, 1068, 1881, 1378, 1413, 1677, 1662, 1799 and 1798 with anti-GFP antiserum (top panel). SDS-PAGE of identical extracts stained by Commassie Brilliant Blue (bottom panel). (E) Immunoblotting against Smc protein using strains BSG1007, 1067, 1002, 1045, 1046, 1008, 2050, 2051. (F) Colony formation assay using strains BSG1002, 1007, 1045, 1046, 1008, 2050 and 2051. (G) ChIP-qPCR using anti-Smc antiserum on strains BSG1002, 1008, 1045, 1046, 2050 and 2051. (H) Quantification of Smc-GFP foci in strains shown in Figure 1C. Number of foci is displayed per unit cell length (µm). Standard deviation is derived from four different fields of view for each genotype. ‘n’ denotes the total number of individual cells counted.

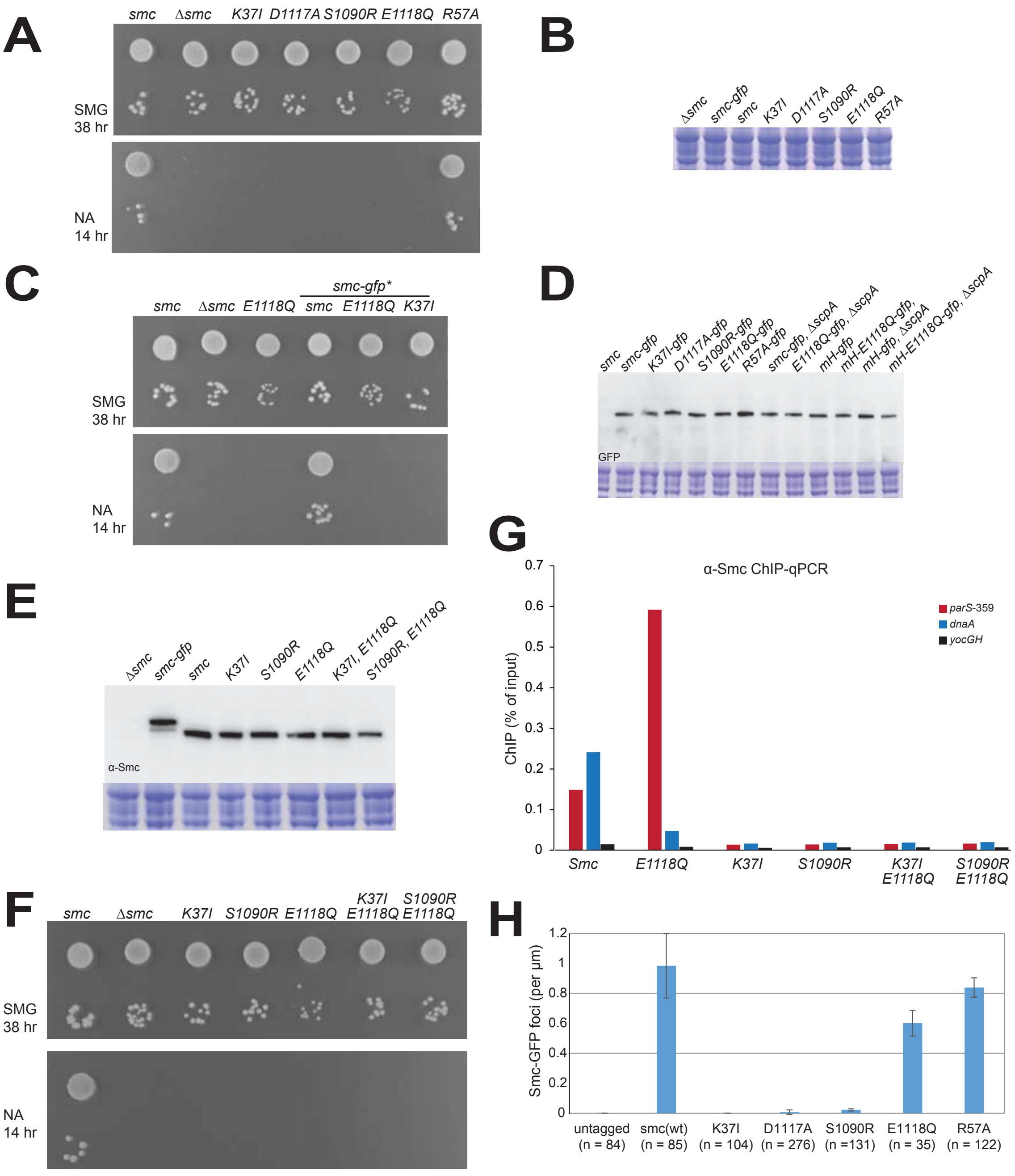
A
smc
Δsmc
K37I
D1117A
S1090R
E1118Q
R57A
SMG
38 hr
NA
14 hr
B
Δsmc
smc-gfp
smc
K37I
D1117A
S1090R
E1118Q
R57A
C
smc
Δsmc
E1118Q
smc-gfp*
smc
E1118Q
K37I
SMG
38 hr
NA
14 hr
D
smc
smc-gfp
K37I-gfp
D1117A-gfp
S1090R-gfp
E1118Q-gfp
R57A-gfp
smc-gfp, ΔscpA
E1118Q-gfp, ΔscpA
mH-gfp
mH-E1118Q-gfp,
mH-gfp, ΔscpA
mH-E1118Q-gfp, ΔscpA
GFP
E
Δsmc
smc-gfp
smc
K37I
S1090R
E1118Q
K37I, E1118Q
S1090R, E1118Q
α-Smc
F
smc
Δsmc
K37I
S1090R
E1118Q
K37I
E1118Q
S1090R
E1118Q
SMG
38 hr
NA
14 hr
G
α-Smc ChIP-qPCR
ChIP (% of input)
0.7
0.6
0.5
0.4
0.3
0.2
0.1
0
parS-359
dnaA
yocGH
Smc
E1118Q
K37I
S1090R
K37I
E1118Q
S1090R
E1118Q
H
Smc-GFP foci (per µm)
1.2
1
0.8
0.6
0.4
0.2
0
untagged
(n = 84)
smc(wt)
(n = 85)
K37I
(n = 104)
D1117A
(n = 276)
S1090R
(n =131)
E1118Q
(n = 35)
R57A
(n = 122)

Figure S1

Figure S2 Smc and ScpB ChIP-Seq in Smc and Smc(EQ) cells. Related to Figure 2.
(A) ChIP-Seq analysis of BSG1002 and 1008 using anti-Smc antiserum. Number of reads in 1 kb windows at 100bp intervals are shown for input (IN) and ChIP (IP) samples without prior normalization for input material. Normalized data of the same experiment is shown in Figure 2A and 2C. (B) ChIP-Seq analysis of strains BSG1470 and BSG1472 using anti-ScpB antiserum. Data analysis and display as in (A). (C) Whole-genome ChIP-Seq profile for anti-ScpB ChIP (on strain BSG1470), (also shown in Fgiure 7B; same experiment as in Figure S2B). Sequencing reads are put into 5 kb bins and normalized for input DNA. Please note the generally high degree of similarity between anti-Smc (Figure 2C) and anti-ScpB ChIP-Seq profiles with the ScpB profile possibly displaying a steeper gradient from the replicaton origin to the terminus (Kleine Borgmann et al., 2013). (D) Localization of Smc, Smc(S1090R) and Smc(E1118Q) to sites located on the chromosome arm analyzed by ChIP-qPCR using strains BSG1002, BSG1046 and BSG1008. Mean and standard deviation are calculated from three replicate experiments. Boxed insert displays results from the same experiment with "background" correction by subtraction of ChIP obtained with Smc(S1090R).

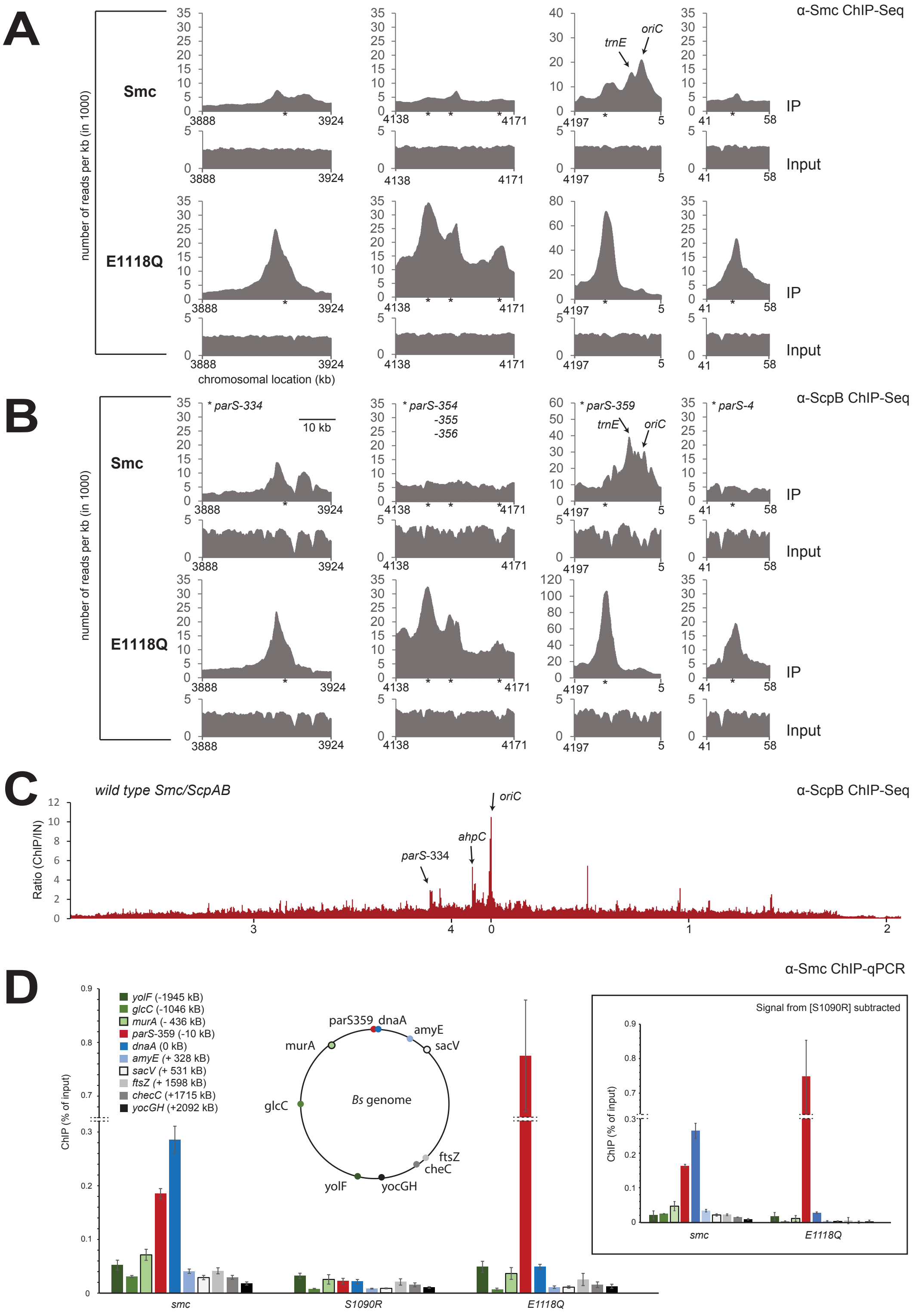
A
α-Smc ChIP-Seq
Smc
E1118Q
number of reads per kb (in 1000)
chromosomal location (kb)
3888
3924
4138
4171
4197
5
41
58
trnE
oriC
IP
Input
B
α-ScpB ChIP-Seq
* parS-334
10 kb
* parS-354
-355
-356
* parS-359
* parS-4
C
wild type Smc/ScpAB
Ratio (ChIP/IN)
parS-334
ahpC
oriC
D
α-Smc ChIP-qPCR
ChIP (% of input)
yolF (-1945 kB)
glcC (-1046 kB)
murA (- 436 kB)
parS-359 (-10 kB)
dnaA (0 kB)
amyE (+ 328 kB)
sacV (+ 531 kB)
ftsZ (+ 1598 kB)
checC (+1715 kB)
yocGH (+2092 kB)
parS359 dnaA
amyE
sacV
murA
glcC
Bs genome
ftsZ
cheC
yolF
yocGH
smc
S1090R
E1118Q
Signal from [S1090R] subtracted

Figure S2

Figure S3 Dimerization at the Smc hinge determines localization of Smc/ScpAB to *parS*. Related to Figure 3.

(A) Immunoblotting of cell extracts from strains BSG1007, 1067, 1002, 1051, 1406, 1052, 1387, 1890, 1893, 1889, 1891 and 1892 using anti-Smc antiserum. (B) Colony formation *Bs* strains BSG1007, 1008, 1889, 1892 and 1891 on minimal medium (SMG). (C) The hinge mutation (GGGG->AAAA) blocks dimerization of headless Smc protein (*Bs*SmcH-CC300). 40 µg of purified proteins was injected onto a gel filtration column and analyzed by multi-angle light scattering (SEC-MALS). Absorbance (at A_{280}) and light scattering is shown for wild-type and hinge mutant *Bs*SmcH-CC300 (curves in red and blue colours, respectively). (D) Analysis of the major peak (in A_{280} absorbance) in SEC-MALS (as in C) of wild-type and hinge-mutant *Bs*SmcH-CC300 indicates the existence of largely dimeric and monomeric protein species, respectively. (E) Immunoblotting of cell extracts from strains BSG1007, 1067, 1002, 1890, 1893, 1892, 1624, 1621 and 1620 using anti-Smc antiserum. (F) Colony formation of strains BSG1007, 1893, 1624, 1621, 1623 and 1620 on minimal medium (SMG). (G) Quantification of Smc-GFP foci in strains shown in Figure 3D. Number of foci is displayed per unit cell length (µm). Standard deviation is derived from four different fields of view for each genotype. ‘n’ denotes the total number of individual cells counted. (H) ChIP-qPCR analysis of strains BSG1893, 1892, 2144-2147 grown in SMG medium with anti-Smc antiserum.

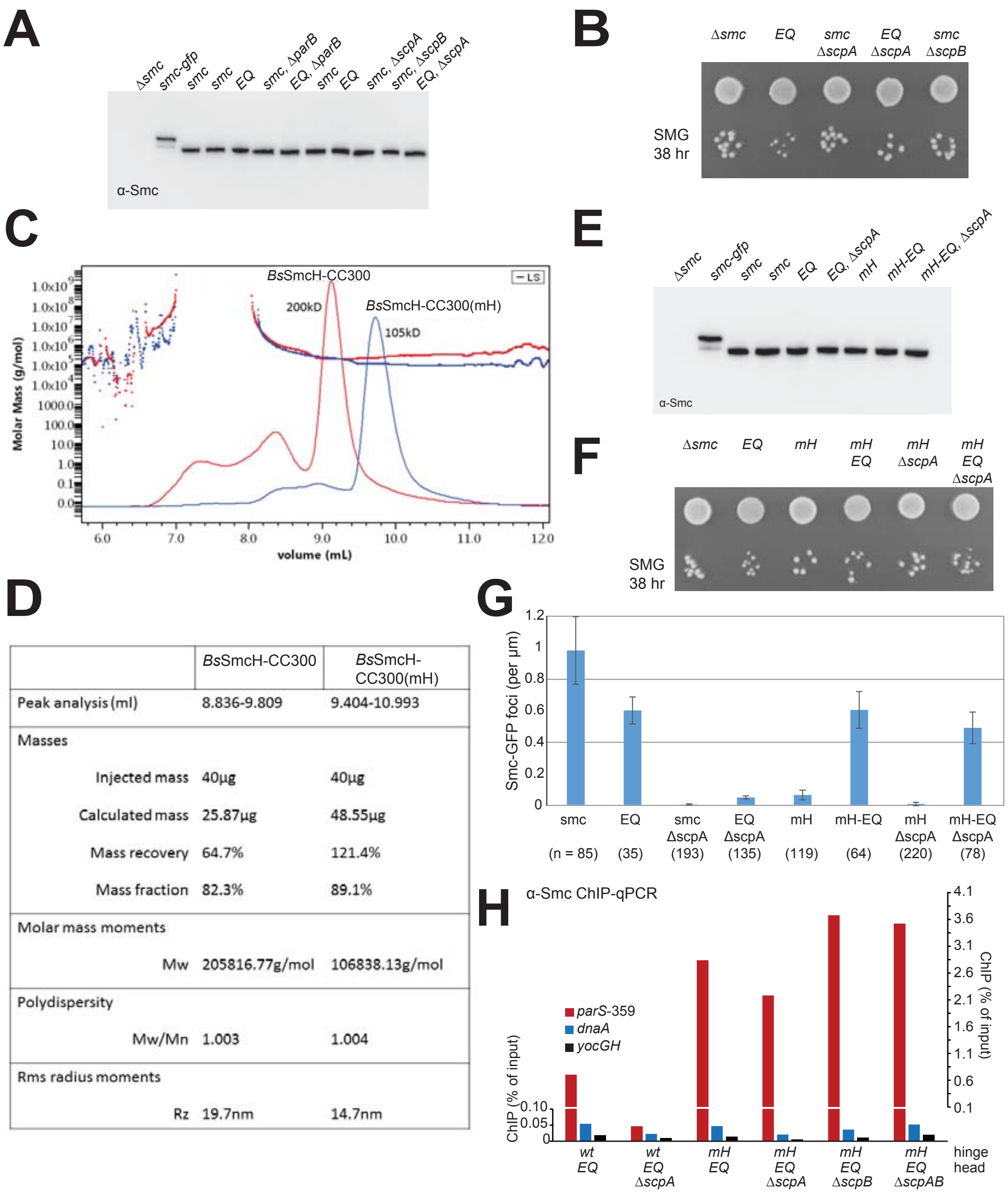

	*Bs*SmcH-CC300	*Bs*SmcH-CC300(mH)
Peak analysis (ml)	8.836-9.809	9.404-10.993
Masses		
Injected mass	40μg	40μg
Calculated mass	25.87μg	48.55μg
Mass recovery	64.7%	121.4%
Mass fraction	82.3%	89.1%
Molar mass moments		
Mw	205816.77g/mol	106838.13g/mol
Polydispersity		
Mw/Mn	1.003	1.004
Rms radius moments		
Rz	19.7nm	14.7nm

Figure S3

Figure S4 Smc(K1151C) –the reporter for head engagement– is functional. Related to Figure 4. (A) Colony formation of strains BSG1002, 1007, 1360 and 1457 on minimal medium (SMG) and nutrient rich medium (NA). (B) Cross-linking of Smc(K1151C) in BSG1607, 1488, 1512 and 1513 with BMOE. Mean values and standard deviation from triplicate experiments are shown.

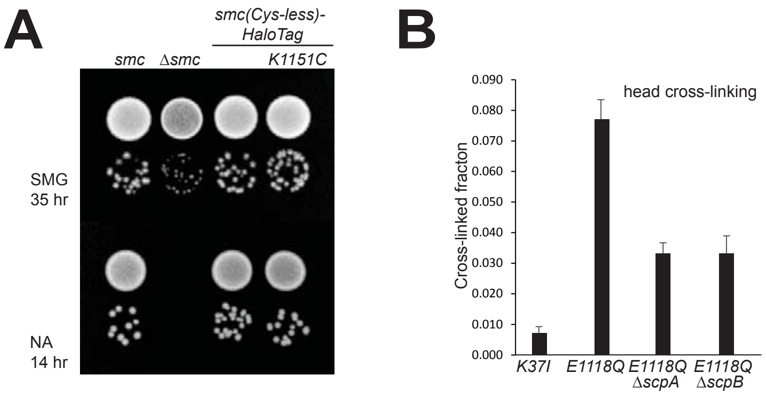
A
B
smc(Cys-less)-
HaloTag
smc
Δsmc
K1151C
SMG
35 hr
NA
14 hr
head cross-linking
Cross-linked fracton
0.090
0.080
0.070
0.060
0.050
0.040
0.030
0.020
0.010
0.000
K37I
E1118Q
E1118Q
ΔscpA
E1118Q
ΔscpB

Figure S4

Figure S5 Expression and functionality of hinge-less Smc protein. Related to Figure 5.
(A) Immunoblotting against the TAP tag on Smc in cell extracts from strains BSG1002, 1016, 1475, 1691, 1896, 1671, 1780, 1672, 1895, 1689 and 1779. Commassie staining of the same extracts is shown in the bottom panel. (B) Colony formation assay using strains BSG1007, 1008, 1626, 1619, 1896 and 1780. (C) Same as in (B) with strains BSG1002, 1007, 1008, 1520, 1689 and 1779. (D) Exemplary image of the SDS-PAGE analysis of disulfide cross-linked *Bs*SmcH-CC300 samples harboring pairs of cysteines as annotated. (E) Quantification of intra- and inter-molecular disulfide formation (after 4 hr incubation) from Commassie stained SDS-PAGE gels for 16 pairs of cysteine mutants. (F) Schematic view of the folding of the Smc coiled coil. Anchor points setting the register of the Smc coiled coils – established by *in vitro* disulfide formation (see D and E)– are given as dashed lines connecting N- and C-terminal helix. Disruptions in the coiled coil register were detected by Marcoil prediction. The length of extra sequences in the C-terminal coiled coil as given by the experimentally determined coiled coil register are indicated at the corresponding positions. Regions relevant for the targeting of mini-Smc to *parS* are highlighted by labels in red colours.

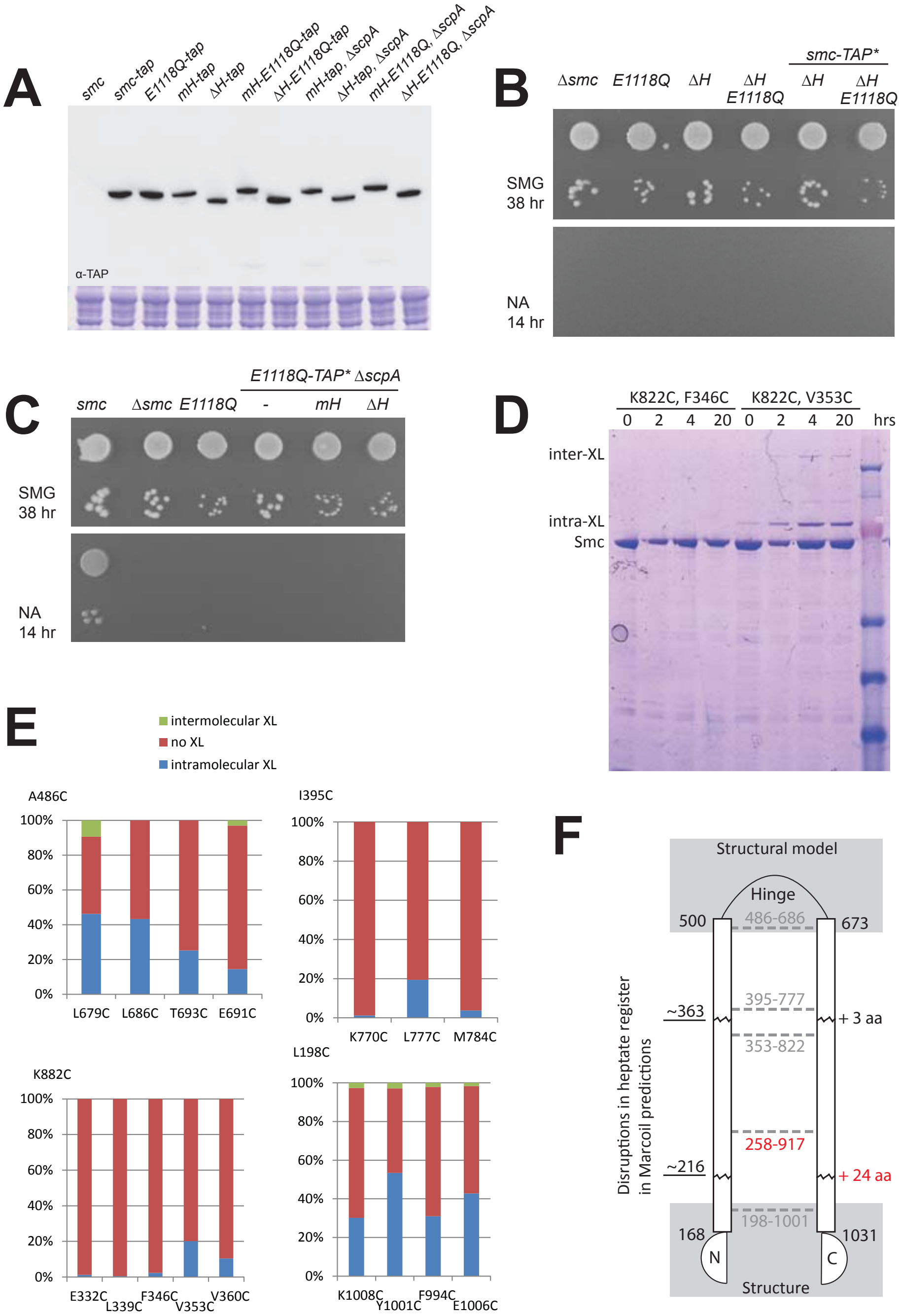
A
smc
smc-tap
E1118Q-tap
mH-tap
ΔH-tap
mH-E1118Q-tap
ΔH-E1118Q-tap
mH-tap, ΔscpA
ΔH-tap, ΔscpA
mH-E1118Q, ΔscpA
ΔH-E1118Q, ΔscpA
α-TAP
B
Δsmc
E1118Q
ΔH
ΔH E1118Q
smc-TAP*
ΔH
ΔH E1118Q
SMG 38 hr
NA 14 hr
C
E1118Q-TAP* ΔscpA
smc
Δsmc
E1118Q
-
mH
ΔH
SMG 38 hr
NA 14 hr
D
K822C, F346C
K822C, V353C
0
2
4
20
0
2
4
20
hrs
inter-XL
intra-XL
Smc
E
intermolecular XL
no XL
intramolecular XL
A486C
100%
80%
60%
40%
20%
0%
L679C
L686C
T693C
E691C
I395C
100%
80%
60%
40%
20%
0%
K770C
L777C
M784C
K882C
100%
80%
60%
40%
20%
0%
E332C
L339C
F346C
V353C
V360C
L198C
100%
80%
60%
40%
20%
0%
K1008C
Y1001C
F994C
E1006C
F
Structural model
Hinge
486-686
500
673
395-777
~363
+ 3 aa
353-822
258-917
~216
+ 24 aa
198-1001
168
1031
N
C
Structure
Disruptions in heptate register in Marcoil predictions

Figure S5

Figure S6 ChIP-Seq of Smc(EQ) to an ectopic *parS* site. Related to Figure 6.
Smc(EQ) is efficiently targeted to *parS-amyE*. ChIP-Seq analysis of BSG1471 (top panel) and BSG1008 (bottom panel) using anti-Smc antiserum. ChIP eluate sequence reads were mapped to 5 kb bins and normalized for input DNA. Please note that Smc(EQ) localization to endogenous parS sites is decreased by the presence of an extra *parS* site, being consistent with a titration effect. The bottom panel is identical to the bottom panel of Figure 2C.

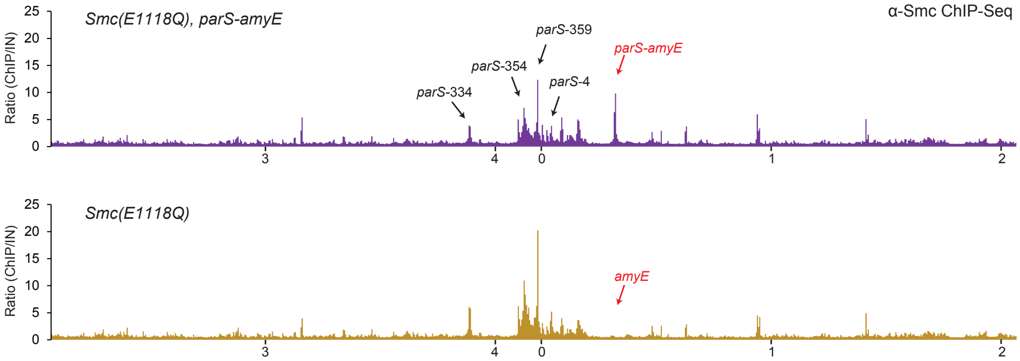
α-Smc ChIP-Seq
Smc(E1118Q), parS-amyE
Ratio (ChIP/IN)
25
20
15
10
5
0
parS-359
parS-amyE
parS-354
parS-4
parS-334
3
4
0
1
2
Smc(E1118Q)
Ratio (ChIP/IN)
25
20
15
10
5
0
amyE
3
4
0
1
2

Figure S6

Minnen, Bürmann et al., Cell Reports 2016 Targeting of Smc/ScpAB to the chromosome

II.) Supplemental Table

Supplemental Table 1 Genotypes

All strains are derivatives of *Bacillus subtilis* 1A700 provided by the BGSC (*Bacillus* Genetic Stock Center). All strains are auxotrophic for tryptophan (*trpC2*).

BSG1002	smc ftsY::ermB
BSG1007	Δsmc ftsY::ermB
BSG1008	smc(E1118Q) ftsY::ermB
BSG1016	smc-TAP ftsY::ermB
BSG1045	smc(K37I) ftsY::ermB
BSG1046	smc(S1090R) ftsY::ermB
BSG1047	smc(D1117A) ftsY::ermB
BSG1051	smc ftsY::ermB, parAB::kanR
BSG1052	smc ftsY::ermB, ΔparB::kanR
BSG1067	smc-mGFPmut1 ftsY::ermB
BSG1068	smc(E1118Q)-mGFP1mut1 ftsY::ermB
BSG1083	smc(R57A) ftsY::ermB
BSG1360	smc(C119S, C437S, C826S, C1114S)-TEV-His12-HaloTag(C61V, C262A) ftsY::ermB
BSG1378	smc-mGFPmut1 ftsY::ermB, specR::ΔscpA
BSG1387	smc(E1118Q) ftsY::ermB, ΔparB::kanR
BSG1406	smc(E1118Q) ftsY::ermB, parAB::kanR
BSG1413	smc(E1118Q)-mGFP1mut1 ftsY::ermB, specR::ΔscpA
BSG1457	smc(C119S, C437S, C826S, C1114S, K1151C)-TEV-His12-HaloTag(C61V, C262A) ftsY::ermB
BSG1469	smc ftsY::ermB, ΔamyE::parS-359::cat
BSG1470	smc ftsY::ermB, ΔamyE::mtparS-359::cat
BSG1471	smc(E1118Q) ftsY::ermB, ΔamyE::parS-359::cat
BSG1472	smc(E1118Q) ftsY::ermB, ΔamyE::mtparS-359::cat
BSG1475	smc(E1118Q)-TAP ftsY::ermB
BSG1488	smc(C119S, C437S, C826S, C1114S, K1151C, E1118Q)-TEV-His12-HaloTag(C61V, C262A) ftsY::ermB
BSG1509	smc(C119S, C437S, C826S, C1114S, K1151C)-TEV-His12-HaloTag(C61V, C262A) ftsY::ermB, specR::ΔscpA
BSG1512	smc(C119S, C437S, C826S, C1114S, K1151C, E1118Q)-TEV-His12-HaloTag(C61V, C262A) ftsY::ermB, specR::ΔscpA
BSG1513	smc(C119S, C437S, C826S, C1114S, K1151C, E1118Q)-TEV-His12-HaloTag(C61V, C262A) ftsY::ermB, specR::scpA ΔscpB
BSG1520	smc(E1118Q)-TAP ftsY::ermB, specR::ΔscpA
BSG1547	smc(G657A, G658A, G662A, G663A, E1118Q)-ftsY::ermB
BSG1597	smc(C119S, C437S, G657A, G658A, G662A, G663A, C826S, C1114S, K1151C)-TEV-His12-HaloTag(C61V, C262A) ftsY::ermB
BSG1598	smc(C119S, C437S, G657A, G658A, G662A, G663A, C826S, C1114S, E1118Q, K1151C)-TEV-His12-HaloTag(C61V, C262A) ftsY::ermB
BSG1607	smc(K37I, C119S, C437S, C826S, C1114S, K1151C)-TEV-His12-HaloTag(C61V, C262A) ftsY::ermB
BSG1619	rncS smc(1-499 GGGSGGGSGGG 674-1186, E1118Q) ftsY::ermB
BSG1620	smc(G657A, G658A, G662A, G663A, E1118Q)-ftsY::ermB, specR::ΔscpA
BSG1621	smc(G657A, G658A, G662A, G663A, E1118Q)-ftsY::ermB, specR::scpAB
BSG1624	smc(G657A, G658A, G662A, G663A) ftsY::ermB, specR::scpAB
BSG1626	rncS smc(1-499 GGGSGGGSGGG 674-1186) ftsY::ermB
BSG1662	smc(G657A, G658A, G662A, G663A, E1118Q)-mGFP-ftsY::ermB
BSG1671	smc(G657A, G658A, G662A, G663A, E1118Q)-TAP-ftsY::ermB, specR::scpAB
BSG1672	smc(G657A, G658A, G662A, G663A)-TAP ftsY::ermB, specR::ΔscpA
BSG1677	smc(G657A, G658A, G662A, G663A)-mGFP-ftsY::ermB

BSG1689	smc(G657A, G658A, G662A, G663A, E1118Q)-TAP ftsY::ermB, specR::ΔscpA
BSG1691	smc(G657A, G658A, G662A, G663A)-TAP ftsY::ermB, specR::scpAB
BSG1779	smc(1-499 GGGSGGGSGGG 674-1186, E1118Q)-TAP::ermB, specR::ΔscpA
BSG1780	smc(1-499 GGGSGGGSGGG 674-1186, E1118Q)-TAP::ermB, specR::scpAB
BSG1791	smc(C119S, C437S, G657A, G658A, G662A, G663A, C826S, C1114S, E1118Q, K1151C)-TEV-His12-HaloTag(C61V, C262A) ftsY::ermB, specR::ΔscpA
BSG1798	smc(G657A, G658A, G662A, G663A, E1118Q)-mGFP-ftsY::ermB, specR::ΔscpA
BSG1799	smc(G657A, G658A, G662A, G663A)-mGFP-ftsY::ermB, specR::ΔscpA
BSG1800	smc(C119S, C437S, G657A, G658A, G662A, G663A, C826S, C1114S, K1151C)-TEV-His12-HaloTag(C61V, C262A) ftsY::ermB, specR::ΔscpA
BSG1824	smc(1-199 GGGSGGGSGGG 999-1186, E1118Q)-TAP::ermB, specR::ΔscpA
BSG1825	smc(1-219 GPG 983-1186, E1118Q)-TAP::ermB, specR::ΔscpA
BSG1826	smc(1-243 GGGSGGGSGGG 957-1186, E1118Q)-TAP::ermB, specR::ΔscpA
BSG1827	smc(1-243 GGGSGGGSGGG 943-1186, E1118Q)-TAP::ermB, specR::ΔscpA
BSG1828	smc(1-261 GGGSGGGSGGG 943-1186, E1118Q)-TAP::ermB, specR::ΔscpA
BSG1829	smc(1-261 GGGSGGGSGGG 912-1186, E1118Q)-TAP::ermB, specR::ΔscpA
BSG1830	smc(1-277 GGGSGGGSGGG 922-1186, E1118Q)-TAP::ermB, specR::ΔscpA
BSG1855	smc(K37I)-mGFP1mut1 ftsY::ermB
BSG1856	smc(S1090R)-mGFP1mut1 ftsY::ermB
BSG1857	smc(D1117A)-mGFP1mut1 ftsY::ermB
BSG1871	smc(1-468 GGGSGGGSGGG 705-1186, E1118Q)-TAP::ermB, specR::ΔscpA
BSG1872	smc(1-437 GGGSGGGSGGG 736-1186, E1118Q)-TAP::ermB, specR::ΔscpA
BSG1873	smc(1-315 GGGSGGGSGGG 858-1186, E1118Q)-TAP::ermB, specR::ΔscpA
BSG1874	smc(1-370 GGGSGGGSGGG 803-1186, E1118Q)-TAP::ermB, specR::ΔscpA
BSG1875	smc(1-414 GGGSGGGSGGG 785-1186, E1118Q)-TAP::ermB, specR::ΔscpA
BSG1881	smc(R57A)-mGFP1mut1 ftsY::ermB
BSG1889	smc ftsY::ermB, specR::ΔscpA
BSG1890	smc ftsY::ermB, specR::scpAB
BSG1891	smc ftsY::ermB, specR::scpA ΔscpB
BSG1892	smc(E1118Q) ftsY::ermB, specR::ΔscpA
BSG1893	smc(E1118Q) ftsY::ermB, specR::scpAB
BSG1895	smc(1-499 GGGSGGGSGGG 674-1186)-TAP ftsY::ermB, specR::ΔscpA
BSG1896	smc(1-499 GGGSGGGSGGG 674-1186)-TAP ftsY::ermB, specR::scpAB
BSG1921	smc(C119S, C437S, A715C, C826S, C1114S)-TEV-His12-HaloTag(C61V, C262A) ftsY::ermB
BSG1922	smc(C119S, C437S, A715C, C826S, C1114S, E1118Q)-TEV-His12-HaloTag(C61V, C262A) ftsY::ermB
BSG1923	smc(C119S, C437S, G657A, G658A, G662A, G663A, A715C, C826S, C1114S)-TEV-His12-HaloTag(C61V, C262A) ftsY::ermB
BSG1924	smc(C119S, C437S, G657A, G658A, G662A, G663A, A715C, C826S, C1114S, E1118Q)-TEV-His12-HaloTag(C61V, C262A) ftsY::ermB
BSG1949	smc(C119S, C437S, A715C, C826S, C1114S)-TEV-His12-HaloTag(C61V, C262A) ftsY::ermB, specR::ΔscpA
BSG1950	smc(C119S, C437S, A715C, C826S, C1114S, E1118Q)-TEV-His12-HaloTag(C61V, C262A) ftsY::ermB, specR::ΔscpA
BSG1951	smc(C119S, C437S, G657A, G658A, G662A, G663A, A715C, C826S, C1114S)-TEV-His12-HaloTag(C61V, C262A) ftsY::ermB, specR::ΔscpA
BSG2036	smc(C119S, C437S, G657A, G658A, G662A, G663A, A715C, C826S, C1114S, E1118Q)-TEV-His12-HaloTag(C61V, C262A) ftsY::ermB, specR::ΔscpA
BSG2050	smc(K37I, E1118Q) ftsY::ermB
BSG2051	smc(S1090R, E1118Q) ftsY::ermB
BSG2144	specR::scpAB, smc(G657A, G658A, G662A, G663A, E1118Q)-ftsY::ermB
BSG2145	specR::ΔscpA, smc(G657A, G658A, G662A, G663A, E1118Q)-ftsY::ermB
BSG2146	specR::scpA ΔscpB, smc(G657A, G658A, G662A, G663A, E1118Q)-ftsY::ermB
BSG2147	specR::ΔscpAB, smc(G657A, G658A, G662A, G663A, E1118Q)-ftsY::ermB

III.) Supplemental Experimental Procedures

In vivo expression of Smc proteins tested by immunoblotting

Cells were grown in SMG at 37°C to an OD_{600} of 0.02-0.03, harvested by centrifugation or filtrations and washed once in 2 ml PBSG (PBS + 0.1% glycerol). The OD_{600} was measured and equivalent amount of cells for all samples were taken (0.02 ml*OD_{600}). Cells were resuspended in PBSG, ß-mercaptoethanol was added to a final concentration of 28.6 mM and kept on ice for 3 min. Lysozyme (12.8U/µl final), *Roche Complete* protease inhibitor cocktail and Benzonase (0.4 U/µl; Sigma-Aldrich) were added and the samples were incubated at 37°C for 20 min. NuPage LDS loading dye (final 1x) and DTT (final conc. 100 mM) were added and the samples incubated at 70°C for 10 min. The extracts were loaded on a 4-12% NuPAGE Bis-Tris gel run in MOPS buffer for 50 min at 200 V. Proteins were transferred to a PVDF membrane which was treated with α-Smc, α-GFP (Life Technologies, A6455) or Peroxidase Anti-Peroxidase (PAP). α-Smc and α-GFP blots were treated with ECL Anti-rabbit IgG, HRP-linked whole antibody (from donkey) (GE healthcare). The blots were incubated with Supersignal West Femto (Thermo Scientific) and were imaged in a LAS4000 scanner.

Chromatin immuno-precipitation (ChIP) and qPCR

Cells were grown in SMG medium at 37ºC overnight and diluted to OD_{600} 0.005 in SMG. At OD 0.02-0.03 40 ml of fixing solution (50mM Tris/HCl pH 8.0, 100mM NaCl, 1mM EDTA, 0.5mM EGTA, 11% formaldehyde) was added to 400 ml of culture and incubated at room temperature for 30 minutes. Cells were harvested by centrifugation or filtration and washed in 2 ml ice-cold PBS and OD_{600} was measured. Cells were resuspended in 1 ml TESS (50mM Tris/HCl 7.4, 10mM EDTA, 50mM NaCl, 500mM sucrose) and protoplasted by incubating in 1 ml TESS supplemented with 20mg/ml lysozyme (Sigma) and Roche Complete protease inhibitor cocktail for 30 min at 37°C shaking. Cells were washed once in 1 ml TESS, aliquoted according to the previously measured OD_{600} and stored at -80°C.

One aliquot of fixed cells was resuspended in 2 ml lysis buffer (50mM Hepes/KOH pH 7.5, 140mM NaCl, 1mM EDTA, 1% (v/v) Triton X-100, 0.1% (w/v) sodium deoxycholate, 100mg/ml RNase, *Roche Complete* protease inhibitor cocktail) and transferred to a 5 ml round-bottom tube. The samples were sonicated 3 x 20 sec on a Bandelin Sonoplus with a MS-72 tip at 90% pulse and 35% power output. Lysates were transferred into 2 ml tubes and centrifuged 5 min at 21000g and the supernatant subsequently 10 min at 21000g at 4°C.

200 µl of the cleared lysates was kept separate as the input sample. 50 µl Protein G coupled dynabead (Invitrogen) were incubated with 50 µl antibody serum (α-Smc, α-ScpB or α-ParB generated in rabbit) for at least 1 hr rotating at 4°C. Beads were washed in lysis buffer and added to 800 µl of the cleared lysates. For experiments involving TAP-tagged strains, rabbit IgG coupled to 50 µl magnetic DynaBeads (Epoxy, M-270) (prepared according to the manufacturer's protocol) was added to 800 µl cleared lysates. The beads with cleared lysates were incubated at 4°C rotating for 2-4 hours. Beads were washed once with each of the following buffers, lysis buffer, lysis buffer with high salt (500mM NaCl) and wash buffer (10mM Tris/HCl pH 8.0, 250mM LiCl, 1mM EDTA, 0.5% (w/v) NP-40, 0.5% (w/v) sodium deoxycholate). Beads were resuspended in 520 µl TES (50mM Tris/HCl pH 8.0, 10mM EDTA, 1% SDS), the input samples were combined with 300 µl TES and 20 µl 10% SDS solution and incubated overnight at 65°C shaking. DNA was purified by phenol chloroform extraction and ethanol precipitation. The DNA was dissolved in 100µl TE at 65°C for 20 min and purified on a Qiagen PCR purification column and eluted in 30 µl EB. For qPCR 4 µl of the input DNA (diluted 1:200) and IP samples (diluted 1:20) was used in a 10 µl reaction using 5 µl Takyon no ROX SYBR Mastermix blue dTTP (Eurogentec) and 1 µl primer pair stock solution (3 µM each primer) on a Qiagen Rotor-Gene Q in a 72 well rotor according to manufacturer's instructions. Primer sequences are given in the table below. Curves were analyzed by determining the maximum of the 2nd derivative using the Real-time PCR miner software (http://ewindup.info) (Zhao and Fernald, 2005). ChIP efficiencies were calculated as follows: [(IP/input)*100] for each primer pair.

List of primer pairs for qPCR:

parS-356	STG236	tgaaaagaatgcccatcaca
	STG237	tgcaagcaacaaccctttac
parS-359	STG097	aaaaagtgattgcggagcag
	STG098	agaaccgcatctttcacagg
dnaA	STG199	gatcaatcggggaaagtgtg
	STG200	gtagggcctgtggatttgtg
trnS	STG404	gggttttgacacccttggta
	STG405	aagcaaaaggaaatggctga
cheC	STG396	tttgcatgaactgggcaata
	STG397	tccgaacatgtccaatgaga
yocGH	STG099	tccatatcctcgctcctacg
	STG100	attctgctgatgtgcaatgg

Protein purification and SEC-MALS

Wild-type and hinge mutant *Bs*SmcH-CC300 protein (Smc residues 188-1011) were overexpressed from plasmid pnEA-tH in *E. coli* with an N-terminal HISx6 tag (Diebold et al., 2011). The proteins were purified via a HisTrap column, concentrated by anion-exchange chromatography (MonoQ HiTrap) and eluted from a size exclusion chromatography column (Superdex 200 10/300) in 200mM NaCl, 25mM Tris/HCl pH 7.4 (4°C). Multi-angle light scattering coupled to size exclusion chromatography (SEC-MALS) was performed as described previously (Soh et al., 2015).

Viability spotting assay

Cells were grown in SMG medium overnight into stationary phase, diluted 81-fold and 59049-fold (in 9x steps) and spotted on nutrient agar plates (Oxoid) or SMG agar plates. Plates were incubated at 37°C for ~12 hr on NA or ~36 hr on SMG agar.

Mapping of the *Bs* Smc coiled coil register by disulfide formation

Intramolecular crosslinking reactions for the determination of the coiled coil register were performed essentially as described in (Waldman et al., 2015) using the BsSmcH-CC300 construct (Soh et al., 2015). The protein was expressed from the pnEA-tH plasmid as a His-Tag fusion protein. For each double cysteine mutant, 50mL cultures were set-up. Cells were lysed by sonication and soluble extract was incubated for one hour with 300uL of Talon resin (Clontech). Beads were washed three times with the lysis buffer (200 mM NaCl, 50 mM NaPi pH7.4, 5 mM Imidazole) and then resuspended in the lysis buffer supplemented with 1 mM magnesium chloride. 1uL of benzonase (Roche) was added to the beads that were shaked for 30min at room temperature to remove the bound DNAs. The beads were washed two more times with the lysis buffer and the proteins were eluted with elution buffer 200 mM NaCl, 500 mM Imidazole, 50 mM NaPi pH7.4.

The proteins were then dialyzed against PBS buffer containing 4 mM DTT for 2 hours. For the crosslinking reaction, the protein was diluted to a concentration of 5 µM. The non-crosslinked sample was prepared by adding 1mM of iodoacetamide and heating at 70°C for 10 min. Disulfide formation was set-up by adding one volume of PBS supplemented with 5 mM $NaAsO_2$ (Fluka) to the protein and 100 µM dithio-bisnitrobenzoic acid DTNB (Merck) and 300 µM beta-mercaptoethanol. The reaction was incubated at 4°C under shaking. Samples were taken after 2, 4, 6 and 20h of reaction, and quenched by addition of 10 mM iodoacetamide at 70°C for 10 min.

After addition of non-reducing SDS-Page loading buffer the samples were boiled for 5 min at 95°C and run on a Bis-Tris 4-16% NuPage acrylamide gel (Novex) using MOPS buffer as running buffer for 50 min at 200 V.

IV.) Supplemental References

Diebold, M.L., Fribourg, S., Koch, M., Metzger, T., and Romier, C. (2011). Deciphering correct strategies for multiprotein complex assembly by co-expression: application to complexes as large as the histone octamer. Journal of structural biology *175*, 178-188.

Gruber, S., and Errington, J. (2009). Recruitment of condensin to replication origin regions by ParB/SpoOJ promotes chromosome segregation in B. subtilis. Cell *137*, 685-696.
Gruber, S., Haering, C.H., and Nasmyth, K. (2003). Chromosomal cohesin forms a ring. Cell *112*, 765-777.

Kleine Borgmann, L.A., Ries, J., Ewers, H., Ulbrich, M.H., and Graumann, P.L. (2013). The bacterial SMC complex displays two distinct modes of interaction with the chromosome. Cell reports *3*, 1483-1492.

Schwartz, M.A., and Shapiro, L. (2011). An SMC ATPase mutant disrupts chromosome segregation in Caulobacter. Molecular microbiology *82*, 1359-1374.

Soh, Y.M., Burmann, F., Shin, H.C., Oda, T., Jin, K.S., Toseland, C.P., Kim, C., Lee, H., Kim, S.J., Kong, M.S.*, et al.* (2015). Molecular basis for SMC rod formation and its dissolution upon DNA binding. Molecular cell *57*, 290-303.

Waldman, V.M., Stanage, T.H., Mims, A., Norden, I.S., and Oakley, M.G. (2015). Structural mapping of the coiled-coil domain of a bacterial condensin and comparative analyses across all domains of life suggest conserved features of SMC proteins. Proteins *83*, 1027-1045.

Wang, X., Tang, O.W., Riley, E.P., and Rudner, D.Z. (2014). The SMC condensin complex is required for origin segregation in Bacillus subtilis. Current biology : CB *24*, 287-292.

4. DISCUSSION

Since their last common ancestor, eukaryotic and prokaryotic SMC complexes gained specialized functions. In eukaryotes these were presumably distributed onto three different SMC complexes: Cohesin, condensin and Smc5/6. In contrast, most bacteria only encode for one SMC complex. It is fairly clear that SMC complexes play important roles in various chromosome-related processes in the cell. But are there still many features being shared between prokaryotes and eukaryotes? We still do not have a complete view into all of their functions and moreover, detailed insights into their molecular action. For example, it is still unclear what exact role Smc-ScpAB plays in chromosome segregation and organization.

We have most data on the function of cohesin. One of its major roles is to establish sister chromatid cohesion by entrapping sister chromosomes inside its ring (reviewed in: Nasmyth & Haering, 2009). Based on this finding various studies mostly in *S. cerevisiae* but also in other eukaryotes investigated the mechanistic details of entrapment and hence other characteristics of SMC complexes were discovered. It is therefore a key question how SMC complexes interact with the chromosome. Before I addressed this question in my thesis, it was unclear if the ability to entrap DNA was a conserved feature between prokaryotes and eukaryotes. The answer to this question is important not only to obtain mechanistic insights on the chromosomal interaction of Smc-ScpAB but also to assess its functional implications. I therefore developed the chromosome entrapment assay. Entrapment has never been assessed using physiologically relevant DNA templates so far. With my assay we are able to look directly at the interaction of proteins with whole chromosomes, which comprises a novel approach (Wilhelm et al., 2015).

In this discussion I will briefly introduce the entrapment assay I developed. I will critically discuss its advantages and disadvantages and compare it to the mini-chromosome assays that have been used to study the entrapment of cohesin and condensin. I will then change from a technical view on the assay to a functional view on the biological relevance of my data and will also compare it to our current knowledge about the eukaryotic SMC complexes. Lastly, I will discuss the implications of my work for the field of SMC research.

4.1. DEVELOPMENT OF A CHROMOSOME-ENTRAPMENT ASSAY

The details on how the entrapment assay was established and how certain steps in the assay are carried out can be found in the first publication part of this thesis (Wilhelm et al., 2015).

In summary, the tripartite ring formed by Smc-ScpAB is specifically cross-linked *in vivo* in a *B. subtilis* culture that is in its exponential growth phase. Importantly, this likely should not alter any interaction with the chromosome as the reaction specifically cross-links within the protein complex and not between DNA and proteins. Complexes entrapping the chromosome inside a ring will be locked in this entrapped state. The chromosome is embedded in an agarose matrix, such as performed for samples subjected to Pulsed-Field Gel Electrophoresis ('PFGE') (Nassonova, 2008). Cells are lysed within the agarose matrix ('agarose plug') and the agarose plug is subjected to harsh protein denaturing conditions. Physical interactions with the chromosome are lost upon denaturation. DNA entrapping proteins will also be denatured, however, cross-links at the Smc-ScpAB ring interfaces stay intact. These proteins will stay on the chromosome, inside the agarose plug and will be specifically isolated. Subsequently these proteins are released by digestion of the bacterial chromosome. In the final steps of the entrapment assay the protein fraction is separated from the agarose, concentrated and loaded onto a SDS-PAGE gel. Only proteins that had entrapped the chromosome should thus be detected in this final gel.

4.1.1. LOCKING SMC-SCPAB RINGS *IN VIVO*

How can Smc-ScpAB rings be locked? As first introduced by Bürmann et al. 2013, residues at the three interfaces of Smc-ScpAB that form the tripartite Smc-ScpAB ring can be specifically cross-linked using the bismaleimide crosslinker bismaleimidoethane ('BMOE'). To do so, pairs of residues at these interfaces need to be mutated to cysteines (*see* **Figure 4.1**): At the 'Cap'-interface: Smc(S19) and ScpA(H235); at the 'Neck'-interface: Smc(R1032) and ScpA(E52); and at the 'Hinge'-interface: Smc(R558, N643). BMOE specifically links two closely juxtaposed sulfhydryl groups, such as present in pairs of cysteine residues. The cross-linker generates a stable and specific thioether linkage between cysteines that are closer than 8Å. Wild-type Smc contains four native cysteines in *B. subtilis* (C119, C437, C826, C1114) while wild-type ScpA contains none. The Smc cysteines are not in close distance to other cysteines. Unwanted linkages between native residues by BMOE do thus apparently not occur. Therefore we did not exchange the endogenous cysteine residues in Smc to generate a 'cysteine-less' version of the protein for the development of the entrapment assay, however, for an experiment in the second publication, where quantification of cross-linking was crucial, such a strain was generated (***see* Figure 4** in Minnen et al. 2016). Loss of function effects by the cysteine mutations were excluded by performing 'viability assays'. In these assays growth of *B. subtilis* strains on nutrient-rich growth medium is assessed as well as their colony sizes on minimal medium.

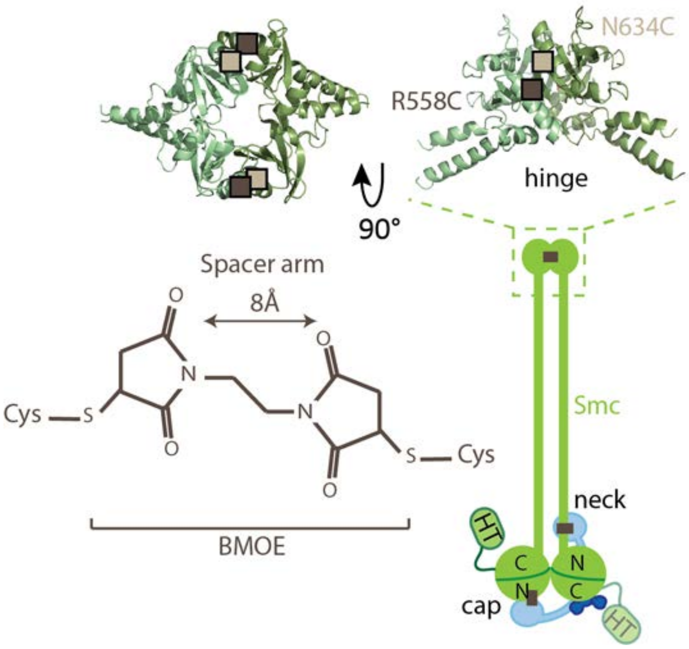

Figure 4.1: Cross-linking the Smc-ScpAB ring. For the entrapment assay residues at the cap, neck and hinge interfaces were mutated to cysteines and cross-linked using BMOE (brown squares). In the crystal structure of the *Thermotoga maritima* hinge (PDB: 1GXL) the R558C mutation (dark brown) and N634C mutation (light brown) are labelled. In each Smc hinge domain, two residues at the dimerization interface were mutated to cysteines. BMOE has a spacer of 8Å in length between two maleimide groups. The Smc protein was C-terminally tagged with a HaloTag (HT).

Strains containing mutations that render the protein dysfunctional are not able to grow on nutrient-rich medium anymore (Bürmann et al., 2013; Minnen et al., 2016; Wilhelm et al., 2015). Moreover, in most strains used in **chapter 3.1** the Smc protein has been C-terminally tagged with the HaloTag (Los et al., 2008). The HaloTag is a mutant version of a bacterial haloalkane dehalogenase that covalently links itself to synthetic ligands linked to moieties such as fluorescent dyes, solid surfaces or affinity molecules such as biotin. The HaloTag has a size of 33 kDa and is therefore rather big when compared to ScpA (29 kDa), DnaN (42 kDa) or even Smc (135 kDa). It has been excluded that the tag grossly affects the proteins function by performing viability assays. The advantage of using HaloTag over Western Blotting is the possibility of precise quantification of proteins. The HaloTag binds a (fluorescent) ligand covalently, one ligand per HaloTag. This enables direct and precise quantification of the tagged protein. Western Blotting, however, largely relies on the blotting efficiency. It cannot be excluded that large cross-linked species are blotted incompletely on the membrane, which would compromise a precise relative quantification of cross-linked species.

4.1.2. EFFICIENCY OF CROSS-LINKING

Key steps in the entrapment assay include cross-linking of Smc-ScpAB rings, embedding the chromosome into the agarose matrix and the specific removal of non-entrapping species during the SDS-PAGE wash.

Cross-linking any protein-protein interaction by BMOE is not achieved with 100% efficiency. The major reason for this is likely a competing reaction attaching the two cysteines to different BMOE molecules.

As we add an excess of BMOE to the cells, the probability is high that an individual BMOE molecule binds to an individual cysteine. This possibly impedes the formation of a high number of cross-links between the cysteine pairs. Therefore incompletely cross-linked Smc-ScpAB rings will be generated (*see* **Figure 2B** in Wilhelm et al 2015). Importantly, only one species – the Smc-ScpAB ring – becomes specifically enriched in the entrapment assay, thus providing additional evidence for the specificity of the assay.

The Smc protein alone has a size of 135 kDa, tagged with HaloTag this gives a protein of approximately 168 kDa in size for monomeric Smc-HaloTag. For the Smc-ScpAB ring the calculated molecular weight is 366 kDa. Proteins of such a size are not easily separable on standard SDS-PAGE gels. Moreover, the complexes differ in their physical shape and cross-linking intermediates will display a mixture of large di- or trimeric linear proteins, X-shaped molecules and a circular protein. Circular proteins move differently than linear proteins in a SDS-PAGE gel (Aaij and Borst, 1972). In order to be able to separate all the cross-linked species of large size we used gels with an acrylamide gradient from 3-8% and let them run for 2.5 hours at 4°C to obtain maximum separation (Gligoris et al. 2014). Under these conditions we were able to identify and analyze most Smc-ScpAB cross-linking species. Unfortunately still some species such as the Smc-ScpAB ring were overlapping with others. This is a major disadvantage and makes it impossible to exactly quantify the efficiency of the chromosome entrapment by Smc-ScpAB.

4.1.2.1. CROSS-LINKING REVERSAL

Are BMOE cross-links stable? A topological entrapment (*see* **chapter 4.1.5**) should be lost upon opening of the Smc-ScpAB ring such as by proteolytic cleavage, linearization of the chromosome or cross-link reversal. The two former cases have largely been excluded for Smc-ScpAB by the optimization of the assay.

A challenging aspect of the assay's development were small amounts of partially cross-linked species that were more or less consistently detected in the assay. In theory, the output sample of the entrapment assay should only contain one cross-linked protein species that is the fully cross-linked Smc-ScpAB tripartite ring. However, some levels of intermediate cross-links were observed in the output gel. Those species corresponded mostly to a Smc_2-ScpA trimer having lost one cross-link at either hinge, cap or neck interface. These intermediate species are also formed during the cross-linking reaction but are efficiently eliminated during the assay as demonstrated by the control samples lacking one out of six cysteines for cross-linking. Therefore the intermediate species observed in the output gel have to have emerged from fully cross-linked rings. One possible reason could be partial cross-link reversal.

As discussed before, the entrapment assay is based on cysteine cross-linking with BMOE. The cross-linker consists of two maleimides that are linked thereby generating a bridge of 8Å in size (*see* **Figure 4.1**). The maleimides specifically form covalent linkages with sulfhydryl groups at physiological pH values of 6.5 to 7.5 (room temperature) within seconds. The reaction can be quenched by addition of excess sulfhydryl groups that compete for BMOE such as β-mercaptoethanol or dithiothreitol. Cross-linking in the entrapment assay is performed by addition of BMOE to living cells - as BMOE can cross the bacterial membrane - in a physiological buffer. The reaction should therefore happen with high efficiency, which can be assessed by quantification of the ratio between monomeric Smc to all other cross-linked Smc-ScpA species. Once cross-linked these bonds are reasonably stable. However, maleimide-based cross-links have been reported to be susceptible to spontaneous elimination especially at basic pH values above pH 8 and high temperatures (Barradas et al., 1976; Fontaine et al., 2015). After isolation of the entrapped fraction, the agarose plugs needs to be melted at 80°C. When we incubated the sample for longer periods of time (> 5 min) at 80°C, indeed increased cross-link reversal was observed. Similarly, we noticed an increase in cross-link reversal when the samples were heated to a temperature ≥70°C for more than 3 minutes before they were loaded onto the output gel. Both indicates an influence of the temperature on cross-link reversal. Looking at all pH conditions during the entrapment assay, a pH above 8 is only reached during the SDS-PAGE wash, when entrapped species are specifically isolated (the SDS-Running Buffer has a pH of 8.3). If cross-linking reversal would happen at that point, ‘opened’ ring species would be lost. Steps following the SDS-PAGE run do not include buffers with a pH above 8, however these steps include temperature changes from room temperature to 37°C, 80°C and -80°C that could influence pH values. Buffers used for washing the agarose plugs after the first SDS-PAGE run contain very low concentrations of Tris, EDTA, SDS and $MgCl_2$, however a 100-fold concentration step of this buffer is performed towards the end of the procedure. Do high salt concentrations, drastic temperature changes and pH changes influence the cross-link stability? Conditions for the reversal or stabilization of maleimide-based cross-linking have been described (Baldwin and Kiick, 2013; Fontaine et al., 2015; Kalia and Raines, 2007). However in case of the entrapment assay, we were not able to pinpoint defined causes for cross-linking reversal. In general cross-link reversal occurred to generally acceptable extends albeit they were not fully reproducibly between assays. Moreover, it should not have an effect on the qualitative results of the entrapment assay as a detected protein signal after the entrapment assay always means that the protein has entrapped the chromosome.

4.1.3. DEGRADATION OF CHROMOSOMAL DNA

The second reason that could cause loss of entrapped Smc-ScpAB rings is degradation or cleavage of the chromosomal DNA causing release of the complexes (i.e. by a sliding-off mechanism). We therefore embedded cells into an agarose matrix to prevent shearing of the chromosome. The steps occurring before casting of the agarose plugs include cell harvesting, washing and cross-linking. We cannot fully exclude the lysis of cells as well as subsequent release and degradation of the chromosome during these steps, however substantial cell lysis should have been visible by a change of the physical appearance of the cells. After embedding cells into the agarose matrix and subsequent lysis, also nucleases could harm the integrity of the chromosome. We do not have a control to exclude digestion of the chromosome, especially between lysis of the cells and loading of the agarose plug onto the SDS-PAGE gel. The SDS-PAGE run is performed in presence of EDTA and SDS. Both should inactivate nucleases, however residual nuclease levels cannot be excluded. We can therefore not exclude that a fraction of cross-linked Smc-ScpAB rings is lost due to residual nuclease activity.

After the SDS-PAGE run the EDTA concentration in the agarose plug is lowered and a purified nuclease was added to the sample to release the entrapped protein fraction. Importantly, the agarose plugs were not washed anymore after this step to prevent loss of released complexes.

4.1.4. QUANTIFICATION OF ENTRAPPING PROTEINS

We used the replicative sliding clamp protein DnaN, known to topologically entrap the bacterial chromosome, for development of the assay (Stukenberg et al., 1991). In cross-linked extracts two additional DnaN-HaloTag bands were detectable in parallel to the monomer (*see* **Figure 1** in Wilhelm et al. 2015). We identified one band as a single cross-linked linear dimer running slightly higher in the gel as the double cross-linked dimer that forms a ring. The entrapment assay specifically enriched for the latter proving that our assay specifically enriches for proteins entrapping the chromosome. Interestingly the ratio of entrapped DnaN compared to the input material was much higher than for Smc-ScpAB. Approximately 50% of the cross-linked DnaN ring in the input material was entrapped. In contrast, only 10% of the Smc-ScpAB ring compared to the input was isolated on average. This might suggest that 5-times more DnaN-rings entrap the chromosome than Smc-ScpAB rings. There is evidence that most of *B. subtilis* DnaN interacts with the chromosome during exponential growth by entrapment (Su'etsugu and Errington, 2011). This indicates that the entrapment assay can detect at least 50% of all entrapping DnaN rings in the cell. Therefore not more than 50% of the entrapped proteins should be lost during the assay.

This also implies that only 10-20% of Smc-ScpAB rings entrap the chromosome. This number could still display a slight under- or overestimation, due to the fact that the quantification of DnaN was more reliable as for Smc-ScpAB. In case of DnaN only two additional cross-linking species are generated and both do not overlap with each other. In contrast, cross-linked Smc-ScpAB generates at least eight different species that are not separated completely due to their high molecular weight. Moreover, the cross-linked Smc-ScpAB ring overlaps with an incompletely cross-linked intermediate species in the protein extract. An absolute quantification of the entrapped Smc-ScpAB ring was therefore not possible. This is a disadvantage of our entrapment assay, especially when high-molecular weight proteins are analyzed. In addition, only two cross-links can theoretically reverse in case of DnaN, compared to three in case of Smc-ScpAB. This might also be a possible reason for an underestimation of Smc-ScpAB rings entrapping the chromosome. How was it then possible to state that 10-20% of Smc-ScpAB rings entrap the chromosome? For the entrapment assays performed with Smc-ScpAB, we had to load only 10% of the protein extracts of the input material in order to obtain similar levels of the in-gel fluorescence signals with the output sample. Therefore we estimated the entrapping Smc-ScpAB complexes to be at least 10% of the input material.

Finally, to obtain an overall view on the number of Smc proteins per *oriC* in *B. subtilis*, we performed quantitative Western- and Southern Blotting. The ratio of Smc protein to a *parS359* DNA fragment (≈9.8 kilo-bps away from *oriC*) revealed 60 ± 12 Smc proteins/*parS359* in nutrient rich medium (Wilhelm et al., 2015). Subsequently we compared the signals of Smc-HaloTag and DnaN-HaloTag in protein extracts using in-gel fluorescence. We detected about 5-fold more DnaN proteins than Smc proteins in the same amount of cells (unpublished results). This suggests that there are 30 Smc dimers (that presumably form Smc-ScpAB complexes) and 150 DnaN dimers per *parS359* in *B. subtilis*. An independent quantification on the number of DnaN proteins per *B. subtilis* cell revealed 500 DnaN dimers per cell (Su'etsu & Errington). This number was obtained by calculating the ratio of the number of DnaN proteins obtained in quantitative Western Blotting, compared to the number of single *B. subtilis* cells per sample. This number is approximately 3 to 5-fold higher than our DnaN quantification. The high difference of these numbers indicates that our absolute quantification of proteins per *parS359* DNA has to be taken with caution. One possibility of this difference could be that it was not stated in their study how many origins of replication on average were present per counted cell. As introduced earlier, replication is reinitiated in *B. subtilis* before the previous round is finished. If one assumes that 3 to 5 origins are present per counted cell, our quantification would perfectly fit to this independent quantification. A second possibility for an overestimation could be their approach to count single *B. subtilis* cells as they often grow in form of cell-chains *in vivo*. It can therefore be difficult to count individual cells. For the entrapment assay our numbers would suggest that we isolate 75 DnaN rings (according to our quantification) but only 3 to 6 Smc-ScpAB rings (i.e. 10-20%). This is a surprising result as it indicates that as little as 3 to 6 complexes might be entrapping the chromosome in wild-type *B. subtilis* cells (*see* **chapter 4.2.1.2**).

4.1.5. A TOPOLOGICAL ENTRAPMENT OR A NON-TOPOLOGICAL ENTRAPMENT

We reproducibly showed that Smc-ScpAB entraps the *B. subtilis* chromosome. Is the entrapment of a topological or non-topological nature? Topology is defined as a property that is preserved under continuous deformations including stretching and bending but not tearing and gluing (modified from: Oxford dictionary definition). A topological interaction between a protein ring and circular DNA would be therefore impossible to be disconnected regardless of the degree of stretching or bending of the protein or the DNA (*see* **Figure 4.2**). Only if one interface of the protein ring or the DNA would be opened, a topological interaction would be resolved.

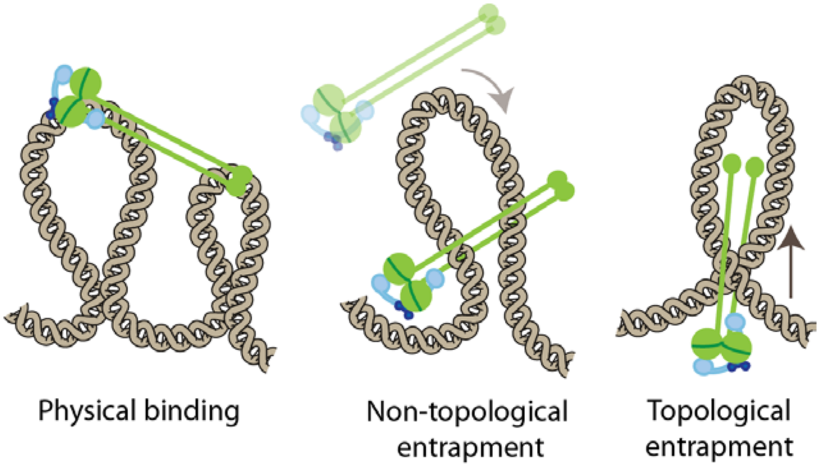

Figure 4.2: Interaction of Smc-ScpAB with the chromosome. On the left side a physical interaction of Smc-ScpAB with chromosomal loops is depicted. The middle scheme depicts a non-topological entrapment of a chromosomal loop whereas the right scheme visualizes topological entrapment of the chromosome. For a topological entrapment one of the interfaces of the Smc-ScpAB ring would have to open (here the hinge is partially opened).

In our entrapment assay the cross-linked Smc-ScpAB ring and the *B. subtilis* chromosome are exposed to harsh protein denaturing conditions in an electric field. Importantly, however, due to the enormous size of the chromosome, we cannot be sure that during the assay the chromosome would be deformed in such a way that large loops of DNA would be released from the protein ring.

So far there is no direct evidence for *B. subtilis* Smc-ScpAB that any of these interfaces has to open up for DNA entrapment. The chromosome is embedded in an agarose matrix capturing the *in vivo* state in which the proteins were cross-linked. Cells are harvested during mid-exponential growth phase, a phase of fast replication, fast growth and cell division (in case of a wild-type strain). Therefore the embedded chromosomes will contain sister chromosomes being inter-linked, replication forks present along the chromosome and different states of chromosome organization within the cell. This probably causes a high quantity of inter-linkages between chromosomal DNA, kept in this state by the agarose. Smc-ScpAB rings that entrap chromosomal loops but not in a topological form, could therefore be hindered from sliding off the chromosome during the SDS-PAGE gel run due to chromosomal DNA loops running into the agarose matrix. With the entrapment assay we can thus not define if non-topologically or topologically entrapped Smc-ScpAB rings or a mixture of both is isolated. In either case we have shown that Smc-ScpAB entraps DNA inside its ring.

A possible solution to distinguish between a topological or non-topological form of binding could be to agitate the DNA inside the agarose plug, e.g. by an alternative electric field such as pulsed-field gel electrophoresis. In PFGE whole chromosomes are embedded in an agarose plug, loaded onto an agarose gel and an electric field with electrodes at different angles of the gel chamber. The angles of the electric field are constantly changed; therefore chromosomal loops are prevented from becoming stuck in the agarose network.

We therefore casted an agarose gel around the agarose plugs prepared for the entrapment assay and let it run in an alternating electric field in a PFGE chamber, in a buffer containing SDS. Plugs that were kept 24 hours under these conditions specifically enriched for the Smc-ScpAB ring species and therefore reflected the result obtained from the entrapment assay (unpublished results). This is consistent with a topological form of interaction with the chromosome. Quantification of the species obtained from PFGE compared to the entrapment assay revealed a signal intensity that was only half of the latter. At the moment it is not clear if the loss of signal happened as a result of protein degradation and/or cross-link reversal or indeed reflects the loss of a non-topologically entrapped fraction. We also performed this experiment with DnaN, known to topologically entrap the chromosome. Plugs were kept 24 hours in the alternating field and the DnaN-ring species was specifically enriched as observed for Smc-ScpAB. However, in this case only between 70-80% of the signal compared to the sample in our entrapment assay, was recovered for DnaN in PFGE. This suggests that a fraction of proteins is lost during PFGE e.g. by protein degradation, cross-link reversal or nuclease activity. Further optimization of this technique will be necessary to control for protein degradation and chromosomal digestion during the run.

4.1.5.1. COMPARISON OF THE ENTRAPMENT ASSAY TO TOPOLOGY ASSAYS

Topological entrapment assays have been first established for cohesin in *S. cerevisiae* (Farcas et al., 2011; Gligoris et al., 2014; Haering et al., 2008; Ivanov and Nasmyth, 2005, 2007). First evidence that cohesin topologically entraps DNA inside its ring came from the mini-chromosome assays of Ivanov et al. (2005). In their assay cohesin was immunoprecipitated and an artificial circular 2.3 kilo-bps plasmid from *S. cerevisiae* was co-purified. Importantly, the co-purification was dependent on the integrity of the cohesin ring and the integrity of the circular mini-chromosome. This provided evidence of a topological interaction of cohesin with DNA (Ivanov and Nasmyth, 2005). Following studies established sucrose gradient sedimentation and gel electrophoresis to purify cohesed (i.e. held together by cohesin) sister mini-chromosomes from *S. cerevisiae* (Haering et al., 2008; Ivanov and Nasmyth, 2007). Moreover, the interfaces of the cohesin (Smc1/Smc3/Scc1) tripartite ring were cross-linked with BMOE (n.b. the Smc3/Scc1 interface was fused) after the isolation of the cohesed mini-chromosomes and treated with SDS. The dimeric mini-chromosomes were resistant to SDS-treatment only in case when all cohesin interfaces were cross-linked. Taken together, this study provided strong evidence that sister DNAs are topologically entrapped by cohesin, most likely within one cohesin ring (Haering et al., 2008).

One of the advantages of using such assays is that purified circular mini-chromosomes are used as templates. In our entrapment assay we look at whole chromosomes and face the problem that we cannot exclude knotting within the chromosome, which is the major reason why we cannot distinguish between a topological and non-topological entrapment (see above). In the mini-chromosome assays the DNA template is purified, and fractions of catenated chromosome dimers (*see* **Figure 1.2** for catenated dimers) can be separated from fractions of cohesed chromosome dimers.

However, one point of criticism has often been that the mini-chromosome assays use small, artificial circular templates while the native eukaryotic chromosomes are much larger, normally linear entities. It is thus possible that the topological association arises as a consequence of an activity that occurs on plasmids but not native chromosomes. The assay as described in Haering et al 2008, was thus extended by a large 26 kilo-bps circular mini-chromosome as well as a 42 kilo-bps linear mini-chromosome as templates (Farcas et al., 2011). Topologically entrapped cohesin should in theory slide off a linear chromosome, if not held back by barriers. This was confirmed using the mini-chromosome assay (Farcas et al., 2011). It was suggested that *in vivo* such barriers could be provided by sites of convergent transcription or telomeres (Glynn et al., 2004; Haering et al., 2008; Lengronne et al., 2004).

Taken together, the mini-chromosome assays established in *S. cerevisiae* are able to identify a topological interaction of SMC-complexes with an artificial DNA template. In contrast, our entrapment assay cannot distinguish between simple entrapment and topological entrapment (*see* **Figure 4.2**). However, the advantage of our assay is that we assess the interaction of Smc-ScpAB with a natural DNA template, namely whole *B. subtilis* chromosomes. Moreover, in our entrapment assay the Smc-ScpAB ring interfaces are cross-linked *in vivo*, whereas in the discussed mini-chromosome assays this was not the case. Only recently the structure of the *S. cerevisiae* Smc3-Scc1 interface was solved, which enabled simultaneous cross-linking of all three interfaces of the cohesin ring *in vivo* (Gligoris et al., 2014). It was shown, that most cohesin forms heterotrimeric rings *in vivo* and that BMOE cross-linking of cohesin *in vivo* causes catenation of sister mini-chromosomes and monomeric DNAs (Gligoris et al., 2014). This result provided evidence that cohesin entraps sister DNAs *in vivo*, such as we have shown for the *B. subtilis* Smc-ScpAB complex.

In conclusion, the entrapment assay that I have developed in course of my thesis provides a novel tool of studying the entrapment of ring-form protein complexes with whole chromosomes *in vivo*. I could show that *B. subtilis* Smc-ScpAB entraps the chromosome *in vivo*. Our assay is not distinguishing between a topological or non-topological interaction. It therefore remains to be established if topological entrapment such as described for eukaryotic cohesin is an evolutionary conserved feature. In the next chapter I will focus on the functional relevance of my results.

4.2. FUNCTIONAL IMPLICATIONS OF CHROMOSOMAL ENTRAPMENT BY SMC-SCPAB

DNA entrapment was for the first time assessed on whole chromosomes *in vivo* by our assay. Entrapment itself is therefore a conserved feature that might be shared between all SMC complexes. However its functional relevance possibly differs between the SMC-complexes. A key question is what the functional implications of chromosomal entrapment in *B. subtilis* are, compared to its eukaryotic relatives. To get an insight it is central to discuss our finding from two points of view. First, I will look directly at the mechanistic basis of the entrapment process and discuss its requirements and how chromosomal entrapment might be established (*see* **chapter 4.2.1**). Second, I will discuss chromosomal entrapment from a cellular perspective and will address how it could contribute to proper chromosome segregation in *B. subtilis* and compare it to findings in eukaryotes (*see* **chapter 4.2.2**).

4.2.1. WHAT IS THE MECHANISTIC BASIS OF CHROMOSOMAL ENTRAPMENT?

In order to address the mechanistic basis of chromosomal entrapment we assessed the influence of ATP hydrolysis on entrapment as well as the requirement of the ParB protein. Additionally, in an independent study to which I contributed to the role of the ATP hydrolysis cycle on the chromosome-wide localization of Smc-ScpAB was assessed.

4.2.1.1. WHAT ARE THE REQUIREMENTS OF CHROMOSOMAL ENTRAPMENT?

I showed that a full cycle of ATP hydrolysis is needed for entrapment of DNA inside its ring (Wilhelm et al., 2015). This was the first time that ATP hydrolysis was shown to be indispensable for entrapment of DNA by any SMC complex in a physiological setting. Experimental evidence for the dependence of DNA entrapment by cohesin or condensin on a full cycle of ATP hydrolysis is still missing. However, in *S. cerevisiae* ATP hydrolysis is required for the normal association of cohesin with the chromosome (Arumugam et al., 2003) and moreover for relocation of cohesin from its initial loading sites (Hu et al., 2011). *In vitro* the topological loading of cohesin depends on the binding and presence of hydrolyzable ATP. However, and very surprisingly, the ATP-hydrolysis mutant (EQ) of cohesin is not defective in DNA loading in the reported *in vitro* system (Murayama and Uhlmann, 2014, 2015).

How might ATP hydrolysis be coupled to DNA entrapment? One hypothesis is that ATP hydrolysis could cause a conformational change of the complex (*see* **Figure 4.3**). Engagement of heads of a Smc-dimer could lead to opening up of an otherwise closed 'rod-like' structure which could make space for capturing DNA (or chromosomal loops). Is there evidence for a conformational change of Smc-ScpAB? The coiled coils emerging from the *B. subtilis* hinge are in close juxtaposition to each other. *In vitro* data suggests that this rod-like conformation of a Smc-dimer is at least partially opened upon engagement of the heads (Soh et al., 2015). In other words, when Smc heads are ATP-engaged the hinge-proximal coiled coils are not closed anymore (*see* **Figure 4.3**).

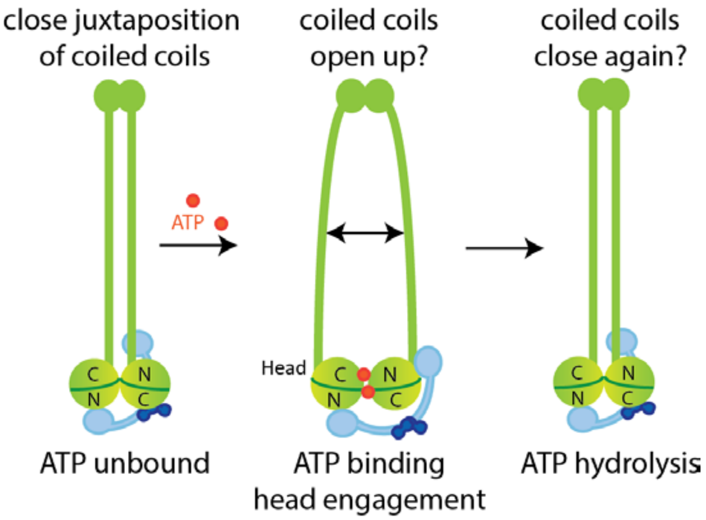
close juxtaposition of coiled coils
coiled coils open up?
coiled coils close again?
ATP
Head
C
N
N
C
ATP unbound
ATP binding head engagement
ATP hydrolysis

Figure 4.3: Conformational change of Smc-ScpAB upon head engagement and ATP hydrolysis. The scheme depicts the Smc-ScpAB complex in a closed conformation in the ATP unbound state (left). Upon binding of ATP the Smc heads dimerize which could lead to opening of the coiled coils (middle). ATP hydrolysis could then again close the coiled coils (right).

This implies that the coiled coils are rather stiff and thereby able to propagate a conformational change along the 45 nm long coiled coils. Opening up the close juxtaposition of the coiled coils could then enable entrapment by simple capture of DNA loops.

Our entrapment assay tests if Smc-ScpAB entraps DNA inside its ring. We do not know in which part of the Smc-ScpAB ring the entrapped DNA resides or how many fibers are entrapped inside the ring (*see* **chapter 4.2.2.1**). Maybe a fiber can also be entrapped in the region between the two Smc heads and the kleisin ScpA? If DNA would indeed be trapped in this region then a rod-conformation would not block entrapment. On the other hand, what would be the reason of the long coiled coils of the complex, if they are not needed to provide enough space for chromosomal entrapment?

Alternatively opening up the close juxtaposition of the coiled coils could enable access of a DNA binding site that could be normally inaccessible such as the proposed basic patch at the inner surface of the hinge described by Hirano (Hirano and Hirano, 2006). Our results do not give any information if the protein has to physically associate with the chromosome before entrapment, or if indeed a conformational change within the protein is needed. To try to answer the first question, the physical association of Smc-ScpAB rings with the chromosome was also assessed using native ChIP by Frank Bürmann (Wilhelm et al., 2015). Smc-ScpAB showed a salt-sensitive association with chromosomal DNA fragments suggesting the existence of electrostatic interactions between the DNA and the complex (*see* **Figure 5** in Wilhelm et al.). In an independent study that I have contributed to, the localization of Smc-ScpAB onto the chromosome and its dependence on ATP hydrolysis was assessed using ChIP, ChIP-seq, fluorescence microscopy and *in vivo* cross-linking (Minnen et al., 2016). This study showed that the EQ-mutant (i.e. increased fraction of engaged heads) of Smc-ScpAB is still able to localize to the chromosome, however only to very specific loci, namely the ParB-bound *parS* sites. In other words, this provides evidence that Smc-ScpAB has to perform ATP hydrolysis to establish a broad wild-type distribution on the chromosome. A comparison of ChIP-seq data between the chromosomal localization of the ParB protein and localization of the Smc EQ-mutant revealed strong similarities in respect to the observed localization patterns. In contrast, Smc mutants that cannot bind ATP or that can bind ATP but are not able to dimerize their heads do not localize to the chromosome at all (Minnen et al., 2016). These findings suggest that a certain conformation of the Smc heads is needed for localization to the ParB-*parS* sites. What could be the underlying reason? One possibility could be that a so far unknown binding site between Smc-ScpAB and ParB is exposed by head engagement of Smc. ParB could then serve as a landing platform for Smc-ScpAB (*see* **Figure 4.4**). Chromosomal entrapment by Smc-ScpAB is dependent on ATP hydrolysis but localization to ParB-*parS* is not, which indicates that the interaction of the EQ-mutant with ParB is unrelated to DNA entrapment. So far, experimental evidence for a direct interaction between Smc-ScpAB and ParB is missing. The last question that remains to be addressed here is why ATP-hydrolysis is needed for DNA entrapment. One possibility could be that engagement of the heads upon ATP binding triggers a first conformational change that opens up the complex and enables the complex to establish contact with the chromosome. Subsequent ATP hydrolysis is needed to stably entrap the complex on the chromosome. Alternatively, ATP hydrolysis itself could open up the ring at the hinge or the Smc-ScpA interface and allow loading of DNA into the Smc-ScpAB ring. It is still unclear if an interface of the Smc-ScpAB ring has to open up for entrapment (*see* **chapter 4.2.1.3**). To obtain mechanistic insights into chromosomal entrapment it will be very important to further address how the conformation of the Smc-ScpAB complex changes during every step of the ATP-hydrolysis cycle.

4.2.1.2. WHY IS THE PARB PROTEIN NEEDED FOR EFFICIENT CHROMOSOMAL ENTRAPMENT?

Chromosomal entrapment is not completely abolished in a *parB* deletion but 80% of the entrapment observed in wild-type is lost (ratio of the percentage of the entrapped fraction in wild type compared to the mutant) (Wilhelm et al., 2015). This implies that the ParB protein itself is not strictly needed for establishing entrapment. However, it could still facilitate the reaction. ParB binds *parS* sites in the vicinity of *oriC* and its ability to bridge and spread on the chromosome possibly leads to chromosomal organization of this region (Graham et al., 2014; Taylor et al., 2015). Moreover, spreading and bridging mutants have been identified (Graham et al., 2014). I combined them with the strain that can be cross-linked into the Smc-ScpAB ring. DNA entrapment was poor in strains of these mutants, comparable to a *parB* deletion. This suggests that both ParB-binding activities are needed for efficient chromosomal entrapment of Smc-ScpAB (Wilhelm et al., 2015). **Figure 4.4** shows a model of how ParB might facilitate entrapment. Maybe chromosomal loops that are possibly generated by bridging and spreading of ParB provide a chromosomal template needed for efficient entrapment.

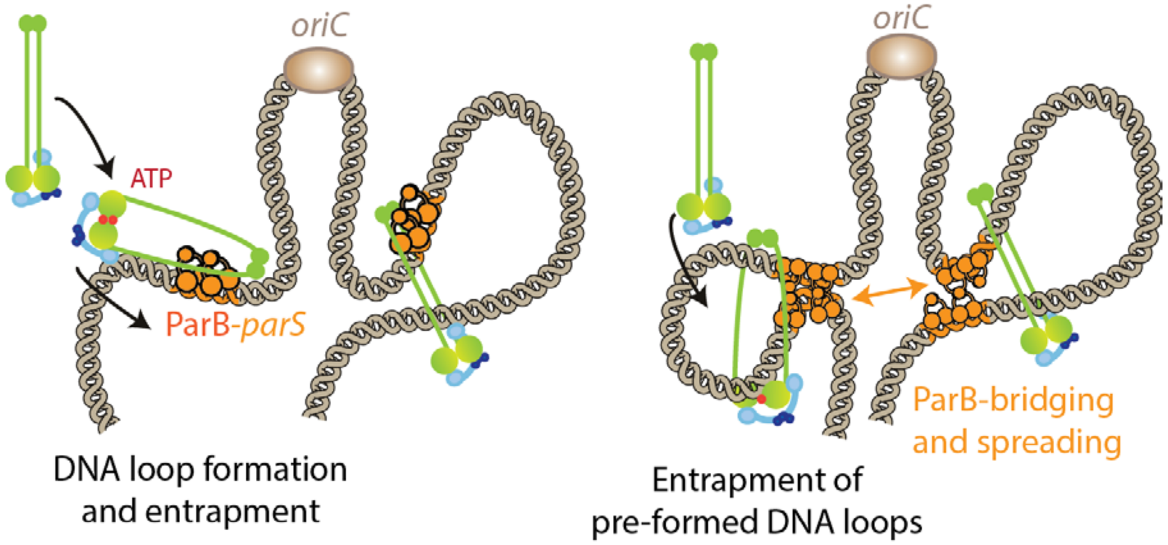
oriC
ATP
ParB-parS
DNA loop formation and entrapment
oriC
ParB-bridging and spreading
Entrapment of pre-formed DNA loops

Figure 4.4: Models of how ParB could facilitate DNA entrapment. In the left scheme ParB (orange) on *parS* (yellow) serves as a landing platform for Smc-ScpAB. Head engagement of Smc could enable entrapment of the chromosome (or chromosomal loops), subsequent ATP hydrolysis could stabilize entrapment. In the right scheme the ability of ParB to spread and bridge on DNA establishes a chromosomal organization that facilitates DNA entrapment by Smc-ScpAB. Also here head engagement could be needed to open the complex for entrapment.

Their absence could hamper the access of Smc-ScpAB to the chromosome. Alternatively ParB could also serve as a landing platform, as mentioned before. In conclusion our data suggests that Smc-ScpAB establishes contact with the chromosome at ParB-*parS,* possibly induced by engagement of its heads (Minnen et al., 2016). The complex has to undergo at least one round of ATP-hydrolysis to stably entrap the chromosome. And entrapment is more efficient in the presence of ParB. Only wild-type Smc-ScpAB shows a broad distribution over the *B. subtilis* chromosome suggesting that the complex can relocate from its initial binding sites after DNA entrapment.

To further emphasize the importance of our studies on the bacterial Smc-ScpAB complex it needs to be mentioned here that there is also evidence that the cohesin complex is loaded in a comparable way on the chromosome. Mutations of Smc1 and Smc3 that block ATP hydrolysis trap cohesin in a head-engaged state and it highly accumulates at centromeres but is less found on the chromosomal arms (Hu et al., 2011). Moreover, the cohesin EQ-mutant co-localizes with its loader complex Scc2/4. Although Scc2/4 and ParB are not homologous proteins, one can draw a parallel between the localization patterns of both SMC EQ-mutants. This also indicates that SMC-complexes could not only have evolutionary kept the ability to entrap DNA but also other mechanistic features of the entrapment process itself. Therefore the study of mechanistic details of the interaction of *B. subtilis* Smc-ScpAB is surely of help to also build a basis for work on its eukaryotic relatives.

4.2.1.3. DOES SMC-SCPAB HAVE AN ENTRY/EXIT GATE FOR DNA?

In order to establish a topological entrapment with the chromosome there are three possibilities (Nasmyth, 2005; Nasmyth and Haering, 2005): 1) *De novo* ring assembly around DNA; 2) A transient double strand break of the chromosome; 3) Transient opening of the SMC-kleisin ring. The first two possibilities seem unlikely. A double strand break would be physiologically unprofitable and SMC-kleisin rings do exist *in vivo* not associated with chromatin (Gruber, 2003). This leaves a high probability that an entry gate and also an exit gate of cohesin rings exists and that one of its interfaces therefore has to partially open up for a topological entrapment of the chromosome.

Cohesin was the only complex shown to topologically entrap DNA. Therefore answering the question of the entry/exit gate has as of yet mainly focused on this complex. There is evidence that the hinge interface has to transiently open to load cohesin onto chromosomes from experiments where this interface was artificially blocked (Gruber et al., 2006b). Loading of cohesin onto chromosomes and establishment of SCC is abolished when the hinge is unable to open. In contrast, a blocked hinge did not interfere with maintenance of SCC once loaded onto chromosomes. Both suggests that the hinge is the entry gate for DNA. Additionally, a permanent fusion of Smc1 and Smc3 to Scc1 does not interfere with the establishment of SCC and is functional in *S. cerevisiae* (Gruber et al., 2006b). Also in *B. subtilis* individual fusions of the cap or neck interface of Smc to ScpA generate functional complexes, suggesting that if Smc-ScpAB topologically entraps the chromosome, this may happen through opening of the hinge domain (Bürmann et al., 2013). However, these results have been recently challenged by an *in vitro* biochemical reconstitution of fission yeast cohesin loading onto DNA. Their experimental data suggest a mechanism in which DNA entry into and exit out of the cohesin ring both take place at the Smc3/Scc1 interface (in fission yeast called: Psm3-Rad21 interface) (Murayama and Uhlmann, 2015). It needs to be established if this mechanism also applies *in vivo* and how both findings can be brought together.

Cohesin has two individual pathways for its dissociation of chromosomes. While most of cohesin is presumably removed from the chromosomal arms during prophase, a fraction mainly at the centromeres stays stably entrapped and is only removed through Scc1 cleavage by separase at the onset of anaphase (reviewed in: Nasmyth and Haering, 2009). Cleavage of Scc1 by separase cuts the cohesin ring irreversibly open. Thereby SCC is resolved and sister chromatids are separated (Uhlmann and Nasmyth, 1998; Uhlmann et al., 1999). The second mechanism is independent of separase and moreover does not irreversibly cleave Scc1. This suggests that an interface of the complex opens to release it from the chromosome. As introduced before, the Wpl1 protein is needed to remove cohesin from chromosomal arms (Gandhi et al., 2006; Kueng et al., 2006). A fusion of the Smc3/Scc1 interface reduces the turnover of cohesin on the chromosome once it has loaded on chromatin suggesting that this interface could be the exit gate (Buheitel and Stemmann, 2013; Chan et al., 2012). Importantly, if all cohesin would be removed by this pathway, then SCC would be resolved, which would impede bipolar attachment of the chromosomes to the mitotic spindle and cause segregation defects. Therefore a mechanism must exist to distinguish between the portion of cohesin that has to stay entrapped to ensure SCC and the one that should be removed in prophase. Acetylation of residues at the Smc3 head domain by Eco1 in *S. cerevisiae* was shown to be essential for maintaining SCC suggesting that acetylation blocks the presumptive exit gate in complexes that have to stay entrapped on the chromosome (Gligoris et al., 2014). No corresponding loading/unloading factors have been found for eukaryotic condensin or prokaryotic Smc-ScpAB so far indicating that either only cohesin complexes unload from the chromosome or that they use a very specialized mechanism for doing so (reviewed in: Hirano, 2016).

Our entrapment assay does not allow us to define whether *B. subtilis* Smc-ScpAB entraps the chromosome topologically. Nevertheless, the question of an entry or exit gate should be addressed for *B. subtilis* as it will not only give us more information about the mechanism of entrapment but potentially also a deeper insight on its interaction with the chromosome and therefore its function. One idea is based on the experiments performed for cohesin and previous work on Smc-ScpAB where fusion proteins of Smc-kleisin were generated (Bürmann et al., 2013; Gruber et al., 2006b). A strain in which both ScpA termini were fused to a Smc protein was generated by my colleague Frank Bürmann (unpublished results). The 'fusion' strains were not viable under conditions supporting fast growth in *B. subtilis* but were expressed and folded correctly as we were able to cross-link the protein into a ring. One copy of Smc was carrying the R558C cysteine in the hinge, whereas the second copy was carrying N634C (*see* **Figure 4.1** for structure of hinge). I could show that the fused protein entraps the chromosome indicating that the head interface of Smc-ScpAB does not need to open for DNA entrapment. When the fusion strain harbored also the EQ-mutation, entrapment was reduced in most of the experiments. Unfortunately the results were not always reproducible and therefore not included in my publication, but they will be carefully repeated in the future to provide a solid basis of our results. From a functional perspective it is ambiguous if prokaryotic Smc-ScpAB needs to unload from the chromosome and hence needs an exit gate. Moreover, unloading could also simply take place by sliding off a chromosomal loop at the terminus after separation of the sister chromosomes. What could be the functional role of unloading? Only limited evidence for a turnover of Smc-ScpAB complexes is available (Kleine Borgmann et al., 2013) but a possible role could lie in recycling of Smc-ScpAB complexes to ensure fast segregation of the chromosome and cell division. In conclusion, we have evidence from our data that Smc-ScpAB establishes contact with the chromosome at ParB-*parS* but only upon engagement of its head domains. Subsequent ATP hydrolysis is needed to entrap the chromosome. It is unclear if this involves opening of one interface. Smc-ScpA-Smc fusion strains indicated that if such an entry gate exists it might be the hinge interface, which would possibly display a conserved mechanism compared to cohesin.

4.2.2. WHAT IS THE ROLE OF CHROMOSOMAL ENTRAPMENT IN *B. SUBTILIS*?

Deletion of Smc-ScpAB leads to partitioning defects of *oriC*. This phenotype can be rescued by a slowdown of the replication speed (Gruber et al., 2014; Wang et al., 2014). Chromosomal entrapment would provide a possibility to ensure that sister chromosomes do not spatially overlap and to minimize their entanglement (*see* **Figure 4.5**). But how could Smc-ScpAB facilitate this process? One idea is that the complex entraps chromosomal loops at certain positions on the chromosome. Subsequently it could move on the chromosome, maybe by a sliding mechanism and might pull DNA constantly through its ring. Such a mechanism was termed ‘loop extrusion’ in the field. There is evidence that eukaryotic condensin entraps DNA inside its ring (Cuylen et al., 2011). As introduced earlier condensin is thought to facilitate compaction and disentanglement of sister chromatids. However, the molecular mechanism of how condensin achieves this is currently unknown. The phenotype of a *smc* deletion in *B. subtilis* suggests that the function of Smc-ScpAB is more related to condensin as to cohesin, which is not helping to separate sister chromosomes from each other but holding them together (i.e. SCC). Hence both Smc-ScpAB and condensin might share a conserved mechanism. One important step to assess the functional relevance of chromosomal entrapment is to ask how many DNA fibers are entrapped by Smc-ScpAB.

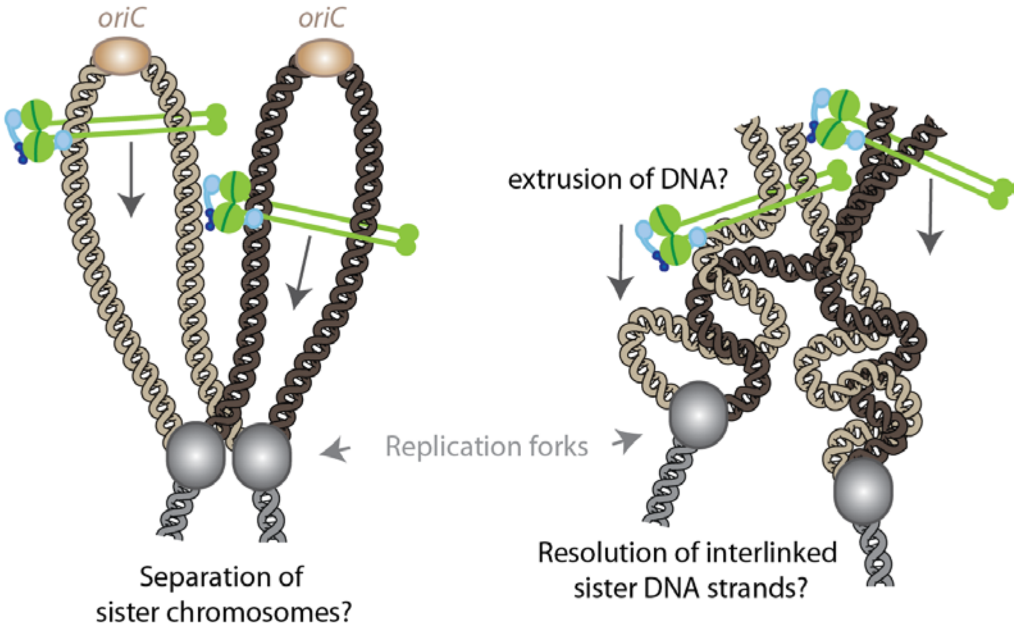
oriC
oriC
extrusion of DNA?
Replication forks
Separation of sister chromosomes?
Resolution of interlinked sister DNA strands?

Figure 4.5: Model for the separation of sister chromosomes by Smc-ScpAB. The left scheme depicts entrapment of the two replicated chromosomal arms of each one sister chromosome, established at *oriC (*brown sphere). The complex slides down from *oriC* in direction towards the terminus, behind the replication forks (grey sphere). Smc-ScpAB complexes could thereby separate sister chromosomes. The right scheme provides a more detailed insight into how Smc-ScpAB could resolve interlinked sister DNA strands behind the replication fork. This could happen by extruding the two replicated chromosomal arms of each sister chromosome through its ring.

4.2.2.1. HOW MANY DNA FIBERS ARE ENTRAPPED BY SMC-SCPAB?

SMC-complexes share their architecture and size throughout all domains of life. Especially the length of coiled coils that is about 45 nm, is a remarkable feature of its architecture. This length is equivalent to the length of 150 bps of double stranded DNA (Hirano, 2016). A naked DNA fiber has a diameter of 2 nm whereas chromatin fibers of eukaryotes are about 10 nm in size (Nasmyth and Haering, 2005). Therefore, in theory both can be fitted inside the Smc-ScpAB ring. However, experimental data on this question is not available. Our entrapment assay does not provide any information on the number of DNA fibers being entrapped inside the ring. We only know that at least one fiber of DNA is entrapped.

Models on how Smc-ScpAB interacts with the bacterial chromosome and how it mediates chromosome segregation mostly propose the entrapment of chromosomal loops or the physical separation of sister chromosomes by entrapment of the two chromosomal arms of each (*see* **Figure 4.5**; Graham et al., 2014; Gruber, 2014; Wang et al., 2015). Direct experimental evidence is missing.

Eukaryotic cohesin was the first complex with experimental support for a topological entrapment of two fibers. The same mechanism of entrapment that applies for establishing SCC could also serve as basis for establishing entrapment in *B. subtilis* despite of its functional differences. Topological entrapment of two sister chromatids by one cohesin ring predicts that proteolytic cleavage of one cohesin subunit such as the kleisin Scc1 releases the two sister chromatids. There is experimental evidence *in vitro* and *in vivo* that disruption of the cohesin ring indeed destroys SCC (Ivanov and Nasmyth, 2005; Nasmyth and Haering, 2005; Uhlmann et al., 1999). However, this does not necessarily imply that two fibers are entrapped inside one cohesin ring. Other models such as the 'handcuff-model' predict that two cohesin rings could be interlinked themselves topologically while each one also entraps one DNA fiber topologically (Nasmyth and Haering, 2009). Experimental evidence for entrapment of sister chromosomes by one individual cohesin ring is thus far only provided indirectly by mini-chromosome assays in yeast. The efficiency of cross-linking the cohesin ring is comparable to the fraction of denaturation-resistant sister-chromosome dimers in mini-chromosome assays (Gligoris et al., 2014; Haering et al., 2008).

Most cohesin is thought to associate with chromosomes from S-phase to G_2/M-phase of the cell cycle. Cells in which expression of cohesin is only induced in G_2/M-phase do not establish SCC, suggesting that the cohesin complexes that are necessary for this function have to associate with chromosomes already in S-phase (reviewed in: Nasmyth and Haering, 2009). Why does SCC need to be established during S-phase? Are the two replicated chromosomal fibers entrapped at once or does the replication fork pass through cohesin rings and thereby eventually lead to entrapment of the two sister chromosomes? There is some evidence pointing towards a partial dependency of cohesion on the replication machinery (Ben-Shahar et al., 2008). On the other hand it was shown that cohesion can also be established in the absence of replication forks (Strom et al., 2007; Unal et al., 2007). The latter suggests that entrapment of two chromosomal fibers does not depend on passing them through the cohesin ring during replication.

A similar mechanism depending on the replication fork, as suggested for cohesin, seems unlikely for Smc-ScpAB as sister chromosomes are presumably separated from each other and not cohesed. Alternatively Smc-ScpAB could be loaded onto the replicated *oriC* of each sister chromosome by entrapping this region inside its ring. Sliding along each sister chromosome behind the replication fork could bring forth a way of separating the two daughter strands from each other by resolving inter-linkages (*see* **Figure 4.5**). There is neither direct experimental evidence for a sliding mechanism of *B. subtilis* Smc-ScpAB (*see* **chapter 4.2.2.2**) nor for entrapment of more than one chromosomal fiber.

During the course of this thesis I therefore aimed at addressing the latter question using a novel *in vivo* approach. Based on the Cre-*loxP* system I inserted two *loxP* sites surrounding the *B. subtilis parS359* site and *oriC* (unpublished results). The Cre-recombinase was expressed with an IPTG-inducible promotor. **Figure 4.6** shows a scheme of the 'loop-out assay'. On the left side, Smc-ScpAB entraps one fiber whereas in the right scheme the complex entraps two chromosomal fibers, such as a chromosomal loop at the *parS359* locus. In the first case upon induction of Cre, *loxP* sites recombine and generate a chromosomal mini-circle, separated from the chromosome. In the second case this circle is linked to the chromosome through entrapment by Smc-ScpAB.

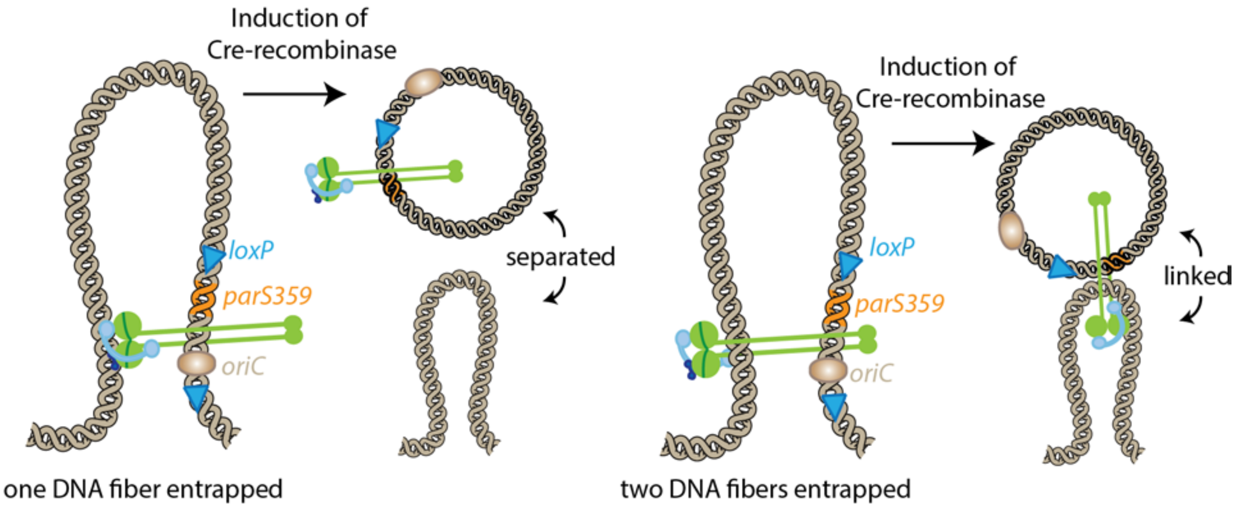

Figure 4.6: Scheme of the chromosomal loop-out assay. Both schemes show a chromosomal loop with Smc-ScpAB entrapping one (left side) or two (right side) DNA fibers. Two *loxP* sites (blue triangle) were inserted on the chromosome surrounding the *parS359* site (orange) and *oriC* (brown sphere). Upon expression of the Cre-recombinase the two *loxP* sites recombine and a chromosomal mini-circle is looped out. If only one fiber was entrapped by Smc-ScpAB, the mini-circle will be separated from the chromosome (left). Upon entrapment of two fibers the mini-circle will stay linked by Smc-ScpAB to the chromosome (right).

We were not able to perform this assay so far. Unfortunately regulation of the promotor for Cre-expression was not tight enough to prevent premature recombination at *loxP* sites, which possibly caused loss of mini-circles during cell divisions, as no mini-circles were detectable in Southern Blots. To exclude technical problems I also used a *B. subtilis* strain carrying a plasmid of approximately the same size of the looped-out mini-circles, which was visible in the Southern Blot.

We have recently established a tighter expression system in the lab, which could help to follow up on this project in the future. In conclusion, the loop out assay that we aimed to establish still needs optimization and moreover, would benefit from a positive control, such as a protein known to entrap more than one chromosomal fiber in *B. subtilis*.

Taken together, there is no experimental evidence for entrapment of two or more chromosomal fibers by *B. subtilis* Smc-ScpAB so far. Also the mechanism of the establishment of SCC by cohesin is still largely unclear and it might not be comparable to prokaryotic Smc-ScpAB. The available experimental data of *B. subtilis* Smc-ScpAB mostly promotes a model where the complex entraps more than one fiber. Important examples are the recent Hi-C studies that propose entrapment of both chromosomal arms by Smc-ScpAB (Marbouty et al., 2015; Wang et al., 2015).

4.2.2.2. DOES SMC-SCPAB SLIDE ON THE BACTERIAL CHROMOSOME?

A second important question in assessing the functional relevance of chromosomal entrapment is to ask if the complex is able to slide along DNA. As mentioned above, sliding could give rise to a mechanism of how Smc-ScpAB could ensure physical separation of replicated daughter strands behind the replication forks (*see* **Figure 4.5**). The recent Hi-C papers introduced earlier, showed that the *B. subtilis* chromosome is organized in a longitudinal fashion from *oriC* to terminus (Marbouty et al., 2015; Wang et al., 2015). This organization is dependent on Smc-ScpAB, ParB and the presence of at least one *parS* site. The position of the *parS* site defines the apex of longitudinal organization, if placed at another position the chromosomal regions flanking *parS* will be juxtaposed emerging from the new position (*see* **Figure 4.7**). It was suggested that Smc-ScpAB could therefore be loaded on the chromosome near *oriC*, at the ParB-bound *parS* sites and then slide towards the terminus, tethering the two chromosomal arms together (Wang et al., 2015). However, direct evidence for a sliding mechanism is missing. A different study provided evidence that ParB bridges distant pieces of DNA in a range of 10-20 kilo-bps. As ParB specifically binds to the ten *parS* sites mainly around *oriC* it seems unlikely that ParB itself triggers the continuous longitudinal organization of the chromosome (Graham et al., 2014; Wang et al., 2015). In wild type *B. subtilis*, Smc-ScpAB is enriched around *oriC* and this is dependent on the presence of the ParB protein (Gruber and Errington, 2009). However, Smc-ScpAB can be found dispersed over the whole bacterial chromosome in contrast to ParB.

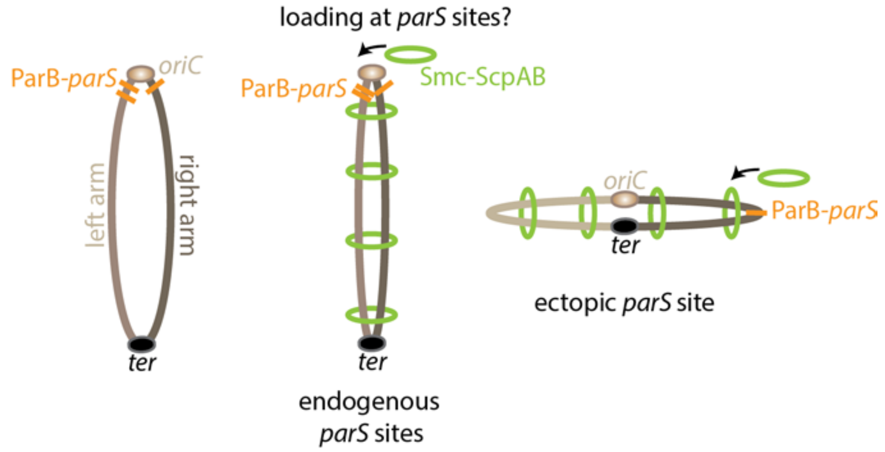

Figure 4.7: Longitudinal organization of the chromosome. The right arm (dark brown) and left arm (light brown) of the *B. subtilis* chromosome are in close juxtaposition to each other as shown by Hi-C studies. In the vicinity of *oriC* the ParB-bound *parS* sites reside (orange). Smc-ScpAB (green ring) could establish contact with the chromosome at ParB-*parS*, subsequently entrap the chromosome and hold both chromosomal arms together in its ring (middle scheme). Only one *parS* site is sufficient to define the apex of the longitudinal organization (left scheme). Here an ectopic *parS* site at a site 90° from *oriC* is depicted, bringing *oriC* and *ter* in close proximity. This image is modified from (Wilhelm and Gruber, 2016).

Additionally, I contributed to a study indicating that a localization gradient is built by wild-type Smc-ScpAB on the bacterial chromosome from *oriC* to terminus which is dependent on presence of ParB (Minnen et al., 2016). All of these findings are in accordance with a model were Smc-ScpAB loads at ParB-bound *parS* sites and then relocates from them in direction to the terminus.

One possibility to address sliding of Smc-ScpAB could be the insertion of a ‘roadblock’ at a certain point on the chromosome and to follow the Smc-ScpAB distribution over the chromosome. If Smc-ScpAB is sliding from *oriC* along the chromosomal arms to the terminus it should be stopped by the roadblock and accumulate which should be detectable by ChIP or ChIP-seq. Experiments with the same question have been recently performed *in vitro* using single-molecule approaches for eukaryotic cohesin (Stigler et al., 2016) suggesting that SMC complexes can indeed be stopped by roadblocks indicating that cohesin slides on DNA. For such assays roadblocks of different sizes have to be generated, as it is unknown how much space the Smc-ScpAB provides for DNA entrapment. Moreover, insertion of roadblocks on the bacterial chromosome *in vivo* could also block other processes such as replication or transcription, and therefore might be experimentally challenging.

Another way of testing diffusion of Smc-ScpAB on the chromosome, its requirements and timely organization would be the use of inducible systems. If one could induce Smc expression and perform ChIP experiments (or ChIP-seq) at several time points after induction, it would be possible to follow the localization of Smc-ScpAB along the chromosome over time. For such experiments tightly regulated promotor systems are needed allowing at the same time wild-type expression levels of Smc.

How could sliding work on a mechanistic basis? The ATP hydrolysis rate of Smc-ScpAB is approximately 11 ATP per minute/mol (Kamada et al., 2013). *B. subtilis* cells divide within 20 minutes. It is unclear if this rate fast enough to push the complex forward along the whole *B. subtilis* chromosome. Another possibility is that Smc-ScpAB does not provide the energy for sliding on its own but that it is being pushed by other proteins moving along DNA such as the transcription or replication machinery (Nasmyth, 2005; Uhlmann, 2016). However genes can be transcribed in both sense and anti-sense direction, which could block Smc-ScpAB movement. Lastly, the appearance of a Smc gradient on the chromosome as judged by ChIP-seq and ChIP-qPCR could also simply be caused by random diffusion of Smc on the chromosome after its loading in the vicinity of *oriC*.

In summary, if and how Smc-ScpAB slides along the chromosome is unclear. From a functional perspective it is a central question especially when taking our quantification of entrapped Smc-ScpAB complexes into account (*see* **Chapter 4.1.4**). The quantification of Smc proteins per *parS359* combined with the quantification of entrapped complexes suggests, that only 3-6 Smc-ScpAB complexes entrap the chromosome in wild-type. If the complex could indeed slide along the chromosome, then presumably this at first glance ‘low number’ would possibly be still sufficient to ensure separation of sister chromosomes, to mediate longitudinal organization of the chromosome seen by Hi-C and hence proper chromosome segregation.

4.3. CONCLUSION

The first SMC-like complex was isolated in *E. coli* in 1989 (Hiraga et al., 1989). Since then almost 30 years have passed and SMC complexes have turned out to be essential cellular machines, ensuring the most essential process of living organisms, cell division. Over the years work in both, eukaryotic and prokaryotic model organisms have built a broad basis for our understanding of SMC complexes. Although we have more basic insights into their general mechanism and function it is now especially important to focus on the molecular details in order to fully understand their action. One of the most vital questions in the field is how SMC complexes interact with the chromosome. Before I started my thesis we knew that the eukaryotic cohesin complex entraps DNA inside its ring and thereby establishes sister chromatid cohesion, which is essential for cell division. However, experimental evidence that entrapment also exists in prokaryotic SMC complexes was missing. With my work on the *B. subtilis* Smc-ScpAB complex I could show that chromosomal entrapment is an evolutionary conserved feature. This has motivated us to establish the requirements of entrapment and in aiming to unravel its functional relevance. My major finding was that chromosomal entrapment is dependent on a full cycle of ATP hydrolysis. This has not been shown for any SMC complex *in vivo* so far. Moreover, the impact of ATP hydrolysis on chromosomal localization of Smc-ScpAB has been assessed in a second publication I contributed to. In combination both studies now allow us to propose mechanisms of how Smc-ScpAB establishes initial contact with the chromosome and then entraps it.

5. REFERENCES

Aaij, C., and Borst, P. (1972). The gel electrophoresis of DNA. BBA Sect. Nucleic Acids Protein Synth. *269*, 192–200.

Adams, D.E., Shekhtman, E.M., Zechiedrich, E.L., Schmid, M.B., and Cozzarelli, N.R. (1992). The role of topoisomerase IV in partitioning bacterial replicons and the structure of catenated intermediates in DNA replication. Cell *71*, 277–288.

Adams, D.W., Wu, L.J., and Errington, J. (2014). Cell cycle regulation by the bacterial nucleoid. Curr. Opin. Microbiol. *22*, 94–101.

Adams, D.W., Wu, L.J., and Errington, J. (2015). Nucleoid occlusion protein Noc recruits DNA to the bacterial cell membrane. EMBO J. *34*, 491–501.

Albano, M., Smits, W.K., Ho, L.T.Y., Kraigher, B., Mandic-Mulec, I., Kuipers, O.P., and Dubnau, D. (2005). The Rok protein of Bacillus subtilis represses genes for cell surface and extracellular functions. J. Bacteriol. *187*, 2010–2019.

Ali Azam, T., Iwata, A., Nishimura, A., Ueda, S., and Ishihama, A. (1999). Growth phase-dependent variation in protein composition of the Escherichia coli nucleoid. J. Bacteriol. *181*, 6361–6370.

Almedawar, S., Colomina, N., Bermúdez-López, M., Pociño-Merino, I., and Torres-Rosell, J. (2012). A SUMO-Dependent Step during Establishment of Sister Chromatid Cohesion. Curr. Biol. *22*, 1576–1581.

Ames, G.F., and Lecar, H. (1992). ATP-dependent bacterial transporters and cystic fibrosis: analogy between channels and transporters. FASEB J. *6*, 2660–2666.

Anderson, D.E., Losada, A., Erickson, H.P., and Hirano, T. (2002). Condensin and cohesin display different arm conformations with characteristic hinge angles. J. Cell Biol. *156*, 419–424.

Arumugam, P., Gruber, S., Tanaka, K., Haering, C.H., Mechtler, K., and Nasmyth, K. (2003). ATP hydrolysis is required for cohesin's association with chromosomes. Curr. Biol. *13*, 1941–1953.

Autret, S., Nair, R., and Errington, J. (2001). Genetic analysis of the chromosome segregation protein Spo0J of Bacillus subtilis: evidence for separate domains involved in DNA binding and interactions with Soj protein. Mol. Microbiol. *41*, 743–755.

Badrinarayanan, A., Lesterlin, C., Reyes-Lamothe, R., and Sherratt, D. (2012). The Escherichia coli SMC Complex, MukBEF, Shapes Nucleoid Organization Independently of DNA Replication. J. Bacteriol. *194*, 4669–4676.

Badrinarayanan, A., Le, T.B.K., and Laub, M.T. (2015). Bacterial Chromosome Organization and Segregation. Annu. Rev. Cell Dev. Biol. *31*, 171–199.

Baldwin, A.D., and Kiick, K.L. (2013). Reversible maleimide-thiol adducts yield glutathione-sensitive poly(ethylene glycol)-heparin hydrogels. Polym. Chem. *4*, 133–143.

Barradas, R.G., Fletcher, S., and Porter, J.D. (1976). The hydrolysis of maleimide in alkaline solution. Can. J. Chem. *54*, 1400–1404.

Ben-Shahar, T.R., Heeger, S., Lehane, C., East, P., Flynn, H., Skehel, M., and Uhlmann, F. (2008). Eco1-Dependent Cohesin Acetylation During Establishment of Sister Chromatid Cohesion. Science *321*, 563–566.

Betts Lindroos, H., Ström, L., Itoh, T., Katou, Y., Shirahige, K., and Sjögren, C. (2006). Chromosomal Association of the Smc5/6 Complex Reveals that It Functions in Differently Regulated Pathways. Mol. Cell *22*, 755–767.

Bhalla, N., Biggins, S., and Murray, A. (2002). Mutation of YCS4, a Budding Yeast Condensin Subunit, Affects Mitotic and Nonmitotic Chromosome Behavior. Mol. Biol. Cell *13*, 632–645.

Bhat, M.A., Philp, A.V., Glover, D.M., and Bellen, H.J. (1996). Chromatid segregation at anaphase requires the barren product, a novel chromosome-associated protein that interacts with topoisomerase II. Cell *87*, 1103–1114.

Bigot, S., Saleh, O. a, Lesterlin, C., Pages, C., El Karoui, M., Dennis, C., Grigoriev, M., Allemand, J.-F., Barre, F.-X., and Cornet, F. (2005). KOPS: DNA motifs that control E. coli chromosome segregation by orienting the FtsK translocase. EMBO J. *24*, 3770–3780.

Bigot, S., Sivanathan, V., Possoz, C., Barre, F.X., and Cornet, F. (2007). FtsK, a literate chromosome segregation machine. Mol. Microbiol. *64*, 1434–1441.

Blakely, G., May, G., McCulloch, R., Arciszewska, L.K., Burke, M., Lovett, S.T., and Sherratt, D.J. (1993). Two related recombinases are required for site-specific recombination at dif and cer in E. coli K12. Cell *75*, 351–361.

Bouet, J., Stouf, M., Lebailly, E., and Cornet, F. (2014). Mechanisms for chromosome segregation. Curr. Opin. Microbiol. *22*, 60–65.

Bowman, G.R., Comolli, L.R., Zhu, J., Eckart, M., Koenig, M., Downing, K.H., Moerner, W.E., Earnest, T., and Shapiro, L. (2008). A Polymeric Protein Anchors the Chromosomal Origin/ParB Complex at a Bacterial Cell Pole. Cell *134*, 945–955.

Bramhill, D., and Kornberg, A. (1988). Duplex opening by dnaA protein at novel sequences in initiation of replication at the origin of the E. coli chromosome. Cell *52*, 743–755.

Bramkamp, M., and van Baarle, S. (2009). Division site selection in rod-shaped bacteria. Curr. Opin. Microbiol. *12*, 683–688.

Breier, A.M., and Grossman, A.D. (2007). Whole-genome analysis of the chromosome partitioning and sporulation protein Spo0J (ParB) reveals spreading and origin-distal sites on the Bacillus subtilis chromosome. Mol. Microbiol. *64*, 703–718.

Britton, R.A., Lin, D.C., and Grossman, A.D. (1998). Characterization of a prokaryotic SMC protein involved in chromosome partitioning. Genes Dev. *12*, 1254–1259.

Broedersz, C.P., Wang, X., Meir, Y., Loparo, J.J., Rudner, D.Z., and Wingreen, N.S. (2014). Condensation and localization of the partitioning protein ParB on the bacterial chromosome. Proc. Natl. Acad. Sci. U. S. A. *111*, 8809–8814.

Bruand, C., Ehrlich, S.D., and Jannière, L. (1995). Primosome assembly site in Bacillus subtilis. EMBO J. *14*, 2642–2650.

Bruand, C., Farache, M., McGovern, S., Ehrlich, S.D., and Polard, P. (2001). DnaB, DnaD and DnaI proteins are components of the Bacillus subtilis replication restart primosome. Mol. Microbiol. *42*, 245–255.

Buheitel, J., and Stemmann, O. (2013). Prophase pathway-dependent removal of cohesin from human chromosomes requires opening of the Smc3-Scc1 gate. EMBO J. *32*, 666–676.

Bürmann, F., Shin, H.-C., Basquin, J., Soh, Y.-M., Giménez-Oya, V., Kim, Y.-G., Oh, B.-H., and Gruber, S. (2013). An asymmetric SMC-kleisin bridge in prokaryotic condensin. Nat. Struct. Mol. Biol. *20*, 371–379.

Chalfie, M., Tu, Y., Euskirchen, G., Ward, W.W., and Prasher, D.C. (1994). Green fluorescent protein as a marker for gene expression. Science *263*, 802–805.

Chan, K.L., Roig, M.B., Hu, B., Beckouët, F., Metson, J., and Nasmyth, K. (2012). Cohesin's DNA exit gate is distinct from its entrance gate and is regulated by acetylation. Cell *150*, 961–974.

Chandler, M., Bird, R.E., and Caro, L. (1975). The replication time of the Escherichia coli K12 chromosome as a function of cell doubling time. J. Mol. Biol. *94*, 127–132.

Chuang, P.T., Albertson, D.G., and Meyer, B.J. (1994). DPY-27: A chromosome condensation protein homolog that regulates C. elegans dosage compensation through association with the X chromosome. Cell *79*, 459–474.

Ciosk, R., Shirayama, M., Shevchenko, A., Tanaka, T., Toth, A., Shevchenko, A., and Nasmyth, K. (2000). Cohesin's binding to chromosomes depends on a separate complex consisting of Scc2 and Scc4 proteins. Mol. Cell *5*, 243–254.

Coelho, P. a, Queiroz-Machado, J., and Sunkel, C.E. (2003). Condensin-dependent localisation of topoisomerase II to an axial chromosomal structure is required for sister chromatid resolution during mitosis. J. Cell Sci. *116*, 4763–4776.

Collas, P. (2010). The current state of chromatin immunoprecipitation. Mol. Biotechnol. *45*, 87–100.

Cooper, S., and Helmstetter, C.E. (1968). Chromosome replication and the division cycle of Escherichia coli. J. Mol. Biol. *31*, 519–540.

Cox, M.M., Goodman, M.F., Kreuzer, K.N., Sherratt, D.J., Sandler, S.J., and Marians, K.J. (2000). The importance of repairing stalled replication forks. Nature *404*, 37–41.

Cuylen, S., Metz, J., and Haering, C.H. (2011). Condensin structures chromosomal DNA through topological links. Nat. Struct. Mol. Biol. *18*, 894–901.

D'Ambrosio, C., Schmidt, C.K., Katou, Y., Kelly, G., Itoh, T., Shirahige, K., and Uhlmann, F. (2008). Identification of cis-acting sites for condensin loading onto budding yeast chromosomes. Genes Dev. *22*, 2215–2227.

Dame, R.T. (2005). The role of nucleoid-associated proteins in the organization and compaction of bacterial chromatin. Mol. Microbiol. *56*, 858–870.

Dame, R.T., Wyman, C., and Goosen, N. (2000). H-NS mediated compaction of DNA visualised by atomic force microscopy. Nucleic Acids Res. *28*, 3504–3510.

Danilova, O., Reyes-Lamothe, R., Pinskaya, M., Sherratt, D., and Possoz, C. (2007). MukB colocalizes with the oriC region and is required for organization of the two Escherichia coli chromosome arms into separate cell halves. Mol. Microbiol. *65*, 1485–1492.

Davidson, A.L., Dassa, E., Orelle, C., and Chen, J. (2008). Structure, Function, and Evolution of Bacterial ATP-Binding Cassette Systems. Microbiol. Mol. Biol. Rev. *72*, 317–364.

Deardorff, M.A., Noon, S.E., and Krantz, I.D. (1993). Cornelia de Lange Syndrome.

Dekker, J., Rippe, K., Dekker, M., and Kleckner, N. (2002). Capturing chromosome conformation. Science *295*, 1306–1311.

Delius, H., and Worcel, A. (1974). Electron microscopic visualization of the folded chromosome of Escherichia coli. J. Mol. Biol. *82*, 107–109.

Dervyn, E., Suski, C., Daniel, R., Bruand, C., Chapuis, J., Errington, J., Janniere, L., and Ehrlich, S.D. (2001). Two Essential DNA Polymerases at the Bacterial Replication Fork. Science *294*, 1716–1719.

Drlica, K. (1992). MicroReview Control of bacterial DNA supercoiling. J. Mol. Biol. *6*, 425–433.

Duggin, I.G., Wake, R.G., Bell, S.D., and Hill, T.M. (2008). The replication fork trap and termination of chromosome replication. Mol. Microbiol. *70*, 1323–1333.

Duro, E., and Marston, A.L. (2015). From equator to pole: Splitting chromosomes in mitosis and meiosis. Genes Dev. *29*, 109–122.

Ebersbach, G., and Gerdes, K. (2005). Plasmid Segregation Mechanisms. Annu. Rev. Genet. *39*, 453–479.

Ebersbach, G., Briegel, A., Jensen, G.J., and Jacobs-Wagner, C. (2008). A Self-Associating Protein Critical for Chromosome Attachment, Division, and Polar Organization in Caulobacter. Cell *134*, 956–968.

Errington, J. (1996). Determination of cell fate in Bacillus subtilis. Trends Genet. *12*, 31–34.

Errington, J. (2003). Regulation of endospore formation in Bacillus subtilis. Nat Rev Microbiol *1*, 117–126.

Espeli, O., Levine, C., Hassing, H., and Marians, K.J. (2003). Temporal regulation of topoisomerase IV activity in E. coli. Mol. Cell *11*, 189–201.

Espeli, O., Mercier, R., and Boccard, F. (2008). DNA dynamics vary according to macrodomain topography in the E. coli chromosome. Mol. Microbiol. *68*, 1418–1427.

Farcas, A.-M., Uluocak, P., Helmhart, W., and Nasmyth, K. (2011). Cohesin's concatenation of sister DNAs maintains their intertwining. Mol. Cell *44*, 97–107.

Feulgen, R., and Rossenbeck, H. (1924). Mikroskopisch-chemischer Nachweis einer Nucleinsäure vom Typus der Thymonucleinsäure und die- darauf beruhende elektive Färbung von Zellkernen in mikroskopischen Präparaten. Hoppe-Seyler´s Zeitschrift Für Physiol. Chemie *135*, 203–248.

Fontaine, S.D., Reid, R., Robinson, L., Ashley, G.W., and Santi, D. V. (2015). Long-term stabilization of maleimide-thiol conjugates. Bioconjug. Chem. *26*, 145–152.

Fousteri, M.I., and Lehmann, A.R. (2000). A novel SMC protein complex in Schizosaccharomyces pombe contains the Rad18 DNA repair protein. EMBO J. *19*, 1691–1702.

Fuentes-Perez, M.E., Gwynn, E.J., Dillingham, M.S., and Moreno-Herrero, F. (2012). Using DNA as a fiducial marker to study SMC complex interactions with the atomic force microscope. Biophys. J. *102*, 839–848.

Fukuoka, T., Moriya, S., Yoshikawa, H., and Ogasawara, N. (1990). Purification and characterization of an initiation protein for chromosomal replication, DnaA, in Bacillus subtilis. J. Biochem. *107*, 732–739.

Gallego-Paez, L.M., Tanaka, H., Bando, M., Takahashi, M., Nozaki, N., Nakato, R., Shirahige, K., and Hirota, T. (2014). Smc5/6-mediated regulation of replication progression contributes to chromosome assembly during mitosis in human cells. Mol. Biol. Cell *25*, 302–317.

Gamba, P., Veening, J.W., Saunders, N.J., Hamoen, L.W., and Daniel, R.A. (2009). Two-step assembly dynamics of the Bacillus subtilis divisome. J. Bacteriol. *191*, 4186–4194.

Gandhi, R., Gillespie, P.J., and Hirano, T. (2006). Human Wapl Is a Cohesin-Binding Protein that Promotes Sister-Chromatid Resolution in Mitotic Prophase. Curr. Biol. *16*, 2406–2417.

Gellert, M. (1981). DNA Topoisomerases. Annu. Rev. Biochem. *50*, 879–910.

Gellert, M., Mizuuchi, K., O'Dea, M.H., and Nash, H.A. (1976). DNA gyrase: an enzyme that introduces superhelical turns into DNA. Proc. Natl. Acad. Sci. U. S. A. *73*, 3872–3876.

Gerlich, D., Koch, B., Dupeux, F., Peters, J.-M., and Ellenberg, J. (2006a). Live-Cell Imaging Reveals a Stable Cohesin-Chromatin Interaction after but Not before DNA Replication. Curr. Biol. *16*, 1571–1578.

Gerlich, D., Hirota, T., Koch, B., Peters, J.-M., and Ellenberg, J. (2006b). Condensin I stabilizes chromosomes mechanically through a dynamic interaction in live cells. Curr. Biol. *16*, 333–344.

Gilbert, N., and Allan, J. (2014). Supercoiling in DNA and chromatin. Curr. Opin. Genet. Dev. *25*, 15–21.

Glaser, P., Sharpe, M.E., Raether, B., Perego, M., Ohlsen, K., and Errington, J. (1997). Dynamic, mitotic-like behavior of a bacterial protein required for accurate chromosome partitioning. Genes Dev. *11*, 1160–1168.

Gligoris, T.G., Scheinost, J.C., Bürmann, F., Petela, N., Chan, K., Uluocak, P., Beckouët, F., Gruber, S., Nasmyth, K., and Löwe, J. (2014). Closing the cohesin ring: structure and function of its Smc3-kleisin interface. Science *346*, 963–967.

Gloyd, M., Ghirlando, R., and Guarné, A. (2011). The role of MukE in assembling a functional MukBEF complex. J. Mol. Biol. *412*, 578–590.

Glynn, E.F., Megee, P.C., Yu, H.-G., Mistrot, C., Unal, E., Koshland, D.E., DeRisi, J.L., and Gerton, J.L. (2004). Genome-Wide Mapping of the Cohesin Complex in the Yeast Saccharomyces cerevisiae. PLoS Biol. *2*, e259.

Goshima, G., and Yanagida, M. (2000). Establishing Biorientation Occurs with Precocious Separation of the Sister Kinetochores, but Not the Arms, in the Early Spindle of Budding Yeast. Cell *100*, 619–633.

Graham, T.G.W., Wang, X., Song, D., Etson, C.M., van Oijen, A.M., Rudner, D.Z., and Loparo, J.J. (2014). ParB spreading requires DNA bridging. Genes Dev. *28*, 1228–1238.

Grainge, I., Bregu, M., Vazquez, M., Sivanathan, V., Ip, S.C.Y., and Sherratt, D.J. (2007). Unlinking chromosome catenanes in vivo by site-specific recombination. EMBO J. *26*, 4228–4238.

Grainger, D.C., Hurd, D., Goldberg, M.D., and Busby, S.J.W. (2006). Association of nucleoid proteins with coding and non-coding segments of the Escherichia coli genome. Nucleic Acids Res. *34*, 4642–4652.

Griese, J.J., and Hopfner, K.P. (2011). Structure and DNA-binding activity of the Pyrococcus furiosus SMC protein hinge domain. Proteins Struct. Funct. Bioinforma. *79*, 558–568.

Gruber, S. (2011). MukBEF on the march: taking over chromosome organization in bacteria? Mol. Microbiol. *81*, 855–859.

Gruber, S. (2014). Multilayer chromosome organization through DNA bending, bridging and extrusion. Curr. Opin. Microbiol. *22*, 102–110.

Gruber, S., and Errington, J. (2009). Recruitment of condensin to replication origin regions by ParB/SpoOJ promotes chromosome segregation in B. subtilis. Cell *137*, 685–696.

Gruber, M., Söding, J., and Lupas, A.N. (2006a). Comparative analysis of coiled-coil prediction methods. J. Struct. Biol. *155*, 140–145.

Gruber, S., Haering, C.H., and Nasmyth, K. (2003). Chromosomal cohesin forms a ring. Cell *112*, 765–777.

Gruber, S., Arumugam, P., Katou, Y., Kuglitsch, D., Helmhart, W., Shirahige, K., and Nasmyth, K. (2006b). Evidence that loading of cohesin onto chromosomes involves opening of its SMC hinge. Cell *127*, 523–537.

Gruber, S., Veening, J.-W., Bach, J., Blettinger, M., Bramkamp, M., and Errington, J. (2014). Interlinked sister chromosomes arise in the absence of condensin during fast replication in B. subtilis. Curr. Biol. *24*, 293–298.

Haering, C.H., and Gruber, S. (2016). SnapShot: SMC Protein Complexes Part I. Cell *164*, 326–326.e1.

Haering, C.H., Löwe, J., Hochwagen, A., and Nasmyth, K. (2002). Molecular architecture of SMC proteins and the yeast cohesin complex. Mol. Cell *9*, 773–788.

Haering, C.H., Schoffnegger, D., Nishino, T., Helmhart, W., Nasmyth, K., and Löwe, J. (2004). Structure and Stability of Cohesin's Smc1-Kleisin Interaction. Mol. Cell *15*, 951–964.

Haering, C.H., Farcas, A.-M., Arumugam, P., Metson, J., and Nasmyth, K. (2008). The cohesin ring concatenates sister DNA molecules. Nature *454*, 297–301.

Hajduk, I. V., Rodrigues, C.D.A., and Harry, E.J. (2016). Connecting the dots of the bacterial cell cycle: Coordinating chromosome replication and segregation with cell division. Semin. Cell Dev. Biol. *53*, 2–9.

Harashima, H., Dissmeyer, N., and Schnittger, A. (2013). Cell cycle control across the eukaryotic kingdom. Trends Cell Biol. *23*, 345–356.

Hauf, S., Waizenegger, I.C., and Peters, J.M. (2001). Cohesin cleavage by separase required for anaphase and cytokinesis in human cells. Science *293*, 1320–1323.

Hayama, R., and Marians, K.J. (2010). Physical and functional interaction between the condensin MukB and the decatenase topoisomerase IV in Escherichia coli. Proc. Natl. Acad. Sci. U. S. A. *107*, 18826–18831.

He, X., Asthana, S., and Sorger, P.K. (2000). Transient sister chromatid separation and elastic deformation of chromosomes during mitosis in budding yeast. Cell *101*, 763–775.

Hegemann, B., Hutchins, J.R.A., Hudecz, O., Novatchkova, M., Rameseder, J., Sykora, M.M., Liu, S., Mazanek, M., Lenart, P., Heriche, J.-K., Poser, I., Kraut, N., Hyman, A.A., Yaffe, M.B., Mechtler, K. and Peters, J.M. (2011). Systematic Phosphorylation Analysis of Human Mitotic Protein Complexes. Sci. Signal. *4*, rs12-rs12.

Hiraga, S., Niki, H., Ogura, T., Ichinose, C., Mori, H., Ezaki, B., and Jaffe, A. (1989). Chromosome partitioning in Escherichia coli: Novel mutants producing anucleate cells. J. Bacteriol. *171*, 1496–1505.

Hirano, M., Anderson, D.E., Erickson, H.P., and Hirano, T. (2001). Bimodal activation of SMC ATPase by intra- and inter-molecular interactions. EMBO J. 20, 3238–3250.

Hirano, T. (2005). SMC proteins and chromosome mechanics: from bacteria to humans. Philos. Trans. R. Soc. Lond. B. Biol. Sci. *360*, 507–514.

Hirano, T. (2012). Condensins: universal organizers of chromosomes with diverse functions. Genes Dev. *26*, 1659–1678.

Hirano, T. (2016). Condensin-Based Chromosome Organization from Bacteria to Vertebrates. Cell *164*, 847–857.

Hirano, M., and Hirano, T. (1998). ATP-dependent aggregation of single-stranded DNA by a bacterial SMC homodimer. EMBO J. *17*, 7139–7148.

Hirano, M., and Hirano, T. (2002). Hinge-mediated dimerization of SMC protein is essential for its dynamic interaction with DNA. EMBO J. *21*, 5733–5744.

Hirano, M., and Hirano, T. (2004). Positive and negative regulation of SMC-DNA interactions by ATP and accessory proteins. EMBO J. *23*, 2664–2673.

Hirano, M., and Hirano, T. (2006). Opening closed arms: long-distance activation of SMC ATPase by hinge-DNA interactions. Mol. Cell *21*, 175–186.

Hirano, T., and Mitchison, T.J. (1993). Topoisomerase II does not play a scaffolding role in the organization of mitotic chromosomes assembled in Xenopus egg extracts. J. Cell Biol. *120*, 601–612.

Hirano, T., and Mitchison, T.J. (1994). A heterodimeric coiled-coil protein required for mitotic chromosome condensation in vitro. Cell *79*, 449–458.

Hirano, T., Kobayashi, R., and Hirano, M. (1997). Condensins, Chromosome Condensation Protein Complexes Containing XCAP-C, XCAP-E and a Xenopus Homolog of the Drosophila Barren Protein. Cell *89*, 511–521.

Hirota, T., Gerlich, D., Koch, B., Ellenberg, J., and Peters, J.M. (2004). Distinct functions of condensin I and II in mitotic chromosome assembly. J Cell Sci *117*, 6435–6445.

Hoa, T.T., Tortosa, P., Albano, M., and Dubnau, D. (2002). Rok (YkuW) regulates genetic competence in Bacillus subtilis by directly repressing comK. Mol. Microbiol. *43*, 15–26.

Hopfner, K.P., Karcher, A., Shin, D.S., Craig, L., Arthur, L.M., Carney, J.P., and Tainer, J. a (2000). Structural biology of Rad50 ATPase: ATP-driven conformational control in DNA double-strand break repair and the ABC-ATPase superfamily. Cell *101*, 789–800.

Houlard, M., Godwin, J., Metson, J., Lee, J., Hirano, T., and Nasmyth, K. (2015). Condensin confers the longitudinal rigidity of chromosomes. Nat. Cell Biol. *17*, 771–781.

Hu, B., Itoh, T., Mishra, A., Katoh, Y., Chan, K.-L., Upcher, W., Godlee, C., Roig, M.B., Shirahige, K., and Nasmyth, K. (2011). ATP hydrolysis is required for relocating cohesin from sites occupied by its Scc2/4 loading complex. Curr. Biol. *21*, 12–24.

Ireton, K., Gunther, N.W., and Grossman, A.D. (1994). spo0J is required for normal chromosome segregation as well as the initiation of sporulation in Bacillus subtilis. J. Bacteriol. *176*, 5320–5329.

Ivanov, D., and Nasmyth, K. (2005). A topological interaction between cohesin rings and a circular minichromosome. Cell *122*, 849–860.

Ivanov, D., and Nasmyth, K. (2007). A physical assay for sister chromatid cohesion in vitro. Mol. Cell *27*, 300–310.

Jensen, R.B., and Shapiro, L. (1999). The Caulobacter crescentus smc gene is required for cell cycle progression and chromosome segregation. Proc Natl Acad Sci U S A *96*, 10661–10666.

Jeppsson, K., Kanno, T., Shirahige, K., and Sjögren, C. (2014). The maintenance of chromosome structure: positioning and functioning of SMC complexes. Nat. Rev. Mol. Cell Biol. *15*, 601–614.

Jun, S., and Mulder, B. (2006). Entropy-driven spatial organization of highly confined polymers: lessons for the bacterial chromosome. Proc. Natl. Acad. Sci. U. S. A. *103*, 12388–12393.

Jun, S., and Wright, A. (2010). Entropy as the driver of chromosome segregation. Nat. Rev. Microbiol. *8*, 600–607.

Kagey, M.H., Newman, J.J., Bilodeau, S., Zhan, Y., Orlando, D.A., van Berkum, N.L., Ebmeier, C.C., Goossens, J., Rahl, P.B., Levine, S.S., Taatjes, D.J., Dekker, J. and Young, R.A. (2010). Mediator and cohesin connect gene expression and chromatin architecture. Nature *467*, 430–435.

Kahramanoglou, C., Seshasayee, A.S.N., Prieto, A.I., Ibberson, D., Schmidt, S., Zimmermann, J., Benes, V., Fraser, G.M., and Luscombe, N.M. (2011). Direct and indirect effects of H-NS and Fis on global gene expression control in Escherichia coli. Nucleic Acids Res. *39*, 2073–2091.

Kaimer, C., González-Pastor, J.E., and Graumann, P.L. (2009). SpoIIIE and a novel type of DNA translocase, SftA, couple chromosome segregation with cell division in Bacillus subtilis. Mol. Microbiol. *74*, 810–825.

Kalia, J., and Raines, R.T. (2007). Catalysis of imido group hydrolysis in a maleimide conjugate. Bioorg. Med. Chem. Lett. *17*, 6286–6289.

Kamada, K., Miyata, M., and Hirano, T. (2013). Molecular basis of SMC ATPase activation: role of internal structural changes of the regulatory subcomplex ScpAB. Structure *21*, 581–594.

Kavenoff, R., and Bowen, B.C. (1976). Electron microscopy of membrane-free folded chromosomes from Escherichia coli. Chromosoma *59*, 89–101.

Kelly, T.J., and Brown, G.W. (2000). Regulation of Chromosome Replication. Annu. Rev. Biochem. *69*, 829–880.

Kimura, K., and Hirano, T. (1997). ATP-dependent positive supercoiling of DNA by 13S condensin: a biochemical implication for chromosome condensation. Cell *90*, 625–634.

Kimura, K., Rybenkov, V. V, Crisona, N.J., Hirano, T., and Cozzarelli, N.R. (1999). 13S condensin actively reconfigures DNA by introducing global positive writhe: implications for chromosome condensation. Cell *98*, 239–248.

Kitajima, T.S., Sakuno, T., Ishiguro, K., Iemura, S., Natsume, T., Kawashima, S. a, and Watanabe, Y. (2006). Shugoshin collaborates with protein phosphatase 2A to protect cohesin. Nature *441*, 46–52.

Kleine Borgmann, L. a K., Ries, J., Ewers, H., Ulbrich, M.H., and Graumann, P.L. (2013). The bacterial SMC complex displays two distinct modes of interaction with the chromosome. Cell Rep. *3*, 1483–1492.

Kornberg, A., and Baker, T.A. (2005). DNA Replication (University Science).

Krantz, I.D., McCallum, J., DeScipio, C., Kaur, M., Gillis, L. a, Yaeger, D., Jukofsky, L., Wasserman, N., Bottani, A., Morris, C. a, et al. (2004). Cornelia de Lange syndrome is caused by mutations in NIPBL, the human homolog of Drosophila melanogaster Nipped-B. Nat. Genet. *36*, 631–635.

Ku, B., Lim, J.H., Shin, H.C., Shin, S.Y., and Oh, B.H. (2010). Crystal structure of the MukB hinge domain with coiled-coil stretches and its functional implications. Proteins Struct. Funct. Bioinforma. *78*, 1483–1490.

Kuempel, P.L., Henson, J.M., Dircks, L., Tecklenburg, M., and Lim, D.F. (1991). dif, a recA-independent recombination site in the terminus region of the chromosome of Escherichia coli. New Biol. *3*, 799–811.

Kueng, S., Hegemann, B., Peters, B.H., Lipp, J.J., Schleiffer, A., Mechtler, K., and Peters, J.M. (2006). Wapl Controls the Dynamic Association of Cohesin with Chromatin. Cell *127*, 955–967.

Lafont, A.L., Song, J., and Rankin, S. (2010). Sororin cooperates with the acetyltransferase Eco2 to ensure DNA replication-dependent sister chromatid cohesion. Proc. Natl. Acad. Sci. U. S. A. *107*, 20364–20369.

Lammens, A., Schele, A., and Hopfner, K.-P. (2004). Structural Biochemistry of ATP-Driven Dimerization and DNA-Stimulated Activation of SMC ATPases. Curr. Biol. *14*, 1778–1782.

Le, T.B.K., Imakaev, M. V, Mirny, L. a, and Laub, M.T. (2013). High-resolution mapping of the spatial organization of a bacterial chromosome. Science *342*, 731–734.

Lee, P.S., and Grossman, A.D. (2006). The chromosome partitioning proteins Soj (ParA) and Spo0J (ParB) contribute to accurate chromosome partitioning, separation of replicated sister origins, and regulation of replication initiation in Bacillus subtilis. Mol. Microbiol. *60*, 853–869.

Lee, P.S., Lin, D.C.H., Moriya, S., and Grossman, A.D. (2003). Effects of the chromosome partitioning protein Spo0J (ParB) on oriC positioning and replication initiation in Bacillus subtilis. J. Bacteriol. *185*, 1326–1337.

Lehmann, a R., Walicka, M., Griffiths, D.J., Murray, J.M., Watts, F.Z., McCready, S., and Carr, a M. (1995). The rad18 gene of Schizosaccharomyces pombe defines a new subgroup of the SMC superfamily involved in DNA repair. Mol. Cell. Biol. *15*, 7067–7080.

Lengronne, A., Katou, Y., Mori, S., Yokobayashi, S., Kelly, G.P., Itoh, T., Watanabe, Y., Shirahige, K., and Uhlmann, F. (2004). Cohesin relocation from sites of chromosomal loading to places of convergent transcription. Nature *430*, 573–578.

Leonard, T.A., Butler, P.J.G., and Löwe, J. (2004). Structural analysis of the chromosome segregation protein Spo0J from Thermus thermophilus. Mol. Microbiol. *53*, 419–432.

Levin, P.A., and Grossman, A.D. (1998). Cell cycle and sporulation in Bacillus subtilis. Curr. Opin. Microbiol. *1*, 630–635.

Lewis, P.J., and Errington, J. (1997). Direct evidence for active segregation of oriC regions of the Bacillus subtilis chromosome and co-localization with the SpoOJ partitioning protein. Mol. Microbiol. *25*, 945–954.

Lewis, P.J., Smith, M.T., and Wake, R.G. (1989). A protein involved in termination of chromosome replication in Bacillus subtilis binds specifically to the terC site. J. Bacteriol. *171*, 3564–3567.

Lewis, P.J., Ralston, G.B., Christopherson, R.I., and Wake, R.G. (1990). Identification of the replication terminator protein binding sites in the terminus region of theBacillus subtilis chromosome and stoichiometry of the binding. J. Mol. Biol. *214*, 73–84.

Li, Y., Stewart, N.K., Berger, A.J., Vos, S., Schoeffler, A.J., Berger, J.M., Chait, B.T., and Oakley, M.G. (2010). Escherichia coli condensin MukB stimulates topoisomerase IV activity by a direct physical interaction. Proc. Natl. Acad. Sci. U. S. A. *107*, 18832–18837.

Lieb, J.D., Albrecht, M.R., Chuang, P.T., and Meyer, B.J. (1998). MIX-1: An essential component of the C. elegans mitotic machinery executes X chromosome dosage compensation. Cell *92*, 265–277.

Lieberman-Aiden, E., van Berkum, N.L., Williams, L., Imakaev, M., Ragoczy, T., Telling, A., Amit, I., Lajoie, B.R., Sabo, P.J., Dorschner, M.O., Sandstrom, R., Bernstein, B., Bender, M.A., Groudine, M., Gnirke, A., Stamatoyannopoulos, J., Mirny, L.A., Lander, E.S. and Dekker, J. (2009). Comprehensive Mapping of Long-Range Interactions Reveals Folding Principles of the Human Genome. Science *326*, 289–293.

Lim, H.C., Surovtsev, I. V., Beltran, B.G., Huang, F., Bewersdorf, J., and Jacobs-Wagner, C. (2014). Evidence for a DNA-relay mechanism in ParABS-mediated chromosome segregation. Elife *2014*, 1–32.

Lin, D.C., and Grossman, A.D. (1998). Identification and characterization of a bacterial chromosome partitioning site. Cell *92*, 675–685.

Lin, D.C., Levin, P. a, and Grossman, A.D. (1997). Bipolar localization of a chromosome partition protein in Bacillus subtilis. Proc. Natl. Acad. Sci. U. S. A. *94*, 4721–4726.

Lindow, J.C., Britton, R.A., and Grossman, A.D. (2002). Structural maintenance of chromosomes protein of Bacillus subtilis affects supercoiling in vivo. J. Bacteriol. *184*, 5317–5322.

Liu, L.F., and Wang, J.C. (1987). Supercoiling of the DNA template during transcription. Proc. Natl. Acad. Sci. U. S. A. *84*, 7024–7027.

Livny, J., Yamaichi, Y., Waldor, M.K., Genomics, C., Livny, J., Yamaichi, Y., and Waldor, M.K. (2007). Distribution of centromere-like parS sites in bacteria: insights from comparative genomics. J. Bacteriol. *189*, 8693–8703.

Lopez-Serra, L., Kelly, G., Patel, H., Stewart, A., and Uhlmann, F. (2014). The Scc2-Scc4 complex acts in sister chromatid cohesion and transcriptional regulation by maintaining nucleosome-free regions. Nat. Genet. *46*, 1147–1151.

Los, G. V., Encell, L.P., McDougall, M.G., Hartzell, D.D., Karassina, N., Zimprich, C., Wood, M.G., Learish, R., Ohana, R.F., Urh, M., Simpson, D., Mendez, J., Zimmerman, K., Otto, P., Vidugiris, G., Zhu, J., Darzins, A., Klaubert, D.H., Bulleit, R.F. and Wood, K.V. (2008). HaloTag: A Novel Protein Labeling Technology for Cell Imaging and Protein Analysis. ACS Chem. Biol. *3*, 373–382.

Losada, A., and Hirano, T. (2001). Intermolecular DNA interactions stimulated by the cohesin complex in vitro: Implications for sister chromatid cohesion. Curr. Biol. *11*, 268–272.

Losada, A., Hirano, M., and Hirano, T. (2002). Cohesin release is required for sister chromatid resolution, but not for condensin-mediated compaction, at the onset of mitosis. Genes Dev. *16*, 3004–3016.

Löwe, J., Cordell, S.C., and van den Ent, F. (2001). Crystal structure of the SMC head domain: an ABC ATPase with 900 residues antiparallel coiled-coil inserted. J. Mol. Biol. *306*, 25–35.

Löwe, J., Ellonen, A., Allen, M.D., Atkinson, C., Sherratt, D.J., and Grainge, I. (2008). Molecular mechanism of sequence-directed DNA loading and translocation by FtsK. Mol. Cell *31*, 498–509.

Lupas, A.N., and Gruber, M. (2005). The structure of alpha-helical coiled coils. Adv. Protein Chem. *70*, 37–78.

Lutkenhaus, J. (2007). Assembly dynamics of the bacterial MinCDE system and spatial regulation of the Z ring. Annu. Rev. Biochem. *76*, 539–562.

Maeshima, K., and Laemmli, U.K. (2003). A Two-step scaffolding model for mitotic chromosome assembly. Dev. Cell *4*, 467–480.

Marbouty, M., Le Gall, A., Cattoni, D.I., Cournac, A., Koh, A., Fiche, J.-B., Mozziconacci, J., Murray, H., Koszul, R., and Nollmann, M. (2015). Condensin- and Replication-Mediated Bacterial Chromosome Folding and Origin Condensation Revealed by Hi-C and Super-resolution Imaging. Mol. Cell *59*, 588–602.

Marsin, S., McGovern, S., Ehrlich, S.D., Bruand, C., and Polard, P. (2001). Early Steps of Bacillus subtilis Primosome Assembly. J. Biol. Chem. *276*, 45818–45825.

Mascarenhas, J., Soppa, J., Strunnikov, A. V., and Graumann, P.L. (2002). Cell cycle-dependent localization of two novel prokaryotic chromosome segregation and condensation proteins in Bacillus subtilis that interact with SMC protein. EMBO J. *21*, 3108–3118.

Mason, D.J., and Powelson, D.M. (1956). Nuclear division as observed in live bacteria by a new technique. J. Bacteriol. *71*, 474–479.

McAleenan, A., Cordon-Preciado, V., Clemente-Blanco, A., Liu, I.C., Sen, N., Leonard, J., Jarmuz, A., and Aragón, L. (2012). SUMOylation of the α-kleisin subunit of cohesin is required for DNA damage-induced cohesion. Curr. Biol. *22*, 1564–1575.

Melby, T.E., Ciampaglio, C.N., Briscoe, G., and Erickson, H.P. (1998). The symmetrical structure of structural maintenance of chromosomes (SMC) and MukB proteins: Long, antiparallel coiled coils, folded at a flexible hinge. J. Cell Biol. *142*, 1595–1604.

Merrikh, H., Zhang, Y., Grossman, A.D., and Wang, J.D. (2012). Replication–transcription conflicts in bacteria. Nat. Rev. Microbiol. *10*, 449–458.

Meyer, B.J. (2010). Targeting X chromosomes for repression. Curr. Opin. Genet. Dev. *20*, 179–189.

Michaelis, C., Ciosk, R., and Nasmyth, K. (1997). Cohesins: Chromosomal proteins that prevent premature separation of sister chromatids. Cell *91*, 35–45.

Minnen, A., Bürmann, F., Wilhelm, L., Anchimiuk, A., Diebold-Durand, M.-L., and Gruber, S. (2016). Control of Smc Coiled Coil Architecture by the ATPase Heads Facilitates Targeting to Chromosomal ParB/parS and Release onto Flanking DNA. Cell Rep. *14*, 2003–2016.

Mirkin, E. V, and Mirkin, S.M. (2007). Replication fork stalling at natural impediments. Microbiol. Mol. Biol. Rev. *71*, 13–35.

Morgan, D.O. (1997). Cyclin-dependent kinases: engines, clocks, and microprocessors. Annu. Rev. Cell Dev. Biol. *13*, 261–291.

Moriya, S., Atlung, T., Hansen, F.G., Yoshikawa, H., and Ogasawara, N. (1992). Cloning of an autonomously replicating sequence (ars) from the Bacillus subtilis chromosome. Mol. Microbiol. *6*, 309–315.

Moriya, S., Firshein, W., Yoshikawa, H., and Ogasawara, N. (1994). Replication of a *Bacillus subtilis oriC* plasmid in vitro. Mol. Microbiol. *12*, 469–478.

Moriya, S., Tsujikawa, E., Hassan, A.K.M., Asai, K., Kodama, T., and Ogasawara, N. (1998). A Bacillus subtilis gene-encoding protein homologous to eukaryotic SMC motor protein is necessary for chromosome partition. Mol. Microbiol. *29*, 179–187.

Murayama, Y., and Uhlmann, F. (2014). Biochemical reconstitution of topological DNA binding by the cohesin ring. Nature *505*, 367–371.

Murayama, Y., and Uhlmann, F. (2015). DNA Entry into and Exit out of the Cohesin Ring by an Interlocking Gate Mechanism. Cell *163*, 1628–1640.

Murray, H., and Errington, J. (2008). Dynamic control of the DNA replication initiation protein DnaA by Soj/ParA. Cell *135*, 74–84.

Murray, H., Ferreira, H., and Errington, J. (2006). The bacterial chromosome segregation protein Spo0J spreads along DNA from parS nucleation sites. Mol. Microbiol. *61*, 1352–1361.

Nasmyth, K. (2002). Segregating sister genomes: the molecular biology of chromosome separation. Science *297*, 559–565.

Nasmyth, K. (2005). How might cohesin hold sister chromatids together? Philos. Trans. R. Soc. B Biol. Sci. *360*, 483–496.

Nasmyth, K., and Haering, C.H. (2005). THE STRUCTURE AND FUNCTION OF SMC AND KLEISIN COMPLEXES. Annu. Rev. Biochem. *74*, 595–648.

Nasmyth, K., and Haering, C.H. (2009). Cohesin: Its Roles and Mechanisms. Annu. Rev. Genet. *43*, 525–558.

Nassonova, E.S. (2008). Pulsed field gel electrophoresis: Theory, instruments and application. Cell Tissue Biol. *2*, 557–565.

Nativio, R., Wendt, K.S., Ito, Y., Huddleston, J.E., Uribe-Lewis, S., Woodfine, K., Krueger, C., Reik, W., Peters, J.-M., and Murrell, A. (2009). Cohesin Is Required for Higher-Order Chromatin Conformation at the Imprinted IGF2-H19 Locus. PLoS Genet. *5*, e1000739.

Navarre, W.W., Porwollik, S., Wang, Y., McClelland, M., Rosen, H., Libby, S.J., and Fang, F.C. (2006). Selective silencing of foreign DNA with low GC content by the H-NS protein in Salmonella. Science *313*, 236–238.

Neuwald, A.F., and Hirano, T. (2000). HEAT repeats associated with condensins, cohesins, and other complexes involved in chromosome-related functions. Genome Res. *10*, 1445–1452.

Nicolas, E., Upton, A.L., Uphoff, S., Henry, O., Badrinarayanan, A., and Sherratt, D. (2014). The SMC Complex MukBEF Recruits Topoisomerase IV to the Origin of Replication Region in Live Escherichia coli. MBio *5*, e01001-13-e01001-13.

Nielsen, H.J., Youngren, B., Hansen, F.G., and Austin, S. (2007). Dynamics of Escherichia coli chromosome segregation during multifork replication. J. Bacteriol. *189*, 8660–8666.

Niki, H., and Hiraga, S. (1998). Polar localization of the replication origin and terminus in Escherichia coli nucleoids during chromosome partitioning. Genes Dev. *12*, 1036–1045.

Niki, H., Jaffe, A., Imamura, R., Ogura, T., and Hiraga, S. (1991). The new gene mukB codes for a 177 kd protein with coiled-coil domains involved in chromosome partitioning of E.coli. EMBO J. *1*, 183–193.

Niki, H., Imamura, R., Kitaoka, M., Yamanaka, K., Ogura, T., and Hiraga, S. (1992). E.coli MukB protein involved in chromosome partition forms a homodimer with a rod-and-hinge structure having DNA binding and ATP/GTP binding activities. EMBO J. *11*, 5101–5109.

Niki, H., Yamaichi, Y., and Hiraga, S. (2000). Dynamic organization of chromosomal DNA in Escherichia coli. Genes Dev. *14*, 212–223.

Nishiyama, T., Ladurner, R., Schmitz, J., Kreidl, E., Schleiffer, A., Bhaskara, V., Bando, M., Shirahige, K., Hyman, A.A., Mechtler, K. and Peters, J.M. (2010). Sororin mediates sister chromatid cohesion by antagonizing Wapl. Cell *143*, 737–749.

Nolivos, S., and Sherratt, D. (2013). The bacterial chromosome: architecture and action of bacterial SMC and SMC-like complexes. FEMS Microbiol. Rev. *38*, 380–392.

Oliferenko, S., Chew, T.G., and Balasubramanian, M.K. (2009). Positioning cytokinesis. Genes Dev. *23*, 660–674.

Oliveira, R.A., Heidmann, S., and Sunkel, C.E. (2007). Condensin I binds chromatin early in prophase and displays a highly dynamic association with Drosophila mitotic chromosomes. Chromosoma *116*, 259–274.

Ono, T., Losada, A., Hirano, M., Myers, M.P., Neuwald, A.F., and Hirano, T. (2003). Differential contributions of condensin I and condensin II to mitotic chromosome architecture in vertebrate cells. Cell *115*, 109–121.

Ono, T., Fang, Y., Spector, D.L., and Hirano, T. (2004). Spatial and temporal regulation of Condensins I and II in mitotic chromosome assembly in human cells. Mol. Biol. Cell *15*, 3296–3308.

Painbeni, E., Caroff, M., and Rouviere-Yaniv, J. (1997). Alterations of the outer membrane composition in Escherichia coli lacking the histone-like protein HU. Proc. Natl. Acad. Sci. U. S. A. *94*, 6712–6717.

Palecek, J.J., and Gruber, S. (2015). Kite Proteins: a Superfamily of SMC/Kleisin Partners Conserved Across Bacteria, Archaea, and Eukaryotes. Structure *23*, 2183–2190.

Panizza, S., Tanaka, T., Hochwagen, A., Eisenhaber, F., and Nasmyth, K. (2000). Pds5 cooperates with cohesin in maintaining sister chromatid cohesion. Curr. Biol. *10*, 1557–1564.

Parelho, V., Hadjur, S., Spivakov, M., Leleu, M., Sauer, S., Gregson, H.C., Jarmuz, A., Canzonetta, C., Webster, Z., Nesterova, T., Cobb, B.S., Yokomori, K., Dillon, N., Aragon, L., Fisher, A.G. and Merkenschlager, M. (2008). Cohesins Functionally Associate with CTCF on Mammalian Chromosome Arms. Cell *132*, 422–433.

Paterczyk, B., and Fornal, J. (1991). Proteins of Caulobacter crescentus strongly binding to DNA. Spectroscopic analysis of major histone-like proteins. Acta Microbiol. Pol. *40*, 37–49.

Pebernard, S., Wohschlegel, J., McDonald, W.H., Yates, J.R., Boddy, M.N., Wohlschlegel, J., and Iii, J.R.Y. (2006). The Nse5-Nse6 dimer mediates DNA repair roles of the Smc5-Smc6 complex. Mol. Cell. Biol. *26*, 1617–1630.

Pérals, K., Capiaux, H., Vincourt, J.B., Louarn, J.M., Sherratt, D.J., and Cornet, F. (2001). Interplay between recombination, cell division and chromosome structure during chromosome dimer resolution in Escherichia coli. Mol. Microbiol. *39*, 904–913.

Peters, J.-M. (2006). The anaphase promoting complex/cyclosome: a machine designed to destroy. Nat. Rev. Mol. Cell Biol. *7*, 644–656.

Peters, J.-M., and Nishiyama, T. (2012). Sister chromatid cohesion. Cold Spring Harb. Perspect. Biol. *4*, 1–18.

Petrushenko, Z.M., She, W., and Rybenkov, V. V. (2011). A new family of bacterial condensins. Mol. Microbiol. *81*, 881–896.

Pettijohn, D.E., and Hecht, R. (1974). RNA molecules bound to the folded bacterial genome stabilize DNA folds and segregate domains of supercoiling. Cold Spring Harb. Symp. Quant. Biol. *38*, 31–41.

Phillips, J.E., and Corces, V.G. (2009). CTCF: Master Weaver of the Genome. Cell *137*, 1194–1211.

De Piccoli, G., Cortes-Ledesma, F., Ira, G., Torres-Rosell, J., Uhle, S., Farmer, S., Hwang, J.-Y., Machin, F., Ceschia, A., McAleenan, A., Cordon-Preciado, V., Clemente-Blanco, A., Vilella-Mitjana, F., Ullal, P., Jarmuz, A., Leitao, B., Bressan, D., Dotiwala, F., Papusha, A., Zhao, X., Myung, K., Haber, J.E., Aguilera, A. and Aragón, L. (2006). Smc5-Smc6 mediate DNA double-strand-break repair by promoting sister-chromatid recombination. Nat. Cell Biol. *8*, 1032–1034.

Piekarski, G. (1937). Zytologische Untersuchungen an Paratyphus- und Coli Bakterien. Arch. Mikrobiol. *8*, 428–429.

Postow, L., Crisona, N.J., Peter, B.J., Hardy, C.D., and Cozzarelli, N.R. (2001). Topological challenges to DNA replication: conformations at the fork. Proc. Natl. Acad. Sci. U. S. A. *98*, 8219–8226.

Postow, L., Hardy, C.D., Arsuaga, J., and Cozzarelli, N.R. (2004). Topological domain structure of the Escherichia coli chromosome. Genes Dev. *18*, 1766-1779.

Potts, P.R., Porteus, M.H., and Yu, H. (2006). Human SMC5/6 complex promotes sister chromatid homologous recombination by recruiting the SMC1/3 cohesin complex to double-strand breaks. EMBO J. *25*, 3377–3388.

Prieto, A.I., Kahramanoglou, C., Ali, R.M., Fraser, G.M., Seshasayee, A.S.N., and Luscombe, N.M. (2012). Genomic analysis of DNA binding and gene regulation by homologous nucleoid-associated proteins IHF and HU in Escherichia coli K12. Nucleic Acids Res. *40*, 3524–3537.

Ptacin, J.L., Lee, S.F., Garner, E.C., Toro, E., Eckart, M., Comolli, L.R., Moerner, W.E., and Shapiro, L. (2010). A spindle-like apparatus guides bacterial chromosome segregation. Nat. Cell Biol. *12*, 791–798.

Rankin, S., Ayad, N.G., and Kirschner, M.W. (2005). Sororin, a Substrate of the Anaphase- Promoting Complex, Is Required for Sister Chromatid Cohesion in Vertebrates. Mol. Cell *18*, 185–200.

Robinow, C., and Kellenberger, E. (1994). The bacterial nucleoid revisited. Microbiol. Rev. *58*, 211–232.

Rodionov, O., Lobocka, M., and Yarmolinsky, M. (1999). Silencing of genes flanking the P1 plasmid centromere. Science *283*, 546–549.

Rubio, E.D., Reiss, D.J., Welcsh, P.L., Disteche, C.M., Filippova, G.N., Baliga, N.S., Aebersold, R., Ranish, J. a, and Krumm, A. (2008). CTCF physically links cohesin to chromatin. Proc. Natl. Acad. Sci. U. S. A. *105*, 8309–8314.

Sakamoto, Y., Nakai, S., Moriya, S., Yoshikawa, H., and Ogasawara, N. (1995). The Bacillus subtilis dnaC gene encodes a protein homologous to the DnaB helicase of Escherichia coli. Microbiology *141*, 641–644.

Sanchez, A., Rech, J., Gasc, C., and Bouet, J.-Y. (2013). Insight into centromere-binding properties of ParB proteins: a secondary binding motif is essential for bacterial genome maintenance. Nucleic Acids Res. *41*, 3094–3103.

Sanchez, A., Cattoni, D.I., Walter, J.C., Rech, J., Parmeggiani, A., Nollmann, M., and Bouet, J.Y. (2015). Stochastic Self-Assembly of ParB Proteins Builds the Bacterial DNA Segregation Apparatus. Cell Syst. *1*, 163–173.

Sanders, G.M., Dallmann, H.G., and McHenry, C.S. (2010). Reconstitution of the B. subtilis Replisome with 13 Proteins Including Two Distinct Replicases. Mol. Cell *37*, 273–281.

Schleiffer, A., Kaitna, S., Maurer-Stroh, S., Glotzer, M., Nasmyth, K., and Eisenhaber, F. (2003). Kleisins: A superfamily of bacterial and eukaryotic SMC protein partners. Mol. Cell *11*, 571–575.

Schmidt, C.K., Brookes, N., and Uhlmann, F. (2009). Conserved features of cohesin binding along fission yeast chromosomes. Genome Biol. *10*, R52.

Sciochetti, S.A., Piggot, P.J., Sherratt, D.J., and Blakely, G. (1999). The ripX locus of Bacillus subtilis encodes a site-specific recombinase involved in proper chromosome partitioning. J. Bacteriol. *181*, 6053–6062.

Sciochetti, S.A., Piggot, P.J., and Blakely, G.W. (2001). Identification and characterization of the dif Site from Bacillus subtilis. J. Bacteriol. *183*, 1058–1068.

Sekimizu, K., Bramhill, D., and Kornberg, A. (1987). ATP activates dnaA protein in initiating replication of plasmids bearing the origin of the E. coli chromosome. Cell *50*, 259–265.

Shebelut, C.W., Guberman, J.M., van Teeffelen, S., Yakhnina, A. a, and Gitai, Z. (2010). Caulobacter chromosome segregation is an ordered multistep process. Proc. Natl. Acad. Sci. U. S. A. *107*, 14194–14198.

Sherratt, D.J., Arciszewska, L.K., Crozat, E., Graham, J.E., and Grainge, I. (2010). The Escherichia coli DNA translocase FtsK. Biochem. Soc. Trans. *38*, 395–398.

Shimomura, O., Johnson, F.H., and Saiga, Y. (1962). Extraction, purification and properties of aequorin, a bioluminescent protein from the luminous hydromedusan, Aequorea. J. Cell. Comp. Physiol. *59*, 223–239.

Shintomi, K., and Hirano, T. (2011). The relative ratio of condensin I to II determines chromosome shapes. Genes Dev. *25*, 1464–1469.

Shintomi, K., Takahashi, T.S., and Hirano, T. (2015). Reconstitution of mitotic chromatids with a minimum set of purified factors. Nat. Cell Biol. *17*, 1014–1023.

Singh, S.S., Singh, N., Bonocora, R.P., Fitzgerald, D.M., Wade, J.T., and Grainger, D.C. (2014). Widespread suppression of intragenic transcription initiation by H-NS. Genes Dev. *28*, 214–219.

Smith, M.T., and Wake, R.G. (1992). Definition and polarity of action of DNA replication terminators in Bacillus subtilis. J. Mol. Biol. *227*, 648–657.

Smith, M.T., de Vries, C.J., Langley, D.B., King, G.F., and Wake, R.G. (1996). The Bacillus subtilis DNA replication terminator. J. Mol. Biol. *260*, 54–69.

Smits, W.K., and Grossman, A.D. (2010). The Transcriptional Regulator Rok Binds A+T-Rich DNA and Is Involved in Repression of a Mobile Genetic Element in Bacillus subtilis. PLoS Genet. *6*, e1001207.

Soh, Y., Bürmann, F., Shin, H., Oda, T., Jin, K.S., Toseland, C.P., Kim, C., Lee, H., Kim, S.J., Kong, M.S., Durand-Diebold, M.-L., Kim, Y.-G., Kim, H.M., Lee, N.K., Sato, M., Oh B.-H. and Gruber, S. (2015). Molecular Basis for SMC Rod Formation and Its Dissolution upon DNA Binding. Mol. Cell *57*, 1–14.

Solomon, M.J., Larsen, P.L., and Varshavsky, A. (1988). Mapping Protein-DNA Interactions In Vivo with Formaldehyde: Evidence That Histone H4 Is Retained on a Highly Transcribed Gene. Cell *53*, 937–947.

Song, D., and Loparo, J.J. (2015). Building bridges within the bacterial chromosome. Trends Genet. *31*, 164–173.

Sonoda, E., Matsusaka, T., Morrison, C., Vagnarelli, P., Hoshi, O., Ushiki, T., Nojima, K., Fukagawa, T., Waizenegger, I.C., Peters, J.M., Earnshaw, W.C. and Takeda, S. (2001). Scc1/Rad21/Mcd1 Is Required for Sister Chromatid Cohesion and Kinetochore Function in Vertebrate Cells. Dev. Cell *1*, 759–770.

Soppa, J., Kobayashi, K., Noirot-Gros, M.-F., Oesterhelt, D., Ehrlich, S.D., Dervyn, E., Ogasawara, N., and Moriya, S. (2002). Discovery of two novel families of proteins that are proposed to interact with prokaryotic SMC proteins, and characterization of the Bacillus subtilis family members ScpA and ScpB. Mol. Microbiol. 45, 59–71.

Stedman, W., Kang, H., Lin, S., Kissil, J.L., Bartolomei, M.S., and Lieberman, P.M. (2008). Cohesins localize with CTCF at the KSHV latency control region and at cellular c-myc and H19/Igf2 insulators. EMBO J. *27*, 654–666.

Steiner, W.W., and Kuempel, P.L. (1998). Sister chromatid exchange frequencies in Escherichia coli analyzed by recombination at the dif resolvase site. J. Bacteriol. *180*, 6269–6275.

Steiner, W., Liu, G., Donachie, W.D., and Kuempel, P. (1999). The cytoplasmic domain of FtsK protein is required for resolution of chromosome dimers. Mol. Microbiol. *31*, 579–583.

Stephan, A.K., Kliszczak, M., Dodson, H., Cooley, C., and Morrison, C.G. (2011). Roles of Vertebrate Smc5 in Sister Chromatid Cohesion and Homologous Recombinational Repair. Mol. Cell. Biol. *31*, 1369–1381.

Stigler, J., Çamdere, G.Ö., Koshland, D.E., and Greene, E.C. (2016). Single-Molecule Imaging Reveals a Collapsed Conformational State for DNA-Bound Cohesin. Cell Rep. *15*, 988–998.

Stille, B. (1937). Zytologische Untersuchungen an Bakterien mit Hilfe der Feulgenschen Nuclealreaktion. Arch. Mikrobiol. *8*, 124–148.

Stouf, M., Meile, J.-C., and Cornet, F. (2013). FtsK actively segregates sister chromosomes in Escherichia coli. Proc. Natl. Acad. Sci. U. S. A. *110*, 11157–11162.

Strick, T.R., Kawaguchi, T., and Hirano, T. (2004). Real-time detection of single-molecule DNA compaction by condensin I. Curr. Biol. *14*, 874–880.

Strom, L., Karlsson, C., Lindroos, H.B., Wedahl, S., Katou, Y., Shirahige, K., and Sjogren, C. (2007). Postreplicative Formation of Cohesion Is Required for Repair and Induced by a Single DNA Break. Science *317*, 242–245.

Strunnikov, A. V, Larionov, V.L., and Koshland, D. (1993). SMC1: an essential yeast gene encoding a putative head-rod-tail protein is required for nuclear division and defines a new ubiquitous protein family. J. Cell Biol. *123*, 1635–1648.

Stukenberg, P.T., Studwell-vaughan, P.S., and Donnell, M.O. (1991). Mechanism of the Sliding beta-Clamp of DNA Polymerase III Holoenzyme. J. Biol. Chem. *266*, 11328–11334.

Su'etsugu, M., and Errington, J. (2011). The replicase sliding clamp dynamically accumulates behind progressing replication forks in Bacillus subtilis cells. Mol. Cell *41*, 720–732.

Sullivan, N.L., Marquis, K.A., and Rudner, D.Z. (2009). Recruitment of SMC by ParB- parS Organizes the Origin Region and Promotes Efficient Chromosome Segregation. Cell *137*, 697–707.

Sumara, I., Vorlaufer, E., Stukenberg, P.T., Kelm, O., Redemann, N., Nigg, E.A., and Peters, J.M. (2002). The dissociation of cohesin from chromosomes in prophase is regulated by polo-like kinase. Mol. Cell *9*, 515–525.

Sundin, O., and Varshavsky, A. (1980). Terminal stages of SV40 DNA replication proceed via multiply intertwined catenated dimers. Cell *21*, 103–114.

Sundin, O., and Varshavsky, A. (1981). Arrest of segregation leads to accumulation of highly intertwined catenated dimers: Dissection of the final stages of SV40 DNA replication. Cell *25*, 659–669.

Sutani, T., Yuasa, T., Tomonaga, T., Dohmae, N., Takio, K., and Yanagida, M. (1999). Fission yeast condensin complex: Essential roles of non-SMC subunits for condensation and Cdc2 phosphorylation of Cut3/SMC4. Genes Dev. *13*, 2271–2283.

Sutani, T., Kawaguchi, T., Kanno, R., Itoh, T., and Shirahige, K. (2009). Budding Yeast Wpl1(Rad61)-Pds5 Complex Counteracts Sister Chromatid Cohesion-Establishing Reaction. Curr. Biol. *19*, 492–497.

Swinger, K.K., Lemberg, K.M., Zhang, Y., and Rice, P.A. (2003). Flexible DNA bending in HU ± DNA cocrystal structures. EMBO J. *22*, 1–12.

Tanaka, T., Cosma, M.P., Wirth, K., and Nasmyth, K. (1999). Identification of cohesin association sites at centromeres and along chromosome arms. Cell *98*, 847–858.

Tanaka, T., Fuchs, J., Loidl, J., and Nasmyth, K. (2000). Cohesin ensures bipolar attachment of microtubules to sister centromeres and resists their precocious separation. Nat. Cell Biol. *2*, 492–499.

Taylor, J. a., Pastrana, C.L., Butterer, A., Pernstich, C., Gwynn, E.J., Sobott, F., Moreno-Herrero, F., and Dillingham, M.S. (2015). Specific and non-specific interactions of ParB with DNA: implications for chromosome segregation. Nucleic Acids Res. *43*, 719–731.

Tedeschi, A., Wutz, G., Huet, S., Jaritz, M., Wuensche, A., Schirghuber, E., Davidson, I.F., Tang, W., Cisneros, D. A., Bhaskara, V., Nishiyama, T., Vaziri, A., Wutz, A., Ellenberg, J. and Peters, J.M. (2013). Wapl is an essential regulator of chromatin structure and chromosome segregation. Nature *501*, 564–568.

Teleman, A.A., Graumann, P.L., Lin, D.C., Grossman, A.D., and Losick, R. (1998). Chromosome arrangement within a bacterium. Curr. Biol. *8*, 1102–1109.

Thadani, R., Uhlmann, F., and Heeger, S. (2012). Condensin, Chromatin Crossbarring and Chromosome Condensation. Curr. Biol. *22*, R1012–R1021.

Toro, E., Hong, S.-H., McAdams, H.H., and Shapiro, L. (2008). Caulobacter requires a dedicated mechanism to initiate chromosome segregation. Proc. Natl. Acad. Sci. U. S. A. *105*, 15435–15440.

Torres-Rosell, J., Machín, F., Farmer, S., Jarmuz, A., Eydmann, T., Dalgaard, J.Z., and Aragón, L. (2005). SMC5 and SMC6 genes are required for the segregation of repetitive chromosome regions. Nat. Cell Biol. *7*, 412–419.

Uhlmann, F. (2016). SMC complexes: from DNA to chromosomes. Nat. Rev. Mol. Cell Biol. *17*, 399–412.

Uhlmann, F., and Nasmyth, K. (1998). Cohesion between sister chromatids must be established during DNA replication. Curr. Biol. *8*, 1095–1101.

Uhlmann, F., Lottspeich, F., and Nasmyth, K. (1999). Sister-chromatid separation at anaphase onset is promoted by cleavage of the cohesin subunit Scc1. Nature *400*, 37–42.

Uhlmann, F., Wernic, D., Poupart, M.-A., Koonin, E. V, and Nasmyth, K. (2000). Cleavage of Cohesin by the CD Clan Protease Separin Triggers Anaphase in Yeast. Cell *103*, 375–386.

Ullsperger, C., and Cozzarelli, N.R. (1996). Contrasting enzymatic activities of topoisomerase IV and DNA gyrase from Escherichia coli. J. Biol. Chem. *271*, 31549–31555.

Unal, E., Heidinger-Pauli, J.M., and Koshland, D. (2007). DNA Double-Strand Breaks Trigger Genome-Wide Sister-Chromatid Cohesion Through Eco1 (Ctf7). Science *317*, 245–248.

Upton, A.L., and Sherratt, D.J. (2013). Breaking symmetry in SMCs. Nat. Struct. Mol. Biol. *20*, 246–249.

Valens, M., Penaud, S., Rossignol, M., Cornet, F., and Boccard, F. (2004). Macrodomain organization of the Escherichia coli chromosome. EMBO J. *23*, 4330–4341.

Varshavsky, A.J., Nedospasov, S.A., Bakayev, V. V, Bakayeva, T.G., and Georgiev, G.P. (1977). Histone-like proteins in the purified Escherichia coli deoxyribonucleoprotein. Nucleic Acids Res. *4*, 2725–2745.

Vecchiarelli, A.G., Han, Y.-W., Tan, X., Mizuuchi, M., Ghirlando, R., Biertümpfel, C., Funnell, B.E., and Mizuuchi, K. (2010). ATP control of dynamic P1 ParA-DNA interactions: a key role for the nucleoid in plasmid partition. Mol. Microbiol. *78*, 78–91.

Vecchiarelli, A.G., Hwang, L.C., and Mizuuchi, K. (2013). Cell-free study of F plasmid partition provides evidence for cargo transport by a diffusion-ratchet mechanism. Proc. Natl. Acad. Sci. *110*, E1390–E1397.

Velten, M., McGovern, S., Marsin, S., Ehrlich, S.D., Noirot, P., and Polard, P. (2003). A two-protein strategy for the functional loading of a cellular replicative DNA helicase. Mol. Cell *11*, 1009–1020.

Vinograd, J., and Lebowitz, J. (1966). Physical and topological properties of circular DNA. J. Gen. Physiol. *49*, 103–125.

Viollier, P.H., Thanbichler, M., McGrath, P.T., West, L., Meewan, M., McAdams, H.H., and Shapiro, L. (2004). Rapid and sequential movement of individual chromosomal loci to specific subcellular locations during bacterial DNA replication. Proc. Natl. Acad. Sci. U. S. A. *101*, 9257–9262.

Vos, S.M., Stewart, N.K., Oakley, M.G., and Berger, J.M. (2013). Structural basis for the MukB-topoisomerase IV interaction and its functional implications in vivo. EMBO J. *32*, 2950–2962.

Waizenegger, I.C., Hauf, S., Meinke, A., and Peters, J.-M. (2000). Two Distinct Pathways Remove Mammalian Cohesin from Chromosome Arms in Prophase and from Centromeres in Anaphase. Cell *103*, 399–410.

Waldman, V.M., Stanage, T.H., Mims, A., Norden, I.S., and Oakley, M.G. (2015). Structural mapping of the coiled-coil domain of a bacterial condensin and comparative analyses across all domains of life suggest conserved features of SMC proteins. Proteins Struct. Funct. Bioinforma. *83*, 1027–1045.

Walker, J.E., Saraste, M., Runswick, M., and Gay, N.J. (1982). Distantly related sequences in the alpha- and beta-subunits of ATP synthase, myosin, kinases and other ATP-requiring enzymes and a common nucleotide binding fold. EMBO J. *1*, 945–951.

Wang, J.C. (1971). Interaction between DNA and an Escherichia coli protein omega. J. Mol. Biol. *55*, 523–533.

Wang, X., and Rudner, D.Z. (2014). Spatial organization of bacterial chromosomes. Curr. Opin. Microbiol. *22*, 66–72.

Wang, X., and Sherratt, D.J. (2010). Independent segregation of the two arms of the Escherichia coli ori region requires neither RNA synthesis nor MreB dynamics. J. Bacteriol. *192*, 6143–6153.

Wang, W., Li, G.-W., Chen, C., Xie, X.S., and Zhuang, X. (2011). Chromosome Organization by a Nucleoid-Associated Protein in Live Bacteria. Science *333*, 1445–1449.

Wang, X., Montero Llopis, P., and Rudner, D.Z. (2013). Organization and segregation of bacterial chromosomes. Nat. Rev. Genet. *14*, 191–203.

Wang, X., Tang, O.W., Riley, E.P., and Rudner, D.Z. (2014). The SMC condensin complex is required for origin segregation in Bacillus subtilis. Curr. Biol. *24*, 287–292.

Wang, X., Le, T.B.K., Lajoie, B.R., Dekker, J., Laub, M.T., and Rudner, D.Z. (2015). Condensin promotes the juxtaposition of DNA flanking its loading site in Bacillus subtilis. Genes Dev. *29*, 1661–1675.

Webb, C.D., Teleman, A., Gordon, S., Straight, A., Belmont, A., Lin, D.C., Grossman, A.D., Wright, A., and Losick, R. (1997). Bipolar Localization of the Replication Origin Regions of Chromosomes in Vegetative and Sporulating Cells of B. subtilis. Cell *88*, 667–674.

Weitzer, S., Lehane, C., and Uhlmann, F. (2003). A Model for ATP Hydrolysis-Dependent Binding of Cohesin to DNA. Curr. Biol. *13*, 1930–1940.

Wendt, K.S., Yoshida, K., Itoh, T., Bando, M., Koch, B., Schirghuber, E., Tsutsumi, S., Nagae, G., Ishihara, K., Mishiro, T., Yahata, K., Imamoto, F., Aburatani, H., Nakao, M., Maeshima, K., Shirahige, K. and Peters, J.M. (2008). Cohesin mediates transcriptional insulation by CCCTC-binding factor. Nature *451*, 796–801.

Wilhelm, L., and Gruber, S. (2016). Chromosom in Schleifen: SMC-Komplexe als molekulare Kabelbinder? BIOspektrum *22*, 356–358.

Wilhelm, L., Bürmann, F., Minnen, A., Shin, H.-C., Toseland, C.P., Oh, B.-H., and Gruber, S. (2015). SMC condensin entraps chromosomal DNA by an ATP hydrolysis dependent loading mechanism in *Bacillus subtilis*. Elife *4*, 1–18.

Woo, J.-S., Lim, J.-H., Shin, H.-C., Suh, M.-K., Ku, B., Lee, K.-H., Joo, K., Robinson, H., Lee, J., Park, S.-Y., et al. (2009). Structural Studies of a Bacterial Condensin Complex Reveal ATP-Dependent Disruption of Intersubunit Interactions. Cell *136*, 85–96.

Wu, L.J., and Errington, J. (2004). Coordination of cell division and chromosome segregation by a nucleoid occlusion protein in Bacillus subtilis. Cell *117*, 915–925.

Yamanaka, K., Ogura, T., Niki, H., and Hiraga, S. (1996). Identification of two new genes, mukE and mukF, involved in chromosome partitioning in Escherichia coli. Mol. Gen. Genet. *250*, 241–251.

Yamazoe, M., Onogi, T., Sunako, Y., Niki, H., Yamanaka, K., Ichimura, T., and Hiraga, S. (1999). Complex formation of MukB, MukE and MukF proteins involved in chromosome partitioning in Escherichia coli. EMBO J. *18*, 5873–5884.

Yeong, F.M., Hombauer, H., Wendt, K.S., Hirota, T., Mudrak, I., Mechtler, K., Loregger, T., Marchler-Bauer, A., Tanaka, K., Peters, J.-M., et al. (2003). Identification of a subunit of a novel Kleisin-beta/SMC complex as a potential substrate of protein phosphatase 2A. Curr. Biol. *13*, 2058–2064.

Zhang, J., Shi, X., Li, Y., Kim, B.J., Jia, J., Huang, Z., Yang, T., Fu, X., Jung, S.Y., Wang, Y., et al. (2008). Acetylation of Smc3 by Eco1 Is Required for S Phase Sister Chromatid Cohesion in Both Human and Yeast. Mol. Cell *31*, 143–151.

Zhao, X., and Blobel, G. (2005). A SUMO ligase is part of a nuclear multiprotein complex that affects DNA repair and chromosomal organization. Proc. Natl. Acad. Sci. U. S. A. *102*, 4777–4782.

6. CURRICULUM VITAE

Personal Data:

Name: Larissa Wilhelm
Date of Birth: March 21st, 1989
Nationality: Austrian

Education and Professional History:

03/2013 – 12/2016	**Doctoral student** at the Max Planck Institute of Biochemistry, Martinsried Supervisor: Dr. Stephan Gruber
03/2015 – 06/2016	**Business economist** with marketing specialization (IWW), Far-distance university Hagen
01/2012 – 01/2013	**Master thesis** in Cell Biology at the Max F. Perutz Laboratories, Vienna Supervisor: Dr. Claudine Kraft Title of thesis: Regulation and function of the Atg1 kinase in autophagy *of Saccharomyces cerevisiae*
10/2010 – 03/2013	**Master of Science** in Molecular Biotechnology University of Applied Sciences FH Campus Vienna
07/2010 – 12/2011	Part-time position as Marketing Associate, eBioscience (now a Thermo Fisher company)
01/2010 – 05/2010	**Bachelor thesis** in the Immunodiagnostics Field Supervisor: Dr. Christina Lobmaier, eBioscience (Thermo Fisher) Title of thesis: Development and optimization of ELISA immunoassays
10/2007 – 05/2010	**Bachelor of Science** in Molecular Biotechnology University of Applied Sciences FH Campus Vienna
06/2007	**A-levels** (Matura) at the Gymnasium Polgarstraße Wien 22, Vienna

Academic achievements and prices

2016	Best Poster Award. Association for General and Applied Microbiology (VAAM) Annual Conference 2016
2015	Junior Research Award of the Max Planck Institute of Biochemistry
2013	Member of the International Max Planck Research School of Molecular and Cellular Life Sciences (IMPRS-LS)
2012	Scholarship for special performance in studies and examinations of the FH Campus Vienna

Publications

2016	Minnen, A*., Bürmann, F*., **Wilhelm, L**., Anchimiuk, A., Diebold-Durand, M.-L., and Gruber, S. 2016. Control of Smc Coiled Coil Architecture by the ATPase Heads Facilitates Targeting to Chromosomal ParB/parS and Release onto Flanking DNA. **Cell Rep**. 14:2003–2016. doi:10.1016/j.celrep.2016.01.066. * Co-Authorship
	Wilhelm L. and Gruber S. Chromosom in Schleifen: SMC-Komplexe als molekulare Kabelbinder? **BIOspektrum.** 04/2016. doi: 10.1007/s12268-016-0696-x
2015	**Wilhelm, L.**, Bürmann, F., Minnen, A., Shin, H.-C., Toseland, C.P., Oh, B.-H., and Gruber, S. 2015. SMC condensin entraps chromosomal DNA by an ATP hydrolysis dependent loading mechanism in Bacillus subtilis. **Elife** 4:1–18. doi:10.7554/eLife.06659.
2014	Papinski, D., Schuschnig, M., Reiter, W., **Wilhelm, L**., Barnes, C.A., Majolica, A., Hansmann, I., Pfaffenwimmer, T., Kijanska, M., Stoffel, I., Lee, S.S., Brezovich, A., Lou, J.H., Turk, B.E., Aebersold, R., Ammerer, G., Peter, M., and Kraft, C. 2014. Early Steps in Autophagy Depend on Direct Phosphorylation of Atg9 by the Atg1 Kinase. **Mol. Cell** :1–13. doi:10.1016/j.molcel.2013.12.011.

Conferences

2016	Annual Conference of the Association for General and Applied Microbiology (VAAM), Jena, Germany
	BACELL Symposium 2016, Paris, France
2015	Interact: The Munich Life Science Symposium for PhD students, Munich, Germany

Languages:

German	Native Speaker
English	Fluent written and oral (Working language since 2012)
Spanish	Basic Knowledge

Other skills:

2014 – 2015	Conference Organizer of the 8th <interact> PhD conference in Munich, Organizer of Marketing activities
2008	Advanced Scuba Diver's Education (PADI)
2004/2006	Voluntary work for environmental projects of the Austrian Alpine Association
2004 – 2005	Education as conflict manager for schools
1996 – 2008	Professional Piano Studies at the Vienna Music School

7. ACKNOWLEDGEMENTS

First of all I want to thank Dr. Stephan Gruber, for offering me the chance to work in his lab. I want to dearly thank you for being a boss who had unlimited time for my questions, for discussions and for sharing your motivation. Stephan, you taught me how to critically question every obtained finding, to think of proper controls for every experiment and to take into account every possible meaning of my obtained results - tasks that are essential to independently work on research projects. Thank you!

My special thanks go to Prof. Dr. Marc Bramkamp, from LMU Munich for serving as my official ‘Doktorvater’ during my PhD studies. Thank you for reviewing my thesis, for being a valuable member of my thesis advisory committee and to always have an open ear for my questions.

I would like to thank all members of my thesis committee for their interest in my thesis and their time. Especially I would like to thank Prof. Dr. Heinrich Jung for serving as second reviewer of my thesis.

I am particularly grateful for the time and interest and the helpful input of the members of my Thesis Advisory Committee in course of my PhD studies - Prof. Dr. Marc Bramkamp and Dr. Zuzana Storchová.

Many thanks go to the coordinators of my graduate program ‘IMPRS-LS’ of the Max Planck Institute of Biochemistry that accompanied me through my PhD studies. Thank you Hans-Jörg Schäffer, Ingrid Wolf and Maximilliane Reif for being extremely open-hearted and for always having an open ear for everything.

I want to dearly thank the people I spent most time with in the past years- the present and past members of the ‘Gruber-lab’. Our lab has an exceptional working atmosphere with a lot of helpfulness, openness, interest and warmth. I am dearly thankful to Marie-Laure, Alex and Ania for our ‘coffee club’ where we drank lots of coffee and ate lots of cake. I want to personally thank Frank, who has had a never-ending patience for questions and provided always a helpful answer. I will miss working with every one of you.

Reaching this point in my life would not have been possible without my family and their support. I want to thank my parents who unconditionally supported me in every decision I made. They motivated me to study what I am interested in and provided financial support, so that I could fully concentrate on my studies. Whenever I was at home, they shared their unconditional warmth and love which always made it possible to ‘re-charge my batteries’ to be fully motivated and concentrated at work. Also I would like to dearly thank my sister. I can talk about everything with you and you always help me to forget about work-related issues for a while.

Last, I cannot thank enough my husband Christopher. I am happy that I found a partner with whom I cannot only critically discuss science-related topics but simply everything. Your patience, love and support make it easy for me to fully concentrate on my career while not forgetting to also enjoy ‘life outside’ the lab.